FINAL REPORT

entitled

TRENDS AND TECHNIQUES FOR SPACE BASE ELECTRONICS

June, 1979

eirs
ENGINEERING & INDUSTRIAL RESEARCH STATION
Electrical Engineering/Mississippi State University

NASA Contract NAS8-26749

(NASA-CR-161270) TRENDS AND TECHNIQUES FOR SPACE BASE ELECTRONICS Final Report, 10 Mar. 1978 - 9 Mar. 1979 (Mississippi State Univ., Mississippi State.) 245 p

by
J. D. Trotter, Principal Investigator
T. E. Wade
J. D. Gassaway

MSSU-EIRS-EE-79-6

TECHNICAL REPORT STANDARD TITLE PAGE

1. REPORT NO.	2. GOVERNMENT ACCESSION NO.	3. RECIPIENT'S CATALOG NO.
4. TITLE AND SUBTITLE TRENDS AND TECHNIQUES FOR SPACE BASE ELECTRONICS		5. REPORT DATE JUNE 1979 6. PERFORMING ORGANIZATION CODE
7. AUTHOR(S) J. D. TROTTER, T. E. WADE, J. D. GASSAWAY		8. PERFORMING ORGANIZATION REPORT # MSU-EE-FIN-1-79
9. PERFORMING ORGANIZATION NAME AND ADDRESS Department of Electrical Engineering Mississippi State University Mississippi State, MS 39762		10. WORK UNIT, NO. 11. CONTRACT OR GRANT NO. NAS8-26749
12. SPONSORING AGENCY NAME AND ADDRESS National Aeronautics and Space Administration Washington, D. C. 20516		13. TYPE OF REPORT & PERIOD COVERED FINAL REPORT March 10, 1978 to March9,1979 14. SPONSORING AGENCY CODE

15. SUPPLEMENTARY NOTES
Prepared by Mississippi State University for George C. Marshall Space Flight Center, Marshall Space Flight Center, Alabama

16. ABSTRACT
During the reporting period of this contract, four activities were in progress: 1) the completion of the 2-D diffusion studies in SOS, (2) the set-up of a sputtering system, furnaces, and photolithography related equipment at MSU, (3) experiments on double layer metal, and (4) the investigation of 2-D modeling of MOSFETs.

Using the 2-D diffusion program developed in the previous contract period, simulations of various phosphorus and boron diffusions in SOS have been completed.

The MSU I. C. Laboratory has in place the furnaces, the photolithography facilities and metallization system to reproduce the NASA/Huntsville double layer process - the only missing equipment being the SiO_2 vapox reactor.

The double layer metal activity initially emphasized wet chemistry techniques. By incorporating the following techniques: (1) ultrasonic etching of the vias, (2) premetal clean using a modified buffered HF, (3) phosphorus doped vapox, and (4) extended sintering, yields of 98% were obtained using the standard test pattern.

A two dimensional modeling program has been written for the simulation of short channel MOSFETs with nonuniform substrate doping. A key simplifying assumption used is that majority carriers can be represented by a sheet charge at the silicon dioxide-silicon interface. The program is not complete. In solving current continuity equation, the program does not converge. However, solving the 2-dimensional Poisson equation for the potential distribution has been achieved. The status of other 2-D MOSFET simulation programs are summarized.

17. KEY WORDS	18. DISTRIBUTION STATEMENT
2-D Diffusion SOS Multi-level metal processes Double layer metal Sintering effects 2-D modeling MOSFET's	

19. SECURITY CLASSIF. (of this report)	20. SECURITY CLASSIF. (of this page)	21. NO. OF PAGES	22. PRICE
Unclassified	Unclassified	237	

MSFC - Form 3292 (May 1969)

For sale by National Technical Information Service, Springfield, Virginia 22151

TABLE OF CONTENTS

LIST OF FIGURES

LIST OF FIGURES (Continued)

LIST OF TABLES

TRENDS AND TECHNIQUES FOR

SPACE BASE ELECTRONICS

Final Report
June 1979

SUMMARY

During the reporting period of this contract, four activities were in progress:

1) the completion of the 2-D diffusion studies in SOS,

2) the set-up of a sputtering system, furnaces, and photolithography related equipment at MSU,

3) experiments on double layer metal, and

4) the investigation of 2-D modeling of MOSFETs.

Using the 2-D diffusion program developed in the previous contract period, simulations of various phosphorus and boron diffusions in SOS have been completed.

The MSU I. C. Laboratory has in place the furnaces, the photolithography facilities and metallization system to reproduce the NASA/Huntsville double layer metal process - the only missing equipment being the SiO_2 vapox reactor.

The double layer metal activity initially emphasized wet chemistry techniques. By incorporating the following techniques:

(1) ultrasonic etching of the vias, (2) premetal clean using a modified buffered HF, (3) phosphorus doped vapox, and (4) extended sintering, yields of 98% were obtained using the standard test pattern.

A two dimensional modeling program has been written for the simulation of short channel MOSFETs with nonuniform substrate doping. A key simplifying assumption used is that the majority carriers can be represented by a sheet charge at the silicon dioxide-silicon interface. The program is not complete. In solving current continuity equation, the program does not converge. However, solving the 2-dimensional Poisson equation for the potential distribution has been achieved. The status of other 2-D MOSFET simulation programs are summarized.

I. REDISTRIBUTION DIFFUSIONS FOR ION-IMPLANTED PREDEPOSITS OF BORON AND PHOSPHORUS IN SOS FILMS

The objective of this work was to produce curves describing the variation with diffusion time and temperature of the junction depth, sheet resistance and integrated impurity dose. This data has been generated for boron and phosphorus redistributed in nitrogen, dry oxygen and steam ambients for <111> oriented SOS films. The following section presents discussions of the implantation and redistribution model, further program develop, the computational procedure and of the computed results.

A. The Redistribution Model

There are three aspects of the redistribution model which are considered: (a) the implanted profile, (b) the oxidation model, and (c) the diffusivity model.

a.) The implanted profile, The implanted profile is described by the Gaussian function,

$$C(y) = C_{max} \exp\{-\tfrac{1}{2} \frac{(y - R_p)^2}{\Delta R_p}\} \qquad (1)$$

where C is the concentration, y is the distance from the entrant silicon surface, R_p is the range and ΔR_p is the straggle for the implant. The peak concentration, C_{max}, is related to the implant dose, Q_{imp} by:

$$C_{max} \propto Q_{imp} / \sqrt{2\pi}\,\Delta R_p \quad . \qquad (2)$$

Redistribution data has been generated for the following conditions: [1.1]

Q_{imp}:	5×10^{12} , 10^{13} , 5×10^{13} , 10^{14} cm^{-2}	
R_p:	0.2735 μm	80 keV boron implant.
	0.1727 μm	150 keV phosphorus.
ΔR_p:	0.0665 μm	80 keV boron implant.
	0.0440 μm	150 keV phosphorus.

The doses are light to moderate resulting in concentrations no heavier than 6×10^{18} cm^{-3}, and the range-straggle values are typical of those employed at MSFC. It is assumed that all of the ions become activated shortly after redistribution begins and thereby diffuse by a substitutional mechanism involving vacancies.

b.) Oxidation model: The oxidation model is assumed to be the same as for bulk silicon and the data of Deal et. al. [1.2] has been used to calculate the oxidation rate according to:

$$\frac{dx_o}{dt} = B/(2x_o + B/C) \quad , \qquad (3)$$

where B and C follow Boltzmann-like temperature dependences. Figures (1) and (2) illustrate the oxide thickness dependence upon time and temperature for both dry O_2 and steam ambients.

During the oxidation, the silicon film thickness is reduced according to:

$$W = W_o - \alpha x_o \quad , \qquad (4)$$

where W_o is the initial film thickness, taken to be 1 μm, and $\alpha = 0.45$ is the ratio of the densities of SiO_2 to silicon. Redistribution data is given for $W_o = 1$ μm and an initial oxide thickness of $x_o = 300$ Å.

c.) Diffusivity model: The diffusivity model for boron was discussed in an earlier report [1.3] and it includes a linear dependence of the diffusivity upon the vacancy concentration as well as the field-enhancement effect. The diffusivity model for phosphorous includes only the field-enhancement effect which is sufficient to describe the non-linear behavior of phosphorous diffusions at concentrations lower than 10^{19} cm^{-3} as shown by Barry [1.4] and Fair and Tsai [1.5]. The diffusivity temperature dependence is after Fair [1.6] and Fair and Tsai [1.5] adaptation of data by Ghostagore [1.6]. For either boron or phosphorous the effective diffusivity is given by:

$$D_{eff} = D(u) \times (1 + u / \sqrt{u^2 + 1}), \qquad (5)$$

where,

$$u = C/2n_i , \qquad (6)$$

and,

$$D(u) = D_B^* u , \text{ for boron,} \qquad (7)$$

$$= D_p^* , \text{ for phosphorus.} \qquad (8)$$

and where n_i is the intrinsic carrier concentration at the diffusion temperature and D_B^* and D_p^* are the intrinsic diffusivities of boron and phosphorus:

$$D_B^* = 3.17 \exp(-3.59\text{eV}/ k_B T)\ \text{cm}^2/\text{sec.},$$

$$D_P^* = 3.85 \exp(-3.66\text{eV}/ k_B T) \qquad (9)$$

B. Further Program Development

The program which was used to generate the data has been described in detail in an earlier report. It was noted that the program was developed in such a way that one could take advantage of a normalization procedure for predeposition diffusions and generate data applicable to different film thicknesses. However, it is not possible to gain such an advantage for redistribution diffusions involving ion-implants or growth of an oxide. Then the program was used to generate data, it was discovered that some other features of the program are extraneous unless further refined.

The program was developed to account for both thin and thick oxides such as would be encountered in some practical situations. However, such a simulation requires the incorporation of a warped grid system, a modification which would require considerably more effort. Therefore, the variable oxide feature is of limited value at this time, since the program, at best, only approximates the conditions for growth of a very thin oxide during redistribution.

A modification was made which allows accurate treatment of redistribution under oxidizing conditions when only a single oxide thickness is involved. The original program treated the oxidation process with regard to the boundary conditions; however, unlike the case of bulk silicon, one must also account for the reduction of

the silicon film thickness. This feature is now included in the program. During the simulation of a redistribution in an oxidizing ambient, the vertical grid spacing continuously shrinks while the horizontal grid spacing is constant. The modification does not show up on logic flow diagrams at the level of detail which has previously been given. For completeness, a new listing of the affected main and sub-programs in given in Appendix C.

C. Computational Procedure

The program described in an earlier report, and modified as described in the preceding, was used to generate the data. Two-dimensional data was obtained in the form of isoconcentration contours for typical situations. The bulk of the data which can be correlated with experimental measurements is generated using a quasi-one-dimensional model in a manner described in a previous report. [1.3] A brief review of the procedure is given in the following.

For generation of sheet resistance, junction depth and integrated impurity dose data as a function of time and temperature, only a one-dimensional profile need be calculated. This is accomplished by making the horizontal grid only three units wide but keeping the field six film thicknesses wide. Periodic boundary conditions for the horizontal dimensions are employed in the program and result in a calculation which produces the vertical profile equivalent to a none-dimensional model. Thus without sacrificing the generality of the program for treating

two-dimensional cases, the amount of computing time is drastically reduced when the data that is desired does not require the full power of the program.

The vertical grid varies from thirty one to sixty one points as required for accuracy in details of the profile, and most of the data is not sensitive to the number of grid points used if the number is chosen in this range. For the purpose of illustrating the unusual nature of phosphorous profiles, the larger number of points was required.

D. Discussion of Results

First, some of the unusual behavior of redistribution diffusions in SOS films will be discussed in this section. Next, the format for the calculated curves will be discussed, and, finally, the bulk of the generated data is given in Appendix A and B without further comment.

Figures (1) and (2) illustrate the oxide thickness growth and silicon film thickness reduction as functions of time for <111> silicon films oxidized in steam and dry O_2 ambients. The evolution traced beginning with an initial oxide of 300 Å thickness on an SOS film of 1 μm initial thickness. The curves are shown for four temperatures. The data are necessary for interpreting some of the results for simulated redistributions.

Figures (3) and (4) show impurity profiles for boron and phosphorus implants being redistributed in a steam ambient at 1000 deg. C. The profiles are all plotted with a common origin as

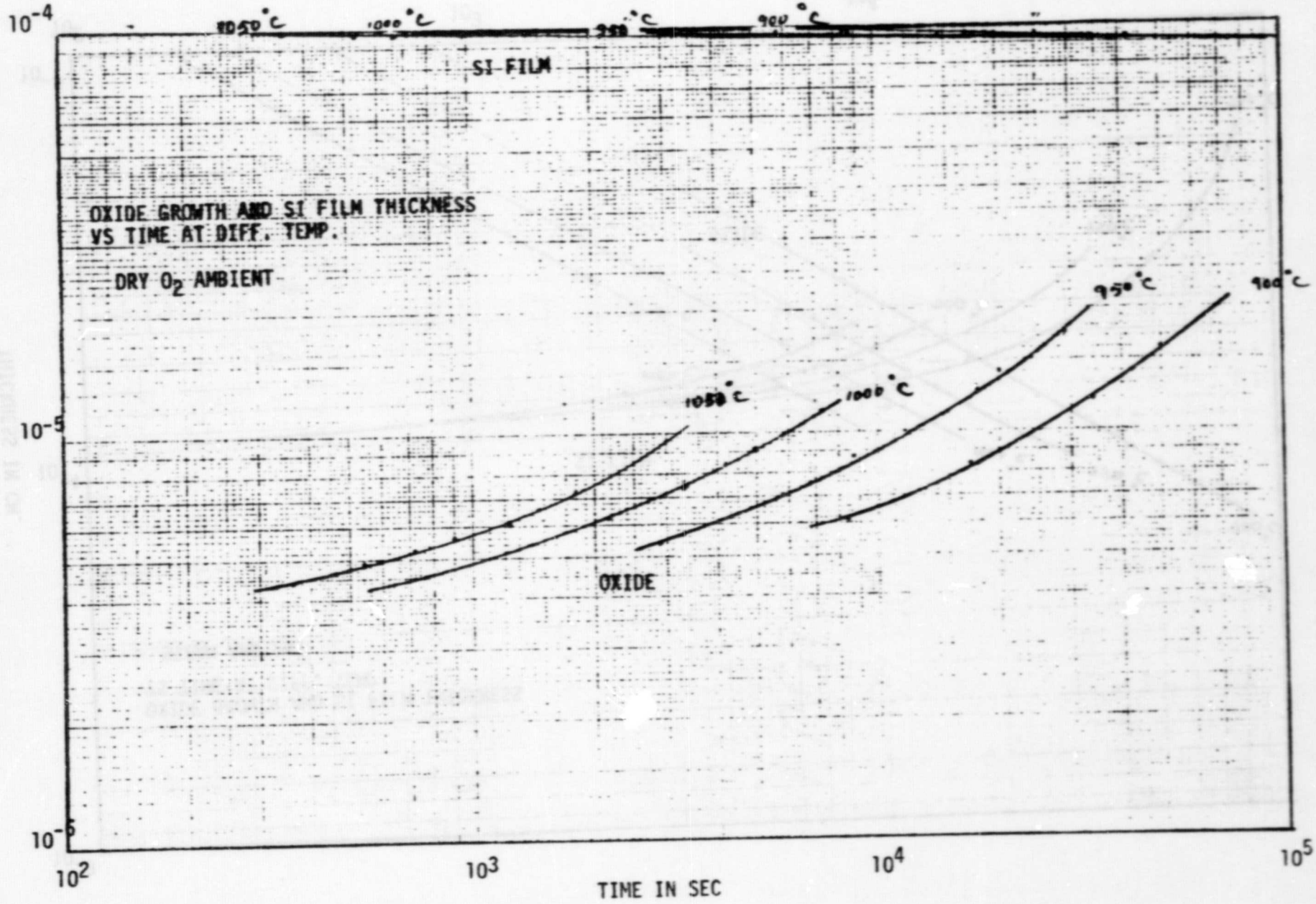

Figure 1.

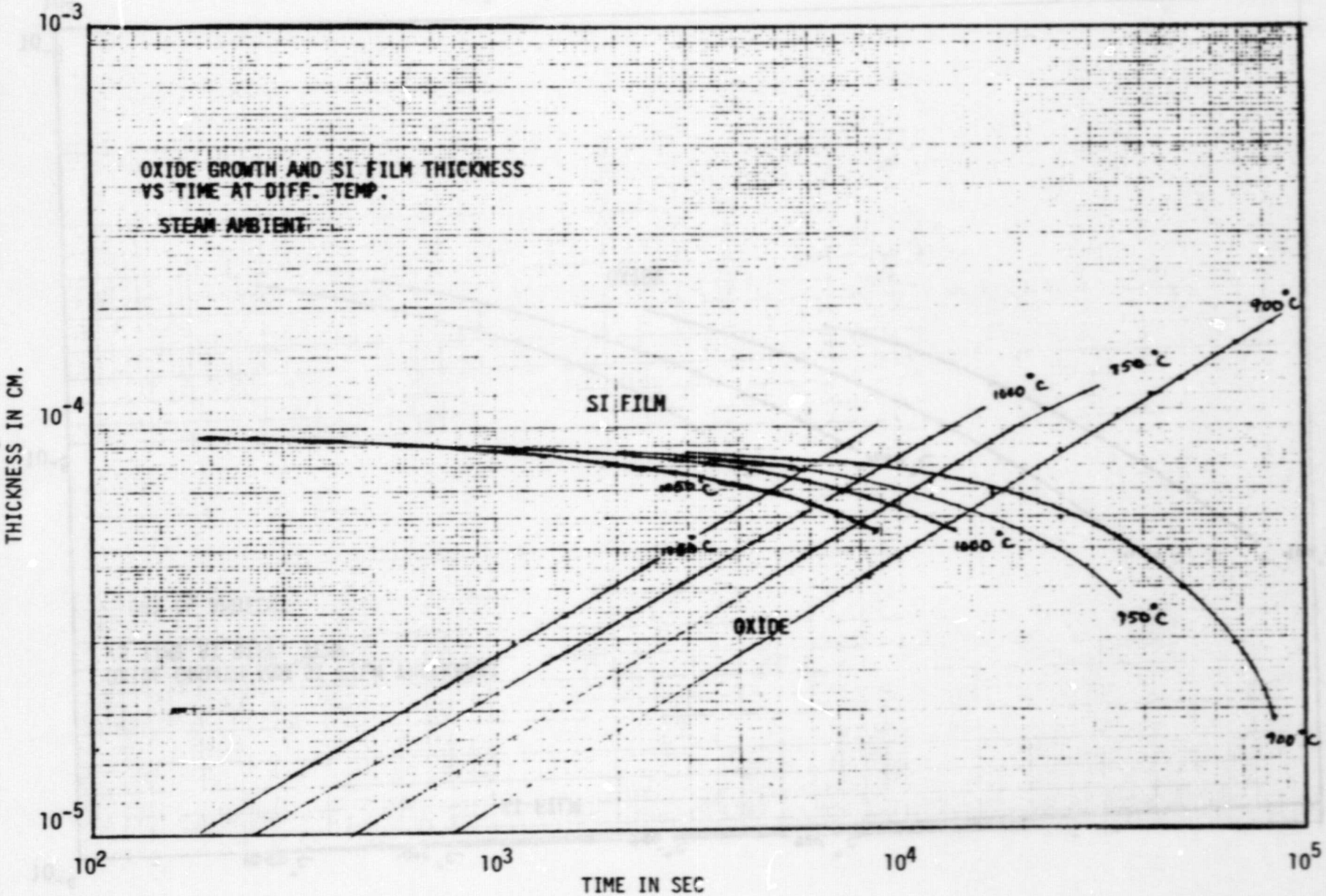
OXIDE GROWTH AND SI FILM THICKNESS
VS TIME AT DIFF. TEMP.
STEAM AMBIENT
SI FILM
OXIDE
900°C
750°C
1000°C
1100°C
1150°C
10^{-3}
10^{-4}
10^{-5}
10^{2}
10^{3}
10^{4}
10^{5}
THICKNESS IN CM.
TIME IN SEC

Figure 2.

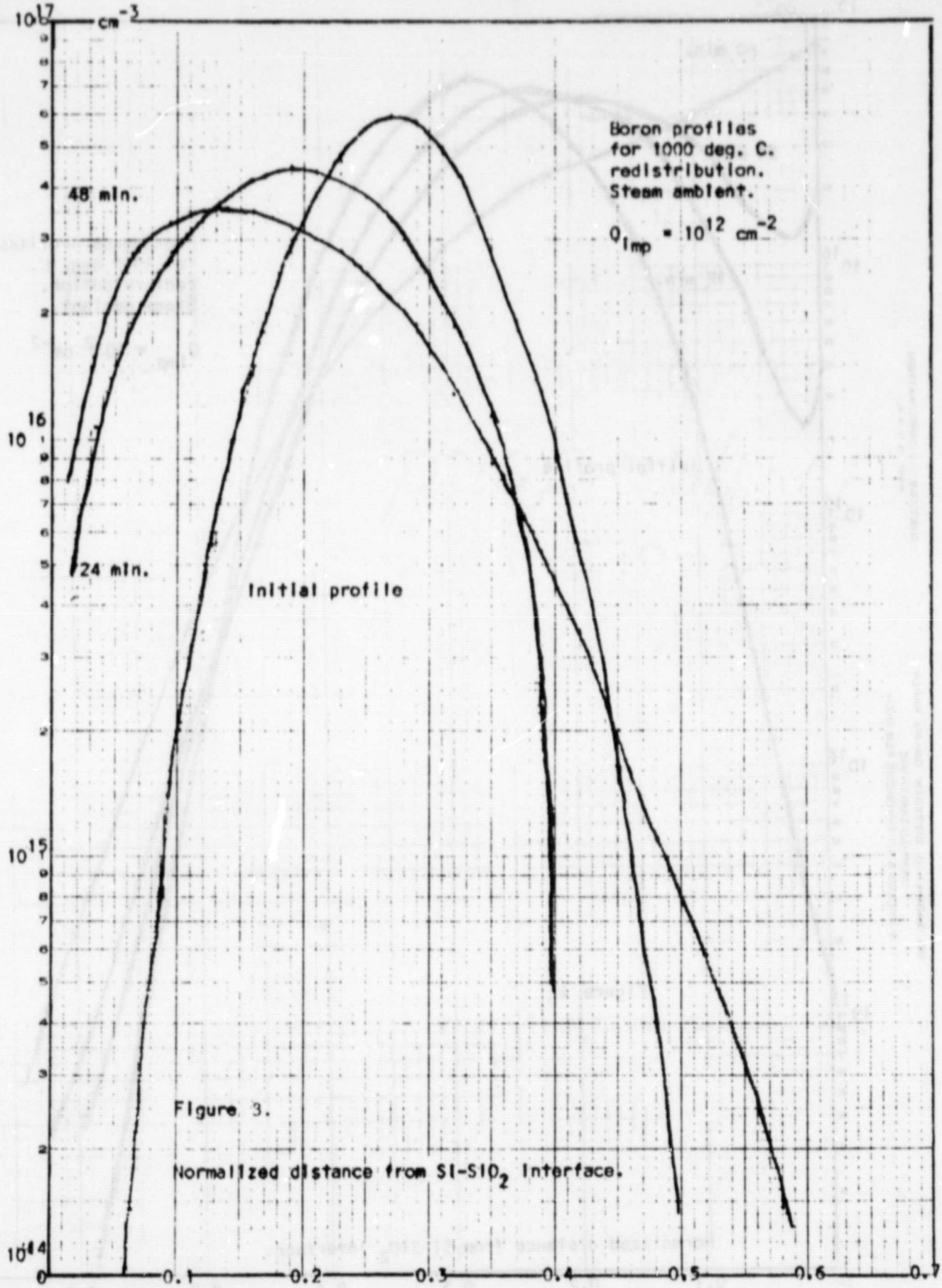
Boron profiles
for 1000 deg. C.
redistribution.
Steam ambient.
$Q_{Imp} = 10^{12}$ cm^{-2}
48 min.
24 min.
Initial profile
10^{17}
cm^{-3}
10^{16}
10^{15}
10^{14}
0.1
0.2
0.3
0.4
0.5
0.6
0.7
Normalized distance from Si-SiO$_2$ Interface.

Figure 3.

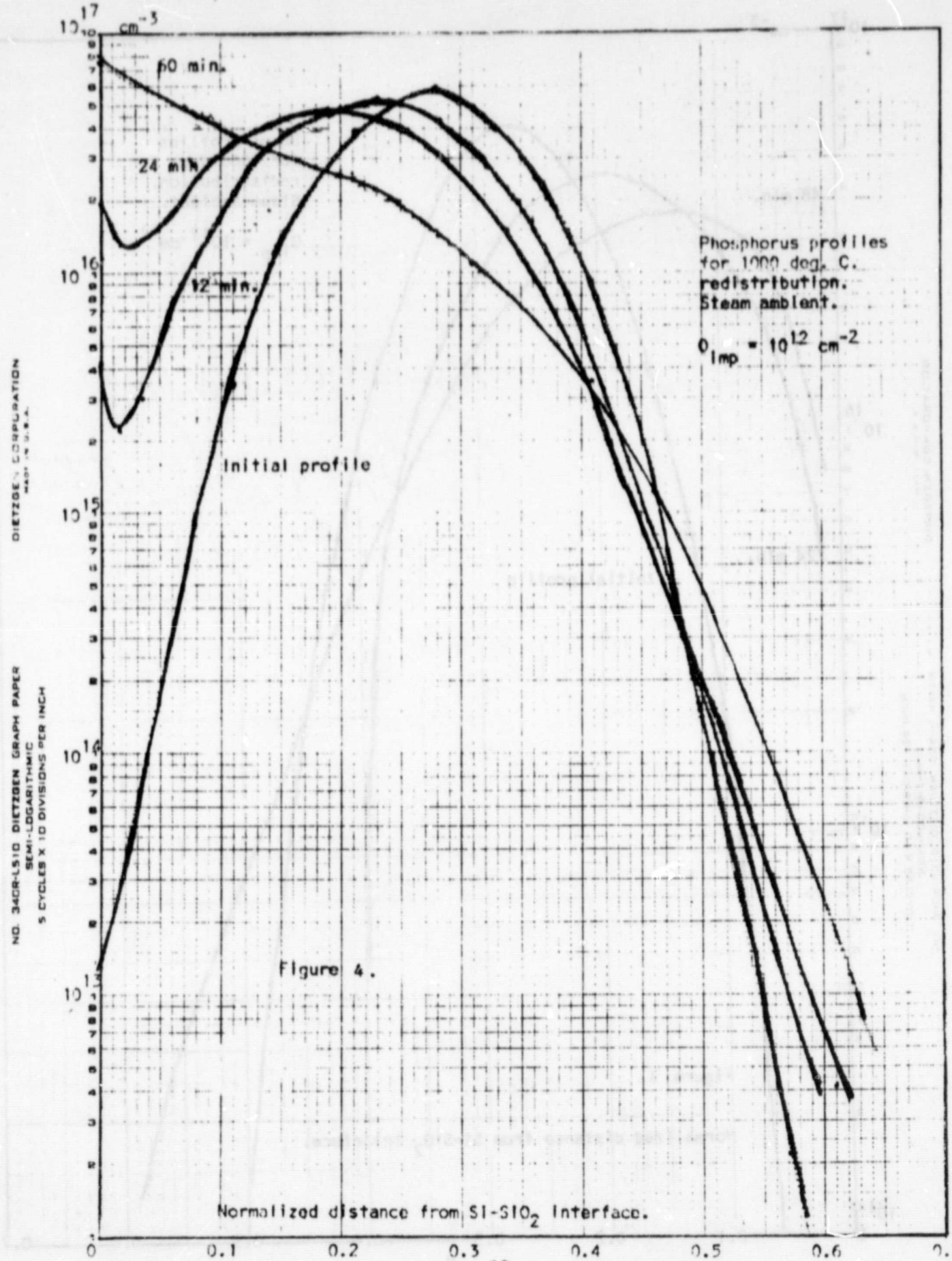

Figure 4.

would be the case for experimentally derived profiles where the Si-SiO_2 interface would serve as the logical origin. However, the profiles are normalized with respect to the film thickness which is of course shrinking. The boron profiles are not unusual but show the wellknown leaching effect due to segregation into the oxide. The phosphorus profiles show the effect of impurities being rejected from the oxide. There is a pile-up of impurities in front of the advancing Si-SiO_2 interface and then a dip which eventually disappears. It is easy for one to draw an erroneous conclusion from observing the profiles, because it appears that the integrated dose should increase or at least remain constant and the sheet resistance should decrease with time. This is not true. Although the segregation coefficient favors phosphorus in silicon vs. SiO_2, eventually all of the phosphorus will be in the SiO_2 when the SOS film is completely oxidized since the model assumes that there is no diffusion into the sapphire.

Figures (5-7) illustrate the behavior of the junction migration, sheet resistance variation, and integrated impurity dose variation over a long period of time. All of the curves are plotted with respect to normalized time, and true time is obtained by multiplying by the normalizing time value given on the plot. Junction depths are in microns, sheet resistance values are in ohms, and dose values are in cm^{-2} units unless otherwise marked. The curves are given in the typical format for all of the data.

For an ion-implanted profile, there are in fact two junctions until one of the junctions emerges at the Si-SiO_2 interface.

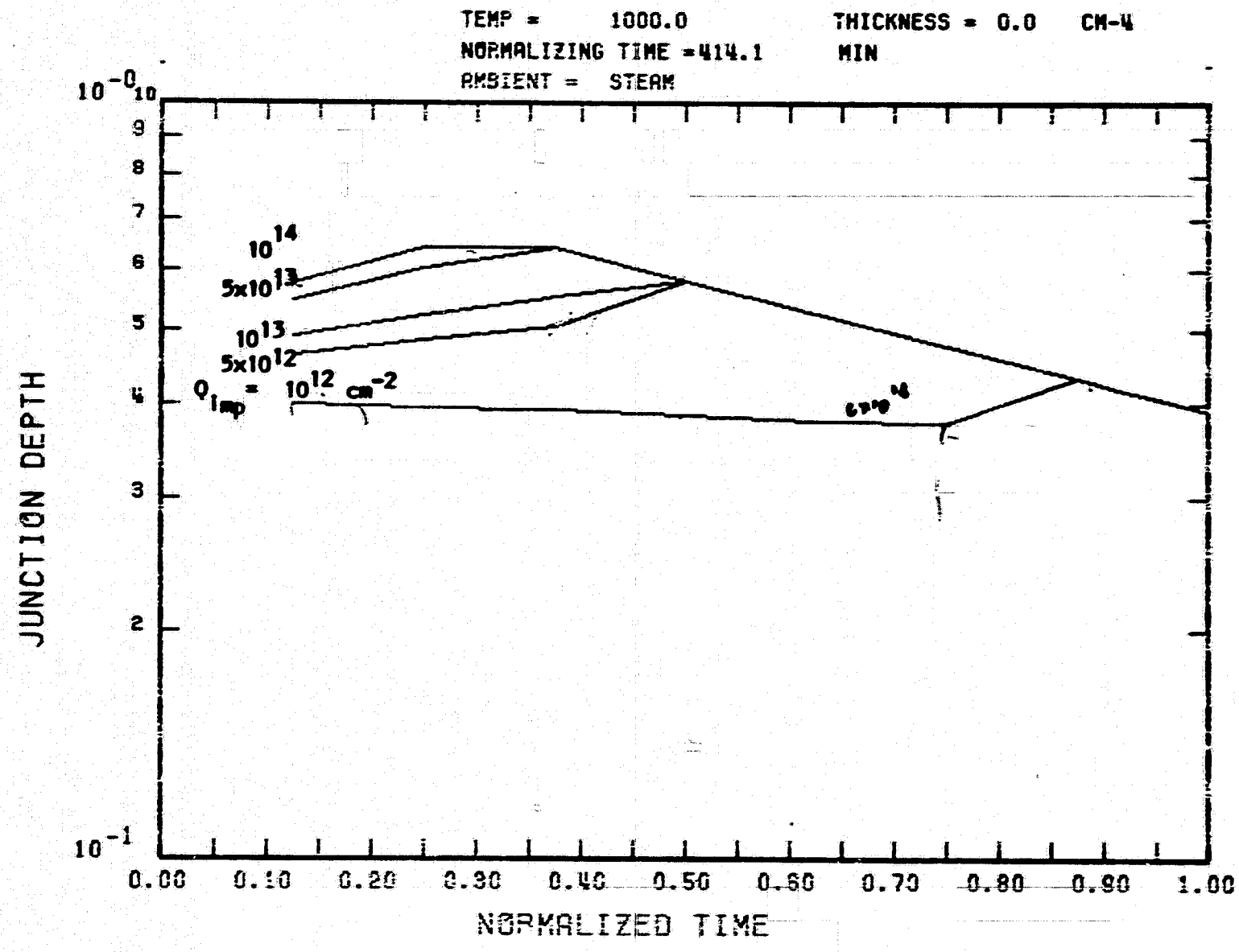

Figure 5. Junction position with respect to Si-SiO_2 Interface for Boron redistribution.

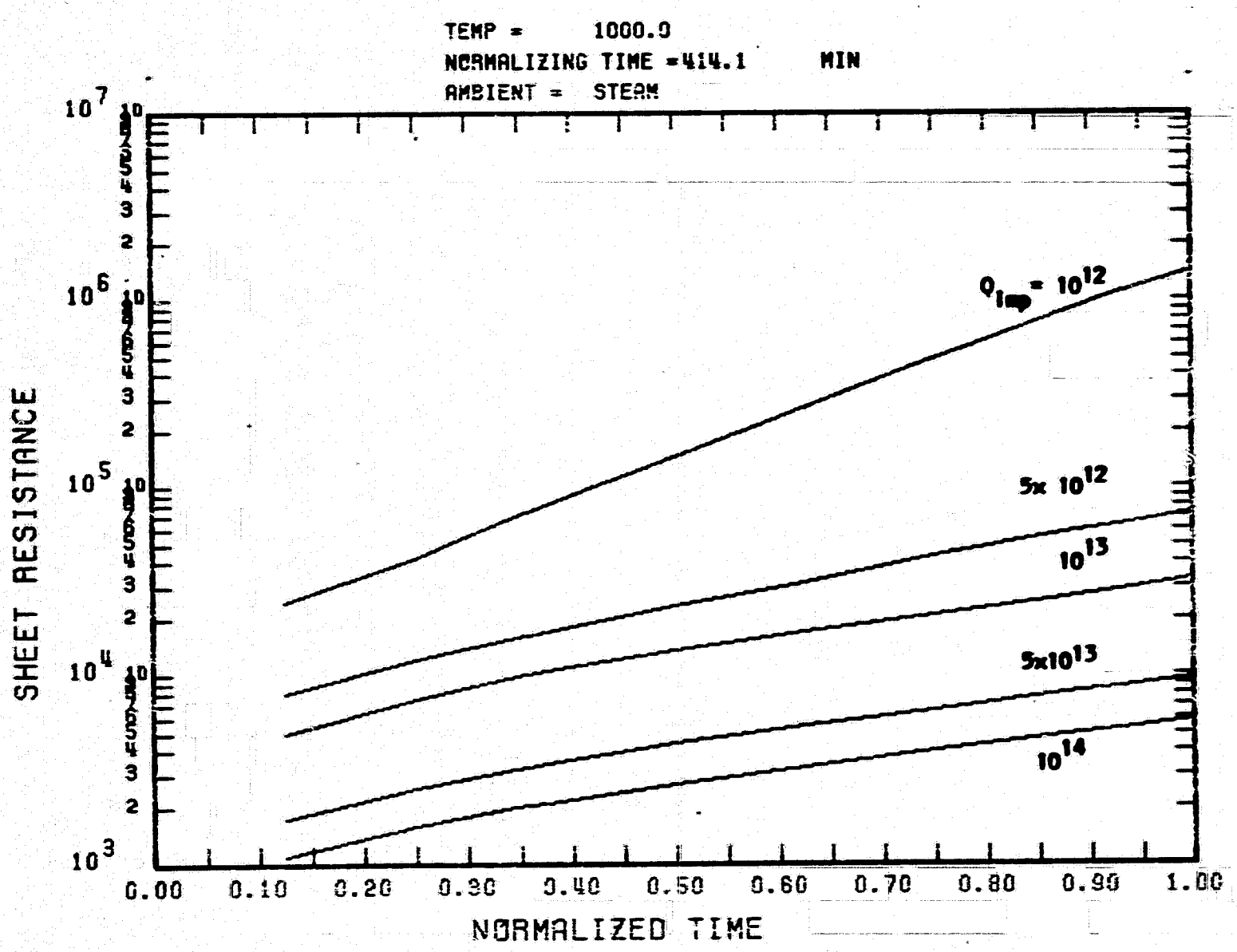

Figure 6. Sheet resistance for Boron redistribution.

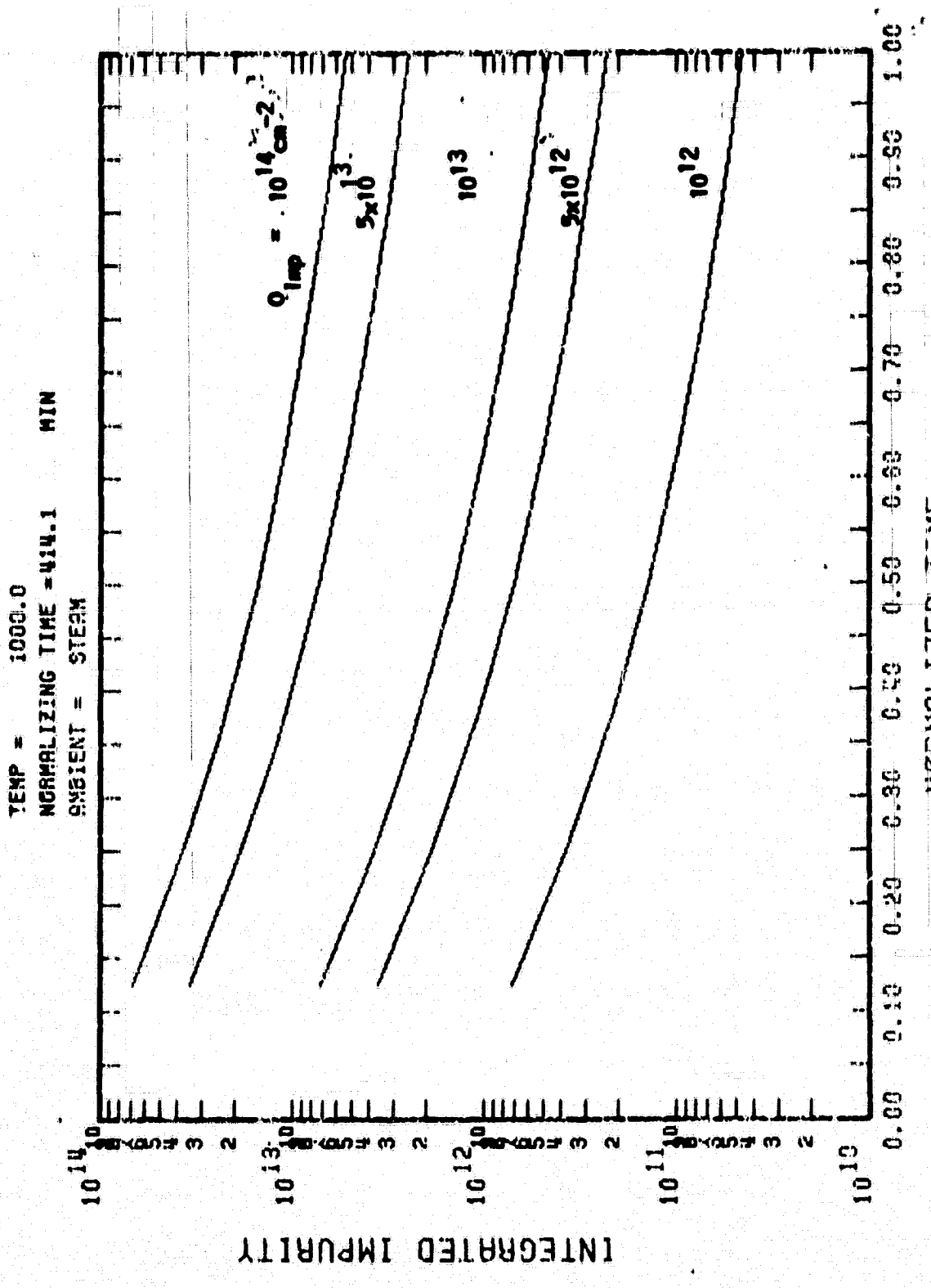

Figure 7. Variation of Dose for Boron redistribution.

Therefore, the sheet resistance values are for the buried layer until the front junction disappears. This typically occurs in a short time compared with that for through-diffusion of the back junction. Figure (5) illustrates the through-diffusion of the back junction for the heavier doses. This always occurs for redistribution in a nitrogen ambient but not necessarily so for an oxidizing ambient. After the through diffusion, or even before for light doses, the junction depth will eventually decrease due to the reduction of the film thickness or due to the relatively slow advancement of the junction with respect to the moving $Si-SiO_2$ interface. In some of the data presented in the appendix, the junction appears to remain almost stationary for this same reason. The variation of the sheet resistance and dose with redistribution time also may appear strange when compared with results for bulk silicon; however, consideration of the previously mentioned factors also explains these results.

Two-dimensional isoconcentration contours are given in the appendix for the various ambients and the two impurity types. The results are not as remarkable as those given in the last report which were for chemically predeposited boron. In that case, there was initially a heavy concentration of fast diffusing impurities at the $Si-SiO_2$ interface which were strongly retarded due to the segregation phenomena. This does not happen with the ion-implanted predeposit because the initial profile lies below the interface at which the segregation phenomena is effective.

II. DOUBLE-LEVEL METALLIZATION TECHNIQUES

A. Long Term Objective

Integrated circuit technologies which incorporate two-levels of metallization into the interconnection scheme are often limited in density and yield because of limitations in the double-layer metal technology itself. With a dual level aluminum and deposited (low temperature) silicon oxide as the base system, the primary objective of this program is to evaluate the basic yield limitations of that system and investigate alternate approaches in order to enhance the yield and/or facilitate improved circuit density. With the pressure of device (or design rule) scaling as an on-going philosophy, high yield for a large number of small vias and small lines becomes extremely important.

B. Fabrication Facilities at Mississippi State University

Most of the facilities work during this contract period was directed toward the development of a sputtering system for preparing aluminum and aluminum-alloy films in support of the double layer metal program. A photograph of the completed system is shown in Figure 8. Briefly, the system consists of the following.

The basic vacuum system is a Varian-NRC 6 inch oil diffusion and mechanical roughing pump equipped for automatic and manual operation. The diffusion pump is equipped for LN_2 cooling of the

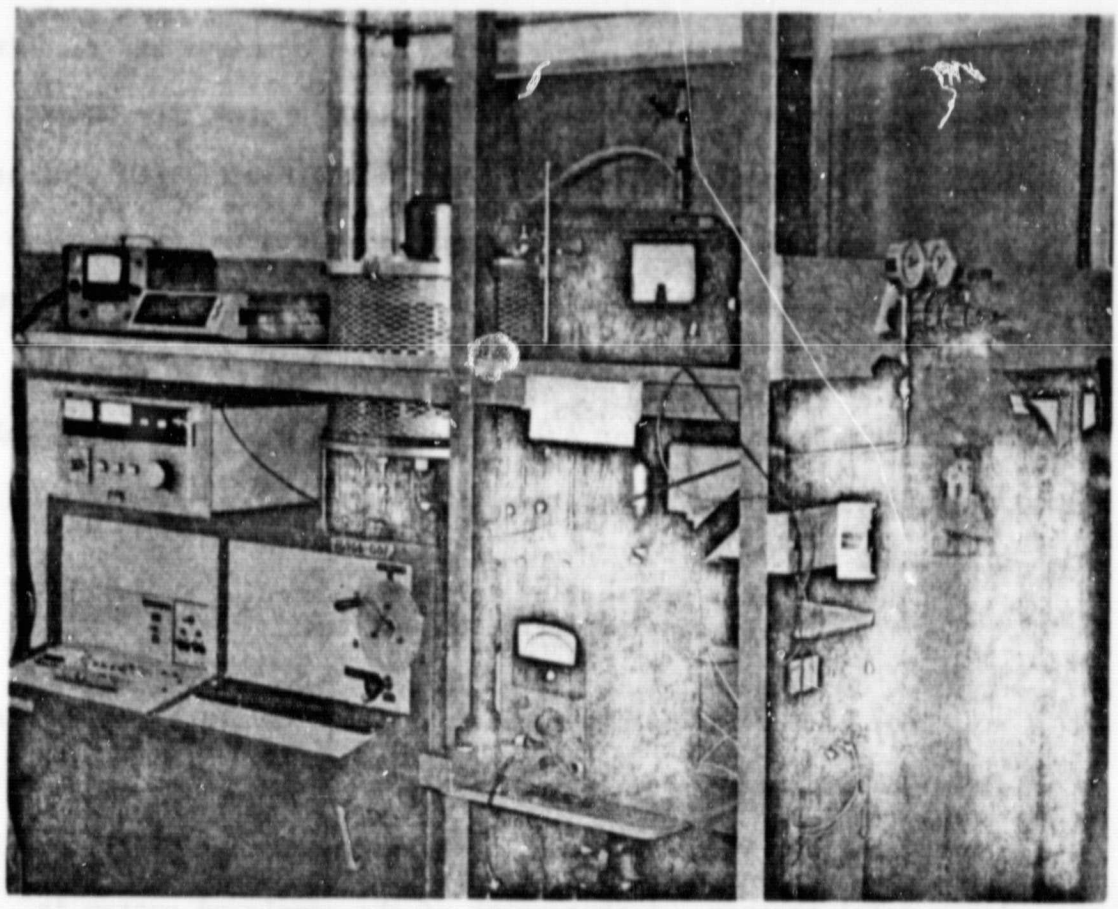

Figure 8. Photograph of metallization system using sputter-gun source.

cold trap. The sputter gun and power supply were obtained from Sloan Technology. The sputtering chamber was designed and built at Mississippi State. It consists of a Corning 12x18 glass cylinder and an aluminum top plate machined to accomodate up to three sputter guns. A cold cathode discharge gauge was constructed and installed in the baseplate of the chamber to measure the pressure during the sputtering operation. A throttle value with several threaded holes for accomodating plugs is operated by one of two mechanical feedthroughs in the baseplate. A lift mechanism with a reversible motor was designed and constructed for raising the top plate and sputter guns.

Inside the chamber is equipped with a rotating table which accomodates up to eight wafers of 1½-2" in diameter. The table is driven by a vacuum sealed shaded pole motor through a magnetic coupling at 7 rpm. The entire motor-table assembly is rotated by a chain-sprocket-mechanical feedthrough arrangement through three sputter-gun and two mask positions. The mask is attached to the rotating assembly and provides one hole through which the sputter-gun deposits metal on the wafers. A crystal film thickness sensor is located beneath the sputter-gun and receives a deposit through a hole at an unused wafer position on the table.

The sputtering chamber opens into a class 100 clean bench in order to maintain a high level of cleanliness. The system is located in the metallizing and bonding room of the microelectronics laboratories in Simrall Engineering Building, and this room was designed with air conditioning and filtering units to maintain a class 10,000 environment.

The installation of a six-tube Thermco Ranger diffusion furnace was completed with the addition of a venting system for exhausting the scavenger boxes.

Complete PMOS circuits have been fabricated in the MSU facilities.

A summary of the microelectronics facility at MSU is provided in Appendix E.

C. Double Layer Metal Experiments

Reviewing the literature has disclosed many investigations relative to the surface oxidation processes of aluminum, including recent reported results by Bell Lab personnel which directly relates to double layer metal processing. These studies show that the aluminum surface is extremely reactive and grows $Al_2O_3 \cdot nH_2O$ films rapidly in water based solutions to thicknesses which cannot be reduced during the sintering operation. Even the growth rate of Al_2O_3 on Al in air at room temperature is reported to be in the range of 30 Å. This compares with the Bell Lab's estimate of 55 Å of Al_2O_3 which can marginally be reduced by sintering.

After careful review of the basic double layer metal process, certain ones stand out as suspect: (1) The via etch using buffered etch, (2) the initial oxidation during vapox deposition, and (3) the photoresist removal.

Consequently, three sets of experiments were initiated:

1) modification of the wet chemistry techniques,

2) dry chemistry processing and/or new insulation materials, e.g., polymide, nitride,

3) the incorporation of in situ back sputtering.

Dramatic improvements in yield were achieved with relatively minor changes in the wet chemistry processing. The effective yield in the number of vias having a total contact resistance of less than 500 ohms has been increased to the 98-99 per cent level for a test pattern having 560 vias of varying sizes by the use of wet chemistry processing techniques and post-heat treatments. Alternations in the process which accounts for these results consists of the following:

1) etching the vias (intermetal contact windows) through C.V.D. - SiO_2 using an ultrasonic etch process in the dark has rendered improved results over that whereby etching was accomplished by dipping the wafer in stirred B.O.E.

2) chemically cleaning the first level metal through the vias with 1:1:1 ethylene glycol: buffered HF:H_2O solution for 20-30 seconds just prior to depositing the second level metal.

3) the use of phosphorus doped vapox to allow for faster via etch times and the ability to perform post heat treatments of temperatures in the 500°C. range without the cracking (crazing) observed with undoped vapox. The use of phosphosilicate glass also tends to give a lower initial contact resistance over that obtained with undoped vapox.

4) the use of post heat treatment (sintering) in the vicinity of 500°C. tends to drastically decrease the total via contact

resistance thereby increasing yield. On wafers exhibiting initial poor yields, sintering can improve this yield by 500-800 percent. On wafers having good yield initially, the contact resistance can be substantially improved. (Average contact resistance of 150 and 200 ohms have been obtained for 560 vias of 0.5 and 0.2 mil square vias, respectively.)

The details of these double layer metal experiments relative to wet chemistry have been reported in a special report, but are included for convenience in Appendix F, "Sintering Effects on Double Layer Metal for VLSI Applications".

The exploratory processing involving dry chemistry required the use of plasma etching and plasma deposition equipment not available at either the Marshall Space Flight Center or Mississippi State University. Consequently, the logistics involved in processing the wafers have been difficult.

Four types of insulators were to be investigated:

1) 5% phosphorus doped silox,
2) plasma nitride,
3) the GAF version of polyimide, and
4) the Hitachi PIQ.

Whenever possible, dry chemistry processing was to be compared with "standard" wet chemistry. The wafers were processed through the first metal mask at Marshall Space Flight Center in standard fashion. The polyimide material was processed at American Microsystems, Inc. (AMI) using the standard recommended procedures by

the manufacturees. The nitride and silox were deposited at AMI using their standard processes, the former on an Applied Materials plasma reactor. The wet chemistry processing was performed at AMI using AMI's standard processing. The plasma etching was performed by Davis and Wilder on one of their production parallel plate plasma system using their proprietary processes.

The wet chemistry split involving silox was lost when the standard "pad" etch attacked the metal completely. The same batch etchant continued to provide good results on AMI material. Since the first layer metal at NASA was deposited via sputtering and with many different impurities, compared with approximately 1% Si:Al deposited with electron beam, the difference in the metal film is believed to be the source of the problem.

The plasma nitride material and silox material, deposited by AMI and plasma etched by Davis & Wilder, was processed without any problems other than long delays. This material plus the polyimide material has finally been received for the final processing here. Although, no electrical results are available at the present, the microscopic examination displays the expected sharper edges of the dry processed material vs. the standard wet chemistry.

In the meantime, the results of the in situ back sputtering experiment were obtained. As was expected, the in situ back sputtering split gave much improved yields over that for the standard material - the detail results being published elsewhere.

The results of these experiments points to the requirement to

very effectively remove the Al_2O_3 prior to the second metalization or minimize its formation during wafer processing to within the order of 30 Å which a good sintering treatment can reduce. The in situ cleaning forgives prior processing which tends to grow the Al_2O_3 such as photoresist removal and buffered HF etching of oxide.

The dry processing has the potential in the future of resolving smaller via sizes and, simultaneously, avoids the harmful H_2O to accelerate the aluminum oxide (and hydrate) formation. Although dry processing to remove the photoresist is routinely done one should expect Al_2O_3 formation due to the presence of active oxygen in the "ashing" process. Some parallel plate reactors can be modified to introduce Ar at low pressure and effectively as in a back sputtering mode. This latter mode could then be used as a clean up step prior to second metal deposition - although not in situ. Undoubtedly, dry processing is going to be extremely important in future double layer metal development work.

III. TWO-DIMENSIONAL MOSFET SIMULATION PROGRAM

A. Long Term Objective

The basic long term objective is to develop a two-dimensional computer program which derives the channel current in steady-state from given values of potentials: source, drain, gate, and substrate. Also given are physical parameters such as gate length, dielectric thickness, doping levels, etc. The substrate doping level should be variable in two dimensions and the substrate potential is independent of the source potential in order to include body-bias effects. The program is intended to model MOSFETs with short channels with particular emphasis on subthreshold and punch-through conduction.

Secondary objective is to utilize techniques in the computer program to minimize computer run time while still maintaining reasonable simulation accuracy.

B. Scope of Work

Review the literature dealing with electrical models for the MOS transistors which takes into account two dimensional effects and investigate their applicability to short channel structures. Identify and demonstrate computer methods suitable for analysis and investigate preliminary problems which need to be solved.

C. Introduction

At the beginning of this project no programs were available which satisfied the specified objectives. There has been considerable work in two-dimensional modelling of JFETs including the works of Kennedy and O'Brien [3.1] and Martin Reiser [3.2]. The MESFET has also received attention in two-dimensional simulation, e.g., Barnes [3.3]. Various modes of MOSFET operation have been simulated or modeled using two-dimensional techniques, e.g. Schroeder and Muller [3.4] (saturation), Barron [3.5] (low level currents), Armstrong e al [3.6] (pinch-off), Kennedy [3.7] (effects of ionizing radiation), Kennedy and Marley [3.8] (saturation), Mock [3.9], Motta [3.10], El-Mansy and Boothroyd [3.11]. Although these works all contribute to the knowledge required in reaching the objective of this task, only the effort by Mock is sufficiently general to meet the objectives--and it is unavailable for public distribution.

The work by Barnes [3.3] described the application of the finite-element method to the analysis of the MESFET.

Further, the finite-element method has been used for some time in solving problems in mechanics and elasticity; however, it has only recently been applied to semiconduction problems. This method has the power to treat some problems, such as eigen-value problems, for which the finite-difference method is awkward if at all applicable. It can also be applied to the solution of field

distributions governed by partial differential equations, and one of the most attractive features as compared to the finite-element method is purported to be the ease of treating non-rectangular geometries and irregular boundaries. For example, the geometry of the VMOS structure could be accomodated. It was decided to further investigate this technique.

The details of this evaluation are included in the appendix. In summary, the evaluation resulted in some skepticism that the finite element method would be sufficiently effective for semiconductor problems to justify the effort. A more recent paper has reinforced this attitude. This paper indicates that the proper formulations of the semiconductor problem for the finite element approach remain to be demonstrated, and, in agreement with out observations, point out that the application of Galerkin's method is subject to skepticism. Therefore, it was concluded that the further work should be based upon the finite-difference method which we have used before although the finite-element method is intriguing and may be further developed in the future.

Key in the development of this task is the proper selection of assumptions. Certain assumptions are required to focus the effort and facilitate convergence expeditiously and, therefore, minimize computer time. On the other hand, too many assumptions lead to loss in utility.

The basic assumptions follow:

1) Recombination/generation is negligible.

2) Hole conduction is negligible.

3) The conventional expression for Poisson's equation is valid [see next section].

4) The mobile majority carriers are included in an infinitesimally thick layer of charge at the $Si-SiO_2$ interface.

5) The current flow in the channel is then described by a one-dimensional equation,

$$J_n = q D \frac{\partial S}{\partial x} + q \mu_n S E_x$$

where

S = density of majority carriers in the channel,

D = majority carrier diffusion constant,

μ = channel carrier mobility, and

E_x = tangential electric field component.

The first three sections are common in the stated literature and restrict the model from covering phenomena associated with breakdown and bulk generated leadage currents. The last assumption is key and separates this work seriously from that of Mock although Kennedy [3.7] used a similar approach for the sake of simplification.

Key also are the normal assumptions which are <u>not</u> made and which are commonly utilized:

1) the gradual channel approximation,

2) constant substrate doping, and

3) zero substrate bias.

Although a constant effective channel mobility is utilized during the initial development of the program, it is not intended to remain a basic assumption.

Assuming step junctions at the source (or drain), the potential in the depletion region and oxide is defined by Poisson's equation with appropriate boundary conditions (Figure 9):

1) fixed potential along the source (or drain) boundary (BCD and IJK),

2) fixed potential deep within the bulk substrate (AL),

3) zero horizontal component of electric field under the source and drain and far from the channel (AB and KL),

4) zero horizontal component of electric field in the oxide far from the channel (EF and KH) and

5) constant potential on the gate electrode (FG).

For convenience the substrate in the basic program is defined as having zero potential. The source, drain, and gate potentials are their respective applied potentials plus their work functions with respect to the substrate, i.e.,

$$\Psi_{source} = V_S + V_{Bi} \ ,$$

$$\Psi_{drain} = V_D + V_{Bi} \ ,$$

$$\Psi_{gate} = V_G + \phi_{ms} \ .$$

For the NMOS example the potential Ψ is always non-negative.

The gate dielectric is assumed to be ideal with infinite resistivity. The charge density in the dielectric is assumed to be zero except for a sheet charge representing the silicon-silicon dioxide interface charge Q_{ss} which is arbitrarily assumed to be 50 Å within the oxide at one grid spacing above the channel grid.

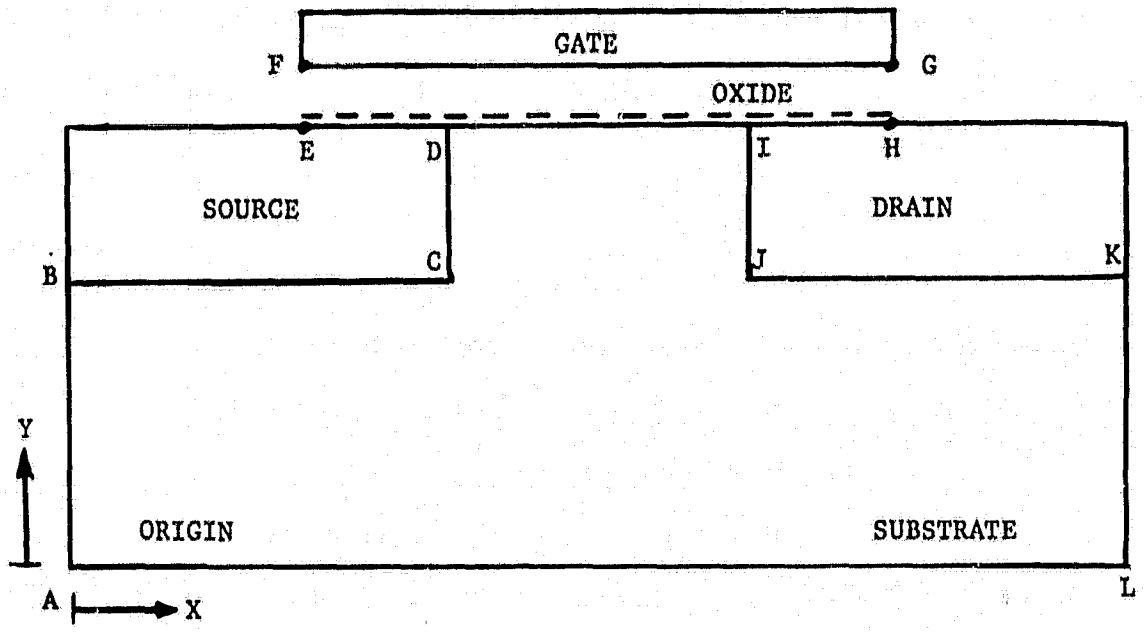

DISTANCES

AB = YDIST - YDIF

CD = JI = YDIF

EF = HG = TOX

BC = JK = XDIF

AL = XDIST

OTHER RELATIONSHIPS

IK5 = IK-5, IL5 = IL +5

JLϕ = JL-1, JK = JK1-1

JMAX1 = JMAX +1

JMAXϕ = JMAX-1

CO-ORDINATES

A = (1,1)

B = (1,JK1)

C = (IK,JKI)

D = (IK,JMAX)

F = (IK5,JL)

G = (IL5,JL)

I = (IL,JMAX)

K = (IMAX,JK1)

L = (IMAX,1)

Figure 9. MOSFET Cross-Section

Key to the simulation of short channel devices is solving the two-dimensional Poisson's equation without making unnecessary approximations. The finite-difference formulation for Poisson's equation is given in the next section. The majority carrier charge is neglected in this formulation except for the sheet charge representation at the oxide interface. The intent is to ignore the charge where it is negligible compared with the ionized doping charge--which is a good assumption everywhere except in the channel.

One can then solve Poisson's equation for the two-dimensional potential distribution more easily and faster than if the coupled majority carrier current equation is included and the majority carrier density variable is included for every mesh node.

After finding the potential distribution one can, after the fact, explicitly solve for the majority carrier densities and current in order to predict punch-thru and subthreshold conduction behavior. This approach is aimed at minimizing computation time while retaining the essential relationships to maintain sufficient accuracy for modeling purposes. One should expect a compromize in accuracy, under certain conditions, when compared with the more general approach of solving the two-dimensional conduction equation.

D. The Poisson Equation, Difference Form

The Poisson equation in different form is

$$\nabla^2\psi = -\rho/\varepsilon \qquad (10)$$

where

Ψ = electrostatic potential,

ρ = charge density, and

ϵ = permittivity of the material.

For acceptor doped material the charge density is

$$\rho = q(p-nN_a) \quad , \quad \text{depletion,} \tag{11}$$

where

q = charge density,

p = hole density,

n = electron density, and

N_a = ionized acceptor density.

The hole density is defined by

$$p = \bar{N}_a \exp(-u) \tag{12}$$

where

u = $q\Psi/kT$, the normalized potential, and

u = 0 in the charge neutral bulk.

Consequently, in the bulk substrate and in the depletion layer where the electron density can be neglected,

$$\rho = - q N_a [1-\exp(-u)] \quad . \tag{13}$$

In the channel region the assumption is made that the electrons exists only in a sheet form of infinitestimal thickness at the silicon dioxide-silicon interface. Since the hole density is insignificant at inversion, the charge density in the channel is

$$\rho_s = -q(N_{aS}+n_S) \quad , \quad \text{channel,} \tag{14}$$

where

N_{aS} is the effective sheet charge due to the ionized acceptors within the grid spacing defined by the interface grid, and n_S is the sheet charge of electrons in the channel.

Near the oxide-silicon interface there are positive interface charges of density N_{SS}, consequently,

$$\rho = q N_{SS} \quad , \quad \text{interface,} \tag{15}$$

with the location being assumed to be 50 Å inside of the oxide. Otherwise in the oxide the charge is assumed neutral.

$$\rho = 0 \quad , \quad \text{oxide,} \tag{16}$$

To solve the Poisson equation numerically, the left hand side can be expanded in difference form as

$$\nabla^2\psi = V_T \nabla^2 U$$

$$= V_T [A U_{i,j-1} + B U_{i-1,j} + C U_{i,j}$$

$$+ D U_{i+1,j} + E U_{i,j+1}] \tag{17}$$

where $V_T = kT/q$,

$$A = 2[h_{j-1}(h_{j-1} + h_j)]^{-1} ,$$

$$B = 2[W_{i-1}(W_{i-1} + W_i)]^{-1} ,$$

$$D = 2[W_i(W_{i-1} + W_i)]^{-1} ,$$

$$E = 2[h_j(h_{j-1} + h_j)]^{-1} \quad , \text{ and}$$

$$C = -(A + B + D + E)$$

with the grid system defined in Figure 10.

Using the charge equation (13) the complete Poisson equation in finite-difference form is written for node (i,j) as

$$A(i,j)U_{i,j-1} + B(i,j)U_{i-1,j} + C(i,j)U_{i,j} + D(i,j)U_{i+1,j}$$

$$+ E(i,j)U_{i,j+1} = \frac{qN_a}{\varepsilon V_T}\,[1-\exp(-U_{i,j})] \qquad (18)$$

The above nonlinear equation can be linearized by defining a function F such that

$$F(U_{i,j-1}, U_{i-1,j}, U_{i,j}, U_{i+1,j}, U_{i,j+1}) = F_{i,j}$$

$$= A_{(i,j)}\,U_{i,j-1} + B_{(i,j)}\,U_{i-1,j} + C(i,j)\,U_{i,j}$$

$$+ D_{(i,j)}\,U_{i+1,j} + E(i,j)\,U_{i,j+1}$$

$$- (qN_a/\varepsilon V_T)\,[1-\exp\,(-U_{i,j})] = 0 \qquad (19)$$

Defining a set of reference value of U's and F such that

$U^r_{i,j-1}$, $U^r_{i-1,j}$, $U^r_{i,j}$, etc. and $F^r_{i,j}$, one can expand F around the reference potentials:

$$F^{r+1}_{i,j} = F^r_{i,j} + \left.\frac{\partial F}{\partial U_{i,j-1}}\right|^r \Delta U_{i,j-1} + \left.\frac{\partial F}{\partial U_{i-1,j}}\right|^r \Delta U_{i-1,j} \qquad (20)$$

$$+ \left.\frac{\partial F}{\partial U_{i,j}}\right|^r \Delta U_{i,j} + \left.\frac{\partial F}{\partial U_{i+1,j}}\right|^r \Delta U_{i+1,j} + \left.\frac{\partial F}{\partial U_{i,j+1}}\right|^r \Delta U_{i,j+1}$$

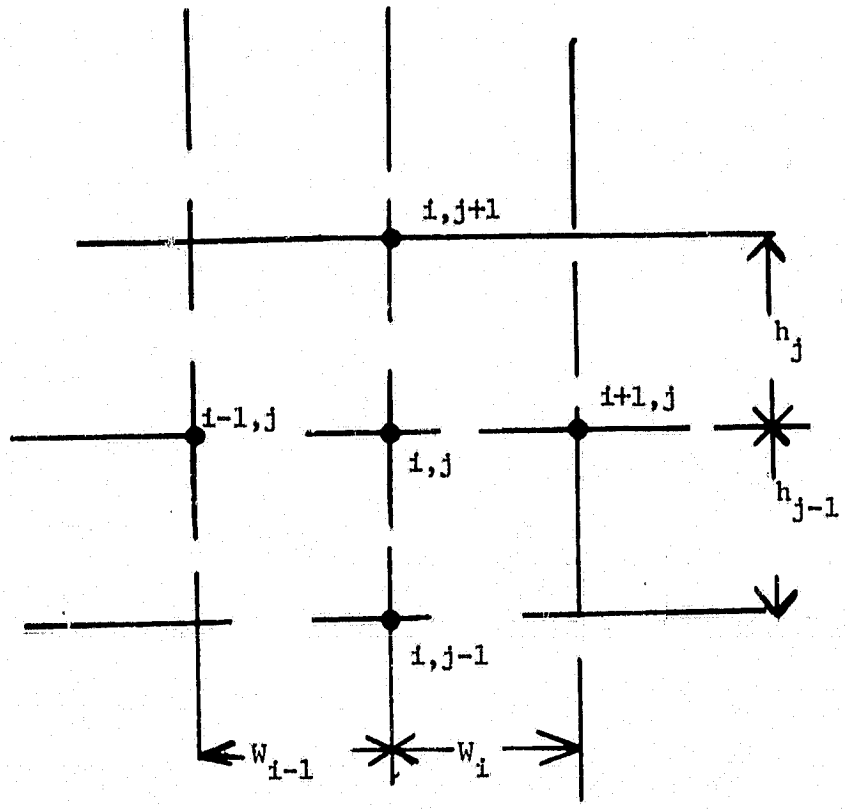

Figure 10. Grid system definition

where

$$\Delta U^{r}_{i,j-1} = U^{r+1}_{i,j-1} - U^{r}_{i,j-1} \quad , \quad \text{etc.}$$

The above expressions defines a system of equations in ΔU as

$$F^{r}_{i,j} = \overline{A}(i,j)\,\Delta U_{i,j-1} + \overline{B}(i,j)\,\Delta U_{i-1,j} + \overline{C}(i,j)\,\Delta U_{i,j} \qquad (21)$$

$$+ \overline{D}(i,j)\,\Delta U_{i+1,j} + \overline{E}(i,j)\,\Delta U_{i,j+1} + F^{r}_{i,j}$$

where

$$\overline{A} = A,\ \overline{B} = B,\ \overline{D} = D,\ \overline{E} = E, \quad \text{and}$$

$$\overline{C} = C - (qNa/kT)\exp\,(-U^{r}_{i,j})$$

with A through E being defined in equation (17). The function F is theoretically zero; therefore, by setting $F^{r+1}_{i,j} = 0$, a system of linear equations in ΔU is obtained. For the node i,j

$$\overline{A}\,\Delta U_{i,j-1} + \overline{B}\,\Delta U_{i-1,j} + \overline{C}\,\Delta U_{i,j} \qquad (22)$$

$$+ \overline{D}\,\Delta U_{i+1,j} + \overline{E}\,\Delta U_{i,j+1} = - F^{r}_{i,j}$$

where $F^{r}_{i,j}$ is defined in equation (19).

By applying the method of lines, the linearized equations are resolved into a tridiagonal matrix form as

$$\overline{A}\,\Delta U_{i,j-1} + \overline{C}\,\Delta U_{i,j} + \overline{E}\,\Delta U_{i,j+1} \qquad (23)$$

$$= - F^{r}_{i,j} - \overline{B}\Delta\tilde{U}_{i-1,j} - \overline{D}\Delta\tilde{U}_{i+1,j}$$

where $\Delta\tilde{U}$ are taken as the most recent updated values of ΔU each iteration, but still keeping the U's fixed until convergence

is achieved. The above equation (23) retains the old values of ΔU along the x-axis and calculates the new values of ΔU along the y-axis. Obviously, equation (23) can be written for the inverse case. By alternating between the vertical and horizontal forms of the tridiagonal matrix, the convergence can be expedited.

Special consideration must be given to Poisson's equation at the silicon-silicon dioxide interface. Figure (11A) illustrates the channel sheet charge S in charge per unit area, the acceptor charge N_a in charge per unit volume, and the discontinuity in permittivity. Applying Gauss's law in one dimension with two surfaces at the midway points between C & C + 1 and C - 1 & C leads to the expression

$$\varepsilon_{ox}E_{1/2} - \varepsilon_{Si}E_{-1/2} = \text{positive charge enclosed} \qquad (24)$$

$$= - q(S + \frac{N_a h_{c-1}}{2})$$

Multiplying through by $\frac{2}{V_T(h_c+h_{c-1})\varepsilon_{Si}}$ leads to

$$\frac{2}{h_c+h_{c-1}}\left[\frac{\varepsilon_{ox}}{\varepsilon_{Si}}\ \frac{(U_{c+1}-U_c)}{h_c} + \frac{U_{c-1}-U_c}{h_{c-1}}\right] = \frac{Zq}{\varepsilon_{Si}V_T}\ \frac{S+\frac{N_a h_{c-1}}{2})}{h_c + h_{c-1}} \qquad (25)$$

which is the one dimension form of Poisson's Law

$$\frac{d^2}{dy^2}\left(\frac{\varepsilon U}{\varepsilon_{Si}}\right) = - \frac{\rho eff}{\varepsilon_{Si}} \qquad (26)$$

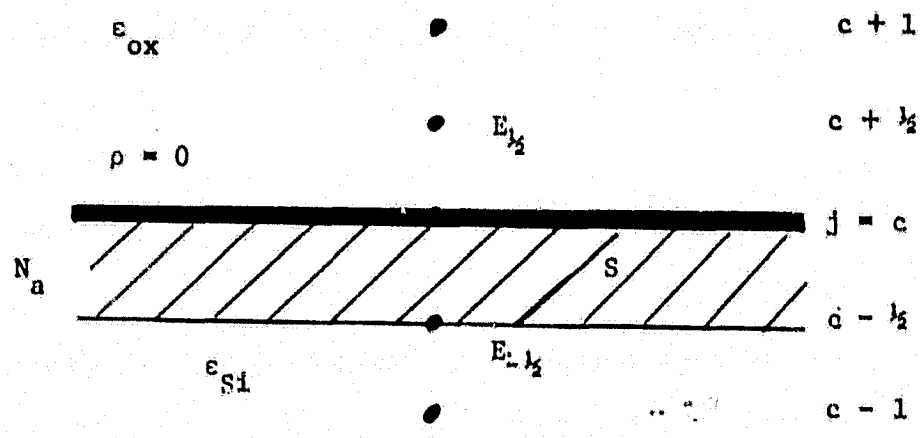

Figure 11A. Gauss's law at the silicon-silicon dioxide interface

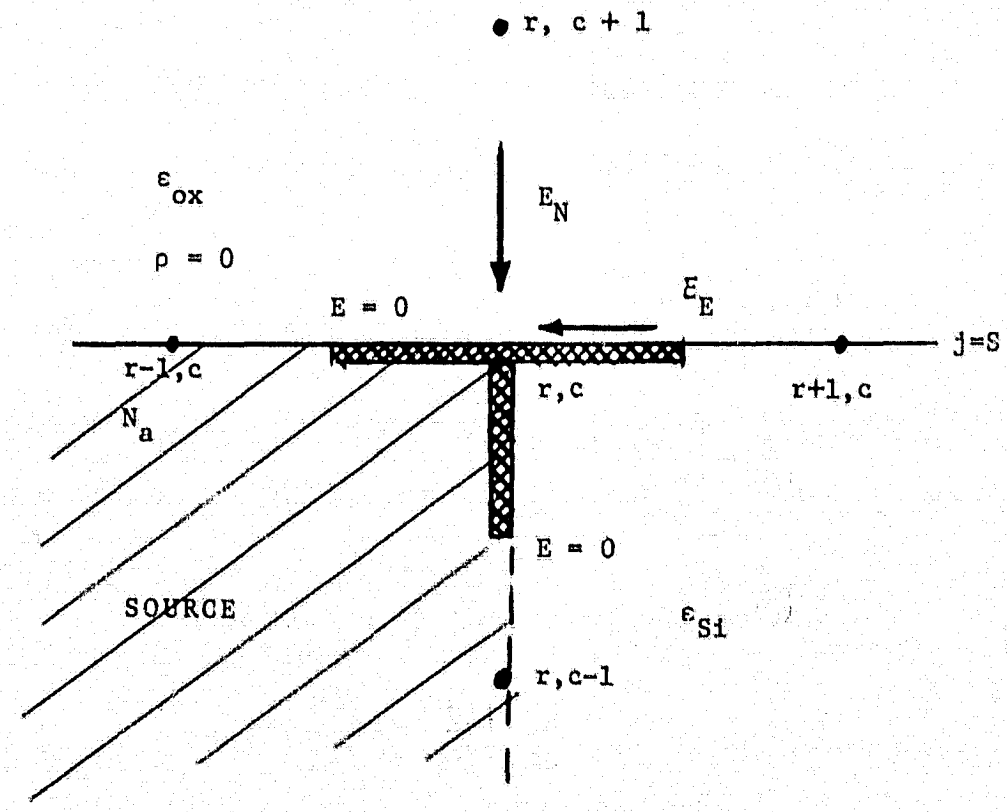

Figure 11. Gauss's law at the source corner

with

$$\rho_{eff} = - \frac{2q(S + N_a h_{c-1}/2)}{V_T (h_c + h_{c-1})}$$

Therefore, the finite difference form of the equation is obtained by modifying the following terms in equation (18):

$$E = 2 \left(\frac{\varepsilon_{ox}}{\varepsilon_{Si}} \right) [h_c (h_{c-1} + h_c)]^{-1} \quad , \tag{27}$$

$$C = -(A + B + D + E) \quad , \quad \text{and}$$

$$\frac{\rho_{eff}}{\varepsilon_{Si}} = \frac{2q}{V_T \varepsilon_{Si}} \frac{(S + N_a h_{c-1}/2)}{(h_c + h_{c-1})}$$

[Note: $y = J_{max}$ for the channel node in the program.]

Similarly the linearized version is modified by

$$\overline{E}_i = E_i, \ \overline{C}_i = C_i, \quad \text{and} \tag{28}$$

$$F^r_{i,c} = A_i U_{i,c-1} + B_i U_{i-1,c} + C_i U_{i,c}$$

$$+ D_i U_{i+1,c} + E_i U_{i,c+1} + \rho_{eff}{}^{i}/\varepsilon_{Si}$$

where the subscript i has been inserted to denote the coefficients for mesh node (i,c).

In the region of Si - SiO_2 interface where the Q_{SS} charges are assumed to exists, one mesh node is assumed inside the oxide, the coefficients are

$$\overline{A} = A, \ \overline{B} = B, \ \overline{C} = C, \ \overline{D} = D, \ \overline{E} = E, \quad \text{and}$$

$$F^r = Au_{i,c} + BU_{i-1,c+1} + CU_{i,c+1} + DU_{i+1,c+1} + EU_{i,c+2}$$

$$+ \frac{2Q_{SS}}{\epsilon_{ox} V_T} [h_c + h_{c+1}]^{-1} \qquad (29)$$

Similarly, in the oxide where $\rho = 0$, the coefficients are

$$\overline{A} = A,\ \overline{B} = B,\ \overline{C} = C,\ \overline{D} = D,\ \overline{E} = E, \quad \text{and} \qquad (30)$$

$$F^r = AU_{i,j-1} + BU_{i-1,j} + CU_{i,j} + DU_{i+1,j} + EU_{i,j+1}$$

E. The Channel Conduction Equation, Difference Form

As noted previously, a significant assumption utilized to facilitate convergence, is that the channel charge is modeled as a sheet charge at the silicon-silicon dioxide interface. The channel current is assumed to obey the single dimensional form of the conventional three dimensional equation, i.e.,

$$J_n = q D_n \frac{\partial S}{\partial x} + q \mu_n S E_x \qquad (31)$$

where S = density of electrons in channel (#per unit area),

D_n = electron diffusion constant,

μ_n = electron mobility, normally field dependent, and

E_x = tangential electric field component.

The above equation can be written in normalized form utilizing

$E_x = V_T \frac{\partial U}{\partial x}$ and $D_n = V_T \mu_n$ (Einstein's relationship):

$$J_n = q V_T \mu_n \left(\frac{\partial S}{\partial x} - S \frac{\partial U}{\partial x}\right) \qquad (32)$$

Then $$f_s = (S' - U'S)\mu_n \qquad (33)$$

where $f_s = J_n (q V_T)^{-1}$, $S' = \frac{\partial S}{\partial x}$, and $U' = \frac{\partial U}{\partial x}$.

At any point x in the channel the general solution of S is

$$S(x) = \exp \int_{x_{i-1}}^{x} U' dx \left\{ \int_{x_{i-1}}^{x} \left(\frac{f_s}{\mu_n} \exp \int_{x_{i-1}}^{x} U' dx \right) dx + C \right\} \qquad (34)$$

which reduces to the specific solution for S(x), given

S at $x = x_{i-1}$:

$$S(x)e^{-U} = S_{i-1} e^{-U_{i-1}} + \frac{J_n}{q V_T} \int_{x_{i-1}}^{x} \frac{e^{-u(\xi)}}{\mu(\xi)} d\xi \qquad (35)$$

Rewriting the above leads to S_i in terms of S_{i-1} :

$$\frac{S_i \exp(-U_i) - S_{i-1} \exp(-U_{i-1})}{\int_{x_{i-1}}^{x_i} \frac{\exp\left[-U(\xi)\right] d\xi}{\mu(\xi)}} = \frac{J_n}{q V_T} \qquad (36)$$

Similarly, integrating between x_i and x_{i+1} leads to

$$\frac{S_{i+1} \exp -(U_{i+1}) - S_i \exp -(U_i)}{\int_{x_i}^{x_{i+1}} \frac{\exp - U(\xi)\, d\xi}{\mu(\xi)}} = \frac{J_n}{q V_T} \qquad (37)$$

Assuming current continuity, i.e., J_n = constant, leads to

$$- \left\{ \exp - (U_{i-1}) \int_{x_i}^{x_{i+1}} \frac{\exp -U(\xi)}{\mu(\xi)} \, d\xi \right\} S_{i-1} \qquad (38)$$

$$+ \left\{ \exp - U_i \int_{x_{i-1}}^{x_{i+1}} \frac{\exp (U(\xi))}{\mu(\xi)} \, d\xi \right\} S_i$$

$$- \left\{ \exp -U_{i+1} \int_{x_{i-1}}^{x_i} \frac{\exp(-U(\xi))}{\mu(\xi)} \, d\xi \right\} S_{i+1} = 0 \, .$$

The above equation is of the form

$$a_i S_{i-1} + b_i S_i + c_i S_{i+1} = 0$$

and define a tridiagonal linear system of equations.

Equation 36 should reduce to a familiar form as $x_i - x_{i-1} = \Delta x \to 0$. Let $S_{i-1} = S_o$, $S_i = S_o + \Delta S$, $U_{i-1} = U_o$, $U_i = U_o + \Delta U$. Then 36 becomes

$$\frac{(S_o + \Delta S) e^{-U_o} (1 - \Delta U) - S_o e^{-U_o}}{\mu^{-1} e^{-U_o} \Delta x} = \frac{J_n}{q V_T} \qquad (39)$$

which reduces to

$$J_n = q V_T \mu \left\{ \frac{\Delta S}{\Delta x} - S_o \frac{\Delta U}{\Delta x} \right\} \qquad (40)$$

which displays the familiar diffusion and drift terms in the limit. The integral form in (36) has the potential of being more accurate with larger grid spacing.

Another observation one may note is that the coefficients a_i, b_i, c_i may be scaled, or normalized, to values less dependent

on the exponential of potential by multiplying them by $\exp(2U_i)$ which gives

$$a_i = -\exp(U_i - U_{i-1}) \int_{x_i}^{x_{i+1}} \mu(\xi) \exp[U_i - U(\xi)]\, d\xi ,$$

$$b_i = \int_{x_{i-1}}^{x_{i+1}} \mu^{-1}(\xi) \exp\,[U_i - U(\xi)]\; d\xi , \quad \text{and}$$

$$c_i = \exp(U_i - U_{i+1}) \int_{x_{i-1}}^{x_i} \mu^{-1}(\xi) \exp\,[U_i - U(\xi)]\; d\xi \; . \qquad (41)$$

And, of course, if the mobility is assumed constant, then it can be removed by multiplying through by μ .

Noting that the integrand varies exponentially with potential whereas the potential is expected to vary with x no worse than the third power, one can approximate the integral by assuming

$$U - U_o = a(x - x_o) \qquad (42)$$

and evaluate the slope $a = \frac{dU}{dx}$ at the lowest value of potential over the range of integration. In this manner the neglected higher order terms contribute very little error since the integrand falls off exponentially with potential. Changing variables for the integration of b_i , as an example, leads to

$$b_i = \int_{U_{i-1}}^{U_{i+1}} \frac{\mu^{-1}(U)}{a} \exp[U_i - U]\; dU \qquad (43)$$

where $a = \frac{dU}{dx}$. Further,

$$b_i = [a\mu]^{-1} \{\exp(U_i - U_{i-1}) - \exp(U_i - U_{i+1})\} \qquad (44)$$

with a and μ evaluated at the lowest value of U which for $a > 0$ is U_{i-1}. Similarly,

$$a_i = [a\mu]_i^{-1}[\exp(U_i - U_{i+1}) - 1] \exp(U_i - U_{i-1})$$

$$c_i = [a\mu]_{i-1}^{-1}[1 - \exp(U_i - U_{i-1})] \exp(U_i - U_{i+1})$$

$$b_i = [a\mu]_{i-1}^{-1}[\exp(U_i - U_{i-1}) - \exp(U_i - U_{i-1})] \qquad (45)$$

where the subscript on $[a\mu]$ denotes the node for evaluating a and μ, assuming $a > 0$..

The boundary conditions for this system of equations association with electron conduction in the channel must be defined in terms of the source and drain corner mesh nodes for the MOSFET operation in the active region. Figure 11 illustrates the application of Gauss's Law at the source corner of the channel. Mesh nodes along the boundary of the source are common poential, therefore, the tangential electric field terms along the boundary of the source are zero. Since the electric field along the channel E_E for operations of interest - at least at this source corner, the surface charge is modelled in a single dimensional manner, i.e.,

$$\varepsilon_{ox} E_N = -qS \qquad (46)$$

or, in terms of potential,

$$\frac{V_T \varepsilon_{ox}(U_{r,c+1} - U_{r,c})}{h_c} = qS \qquad (47)$$

An alternate scheme involves the solution of the one dimensional Poisson equation:

$$-\frac{\varepsilon_{ox}}{t_{ox}}\left\{(V_G - \phi_{ms}) - (V_C + V_{Bi})\right\} = Q_{ss} - qS + Q_B \qquad (48)$$

where V_G = the applied bias to the gate

ϕ_{ms} = the gate work function relative to the substrate,

V_C = the applied channel potential,

V_{Bi} = the work function of the drain/source,

t_{ox} = oxide thickness,

ε_{ox} = oxide permitivity,

Q_{SS} = silicon dioxide-silicon interface charge,

q = electronic charge, and

Q_B = the bulk charge density (per unit area)

= 0 for drain and source.

The Q_B expression can be defined in terms of the vertical electric field in the channel region:

$$Q_B = \varepsilon V_T \frac{(U_{c-1} - U_c)}{h_{c-1}} - q\,Na\,\frac{h_{c-1}}{2}$$

where the subscript c refers to the channel node.

F. Channel Coupled Equations

Although the channel conduction equation (38) is linear in S, it is nonlinear in potential. The simultaneous solution of the conduction equation and the Poisson equation along the channel

requires linearizing (38).

Let $F^r_{ci} = a_i S_{i-1} + b_i S_i + c_i S_{i+1}$ where a_i, b_i, c_i are defined in (45). Since the terms $[a\mu]^{-1}$ vary more slowly than the exponential terms, the term is assumed constant for any particular iteration, using the last known values of u's for its evaluation. Then, the linearized conduction equation becomes

$$A_{ci} = \frac{\partial F^r_{ci}}{\partial U_{i-1}} = - a_i S_{i-1} - [a\mu]^{-1}_{i-1} S_i \exp(U_i - U_{i-1})$$

$$+ c_i S_{i+1} \exp(U_i - U_{i-1}) [1 - \exp(U_i - U_{i-1})]^{-1} ,$$

$$B_{ci} = a_i ,$$

$$C_{ci} = \frac{\partial F^r_{ci}}{\partial U_i} = - a_i S_{i-1} [\exp(U_i - U_{i+1}) - 1]^{-1} + b_i S_i$$

$$+ c_i S_{i+1} [1 - \exp(U_i - U_{i-1})]^{-1} [1 - 2 \exp(U_i - U_{i-1})],$$

$$D_{ci} = b_i ,$$

$$E_{ci} = \frac{\partial F^r_{ci}}{\partial U_{i+1}} = -a_i S_{i-1} \exp(U_i - U_{i+1}) [\exp(U_i - U_{i-1}) - 1]^{-1}$$

$$+ b_i S_i \exp(U_i - U_{i+1}) [\exp(U_i - U_{i-1}) - \exp(U_i - U_{i+1})]^{-1}$$

$$- c_i S_{i+1} ,$$

$$G_{ci} = c_i , \text{ and}$$

$$F^{r+1}_{ci} = F^r_{ci} + A_{ci} \Delta U_{i-1} + B_{ci} \Delta S_{i-1} + C_{ci} \Delta U_i + D_{ci} \Delta S_i \quad (49)$$

$$+ E_{ci} \Delta U_{i+1} + G_{ci} \Delta U_{i+1} = 0 .$$

The Poisson equation has been previously derived, equations (27) and (28), with the coefficients being defined below for the new system of equations:

$$\overline{B}_i \Delta U_{i-1,c} + \overline{C}_i \Delta U_{ic} + \overline{H}_i \Delta S_i + D_i \Delta U_{i+1,c}$$

$$= -\overline{A}_i \Delta U_{i,c-1} - \overline{E}_i \Delta U_{i,c+1} - F^r_{i,c} = T^r_{ic} \qquad (50)$$

where

$$\overline{H}_i = -2q[\varepsilon_{si} V_T (h_{i,c} + h_{i,c-1})]^{-1} ,$$

$$\overline{A}_i = A_i \quad \text{from (17)} ,$$

$$\overline{B}_i = B_i \quad \text{from (17)} ,$$

$$\overline{D}_i = D_i \quad \text{from (17)} ,$$

$$\overline{E}_i = E_i \quad \text{from (17)} ,$$

$$C_i = C_i \quad \text{from (17)} ,$$

$$\overline{F}^r_{i,c} = \text{as defined in (28)} .$$

Simultaneously solving for the channel potential and the change charge requires the simultaneous solution of the above two equations (49) and (50) which results in the following system of equation in matrix form:

$$\begin{bmatrix} \overline{C} & \overline{H} & \overline{D} & 0 & 0 & 0 & \cdots \\ C & D & E & G & 0 & 0 & \cdots \\ \overline{B} & 0 & \overline{C} & \overline{H} & \overline{D} & 0 & \cdots \\ A & B & C & D & E & G & \cdots \\ 0 & 0 & \overline{B} & 0 & \overline{C} & \overline{H} & \cdots \\ 0 & 0 & A & B & C & D & \cdots \\ & & & / & / & / & \end{bmatrix} \begin{bmatrix} \Delta U_2 \\ \Delta S_2 \\ \Delta U_3 \\ \Delta S_3 \\ \vdots \\ \Delta U_{N-1} \\ \Delta S_{N-1} \end{bmatrix} = \begin{bmatrix} T_{2c} \\ -F_{2c} \\ T_{3c} \\ -F_{3c} \\ \vdots \\ T_{N-1,c} \\ -F_{N-1,c} \end{bmatrix}$$

The matrix is a 6 diagonal matrix. The number of variables is twice the number of grid points within the channel--not counting the boundary nodes at the source or drain. The solution can be conveniently solved by using a Guassian elimination technique.

G. Overall Flow Chart

In order to expedite convergence, initially, the gradual channel approximation is assumed and the potential is calculated along the channel. This analytical approach divides the device cross-section into two regions, the channel, silicon substrate region and the oxide region.

In each of the two regions an initial approximation of the potential distribution is obtained by solving the one-dimensional form of Poisson's equation utilizing the given boundary potentials including the channel potential derived in the previous step. The one-dimensional equation is equivalent to setting $dU/dx = 0$. The potential distribution is found along one column (vertical) simultaneously. By sweeping in the x direction, i.e., repeat the solution on another column, the potential distribution for the entire region(s) is obtained.

Next the solution to the two dimensional P. E. is obtained in each region. In the oxide the potential along a column is obtained with the region being swept in the x-direction. In the silicon convergence is expedited by using the alternating direction implicit (ADI) scheme. First, the potential in the row below the channel (JMAX0) is obtained. Next the potential distributions for

each row between the source and drain are obtained by sweeping in the negative y-direction. When the solution to row JK1 is obtained, the solution to the column I = 1 is obtained The column solutions are obtained by sweeping in the positive x-direction. This ADI scheme is repeated until satisfactory convergence is obtained.

With the two-dimensional potential distribution obtained for both regions based on the gradual channel assumption, a new estimate of the channel potential and the channel charge is obtained by solving simultaneously the P. E. and current equation along the channel row. The 2-D P. E. is then solved along the rows between the source and drain by sweeping y in the negative direction. Next the columns solutions are obtained sweeping the x-direction for the entire regions--thus crossing the channel in the appropriate locations (I = IK + 1 to IL-1) . This ADI scheme starting at the simultaneous solution of the P. E. and the current equation along the channel row is repeated until satisfactory convergence is obtained.

The channel current is obtained from an explicit solution to the channel current equation after the channel charge and potential are found.

H. Progress Report

The basic program has been written which provides user flexibility for defining the physical dimensions, the number of grid points, p or n type device, metal or silicon gate, type orientation of substrate, etc. Provisions have been incorporated

for sweeping multiple bias points in order to plot, for example, drain or transfer characteristics. In addition, provisions are provided to plot the two dimension potential distribution as well as, print out this data in table form.

Using an example bias the program has successfully completed the steps through the solution of the two dimensional P. E. using the fixed channel potential as a boundary condition. However, at the next step, the channel charge is found to diverge. Time has not allowed the resolution of the problem; however, an error has been found in the current equation program which may be the cause. Of deeper concern is the possibility that the channel charge is not directly tied to the channel potential through the P. E., but only indirectly. This may require the formulation of an expression for channel charge q_S as a function of potential and electric field which is then inserted into the Poisson equation. Further investigation of this problem is required before the best solution can be determined.

I. Availability of 2-D MOSFET Simulators

The first 2-D simulator program which could provide I-V characteristics was developed by Mock [3.9] and Kennedy [3.8] at IBM in the 1970 to 1972 timeframe. The program, based on finite difference techniques, is proprietary to IBM. However, a modified version of this program has been developed by Sutherland [3.14] (and Kennedy) at the University of Florida under contract to ARPA. This program is restricted to uniformily doped substrates and zero

substrate bias.

Kennedy at the Applied Electronics Research Corporation has modified the Sutherland program to include provisions for

1) 1-D substrate impurity profile,

2) mobility dependence on gate voltage, and

3) substrate bias

and is now licensing the program (NEMOS) for $10,000 for one year and $7,500 for each succeeding year.

In addition, Hitachi has developed a finite element version with provisions, at least, for substrates with 1-D impurity profiles. Dr. Asai of Hitachi has indicated the possibility of licensing the program to Universities, government and industry in the United States. The Hitachi program called CADDET was developed in 1977-1978.

At least one other 2-D simulation program is under development. Jim Meindl at Stanford is under contract with ARPA to continue the work by Sutherland.

At this writing the author has been unable to determine when the program under development at Stanford will be available for distribution.

J. Recommendations

In view of the recent "availability" of alternate sources of the 2-D simulator, it seems prudent to evaluate more seriously the availability and cost for achieving a satisfactory and working program from the four possible sources. The compatibility with existing computers and the difficulty in modifying them to meet

the stated objectives must be considered. The authors believe this should be accomplished before seriously continuing with the present program. After all, the 2-D MOSFET simulator is just the means with which to evaluate various short channel MOSFET device structures and not the end product.

APPENDIX A

BORON DATA

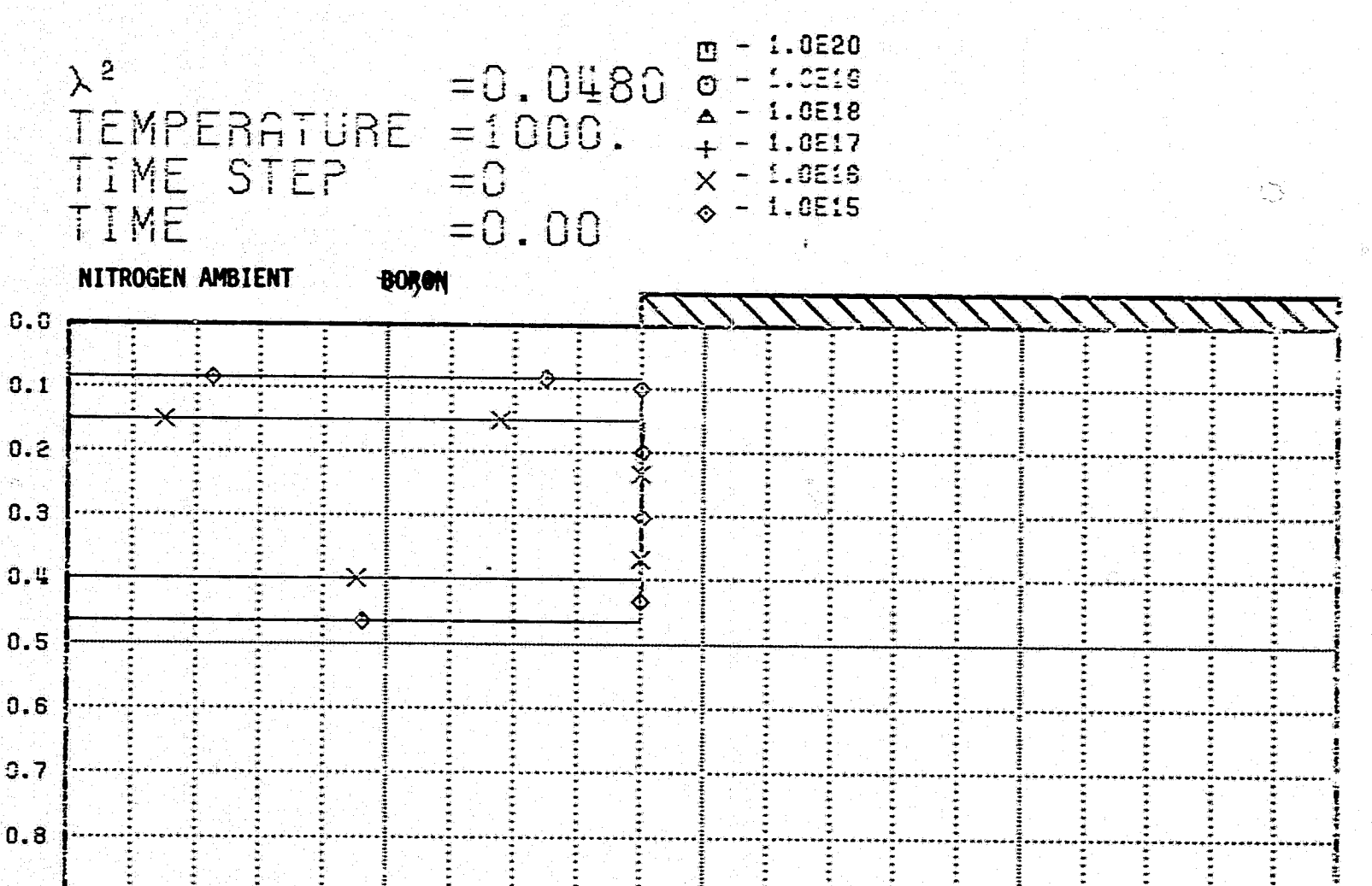
λ² =0.0480
TEMPERATURE =1000.
TIME STEP =0
TIME =0.00
□ - 1.0E20
○ - 1.0E19
△ - 1.0E18
+ - 1.0E17
× - 1.0E16
◇ - 1.0E15
NITROGEN AMBIENT
BORON
0.0
0.1
0.2
0.3
0.4
0.5
0.6
0.7
0.8
0.9
1.0
0.0 0.2 0.4 0.6 0.8 1.0 1.2 1.4 1.6 1.8 2.0 2.2 2.4 2.6 2.8 3.0 3.2 3.4 3.6 3.8 4.0

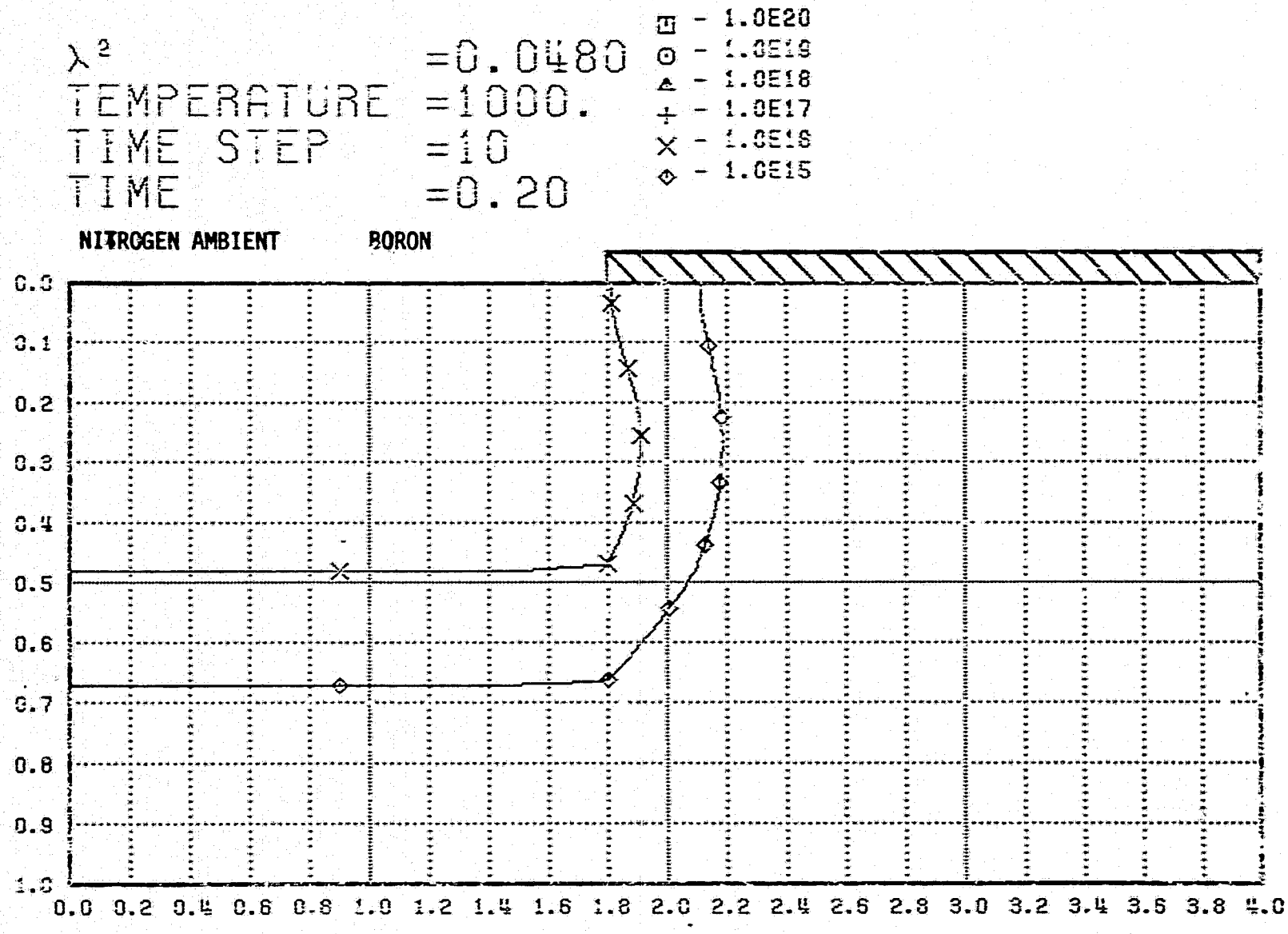
λ² =0.0480
TEMPERATURE =1000.
TIME STEP =10
TIME =0.20
- 1.0E20
- 1.0E19
- 1.0E18
- 1.0E17
- 1.0E16
- 1.0E15
NITROGEN AMBIENT
BORON
0.0
0.1
0.2
0.3
0.4
0.5
0.6
0.7
0.8
0.9
1.0
0.0 0.2 0.4 0.6 0.8 1.0 1.2 1.4 1.6 1.8 2.0 2.2 2.4 2.6 2.8 3.0 3.2 3.4 3.6 3.8 4.0

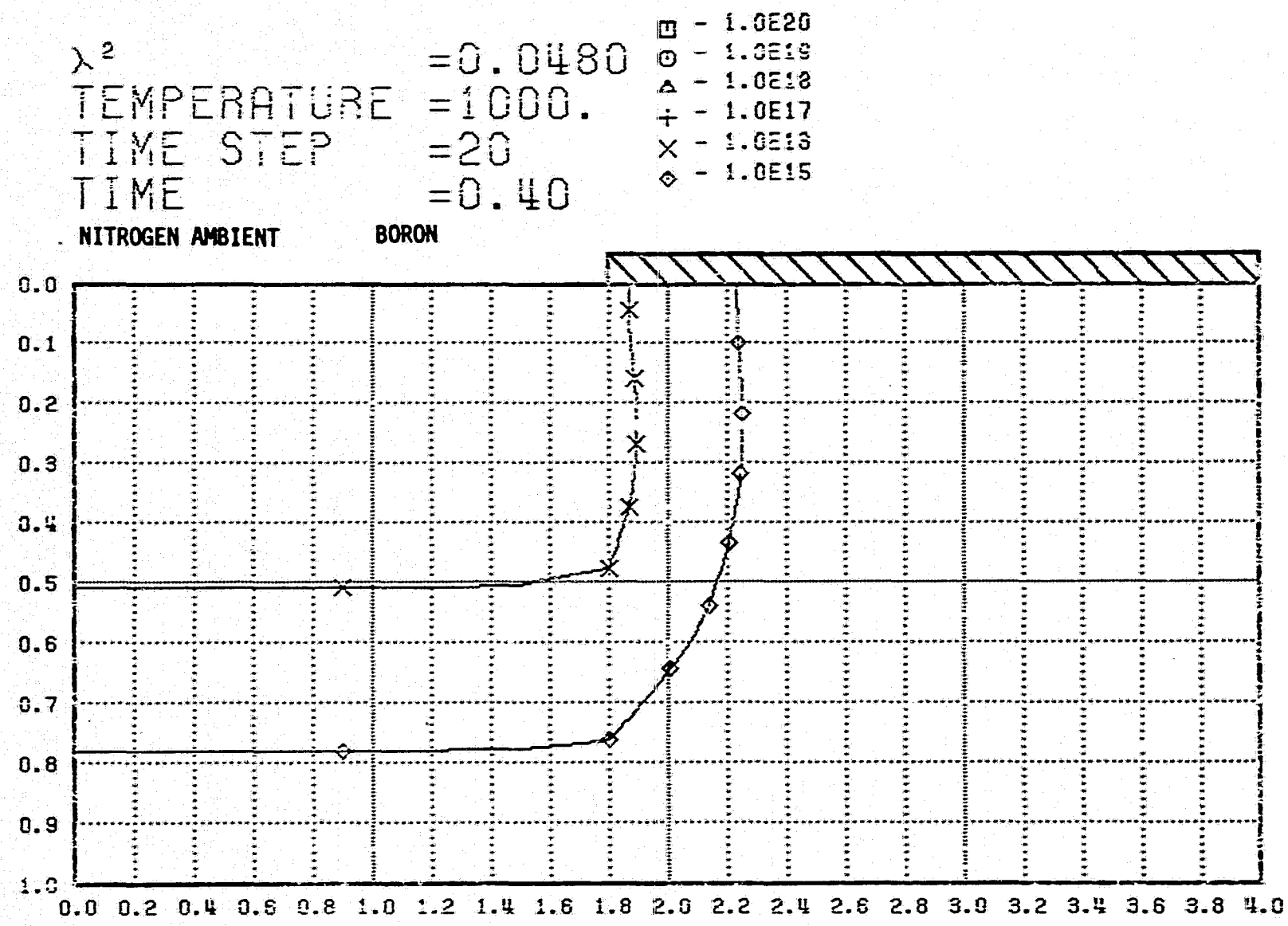
λ² =0.0480
TEMPERATURE =1000.
TIME STEP =20
TIME =0.40
NITROGEN AMBIENT
BORON
- 1.0E20
- 1.0E19
- 1.0E18
- 1.0E17
- 1.0E16
- 1.0E15
0.0
0.1
0.2
0.3
0.4
0.5
0.6
0.7
0.8
0.9
1.0
0.0 0.2 0.4 0.6 0.8 1.0 1.2 1.4 1.6 1.8 2.0 2.2 2.4 2.6 2.8 3.0 3.2 3.4 3.6 3.8 4.0

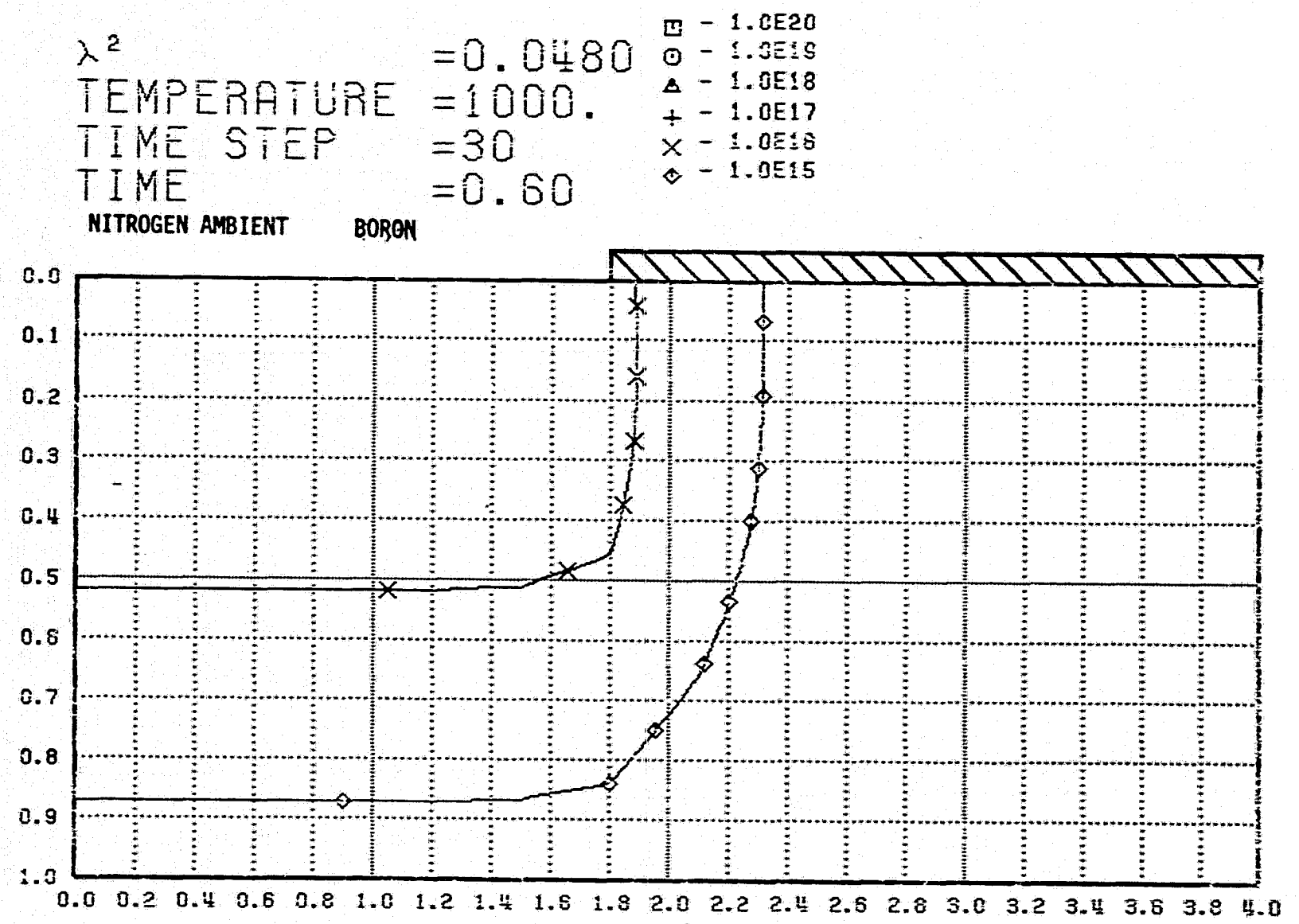
λ² =0.0480
TEMPERATURE =1000.
TIME STEP =30
TIME =0.60
NITROGEN AMBIENT BORON
□ - 1.0E20
⊙ - 1.0E19
△ - 1.0E18
+ - 1.0E17
× - 1.0E16
◇ - 1.0E15
0.0
0.1
0.2
0.3
0.4
0.5
0.6
0.7
0.8
0.9
1.0
0.0 0.2 0.4 0.6 0.8 1.0 1.2 1.4 1.6 1.8 2.0 2.2 2.4 2.6 2.8 3.0 3.2 3.4 3.6 3.8 4.0

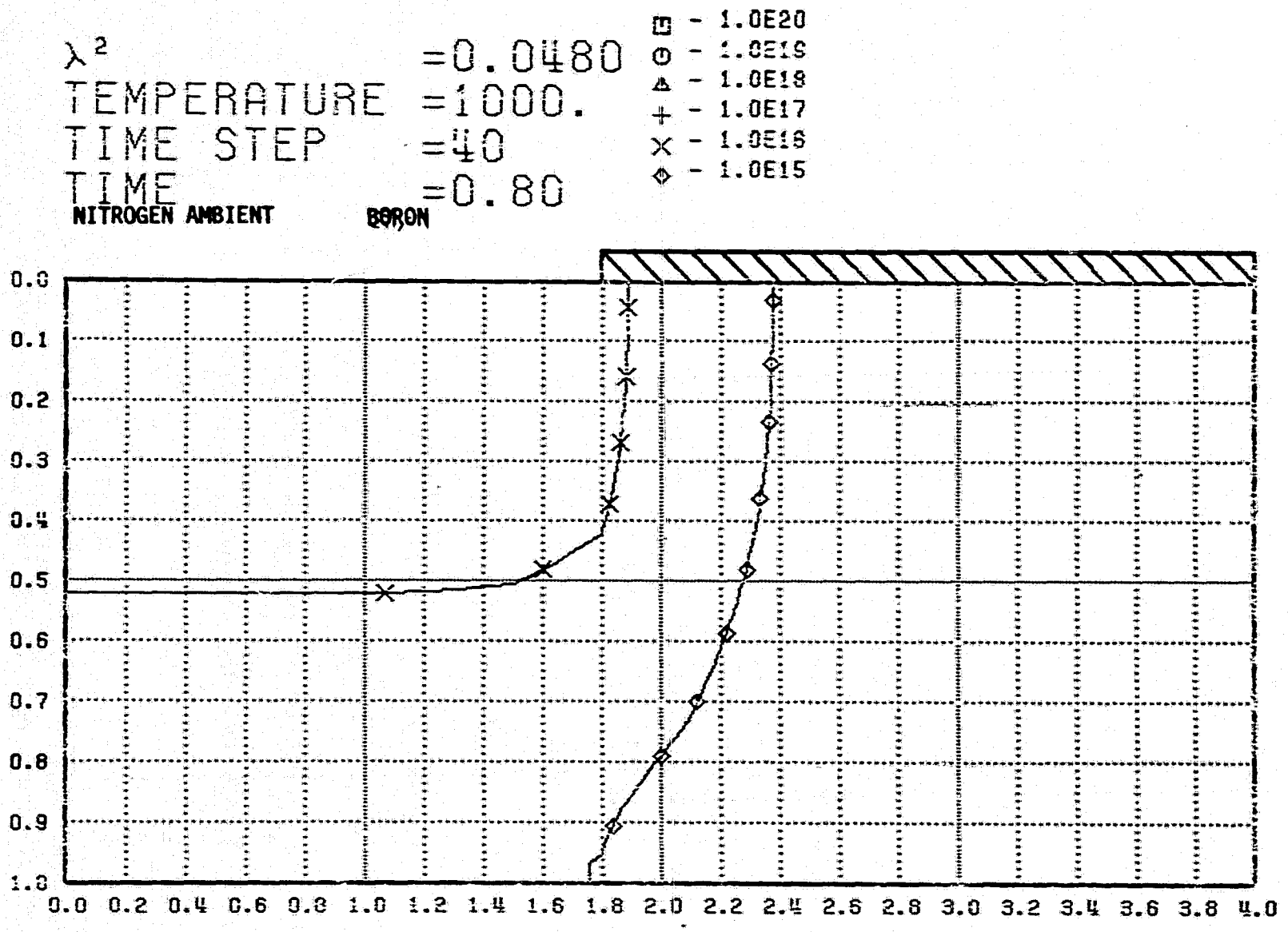
λ² =0.0480
TEMPERATURE =1000.
TIME STEP =40
TIME =0.80
NITROGEN AMBIENT
BORON
- 1.0E20
- 1.0E19
- 1.0E18
- 1.0E17
- 1.0E16
- 1.0E15
0.0
0.1
0.2
0.3
0.4
0.5
0.6
0.7
0.8
0.9
1.0
0.0 0.2 0.4 0.6 0.8 1.0 1.2 1.4 1.6 1.8 2.0 2.2 2.4 2.6 2.8 3.0 3.2 3.4 3.6 3.8 4.0

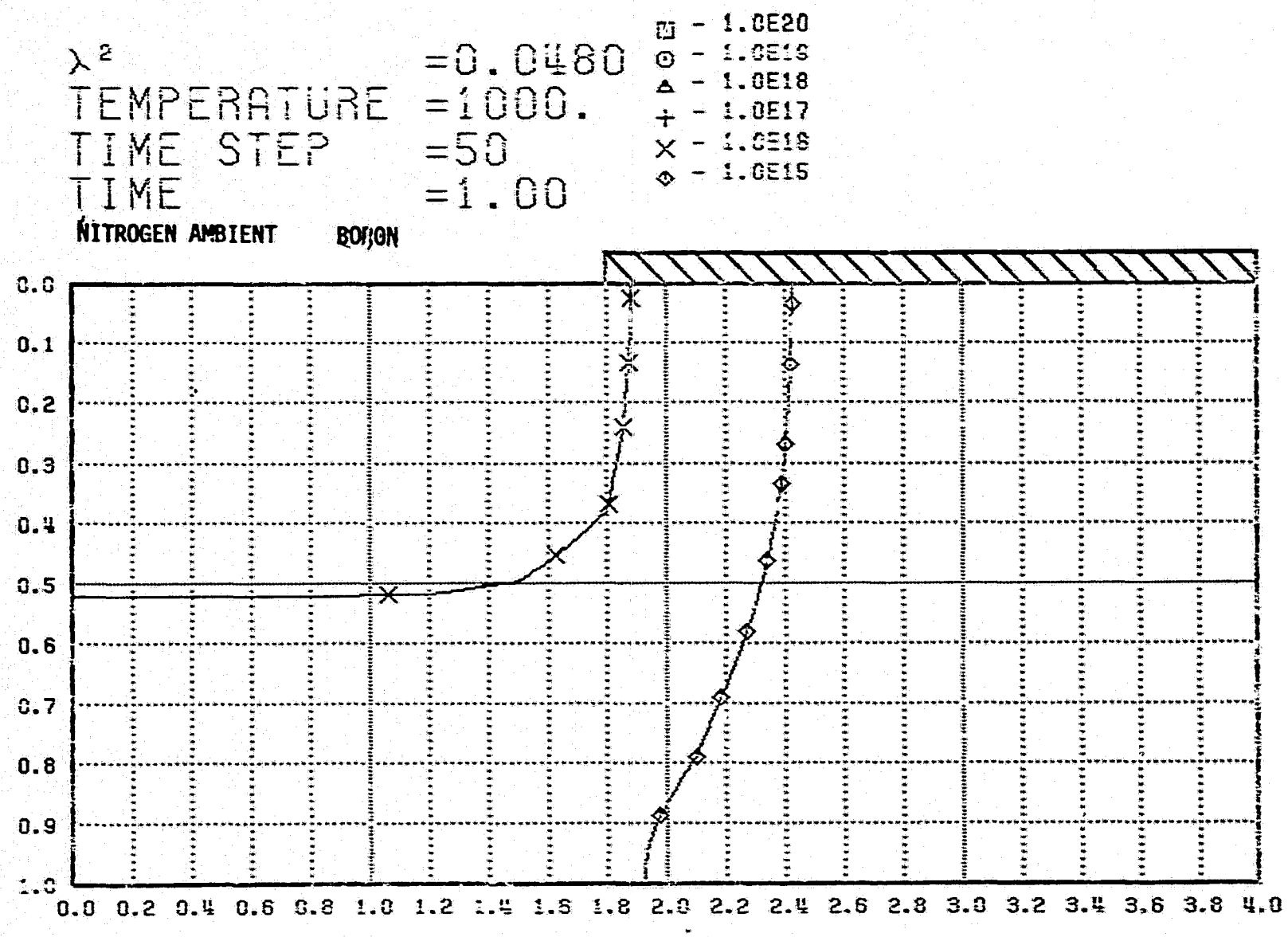
χ^2 =0.0480
TEMPERATURE =1000.
TIME STEP =50
TIME =1.00
NITROGEN AMBIENT BORON
- 1.0E20
- 1.0E19
- 1.0E18
- 1.0E17
- 1.0E16
- 1.0E15
0.0 0.1 0.2 0.3 0.4 0.5 0.6 0.7 0.8 0.9 1.0
0.0 0.2 0.4 0.6 0.8 1.0 1.2 1.4 1.6 1.8 2.0 2.2 2.4 2.6 2.8 3.0 3.2 3.4 3.6 3.8 4.0

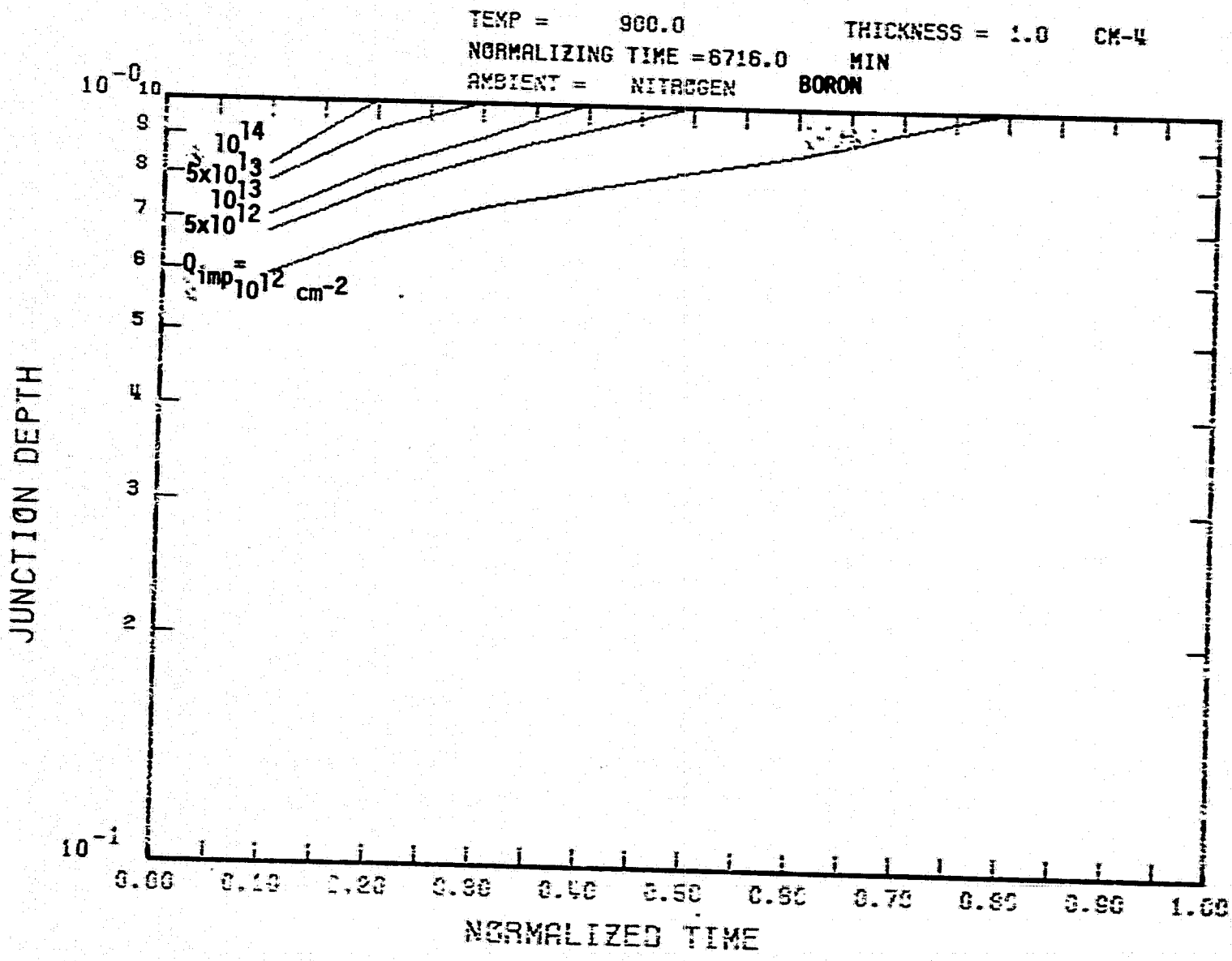

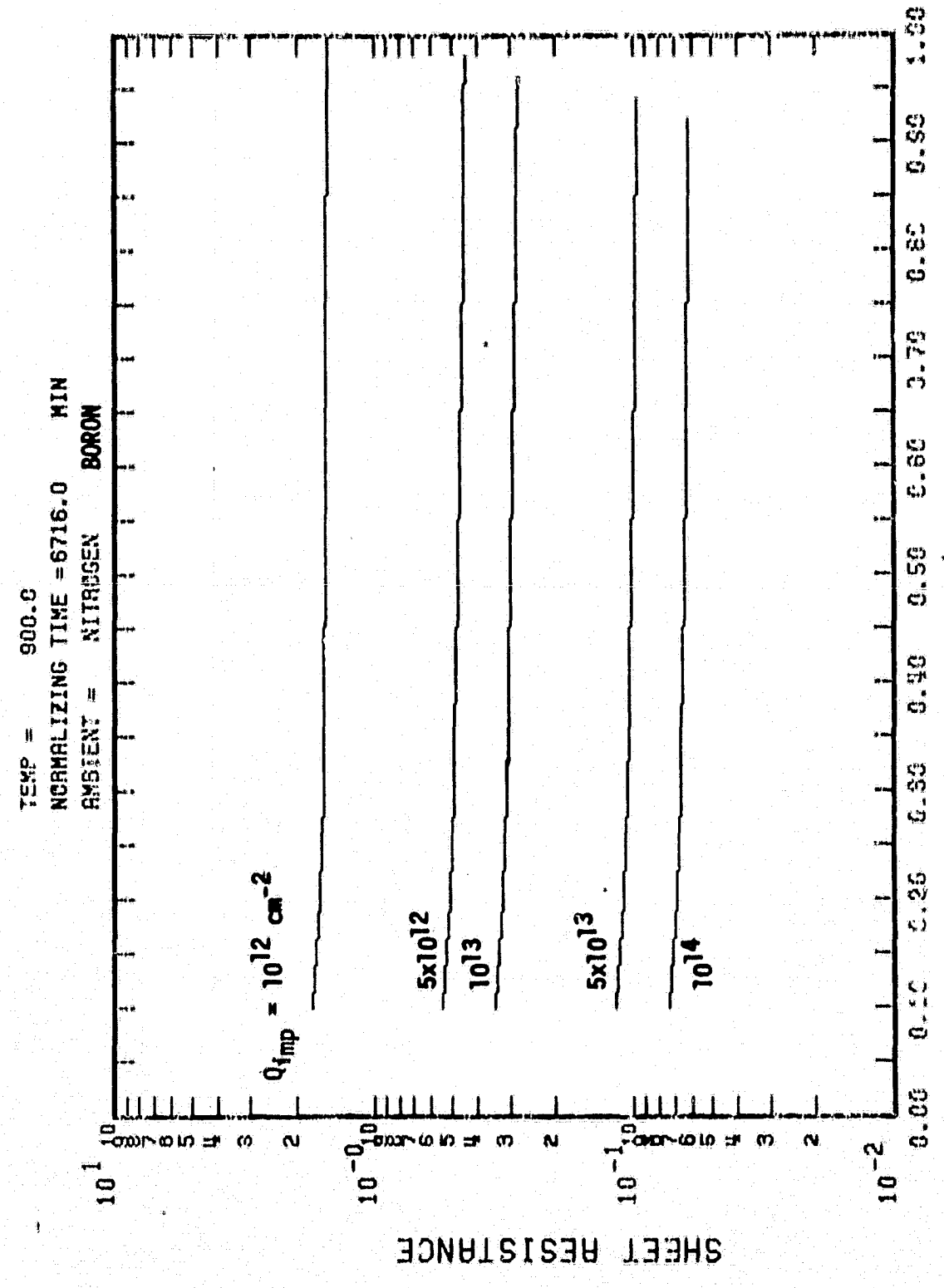
TEMP = 900.0
NORMALIZING TIME =6716.0 MIN
AMBIENT = NITROGEN BORON
$Q_{imp} = 10^{12}$ cm^{-2}
$5x10^{12}$
10^{13}
$5x10^{13}$
10^{14}
SHEET RESISTANCE
NORMALIZED TIME

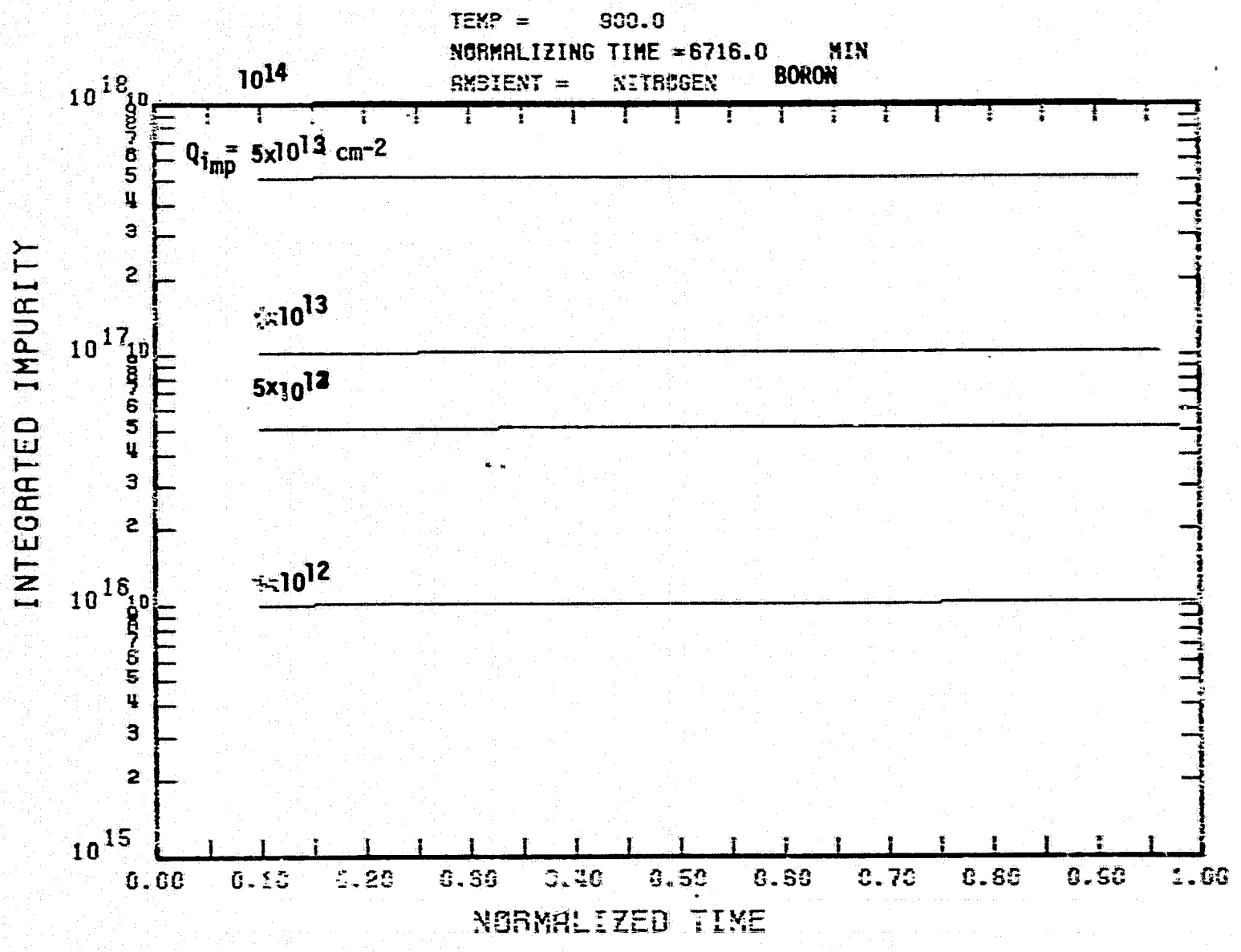
TEMP = 900.0
NORMALIZING TIME =6716.0 MIN
AMBIENT = NITROGEN
BORON
10^{14}
Q_{imp} = 5x10^{13} cm^{-2}
10^{13}
5x10^{12}
10^{12}
10^{18}
10^{17}
10^{16}
10^{15}
INTEGRATED IMPURITY
0.00
0.10
0.20
0.30
0.40
0.50
0.60
0.70
0.80
0.90
1.00
NORMALIZED TIME

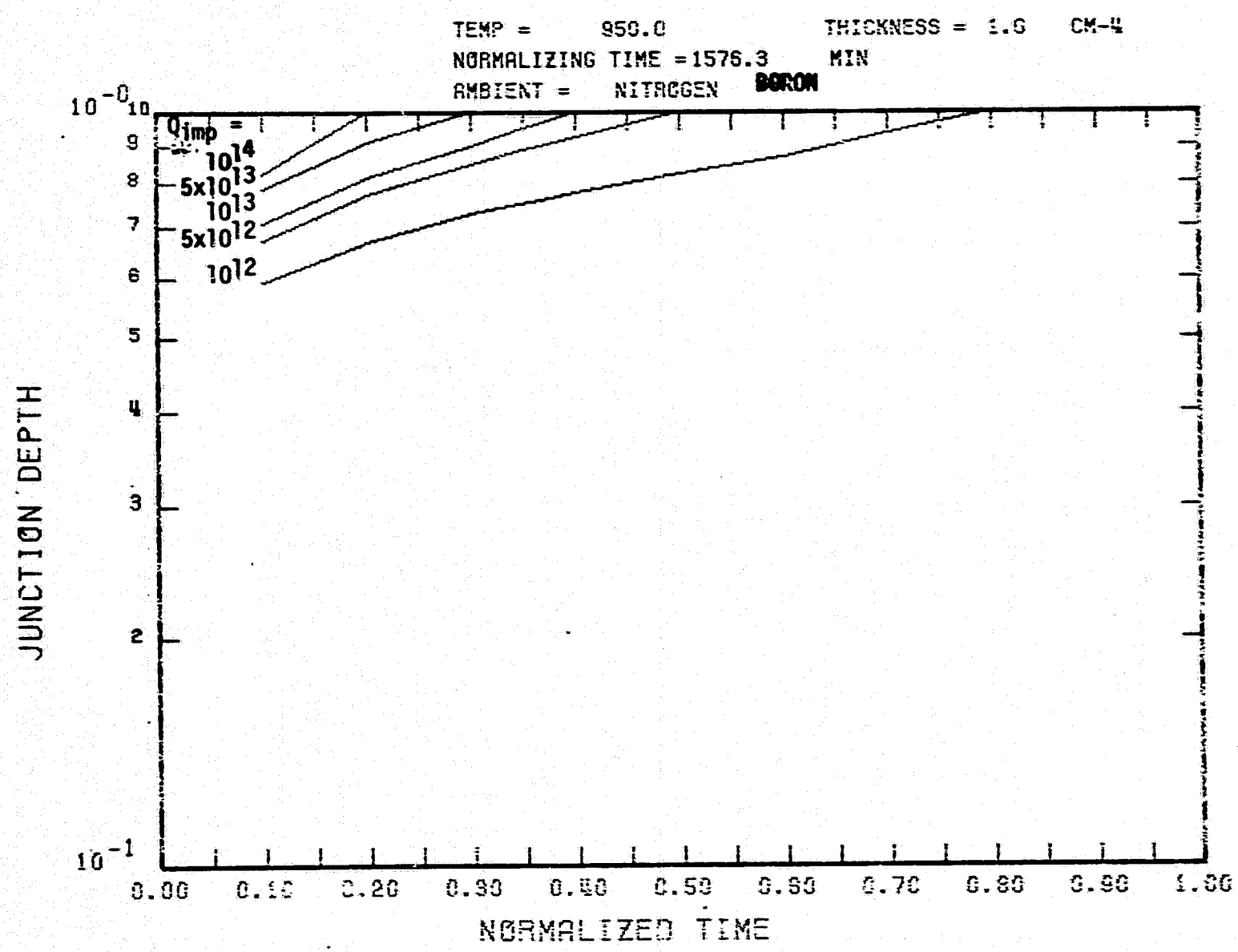
TEMP = 950.0 THICKNESS = 1.6 CM-4
NORMALIZING TIME = 1576.3 MIN
AMBIENT = NITROGEN
BORON
Qimp =
10^14
5x10^13
10^13
5x10^12
10^12
10^-0
10^-1
JUNCTION DEPTH
NORMALIZED TIME
0.00
0.10
0.20
0.30
0.40
0.50
0.60
0.70
0.80
0.90
1.00

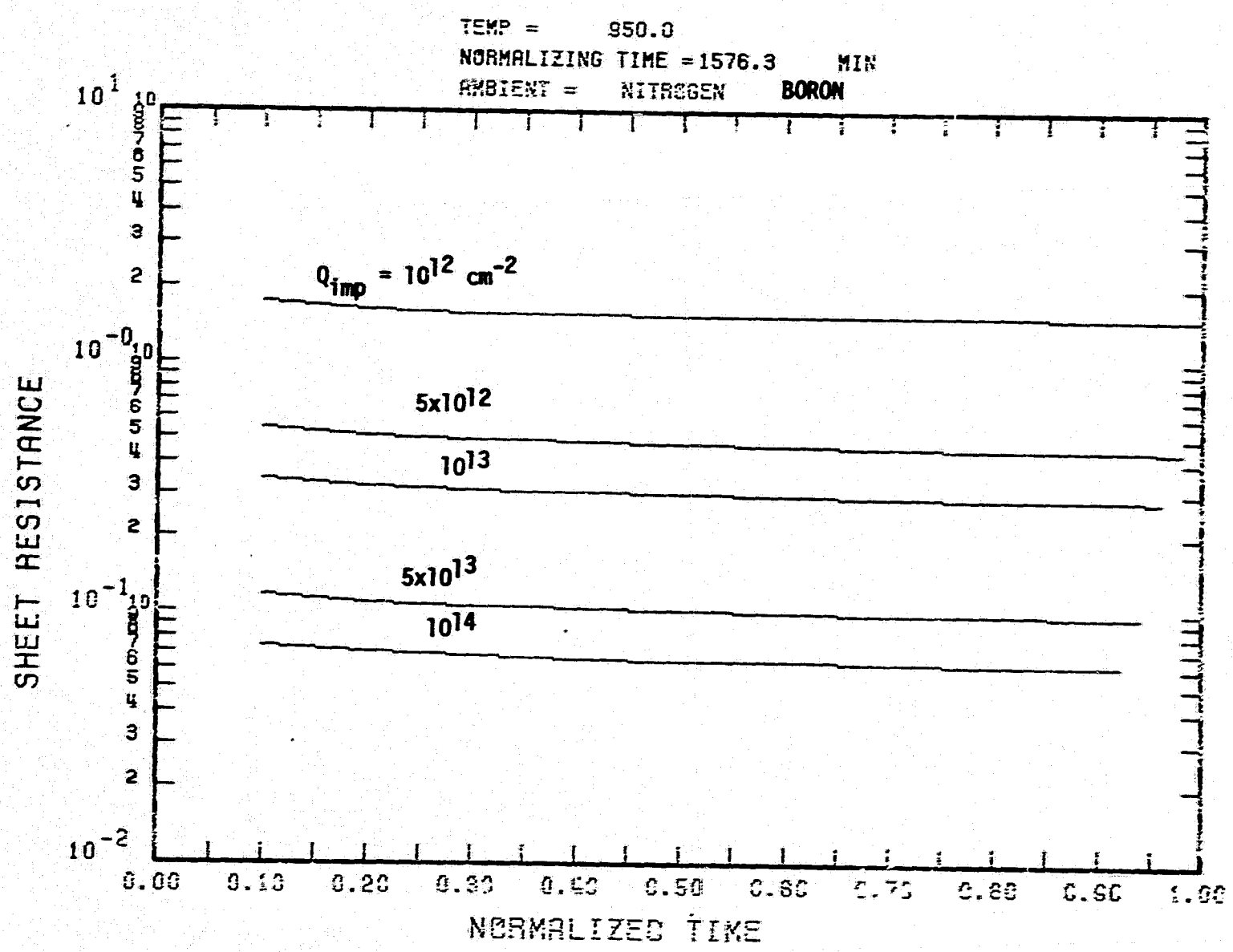
TEMP = 950.0
NORMALIZING TIME = 1576.3 MIN
AMBIENT = NITROGEN BORON
SHEET RESISTANCE
NORMALIZED TIME
Q_{imp} = 10^{12} cm^{-2}
5x10^{12}
10^{13}
5x10^{13}
10^{14}
10^{1}
10^{0}
10^{-1}
10^{-2}
0.00
0.10
0.20
0.30
0.40
0.50
0.60
0.70
0.80
0.90
1.00

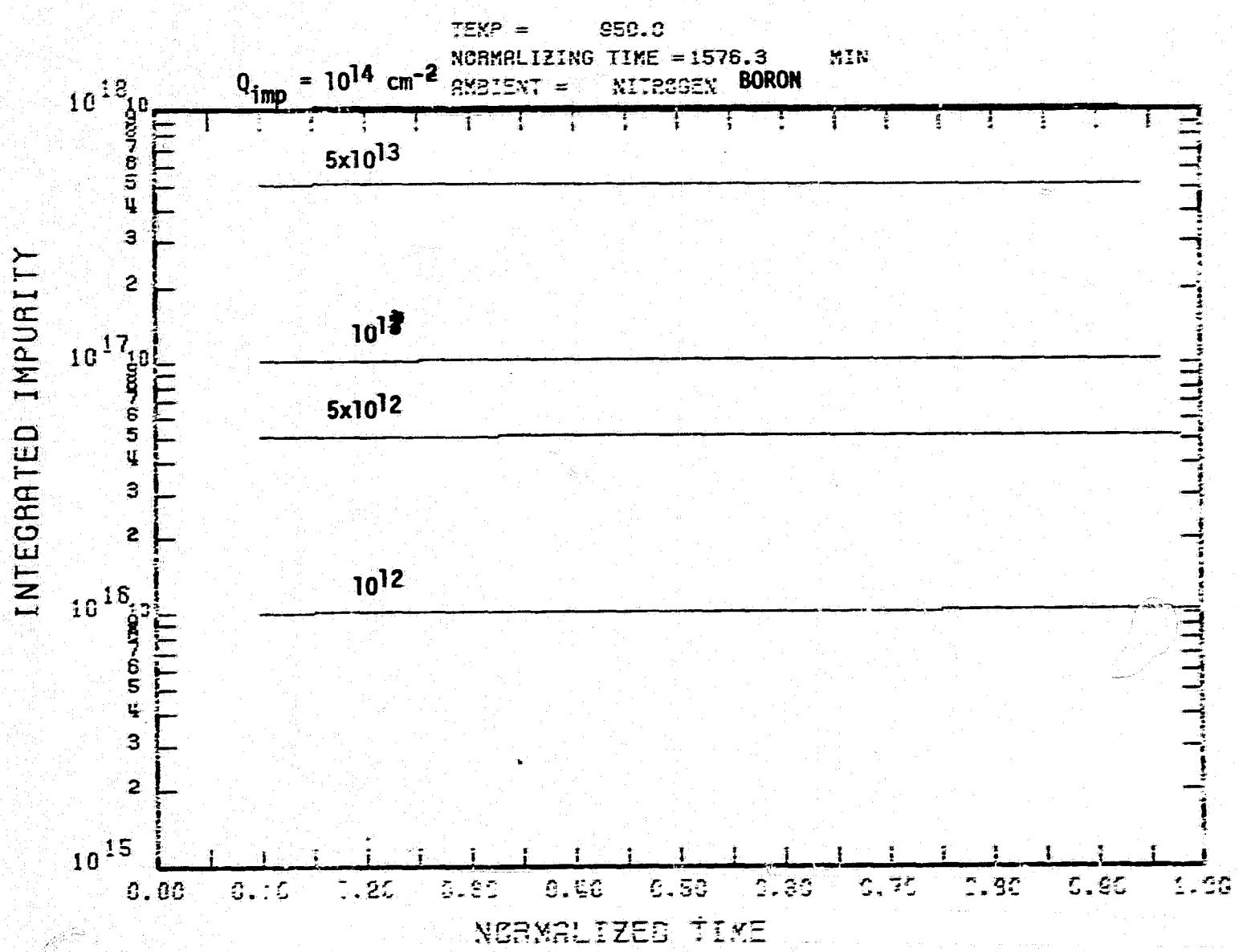
TEMP = 950.0
NORMALIZING TIME = 1576.3 MIN
Q_{imp} = 10^{14} cm^{-2}
AMBIENT = NITROGEN
BORON
$5x10^{13}$
10^{13}
$5x10^{12}$
10^{12}
INTEGRATED IMPURITY
NORMALIZED TIME

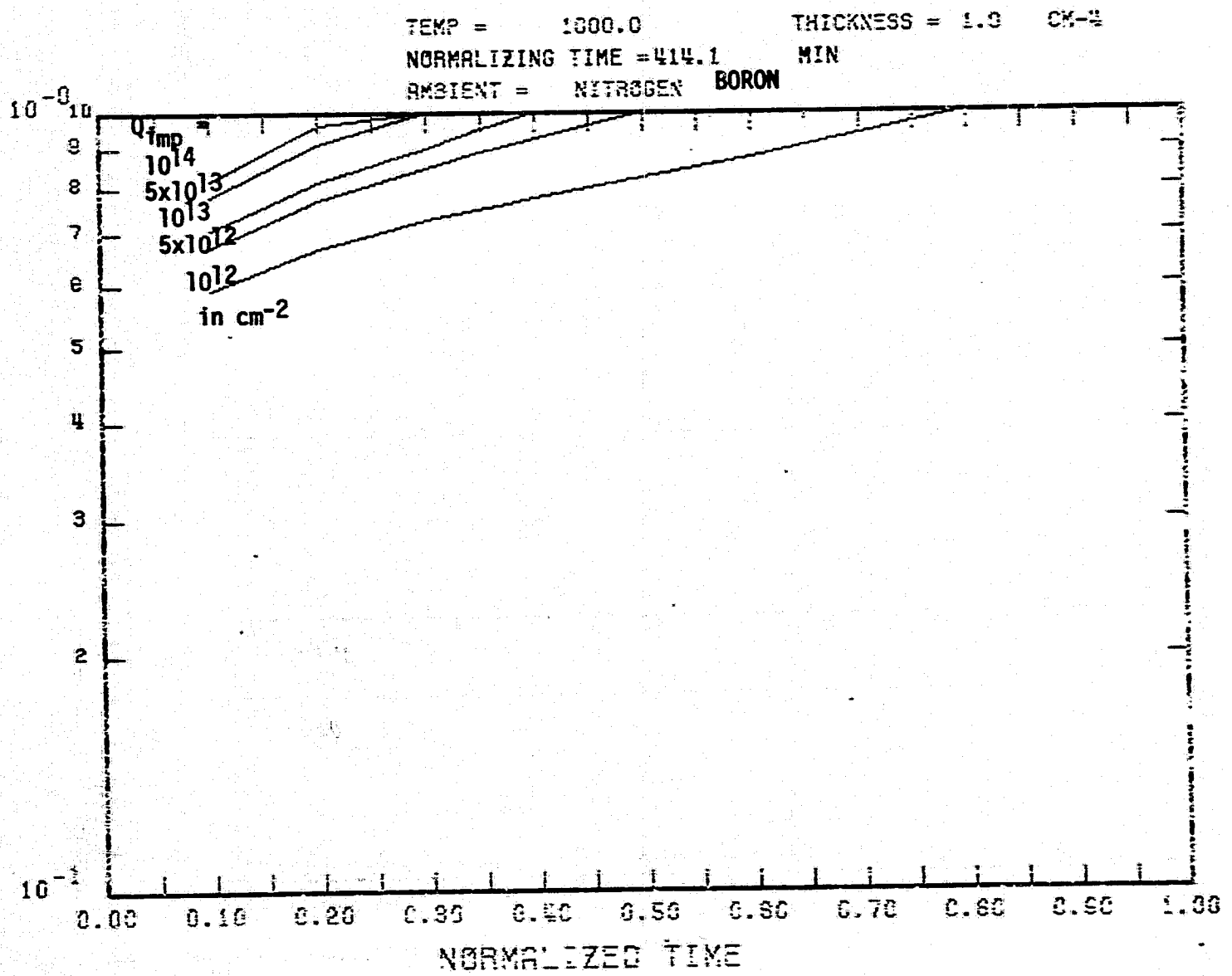

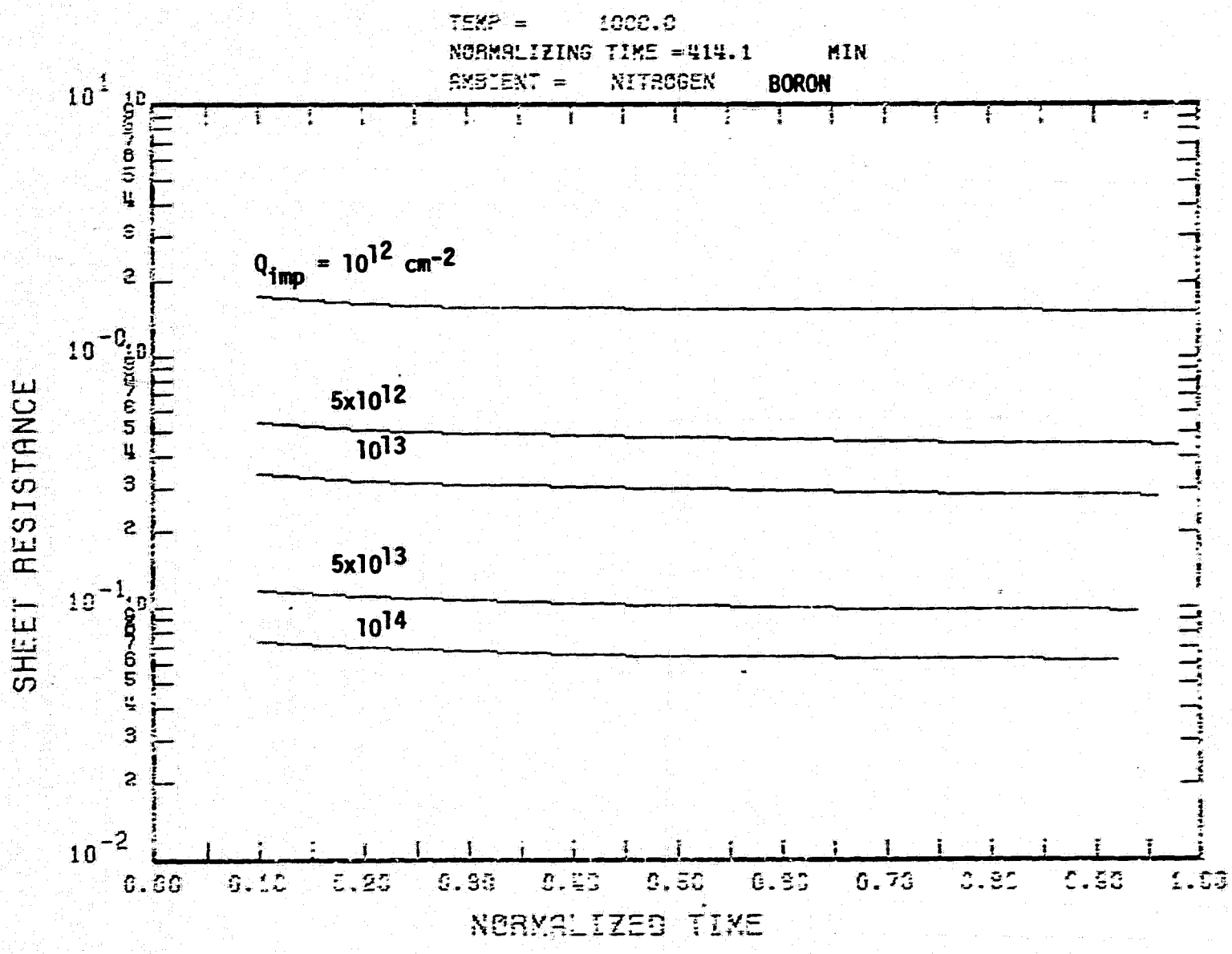
TEMP = 1000.0
NORMALIZING TIME =414.1 MIN
AMBIENT = NITROGEN BORON
Q_{imp} = 10^{12} cm^{-2}
5x10^{12}
10^{13}
5x10^{13}
10^{14}
SHEET RESISTANCE
NORMALIZED TIME

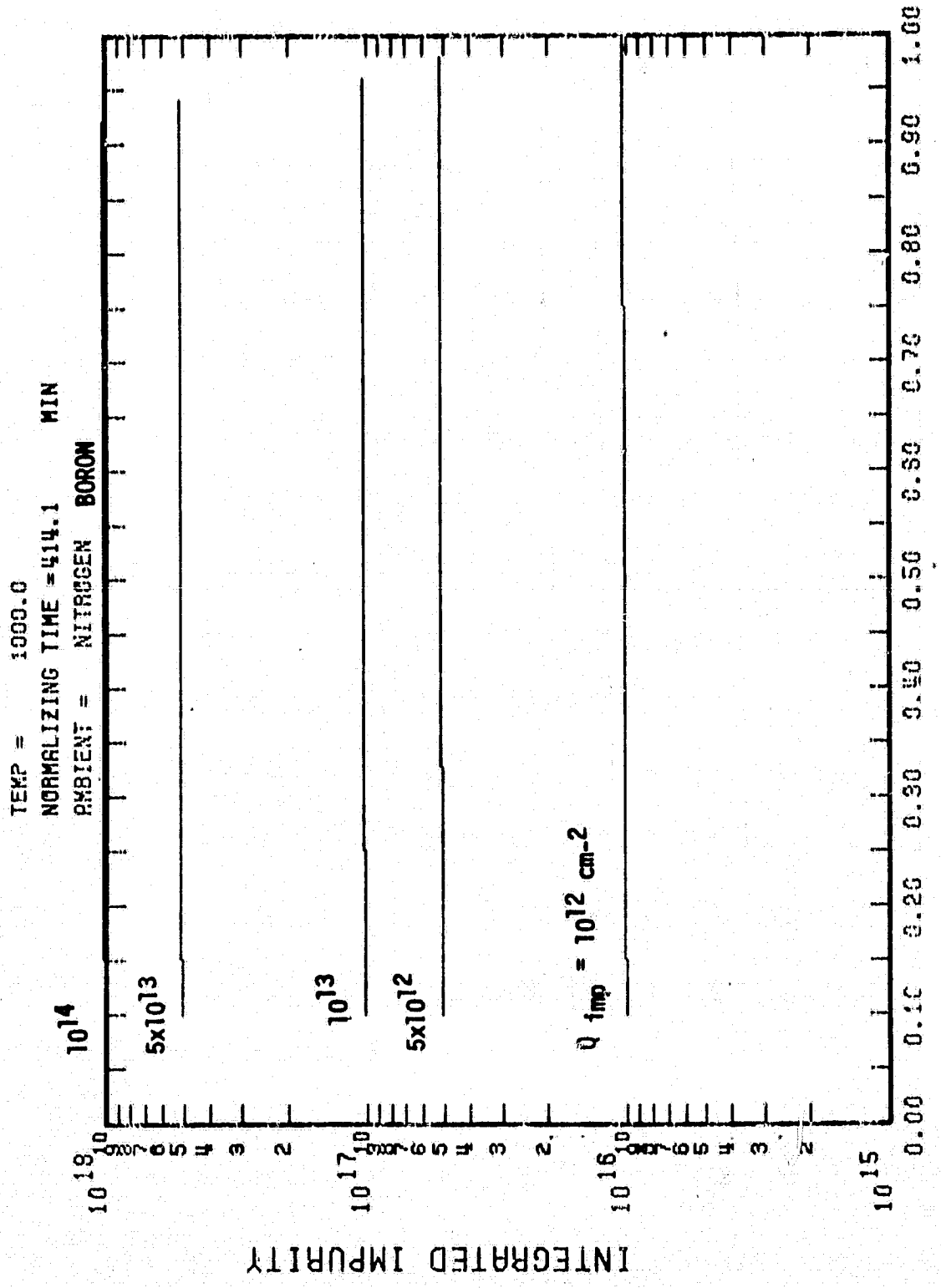

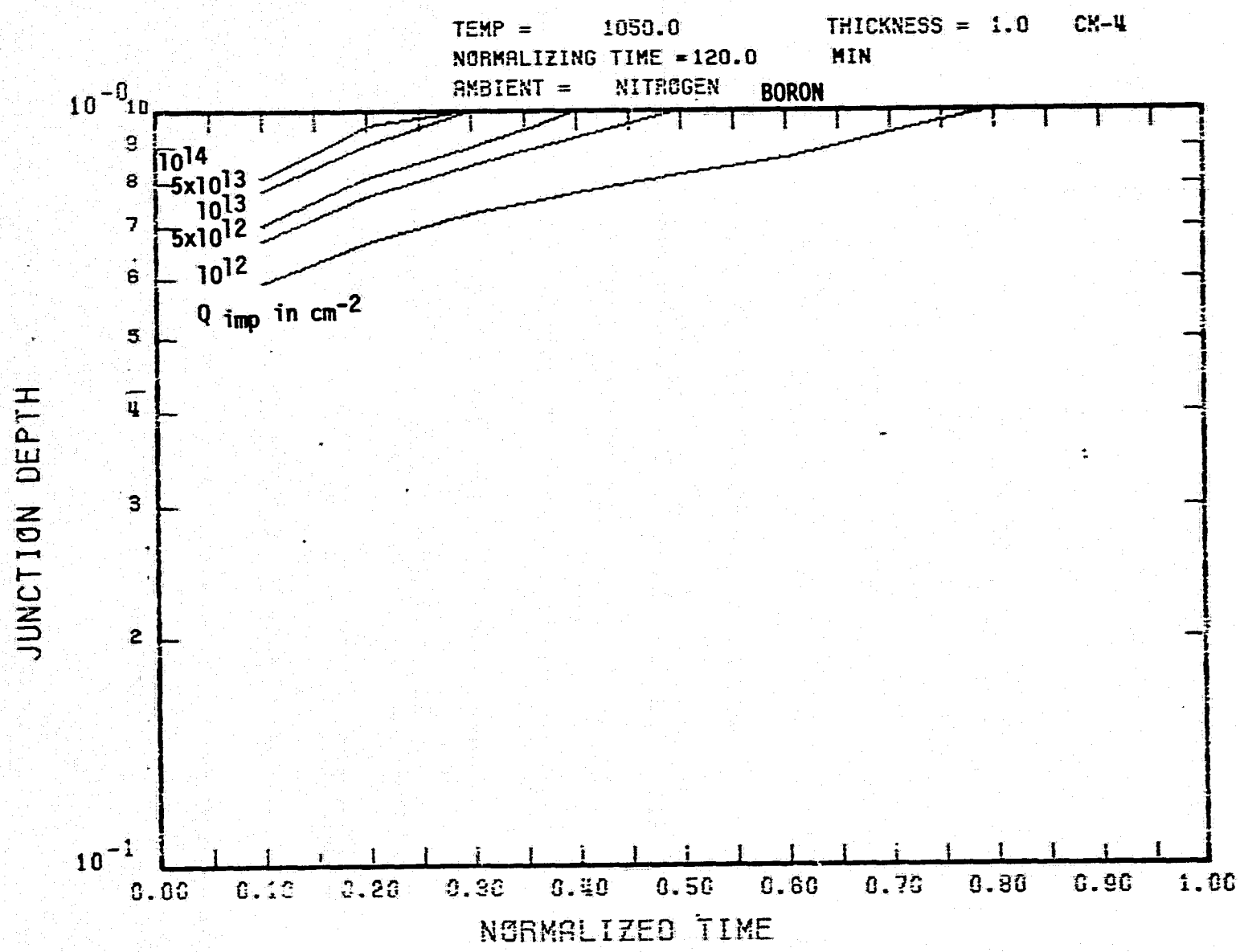
TEMP = 1050.0 THICKNESS = 1.0 CK-4
NORMALIZING TIME =120.0 MIN
AMBIENT = NITROGEN BORON
10^{14}
$5x10^{13}$
10^{13}
$5x10^{12}$
10^{12}
Q imp in cm^{-2}
JUNCTION DEPTH
NORMALIZED TIME
10^{-0}
10^{-1}
10
9
8
7
6
5
4
3
2
0.00
0.10
0.20
0.30
0.40
0.50
0.60
0.70
0.80
0.90
1.00

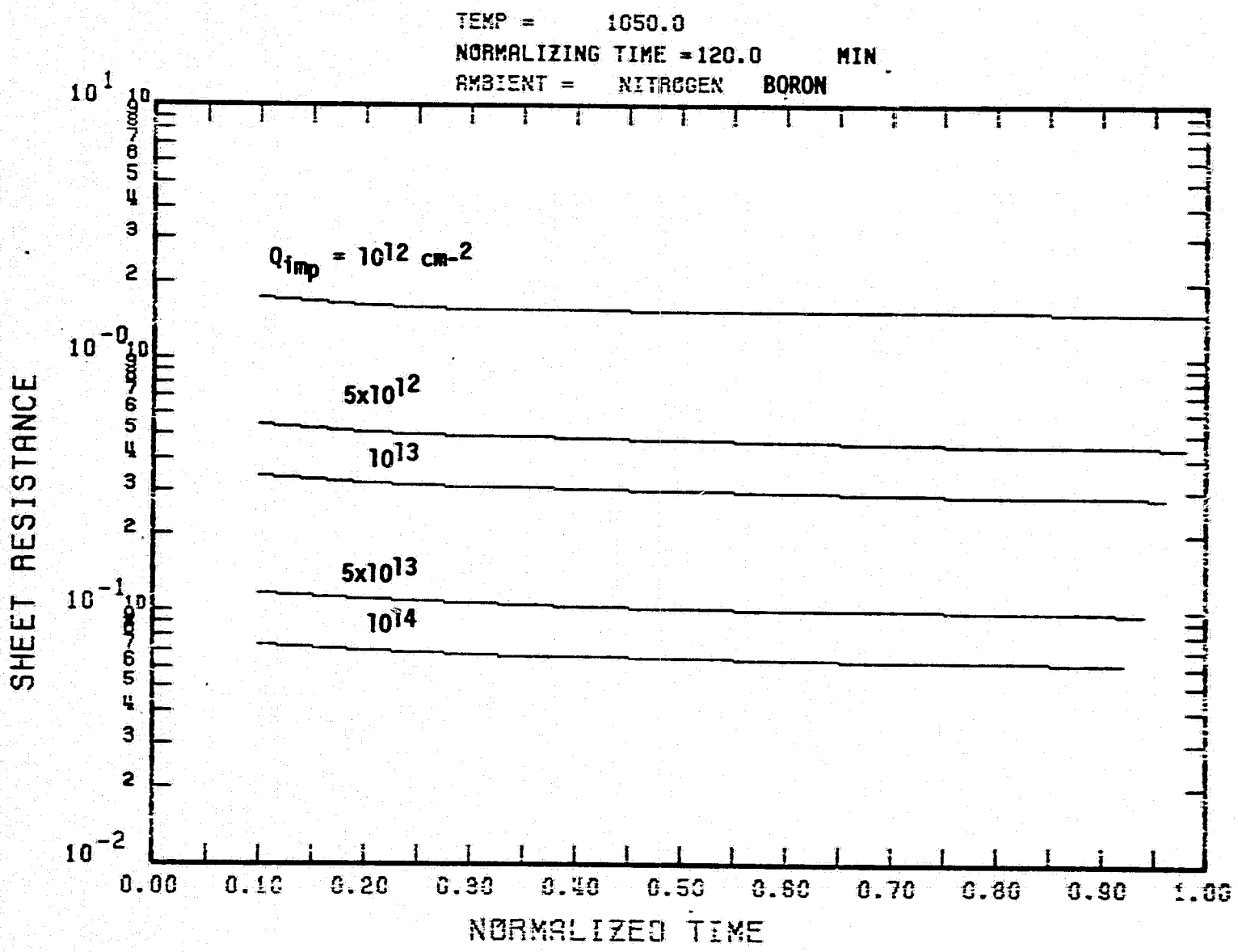
TEMP = 1050.0
NORMALIZING TIME = 120.0 MIN
AMBIENT = NITROGEN BORON
Q_{imp} = 10^{12} cm^{-2}
$5x10^{12}$
10^{13}
$5x10^{13}$
10^{14}
SHEET RESISTANCE
NORMALIZED TIME
10^{1}
10^{0}
10^{-1}
10^{-2}
0.00
0.10
0.20
0.30
0.40
0.50
0.60
0.70
0.80
0.90
1.00

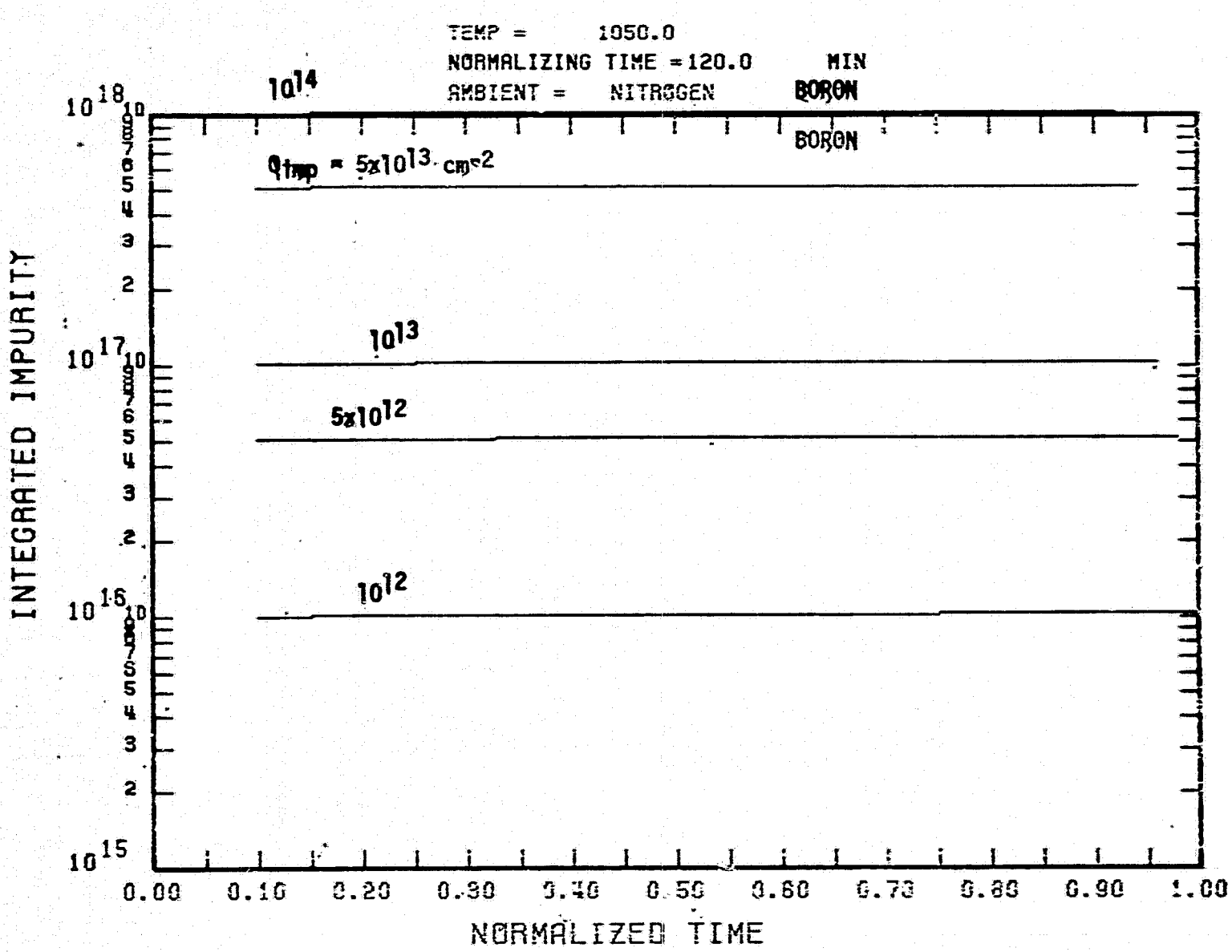
TEMP = 1050.0
NORMALIZING TIME = 120.0 MIN
AMBIENT = NITROGEN
BORON
BORON
10^{14}
$Q_{imp} = 5x10^{13}$ cm^{-2}
10^{13}
$5x10^{12}$
10^{12}
INTEGRATED IMPURITY
10^{18}
10^{17}
10^{16}
10^{15}
0.00 0.10 0.20 0.30 0.40 0.50 0.60 0.70 0.80 0.90 1.00
NORMALIZED TIME

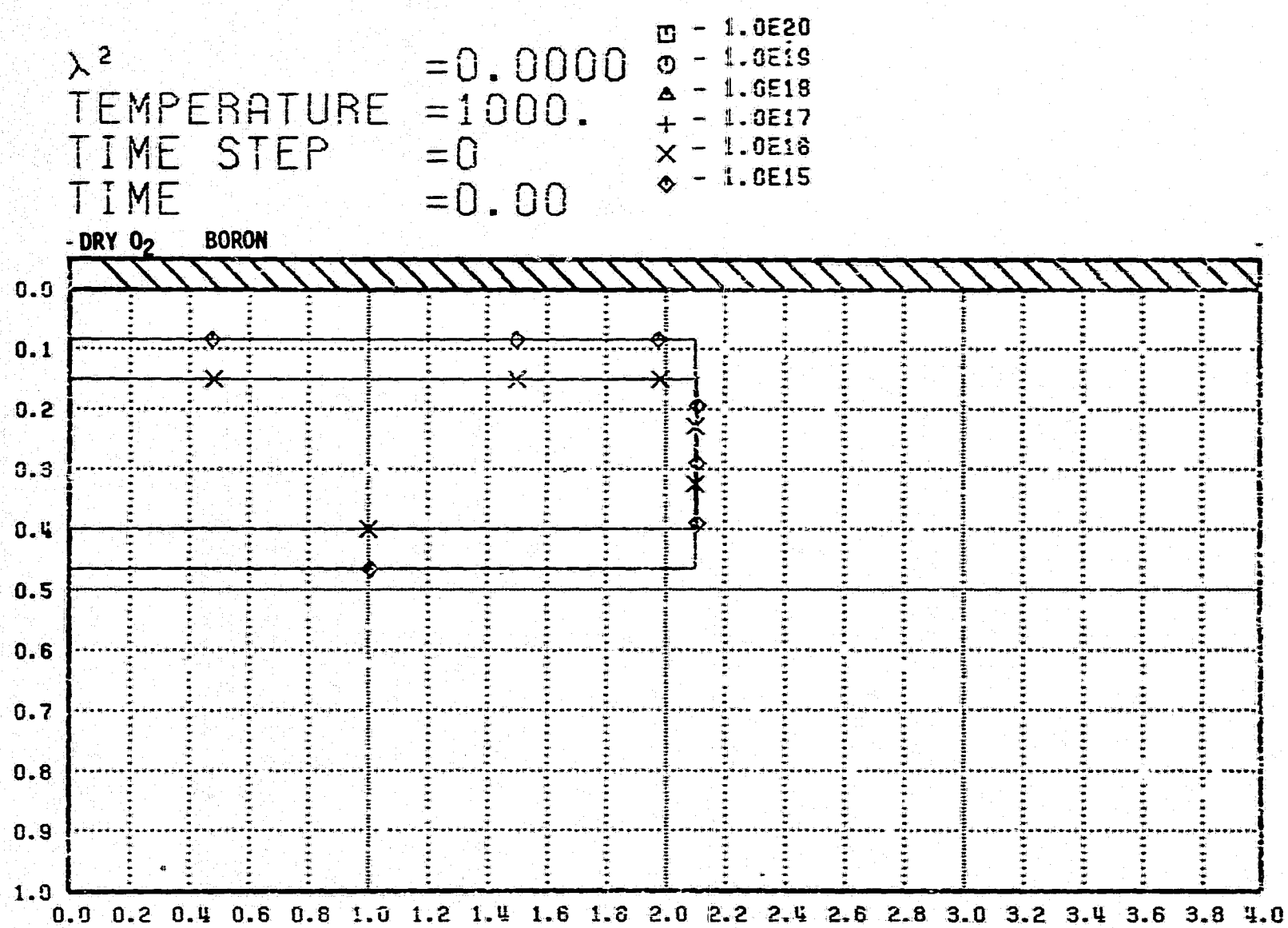
λ² =0.0000
TEMPERATURE =1000.
TIME STEP =0
TIME =0.00
- 1.0E20
- 1.0E19
- 1.0E18
- 1.0E17
- 1.0E16
- 1.0E15
- DRY O2 BORON
0.0
0.1
0.2
0.3
0.4
0.5
0.6
0.7
0.8
0.9
1.0
0.0 0.2 0.4 0.6 0.8 1.0 1.2 1.4 1.6 1.8 2.0 2.2 2.4 2.6 2.8 3.0 3.2 3.4 3.6 3.8 4.0

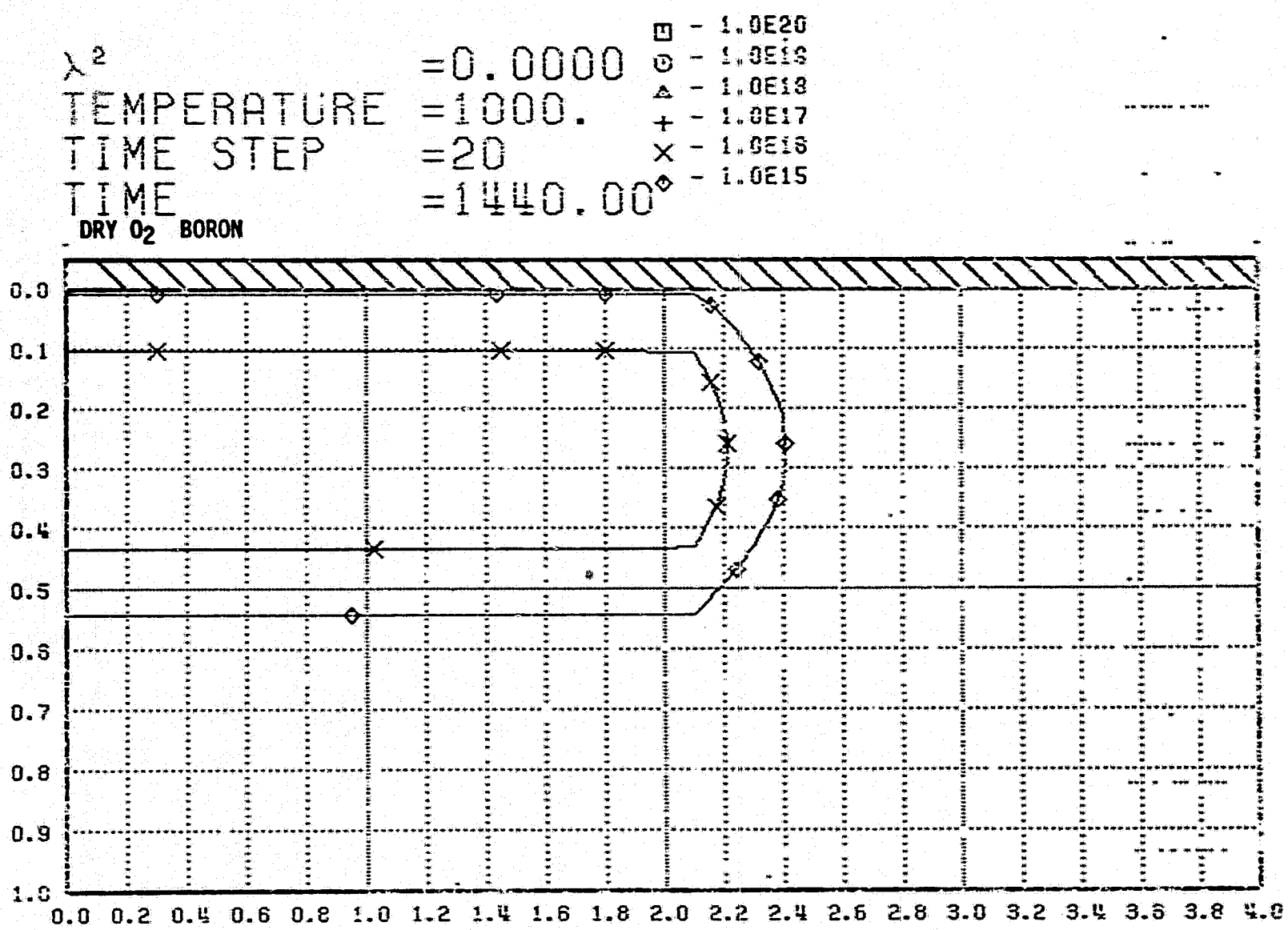

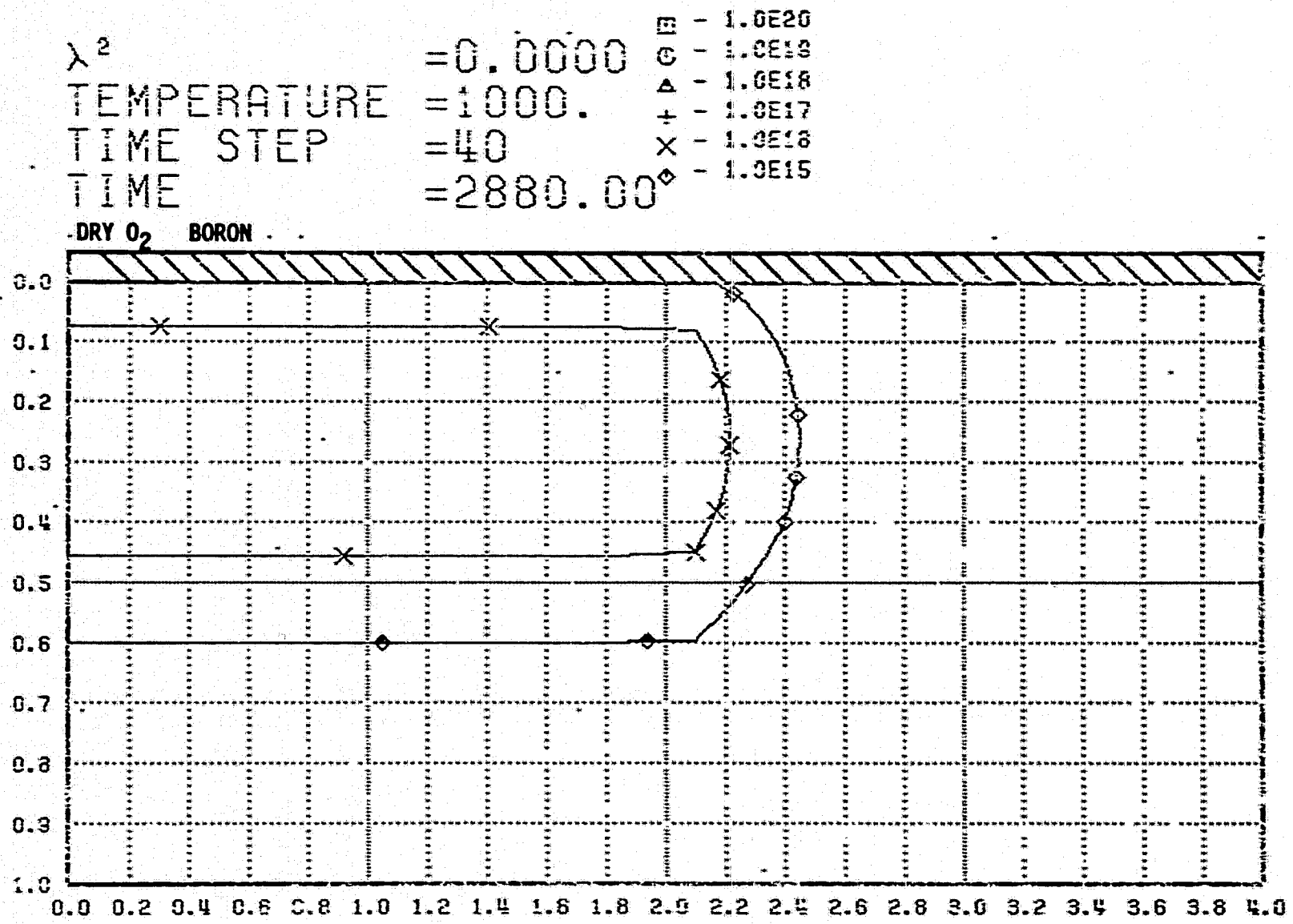
λ² =0.0000
TEMPERATURE =1000.
TIME STEP =40
TIME =2880.00
□ - 1.0E20
○ - 1.0E19
△ - 1.0E18
+ - 1.0E17
× - 1.0E16
◇ - 1.0E15
DRY O2 BORON
0.0
0.1
0.2
0.3
0.4
0.5
0.6
0.7
0.8
0.9
1.0
0.0 0.2 0.4 0.6 0.8 1.0 1.2 1.4 1.6 1.8 2.0 2.2 2.4 2.6 2.8 3.0 3.2 3.4 3.6 3.8 4.0

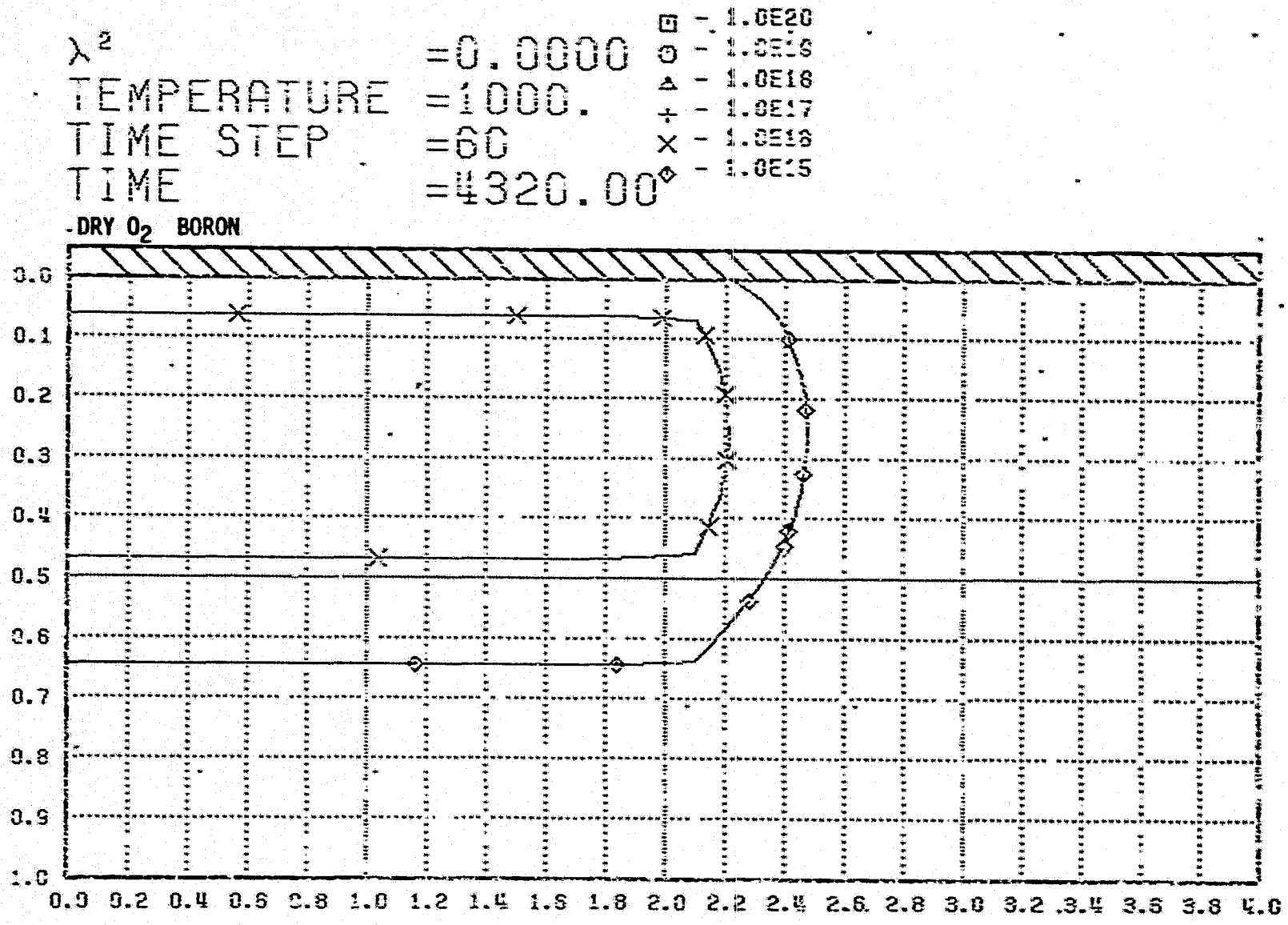
χ^2 =0.0000
TEMPERATURE =1000.
TIME STEP =60
TIME =#320.00
□ - 1.0E20
○ - 1.0E19
△ - 1.0E18
+ - 1.0E17
× - 1.0E16
◇ - 1.0E15
DRY O_2 BORON
0.0
0.1
0.2
0.3
0.4
0.5
0.6
0.7
0.8
0.9
1.0
0.0 0.2 0.4 0.6 0.8 1.0 1.2 1.4 1.6 1.8 2.0 2.2 2.4 2.6 2.8 3.0 3.2 3.4 3.6 3.8 4.0

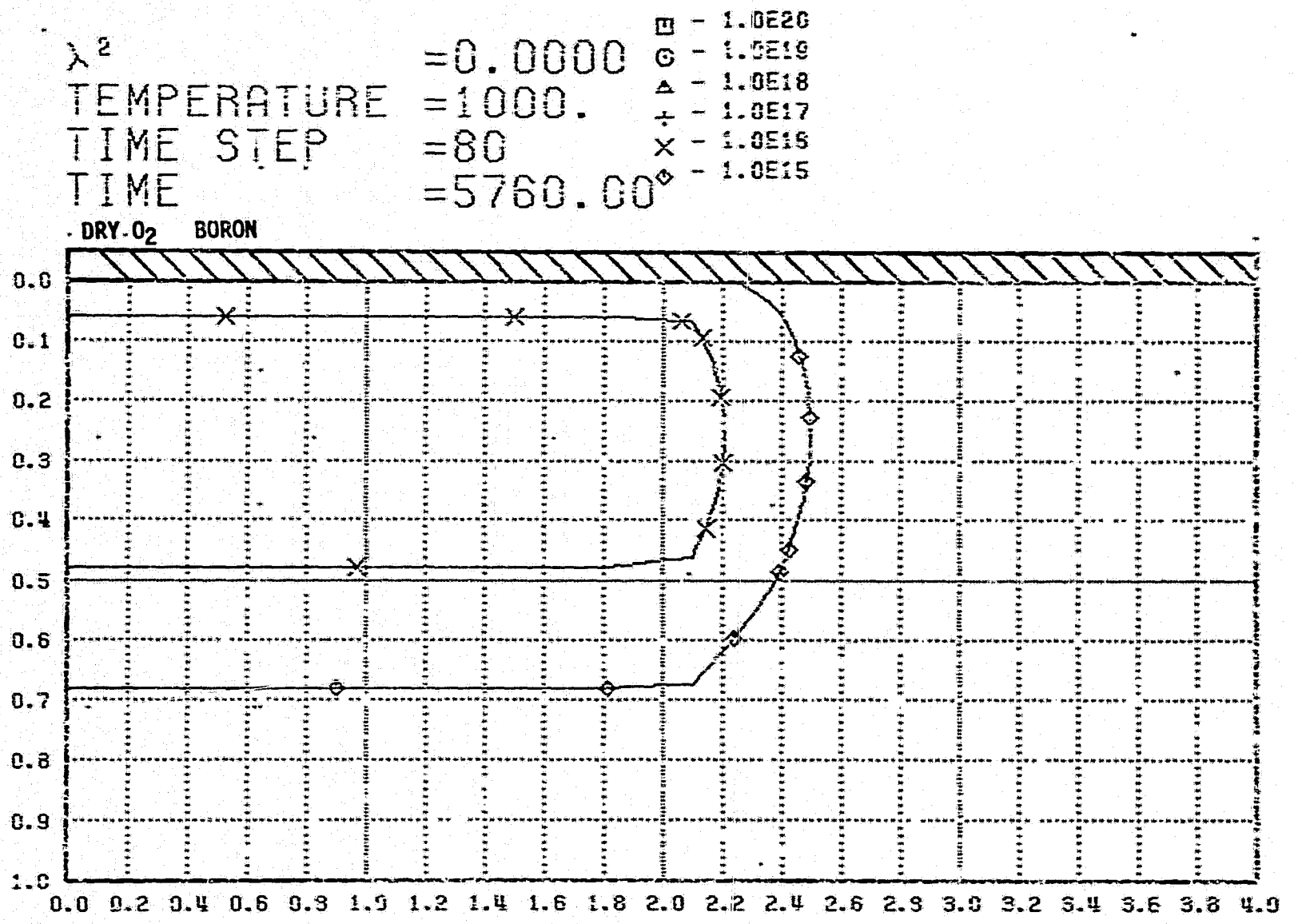
χ^2 =0.0000
TEMPERATURE =1000.
TIME STEP =80
TIME =5760.00
⊞ - 1.0E20
⊙ - 1.0E19
△ - 1.0E18
+ - 1.0E17
× - 1.0E16
◇ - 1.0E15
DRY-O2 BORON
0.0 0.1 0.2 0.3 0.4 0.5 0.6 0.7 0.8 0.9 1.0
0.0 0.2 0.4 0.6 0.8 1.0 1.2 1.4 1.6 1.8 2.0 2.2 2.4 2.6 2.8 3.0 3.2 3.4 3.6 3.8 4.0

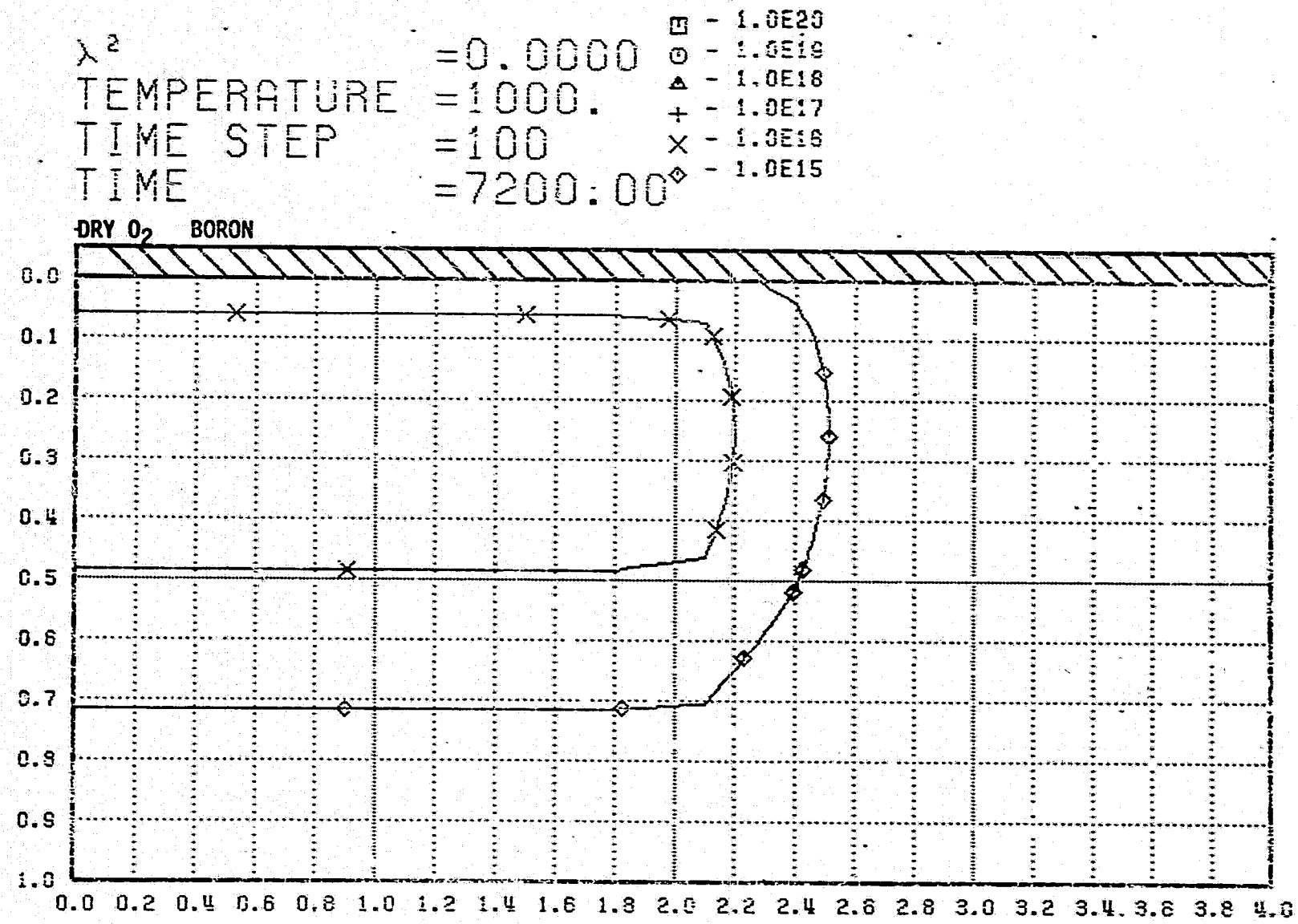
λ² =0.0000
TEMPERATURE =1000.
TIME STEP =100
TIME =7200:00
□ - 1.0E20
⊙ - 1.0E19
△ - 1.0E18
+ - 1.0E17
× - 1.0E16
◇ - 1.0E15
DRY O2 BORON
0.0
0.1
0.2
0.3
0.4
0.5
0.6
0.7
0.8
0.9
1.0
0.0 0.2 0.4 0.6 0.8 1.0 1.2 1.4 1.6 1.8 2.0 2.2 2.4 2.6 2.8 3.0 3.2 3.4 3.6 3.8 4.0

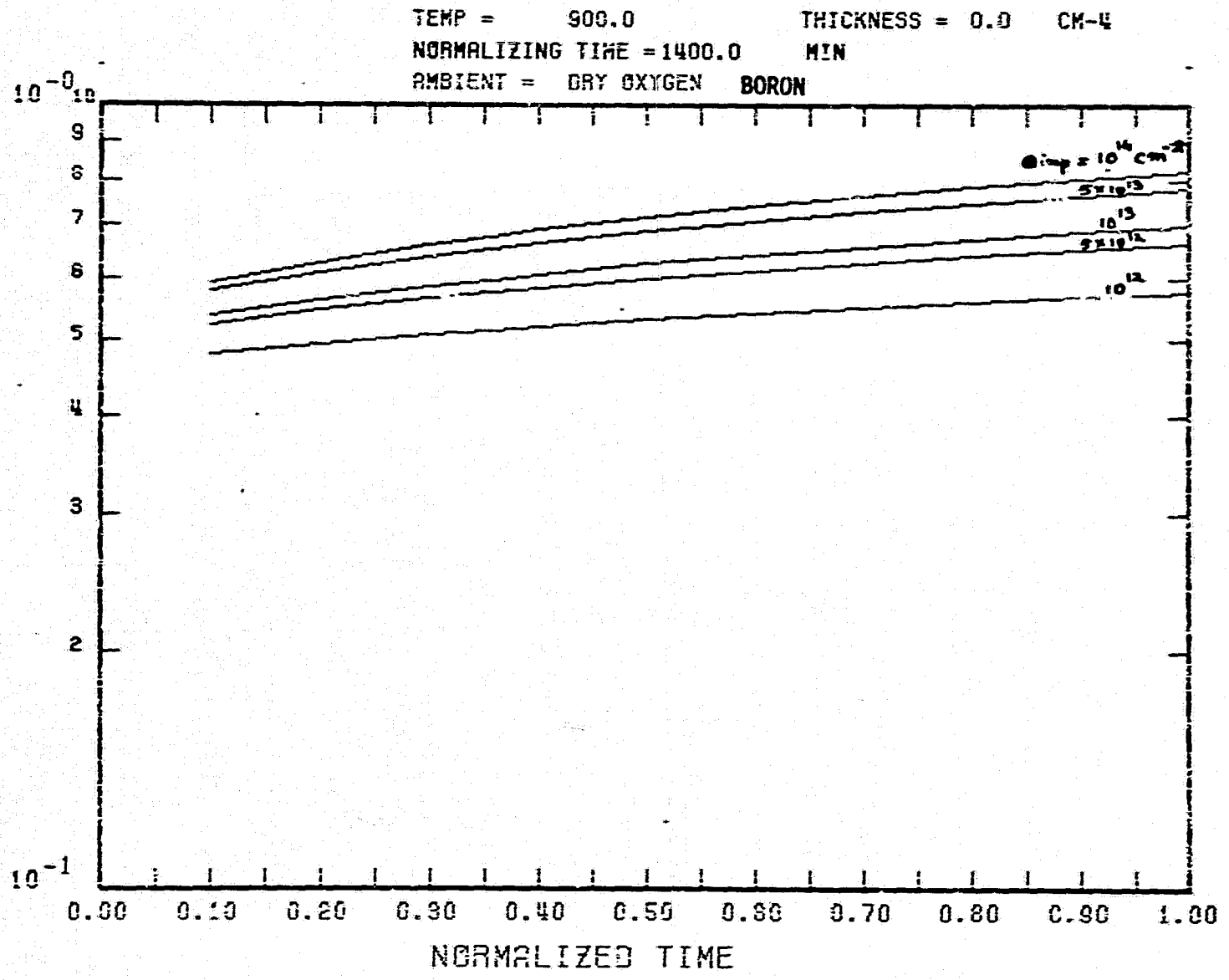
TEMP = 900.0 THICKNESS = 0.0 CM-4
NORMALIZING TIME = 1400.0 MIN
AMBIENT = DRY OXYGEN BORON
10^{-0}
10
9
8
7
6
5
4
3
2
10^{-1}
JUNCTION DEPTH
0.00 0.10 0.20 0.30 0.40 0.50 0.60 0.70 0.80 0.90 1.00
NORMALIZED TIME
10^{12}

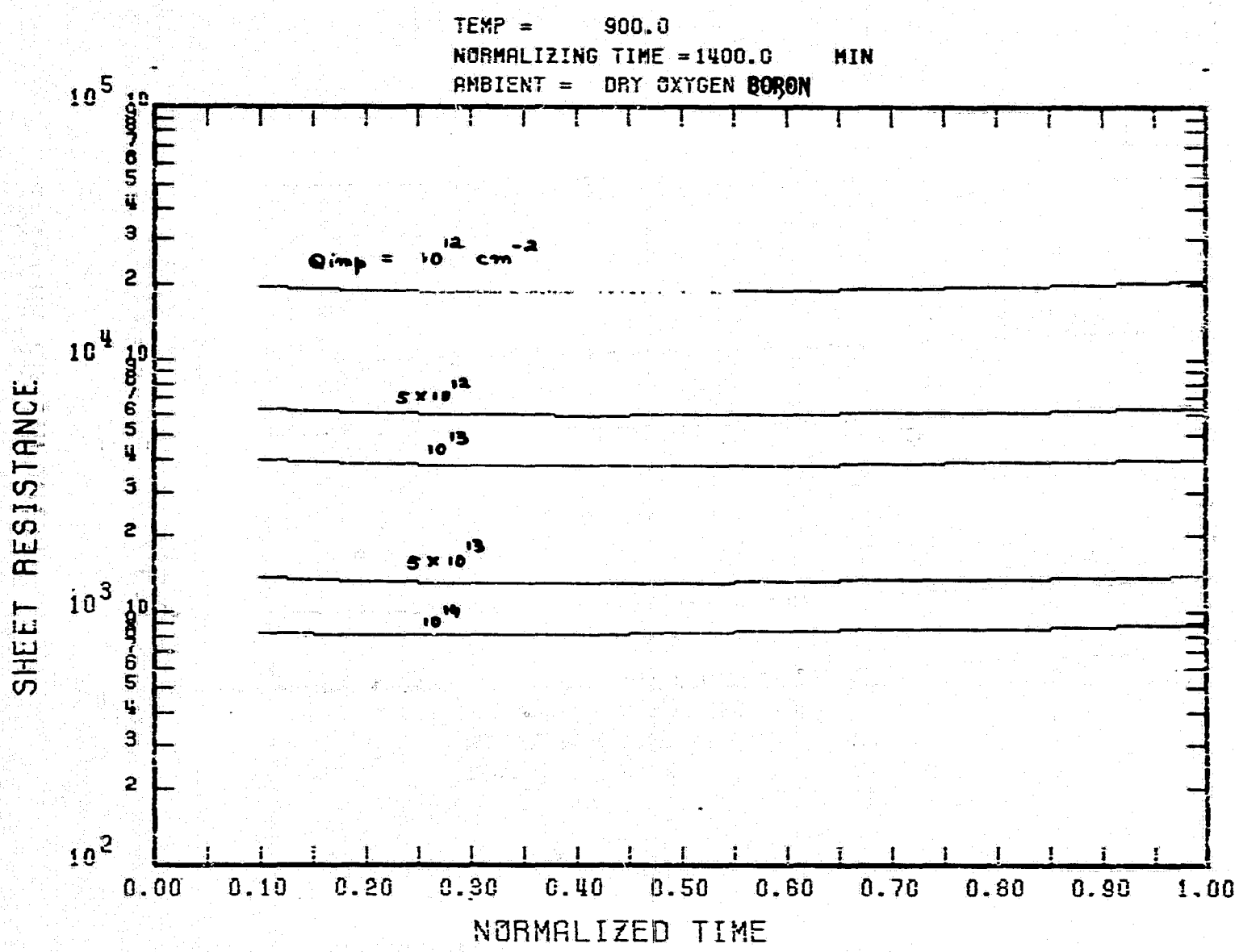
TEMP = 900.0
NORMALIZING TIME = 1400.0 MIN
AMBIENT = DRY OXYGEN BORON
Qimp = 10^12 cm^-2
5x10^12
10^13
5x10^13
10^14
SHEET RESISTANCE
NORMALIZED TIME
0.00
0.10
0.20
0.30
0.40
0.50
0.60
0.70
0.80
0.90
1.00

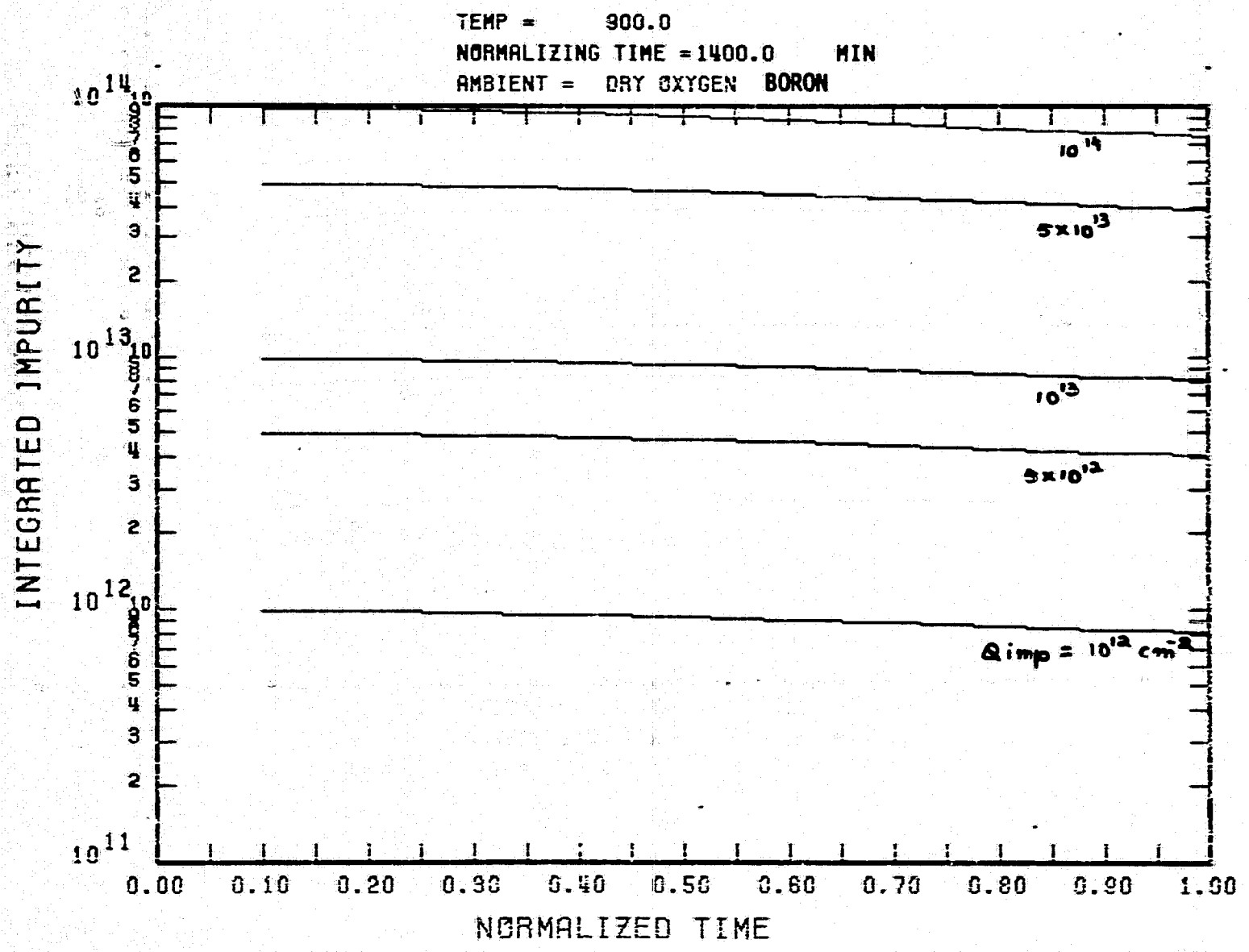
TEMP = 900.0
NORMALIZING TIME = 1400.0 MIN
AMBIENT = DRY OXYGEN BORON
INTEGRATED IMPURITY
NORMALIZED TIME
10^{14}
10^{13}
10^{12}
10^{11}
0.00
0.10
0.20
0.30
0.40
0.50
0.60
0.70
0.80
0.90
1.00
10^{14}
5×10^{13}
10^{13}
5×10^{12}
$Q_{imp} = 10^{12}\ cm^{-2}$

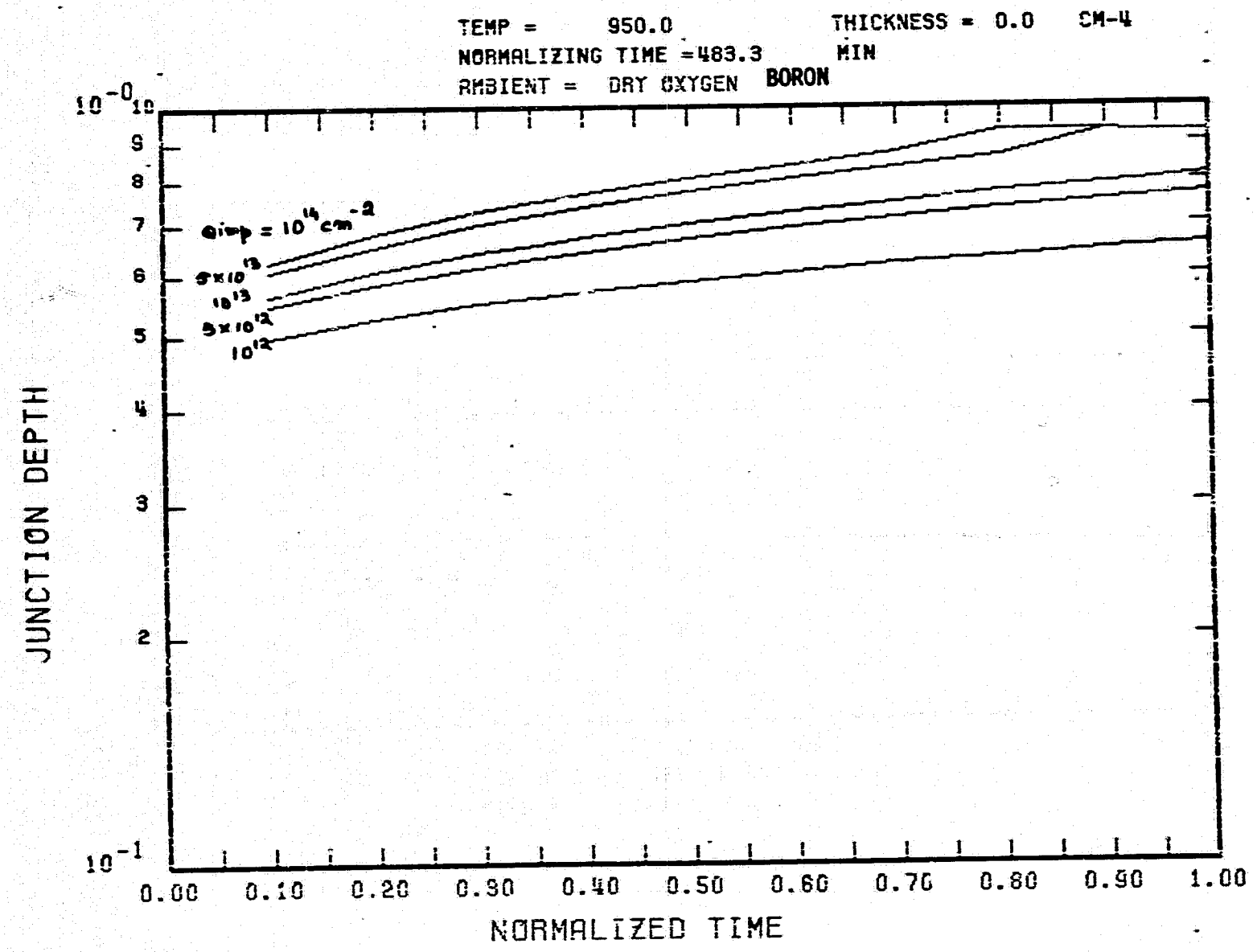
TEMP = 950.0 THICKNESS = 0.0 CM-4
NORMALIZING TIME =483.3 MIN
AMBIENT = DRY OXYGEN BORON
10^{-0}
10
9
8
7
6
5
4
3
2
10^{-1}
$Q_{imp} = 10^{14} cm^{-2}$
5×10^{13}
10^{13}
5×10^{12}
10^{12}
JUNCTION DEPTH
0.00
0.10
0.20
0.30
0.40
0.50
0.60
0.70
0.80
0.90
1.00
NORMALIZED TIME

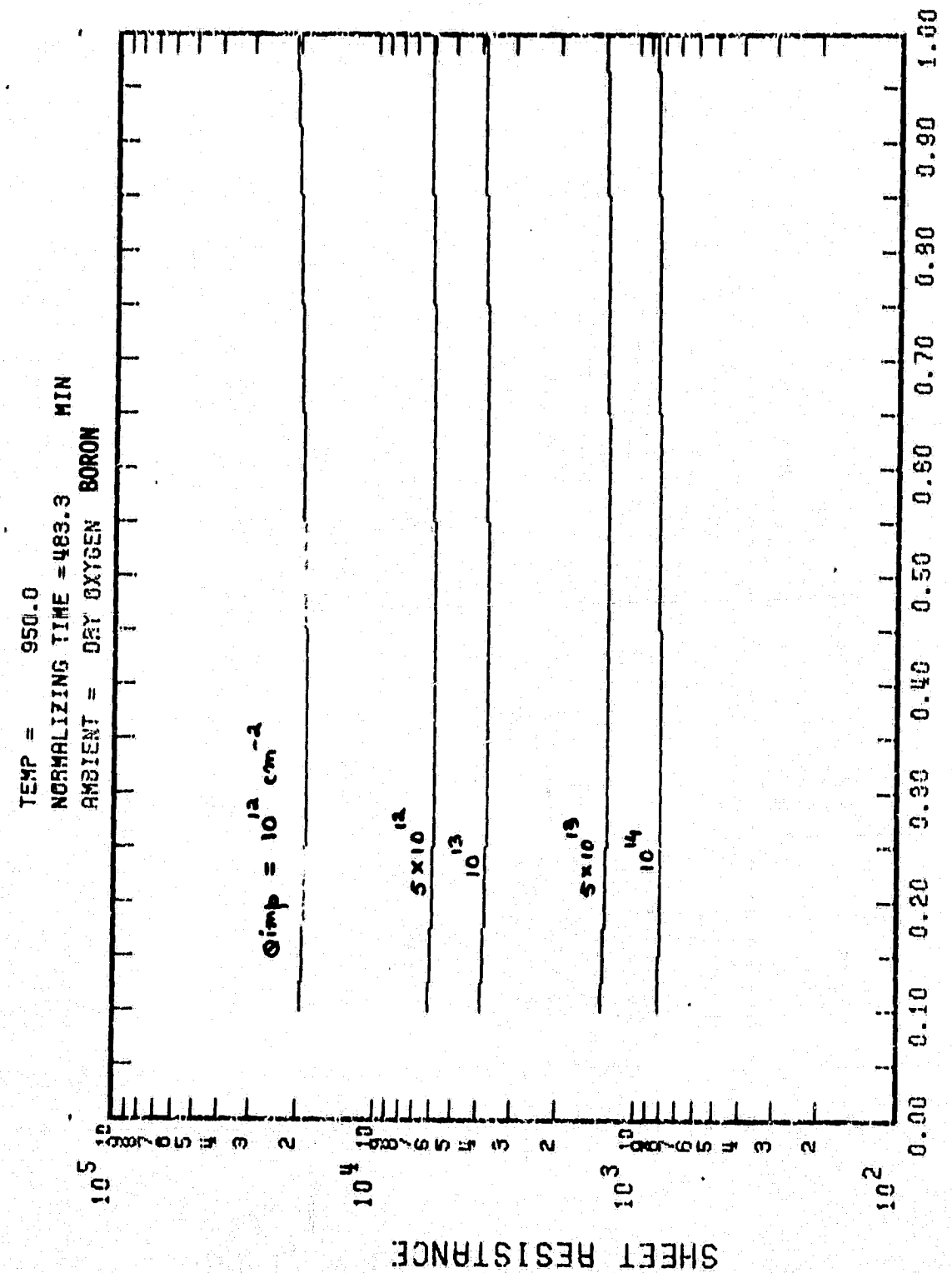
TEMP = 950.0
NORMALIZING TIME =483.3 MIN
AMBIENT = DRY OXYGEN BORON
Φimp = 10^12 cm^-2
5×10^12
10^13
5×10^13
10^14
SHEET RESISTANCE
NORMALIZED TIME
0.00
0.10
0.20
0.30
0.40
0.50
0.60
0.70
0.80
0.90
1.00

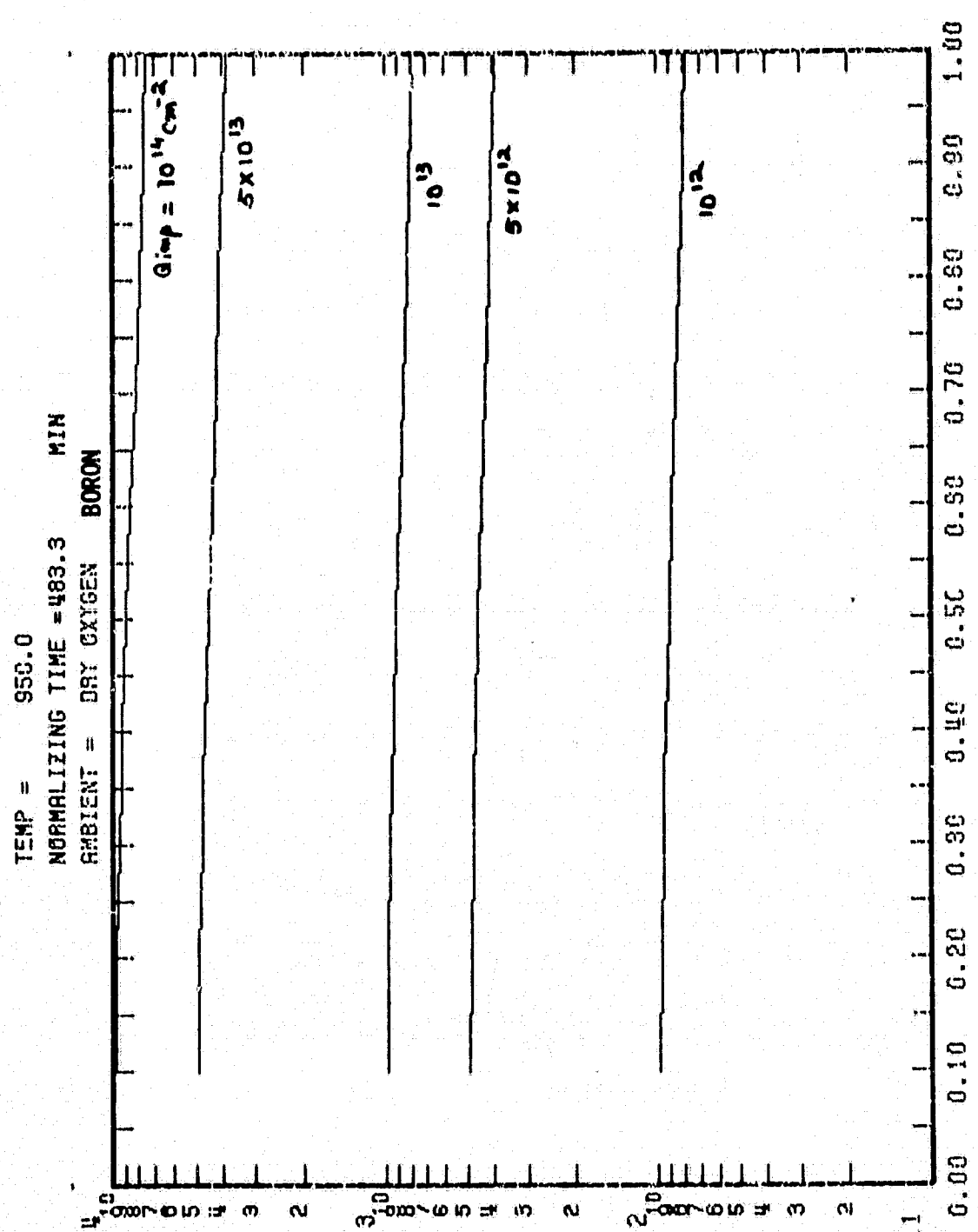
TEMP = 950.0
NORMALIZING TIME =483.3 MIN
AMBIENT = DRY OXYGEN BORON
Qimp = 10^14 cm^-2
5x10^13
10^13
5x10^12
10^12
INTEGRATED IMPURITY
NORMALIZED TIME
0.00
0.10
0.20
0.30
0.40
0.50
0.60
0.70
0.80
0.90
1.00

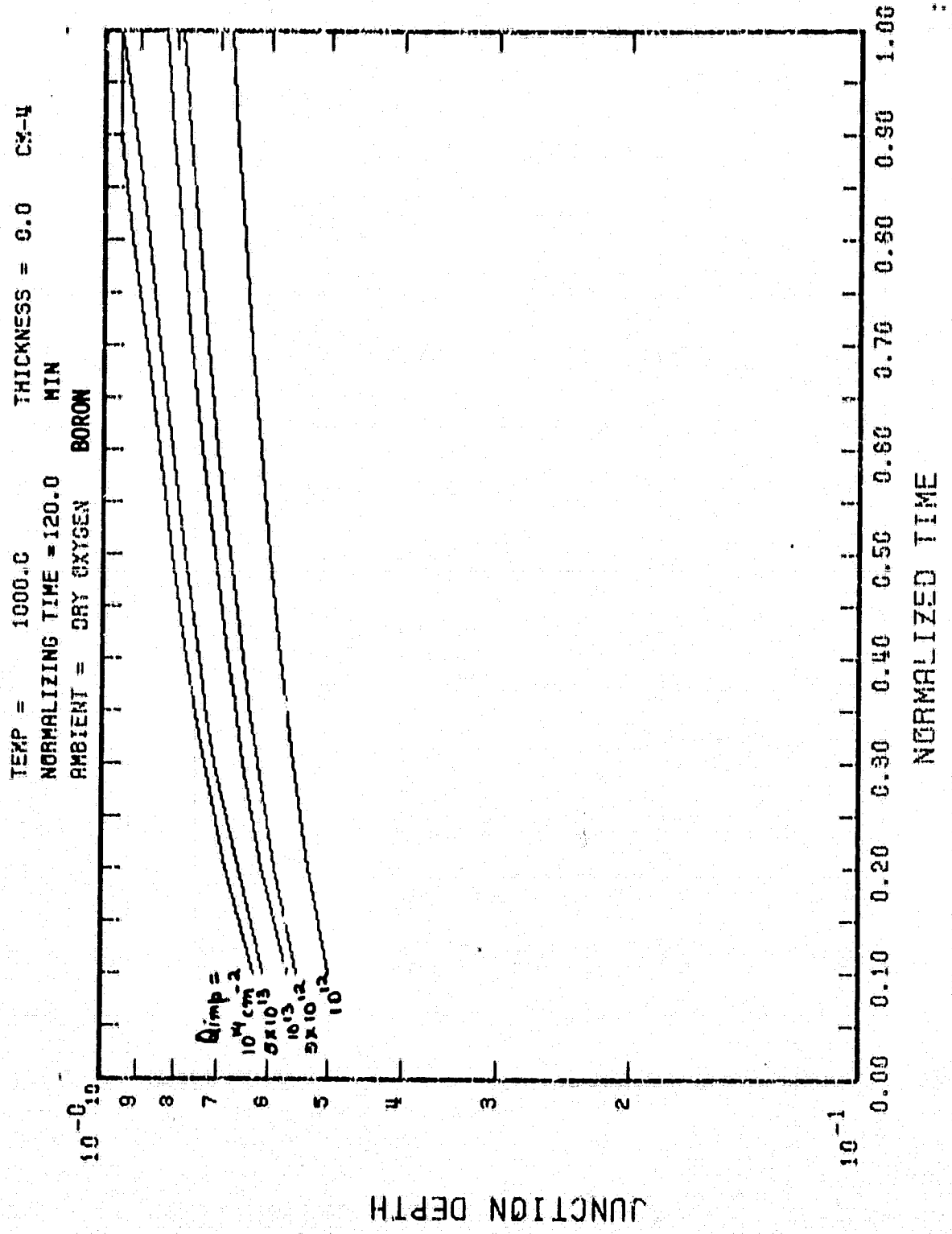
TEMP = 1000.0 THICKNESS = 0.0 CM-4
NORMALIZING TIME =120.0 MIN
AMBIENT = DRY OXYGEN BORON
Qimp =
10^{14} cm^{-2}
8×10^{13}
10^{13}
5×10^{12}
10^{12}
JUNCTION DEPTH
NORMALIZED TIME
10^{-0}
10^{-1}
9
8
7
6
5
4
3
2
0.00
0.10
0.20
0.30
0.40
0.50
0.60
0.70
0.80
0.90
1.00

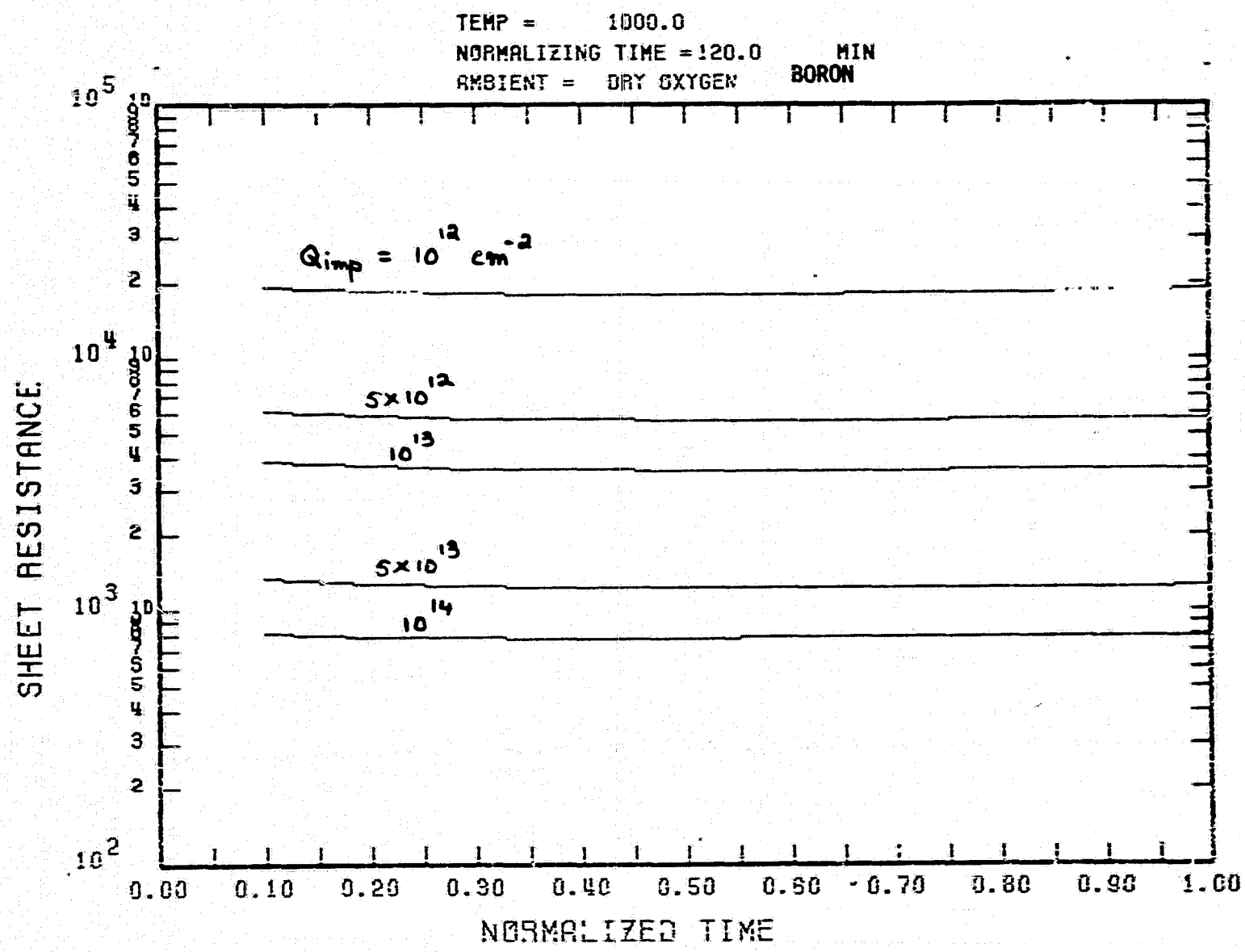
TEMP = 1000.0
NORMALIZING TIME = 120.0 MIN
AMBIENT = DRY OXYGEN
BORON
$Q_{imp} = 10^{12}$ cm^{-2}
5×10^{12}
10^{13}
5×10^{13}
10^{14}
SHEET RESISTANCE
10^5
10^4
10^3
10^2
0.00 0.10 0.20 0.30 0.40 0.50 0.60 0.70 0.80 0.90 1.00
NORMALIZED TIME

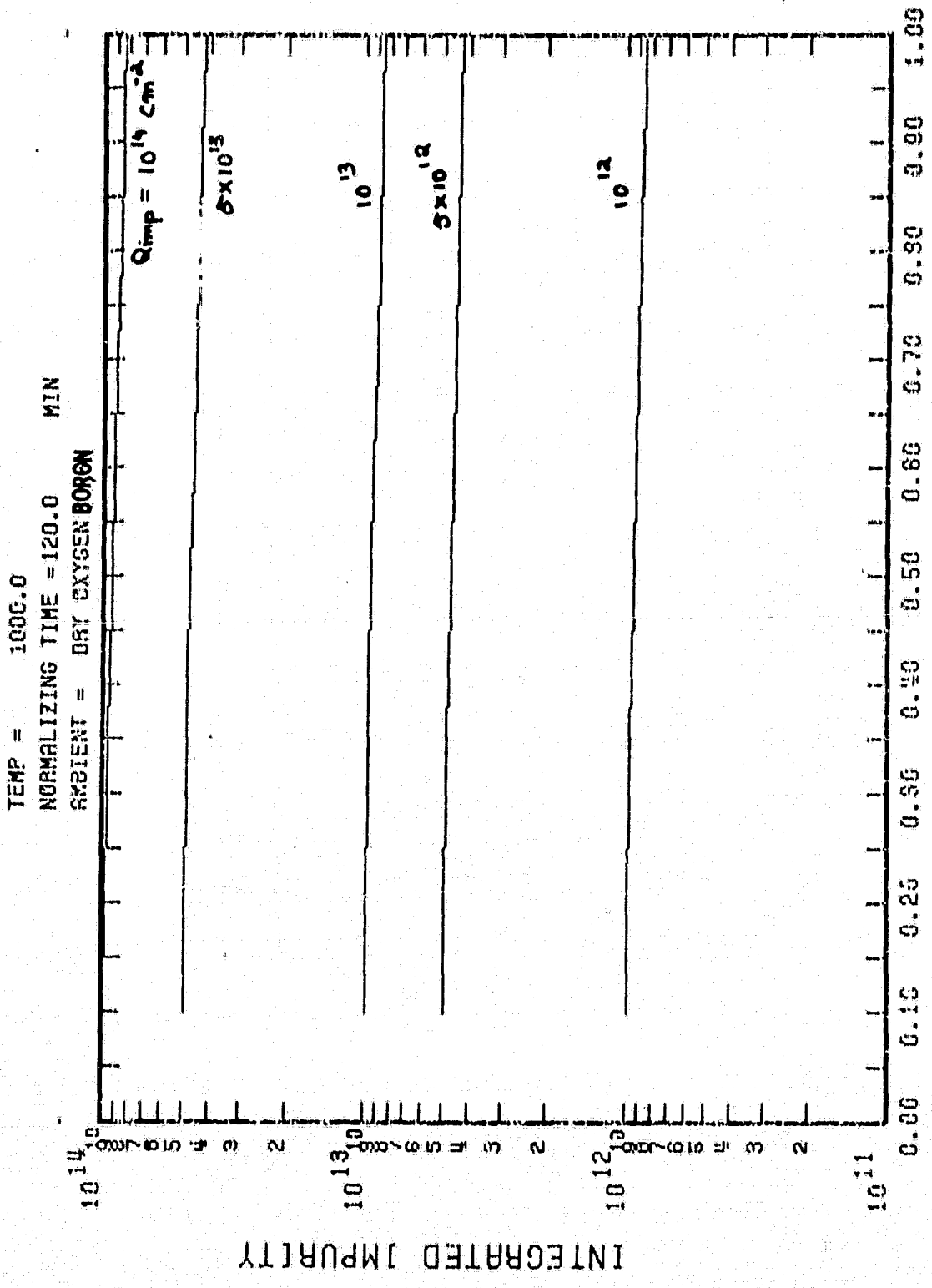
TEMP = 1000.0
NORMALIZING TIME = 120.0 MIN
AMBIENT = DRY OXYGEN BORON
Qimp = 10^14 cm^-2
5x10^13
10^13
5x10^12
10^12
INTEGRATED IMPURITY
NORMALIZED TIME
0.00
0.13
0.25
0.38
0.50
0.63
0.75
0.88
1.00

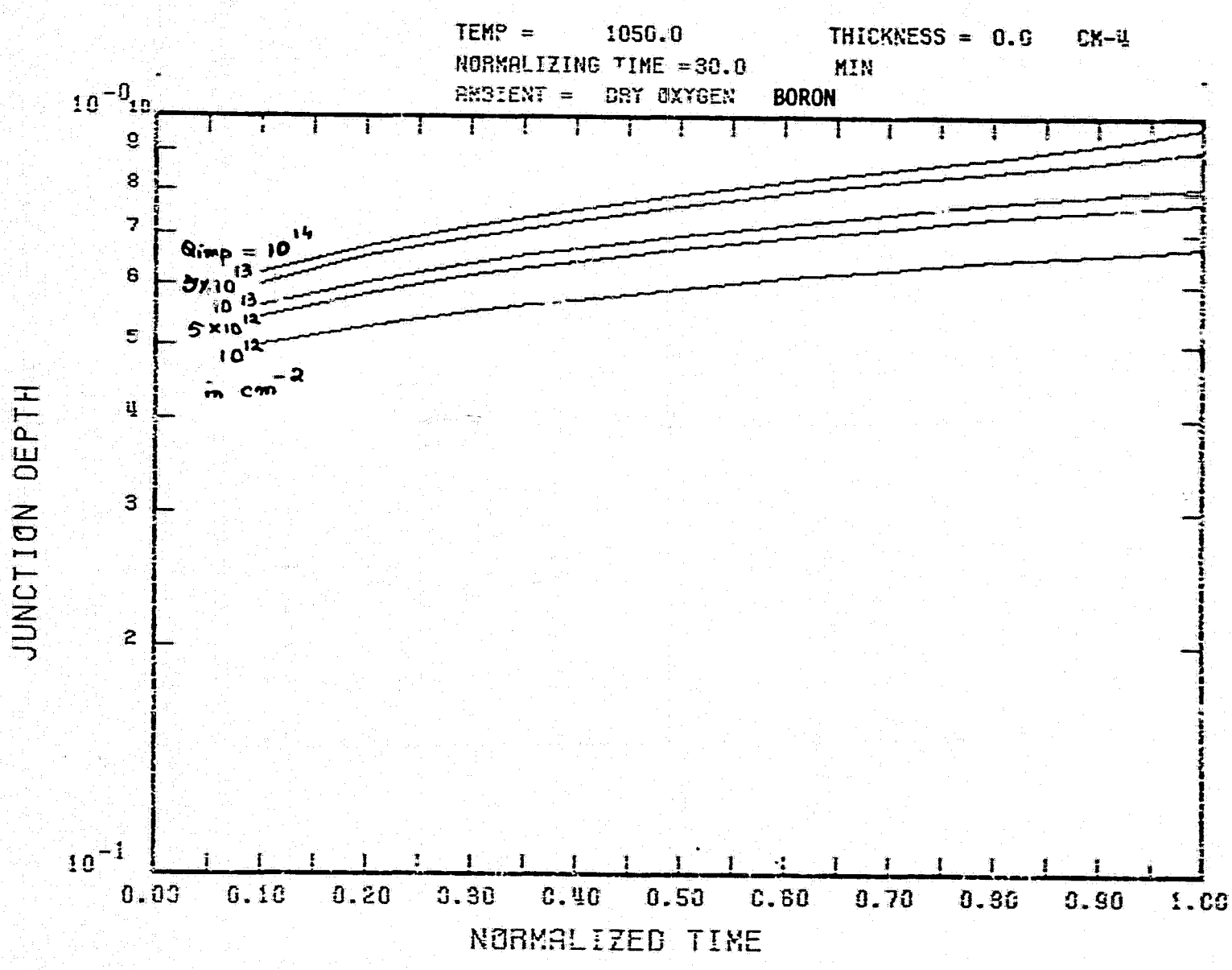
TEMP = 1050.0 THICKNESS = 0.0 CM-4
NORMALIZING TIME =30.0 MIN
AMBIENT = DRY OXYGEN BORON
JUNCTION DEPTH
NORMALIZED TIME
0.00
0.10
0.20
0.30
0.40
0.50
0.60
0.70
0.80
0.90
1.00
Qimp = 10^14
5x10^13
10^13
5x10^12
10^12
in cm^-2

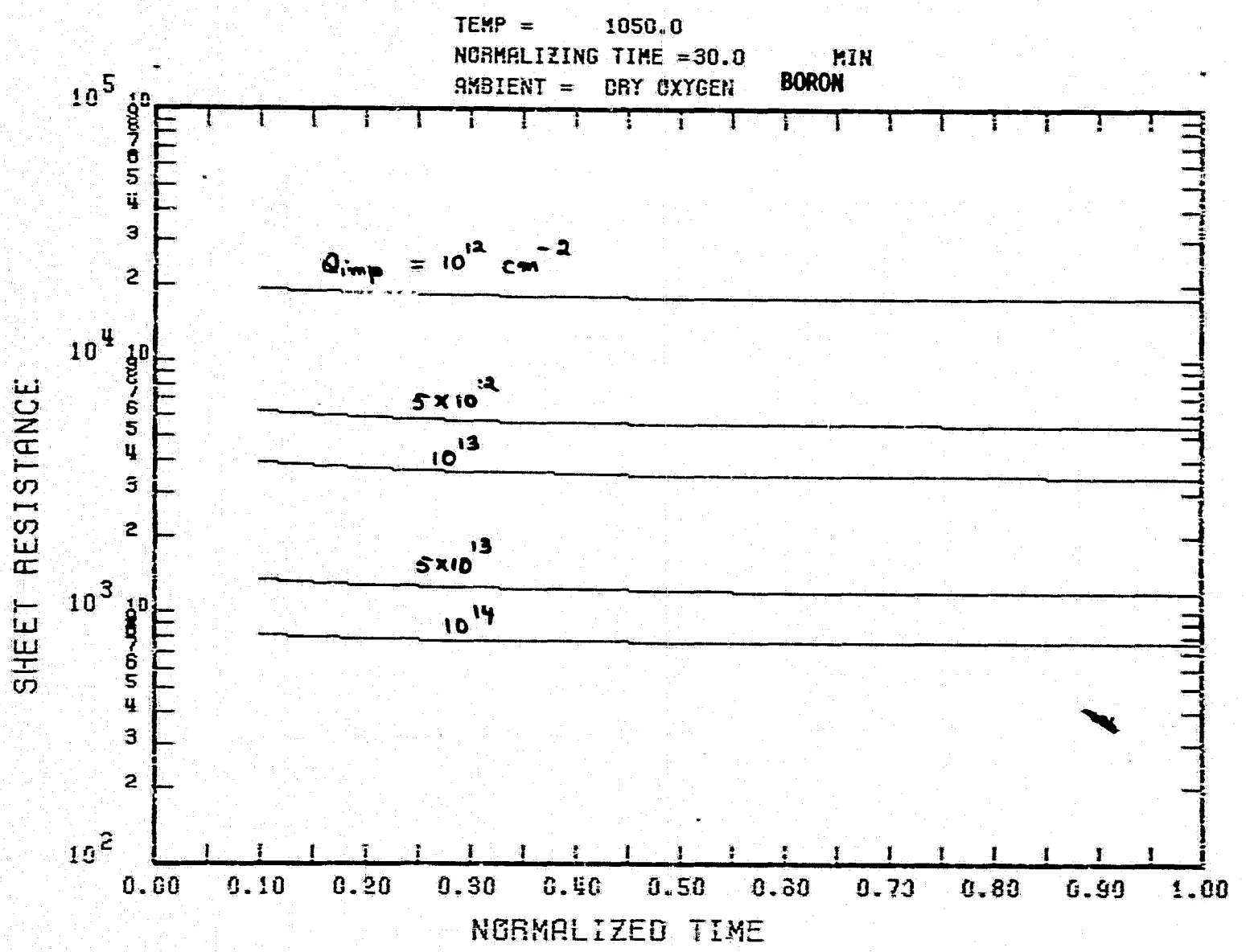
TEMP = 1050.0
NORMALIZING TIME =30.0 MIN
AMBIENT = DRY OXYGEN
BORON
$Q_{imp} = 10^{12}$ cm^{-2}
5×10^{12}
10^{13}
5×10^{13}
10^{14}
SHEET RESISTANCE
NORMALIZED TIME
10^5
10^4
10^3
10^2
0.00
0.10
0.20
0.30
0.40
0.50
0.60
0.70
0.80
0.90
1.00

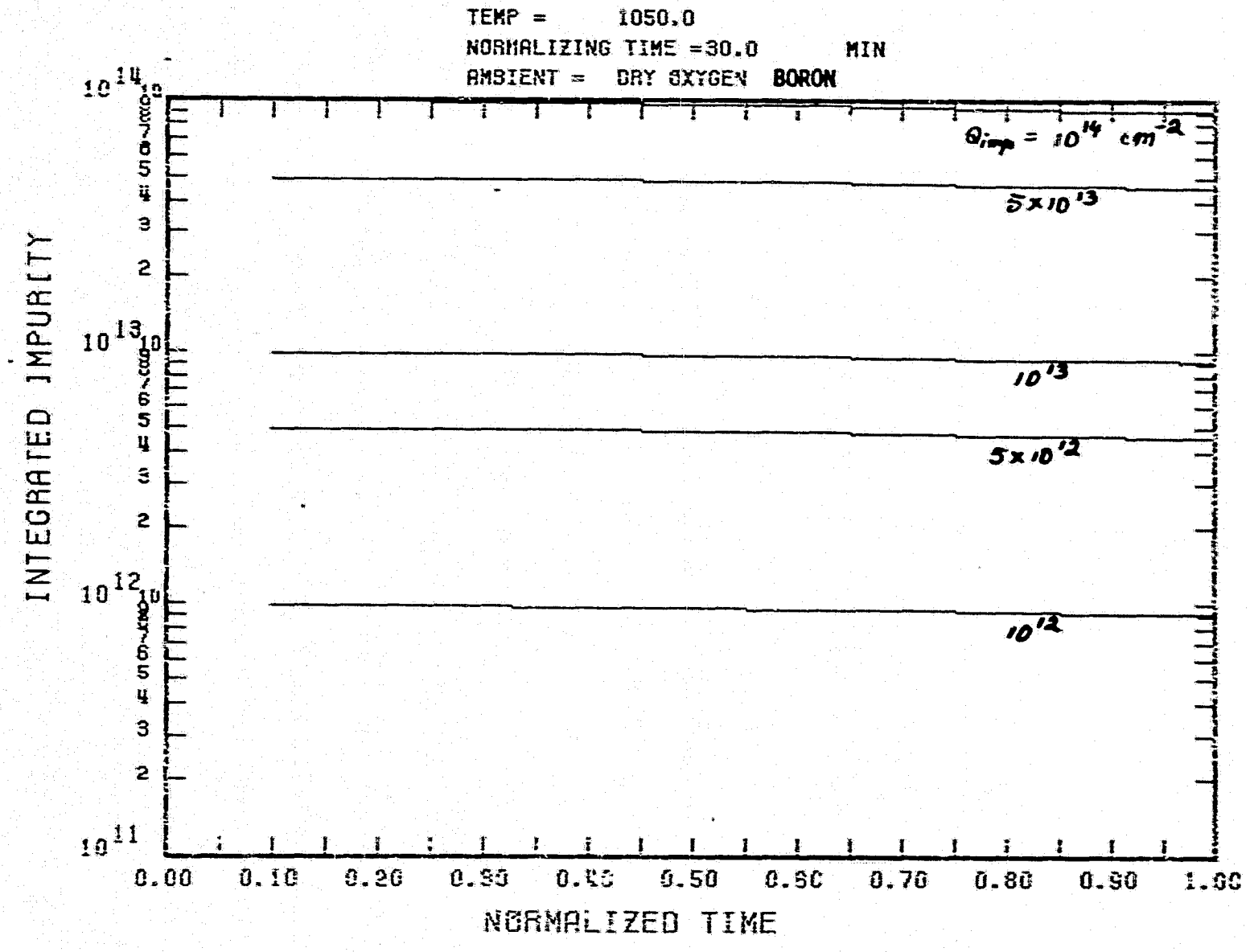
TEMP = 1050.0
NORMALIZING TIME =30.0 MIN
AMBIENT = DRY OXYGEN BORON
$Q_{imp} = 10^{14}$ cm^{-2}
5×10^{13}
10^{13}
5×10^{12}
10^{12}
INTEGRATED IMPURITY
10^{14}
10^{13}
10^{12}
10^{11}
0.00 0.10 0.20 0.30 0.40 0.50 0.60 0.70 0.80 0.90 1.00
NORMALIZED TIME

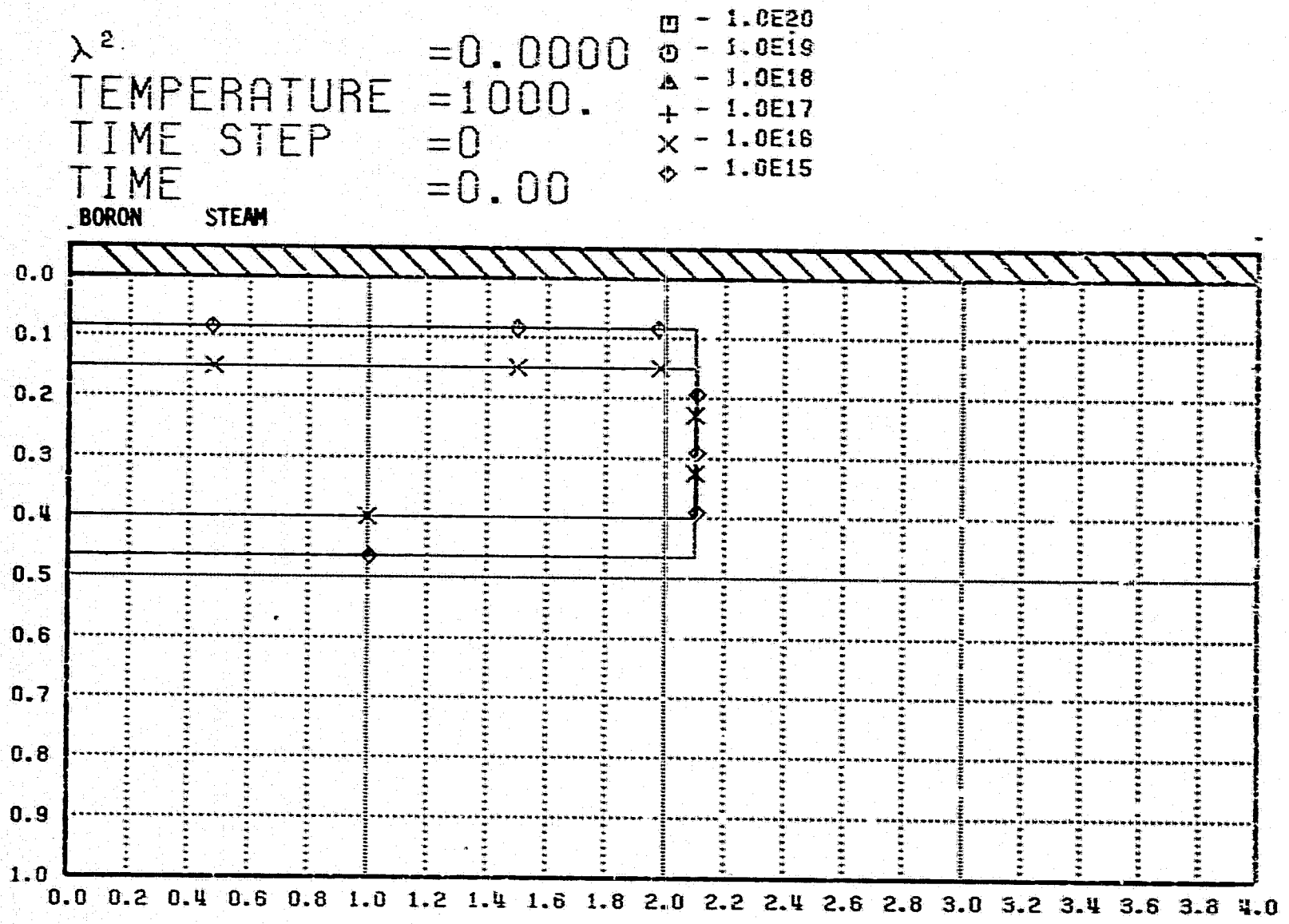
λ² =0.0000
TEMPERATURE =1000.
TIME STEP =0
TIME =0.00
□ - 1.0E20
○ - 1.0E19
△ - 1.0E18
+ - 1.0E17
× - 1.0E16
◇ - 1.0E15
BORON STEAM
0.0
0.1
0.2
0.3
0.4
0.5
0.6
0.7
0.8
0.9
1.0
0.0 0.2 0.4 0.6 0.8 1.0 1.2 1.4 1.6 1.8 2.0 2.2 2.4 2.6 2.8 3.0 3.2 3.4 3.6 3.8 4.0

X
TEMPERATURE = 0.0000
TIME STEP = 1000.
TIME = 1440.00
1.0E20
1.0E19
1.0E18
1.0E17
1.0E16
1.0E15
BORON
STEAM
0.0 0.2 0.4 0.6 0.8 1.0 1.2 1.4 1.6 1.8 2.0 2.2 2.4 2.5 2.8 3.0 3.2 3.4 3.6 3.8 4.0
0.0 0.1 0.2 0.3 0.4 0.5 0.6 0.7 0.8 0.9 1.0

C-2

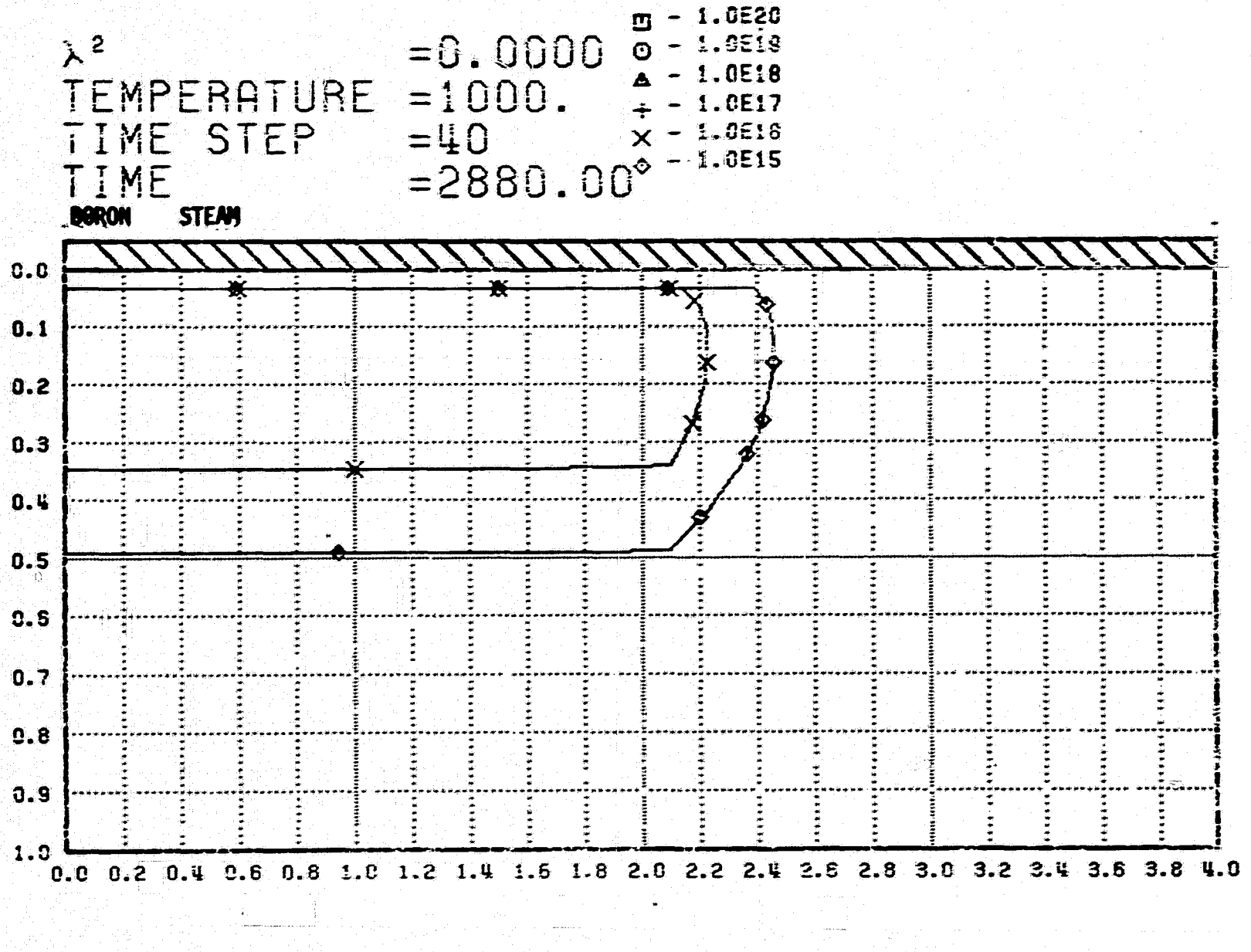
λ² =0.0000
TEMPERATURE =1000.
TIME STEP =40
TIME =2880.00
□ - 1.0E20
○ - 1.0E19
△ - 1.0E18
+ - 1.0E17
× - 1.0E16
◇ - 1.0E15
BORON STEAM
0.0
0.1
0.2
0.3
0.4
0.5
0.6
0.7
0.8
0.9
1.0
0.0 0.2 0.4 0.6 0.8 1.0 1.2 1.4 1.6 1.8 2.0 2.2 2.4 2.6 2.8 3.0 3.2 3.4 3.6 3.8 4.0

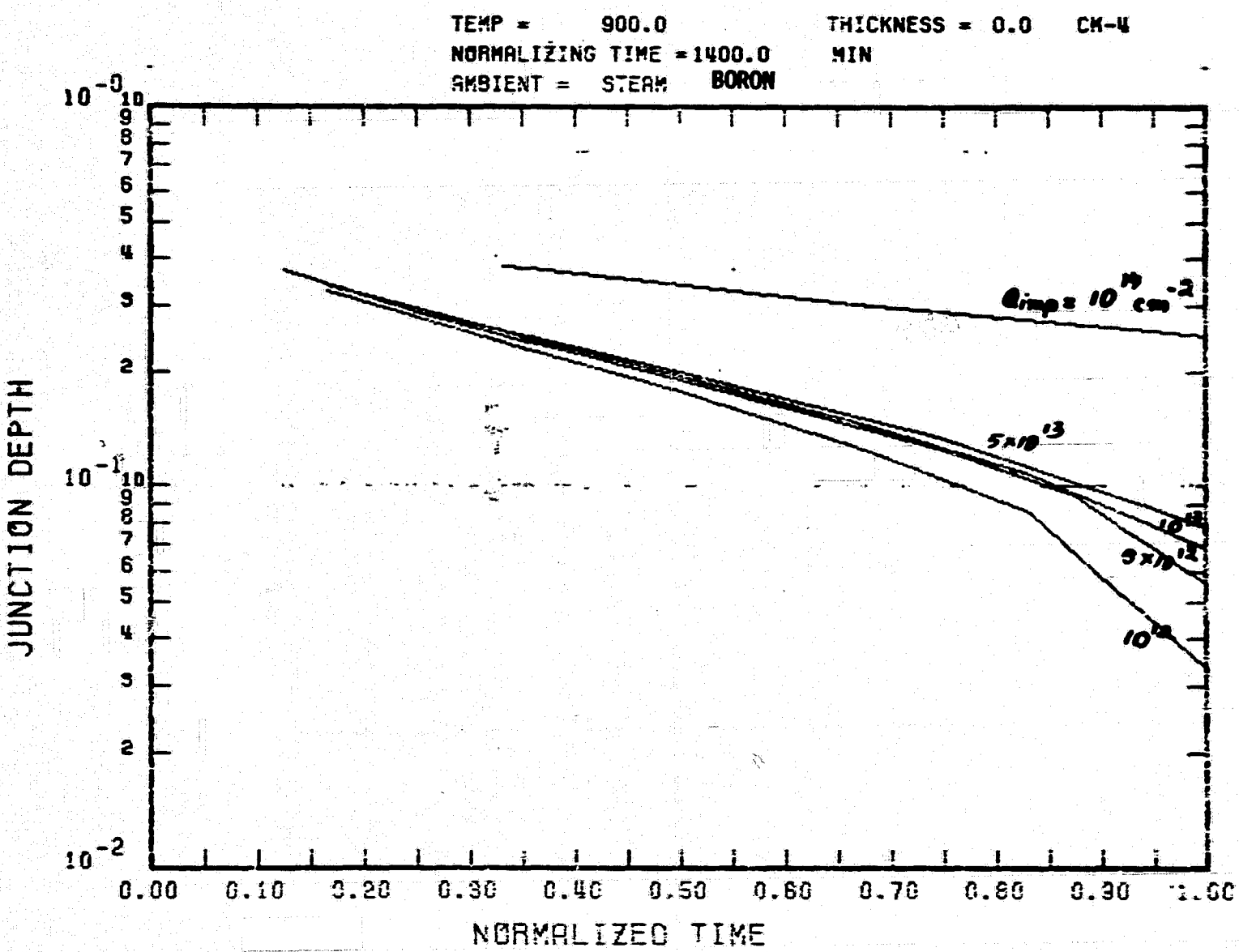
TEMP = 900.0 THICKNESS = 0.0 CM-4
NORMALIZING TIME = 1400.0 MIN
AMBIENT = STEAM BORON
JUNCTION DEPTH
NORMALIZED TIME
10^{-0}
10^{-1}
10^{-2}
0.00
0.10
0.20
0.30
0.40
0.50
0.60
0.70
0.80
0.90
1.00
$Q_{imp} = 10^{14}\ cm^{-2}$
5×10^{13}
10^{13}
9×10^{12}
10^{12}

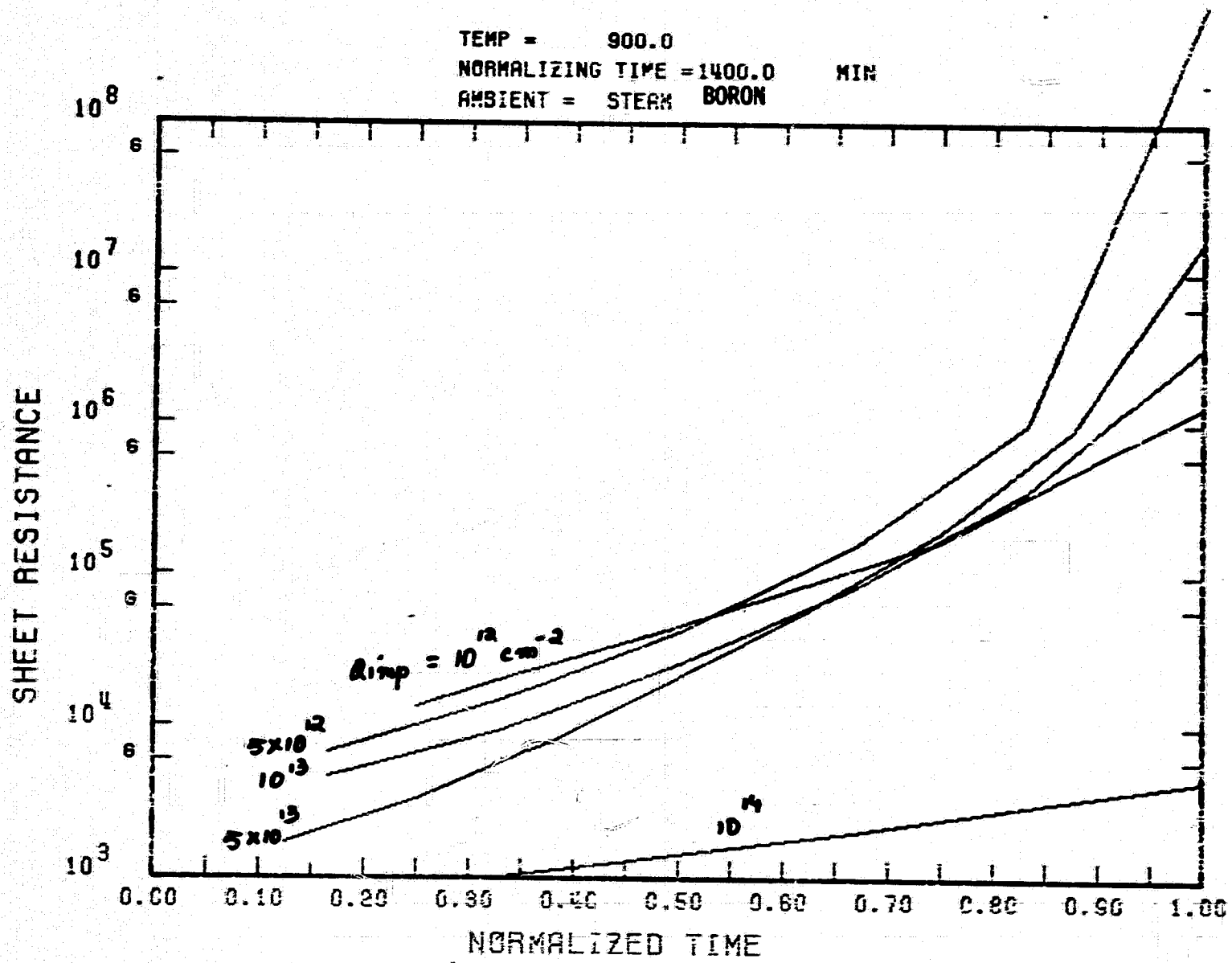
TEMP = 900.0
NORMALIZING TIME = 1400.0 MIN
AMBIENT = STEAM BORON
SHEET RESISTANCE
NORMALIZED TIME
10^8
10^7
10^6
10^5
10^4
10^3
0.00
0.10
0.20
0.30
0.40
0.50
0.60
0.70
0.80
0.90
1.00
$R_{imp} = 10^{12}$ cm^{-2}
5×10^{12}
10^{13}
5×10^{13}
10^{14}

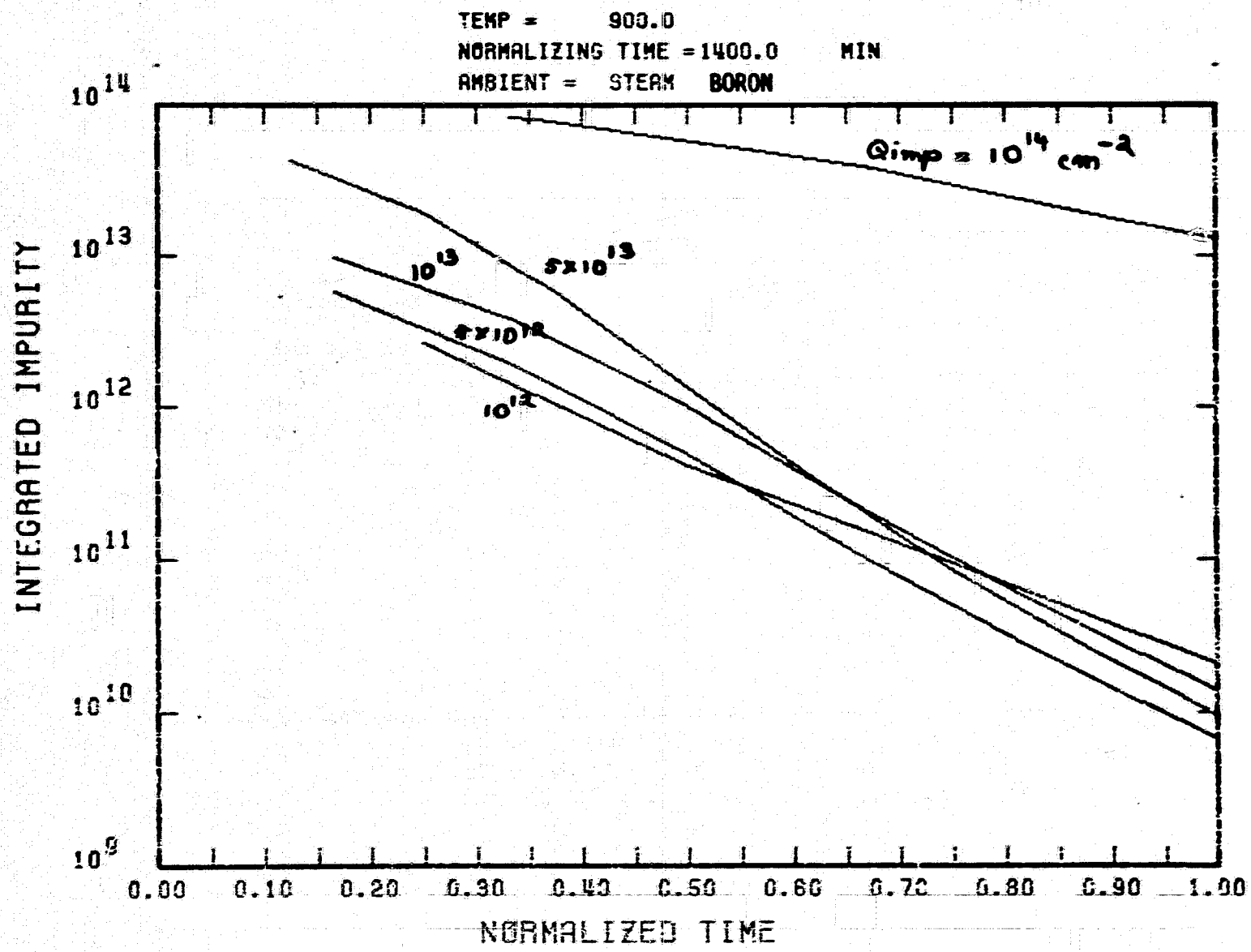
TEMP = 900.0
NORMALIZING TIME = 1400.0 MIN
AMBIENT = STEAM BORON
Qimp = 10^14 cm^-2
5x10^13
10^13
5x10^12
10^12
INTEGRATED IMPURITY
10^14
10^13
10^12
10^11
10^10
10^9
0.00
0.10
0.20
0.30
0.40
0.50
0.60
0.70
0.80
0.90
1.00
NORMALIZED TIME

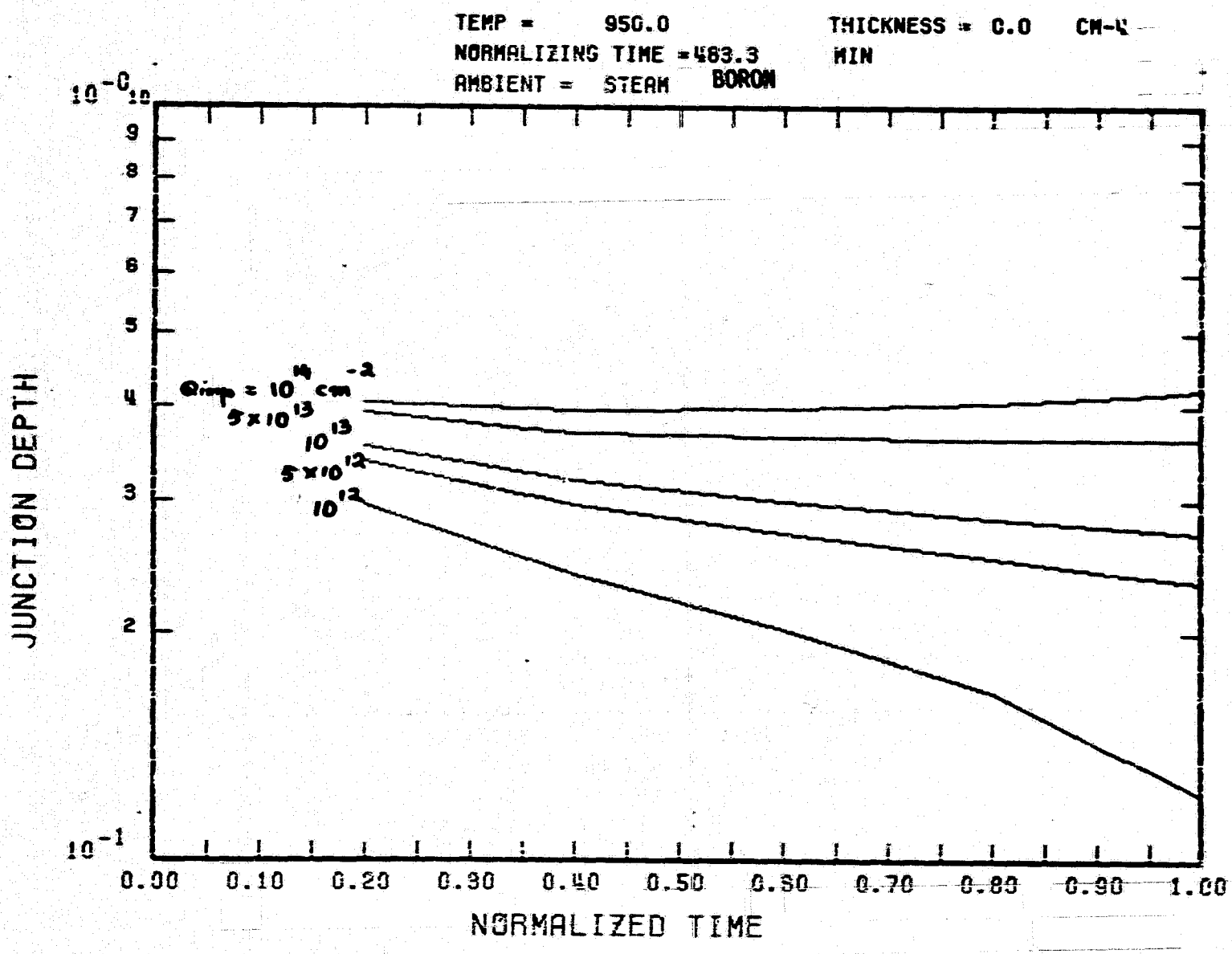
TEMP = 950.0
THICKNESS = 0.0 CM-4
NORMALIZING TIME = 483.3 MIN
AMBIENT = STEAM
BORON
10^{-C} 10
9
8
7
6
5
4
3
2
10^{-1}
JUNCTION DEPTH
$Q_{imp} = 10^{14}$ cm^{-2}
5×10^{13}
10^{13}
5×10^{12}
10^{12}
0.00
0.10
0.20
0.30
0.40
0.50
0.60
0.70
0.80
0.90
1.00
NORMALIZED TIME

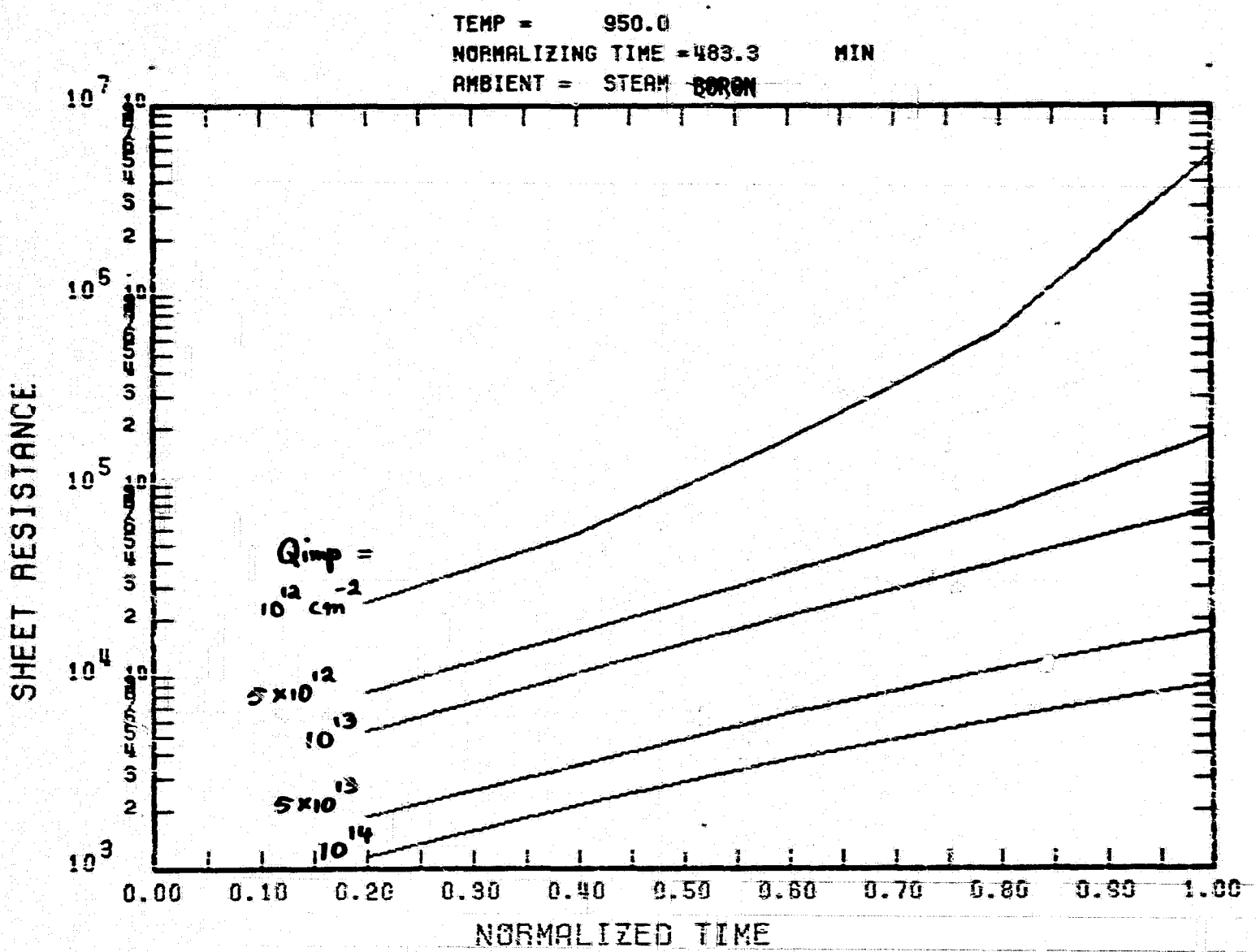
TEMP = 950.0
NORMALIZING TIME =483.3 MIN
AMBIENT = STEAM BORON
SHEET RESISTANCE
NORMALIZED TIME
Qimp =
10^12 cm^-2
5x10^12
10^13
5x10^13
10^14
10^7
10^6
10^5
10^4
10^3
0.00
0.10
0.20
0.30
0.40
0.50
0.60
0.70
0.80
0.90
1.00

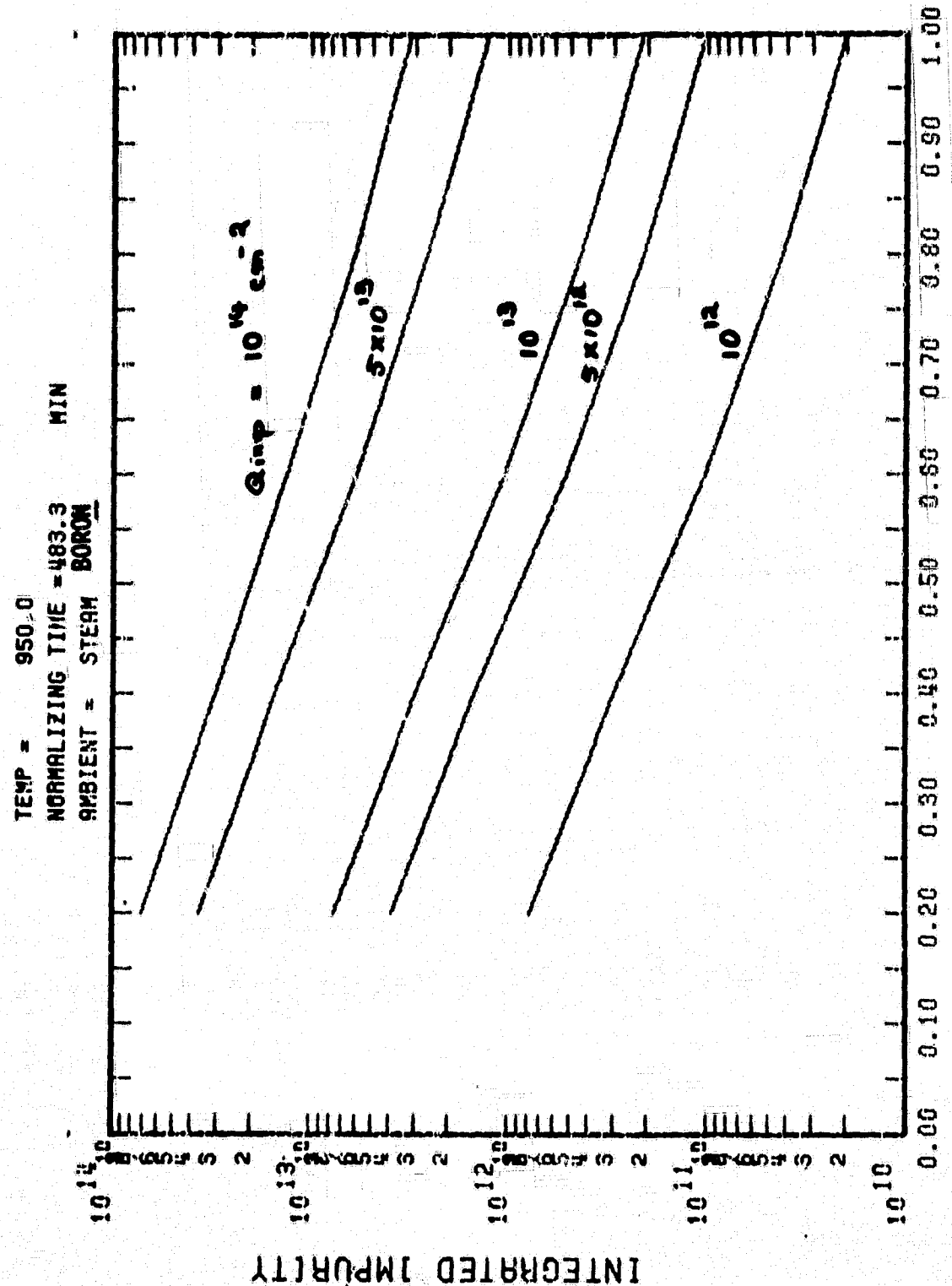
TEMP = 950.0
NORMALIZING TIME =483.3 MIN
AMBIENT = STEAM BORON
Qinp = 10^14 cm^-2
5x10^13
10^13
5x10^12
10^12
INTEGRATED IMPURITY
NORMALIZED TIME
0.00
0.10
0.20
0.30
0.40
0.50
0.60
0.70
0.80
0.90
1.00

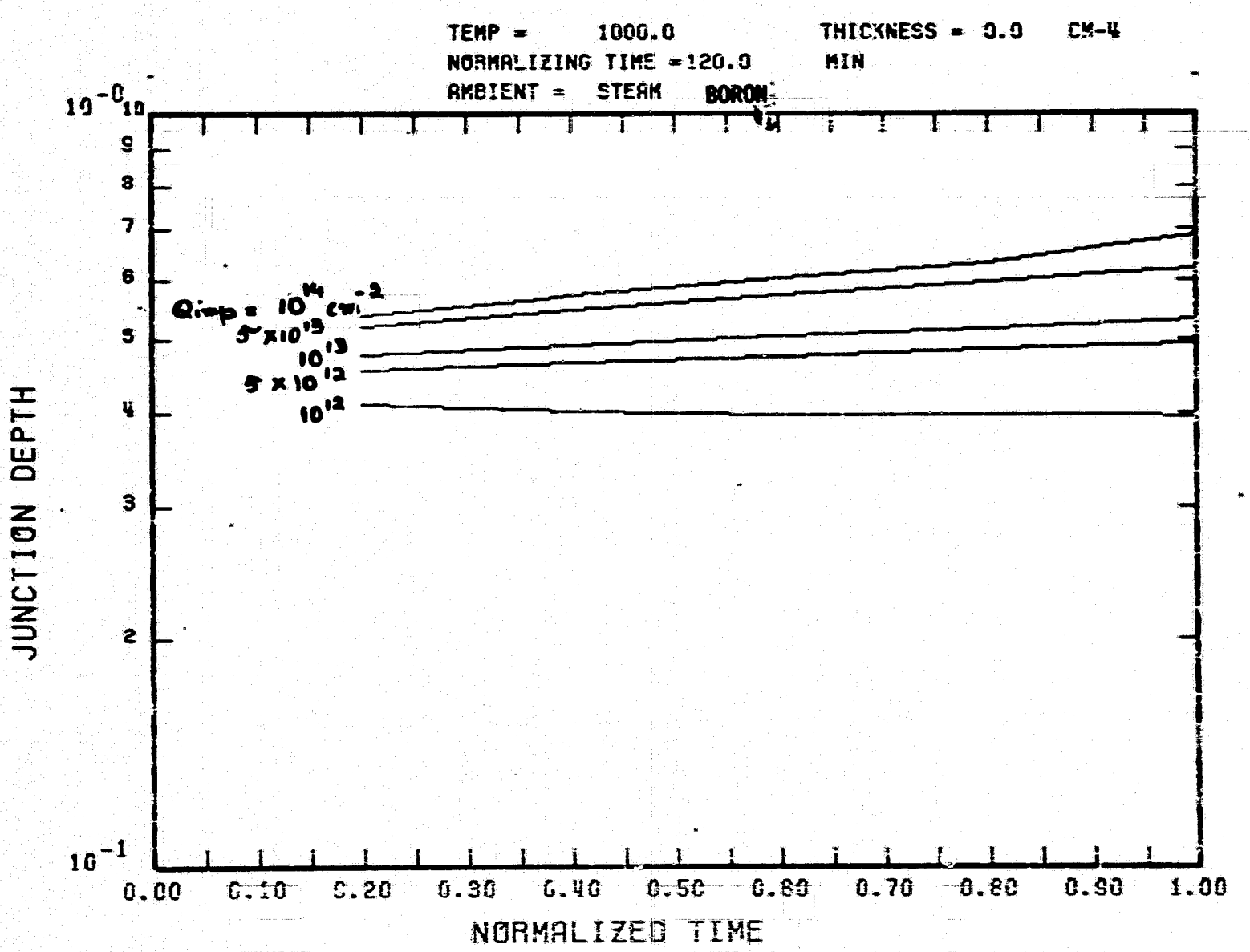
TEMP = 1000.0 THICKNESS = 0.0 CM-4
NORMALIZING TIME =120.0 MIN
AMBIENT = STEAM BORON
10^{-0}
10
9
8
7
6
5
4
3
2
10^{-1}
$Q_{imp} = 10^{14}$ (cm)$^{-2}$
5×10^{13}
10^{13}
5×10^{12}
10^{12}
JUNCTION DEPTH
0.00 0.10 0.20 0.30 0.40 0.50 0.60 0.70 0.80 0.90 1.00
NORMALIZED TIME

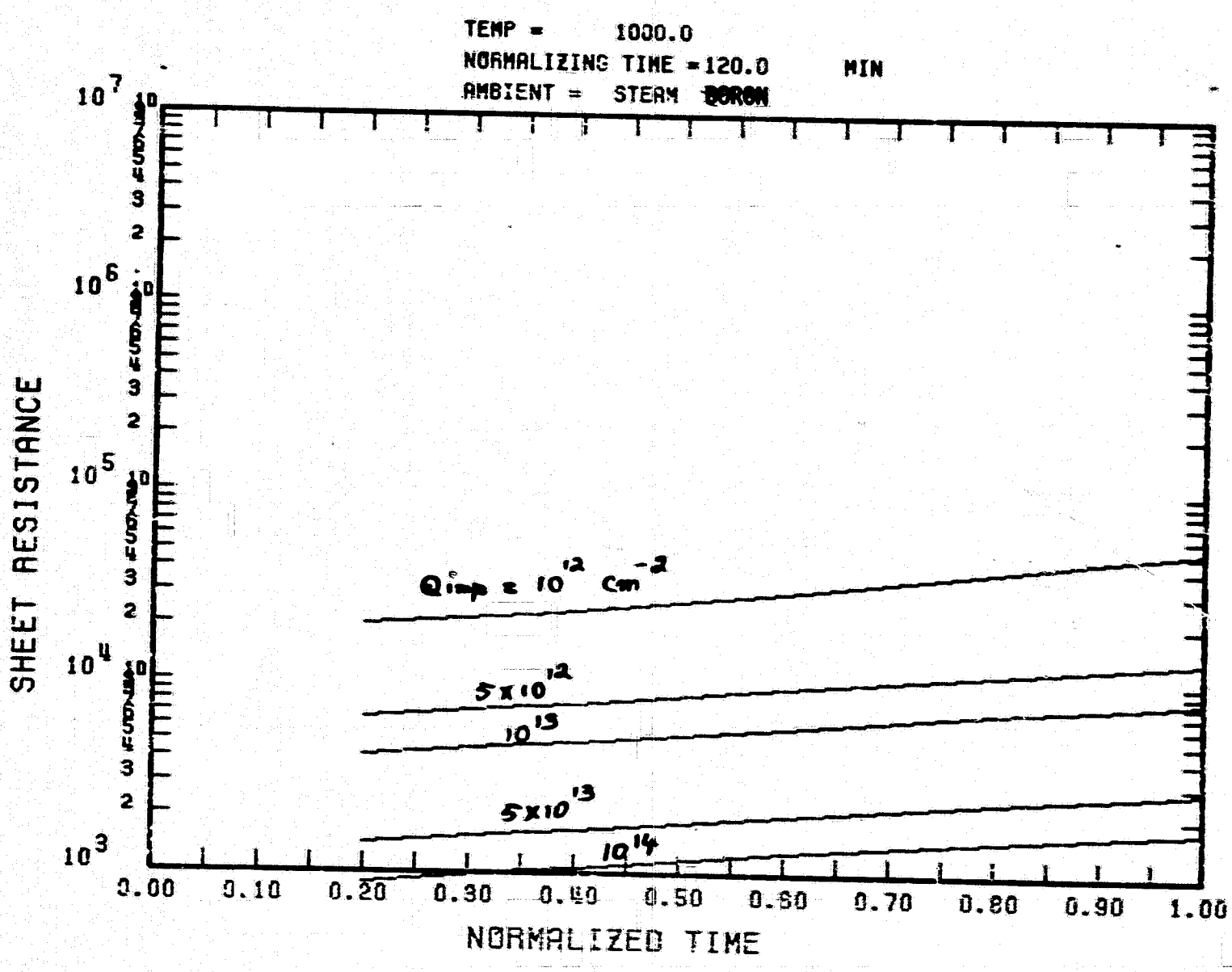
TEMP = 1000.0
NORMALIZING TIME = 120.0 MIN
AMBIENT = STEAM BORON
SHEET RESISTANCE
NORMALIZED TIME
10^7
10^6
10^5
10^4
10^3
0.00
0.10
0.20
0.30
0.40
0.50
0.60
0.70
0.80
0.90
1.00
$Q_{imp} = 10^{12}$ cm^{-2}
5×10^{12}
10^{13}
5×10^{13}
10^{14}

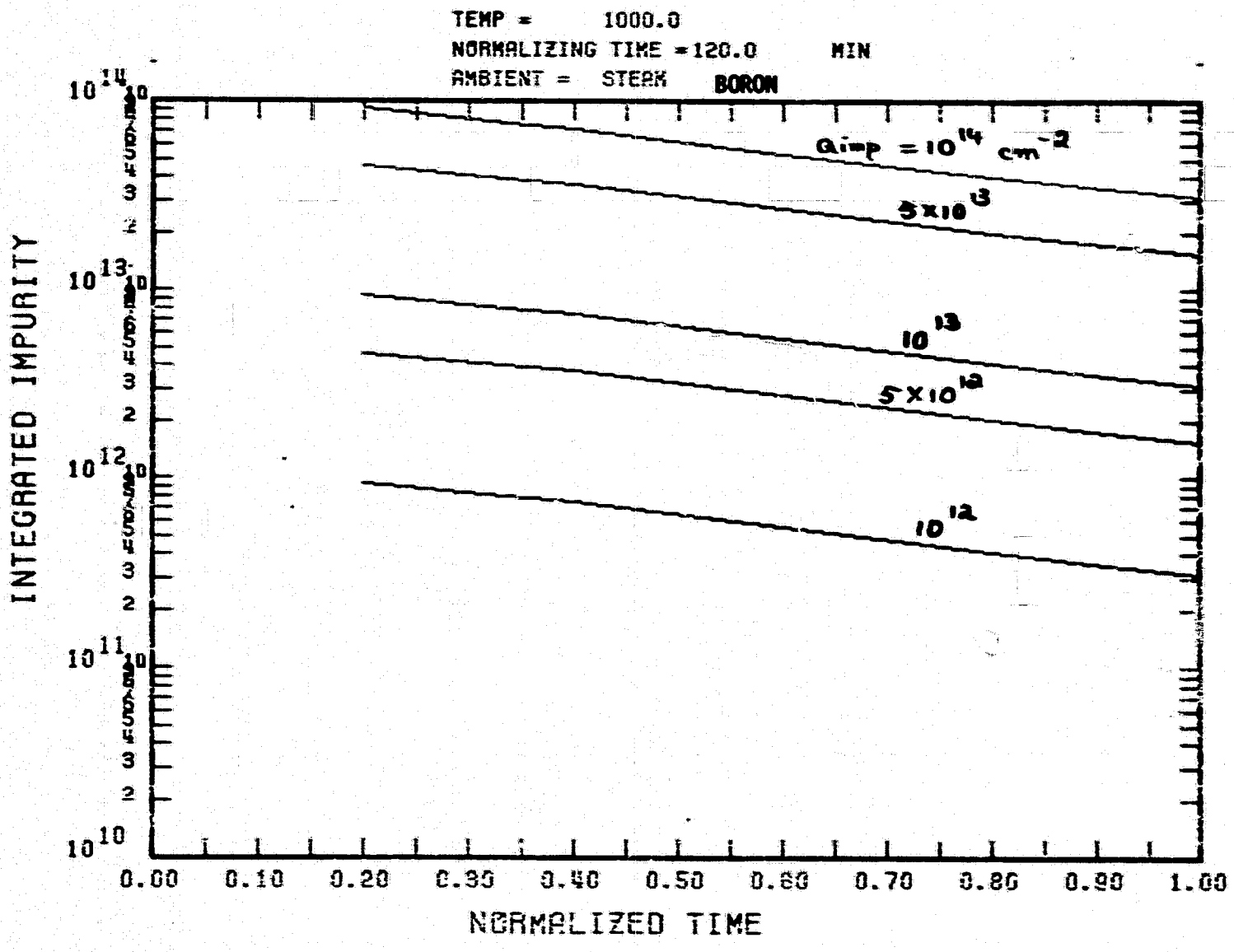
TEMP = 1000.0
NORMALIZING TIME =120.0 MIN
AMBIENT = STEAM
BORON
$Q_{imp} = 10^{14}$ cm^{-2}
5×10^{13}
10^{13}
5×10^{12}
10^{12}
INTEGRATED IMPURITY
10^{14}
10^{13}
10^{12}
10^{11}
10^{10}
0.00 0.10 0.20 0.30 0.40 0.50 0.60 0.70 0.80 0.90 1.00
NORMALIZED TIME

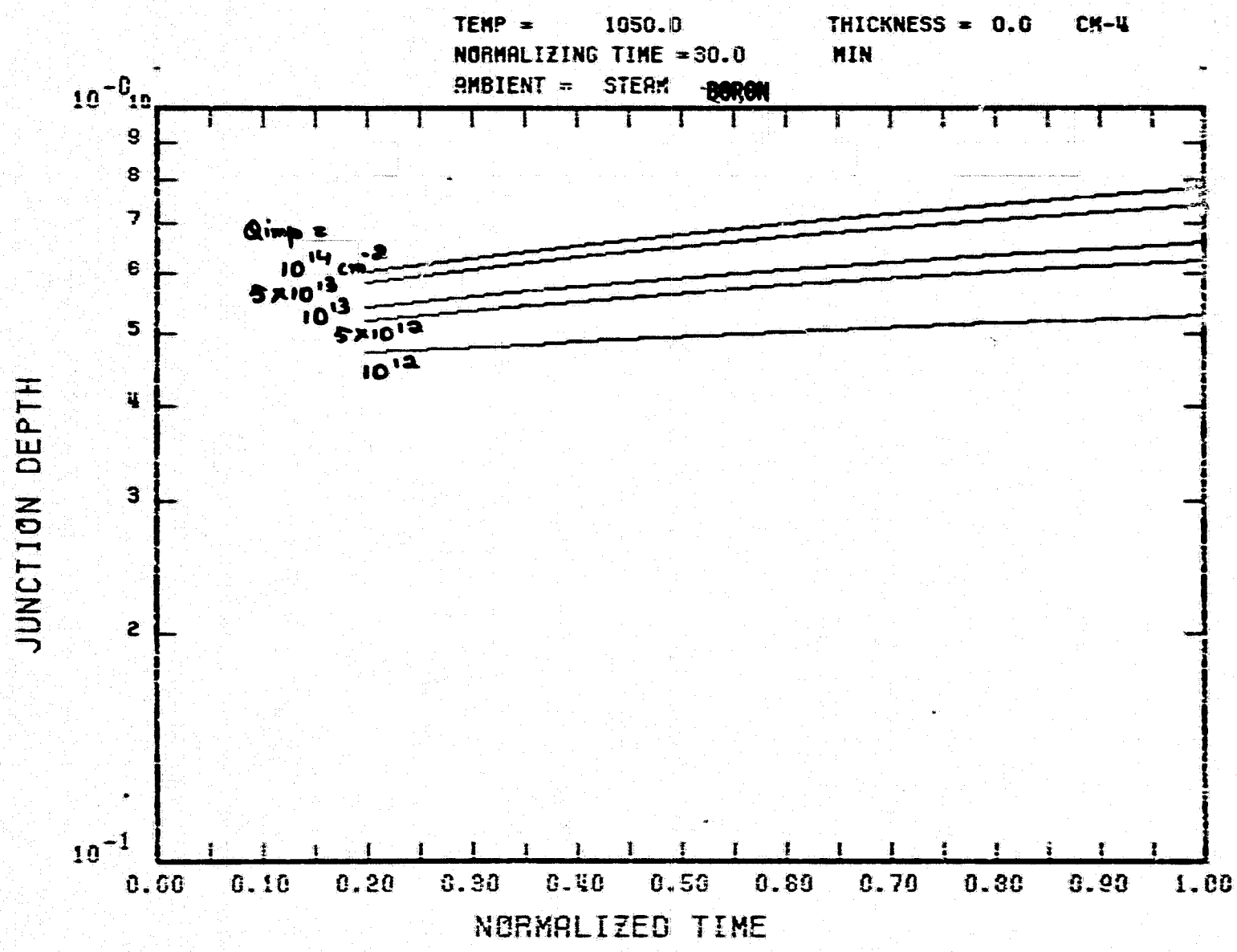
TEMP = 1050.0
THICKNESS = 0.0 CM-4
NORMALIZING TIME = 30.0 MIN
AMBIENT = STEAM
BORON
Qimp =
10^14 cm^-2
5x10^13
10^13
5x10^12
10^12
JUNCTION DEPTH
10^-1
2
3
4
5
6
7
8
9
10^-0
0.00
0.10
0.20
0.30
0.40
0.50
0.60
0.70
0.80
0.90
1.00
NORMALIZED TIME

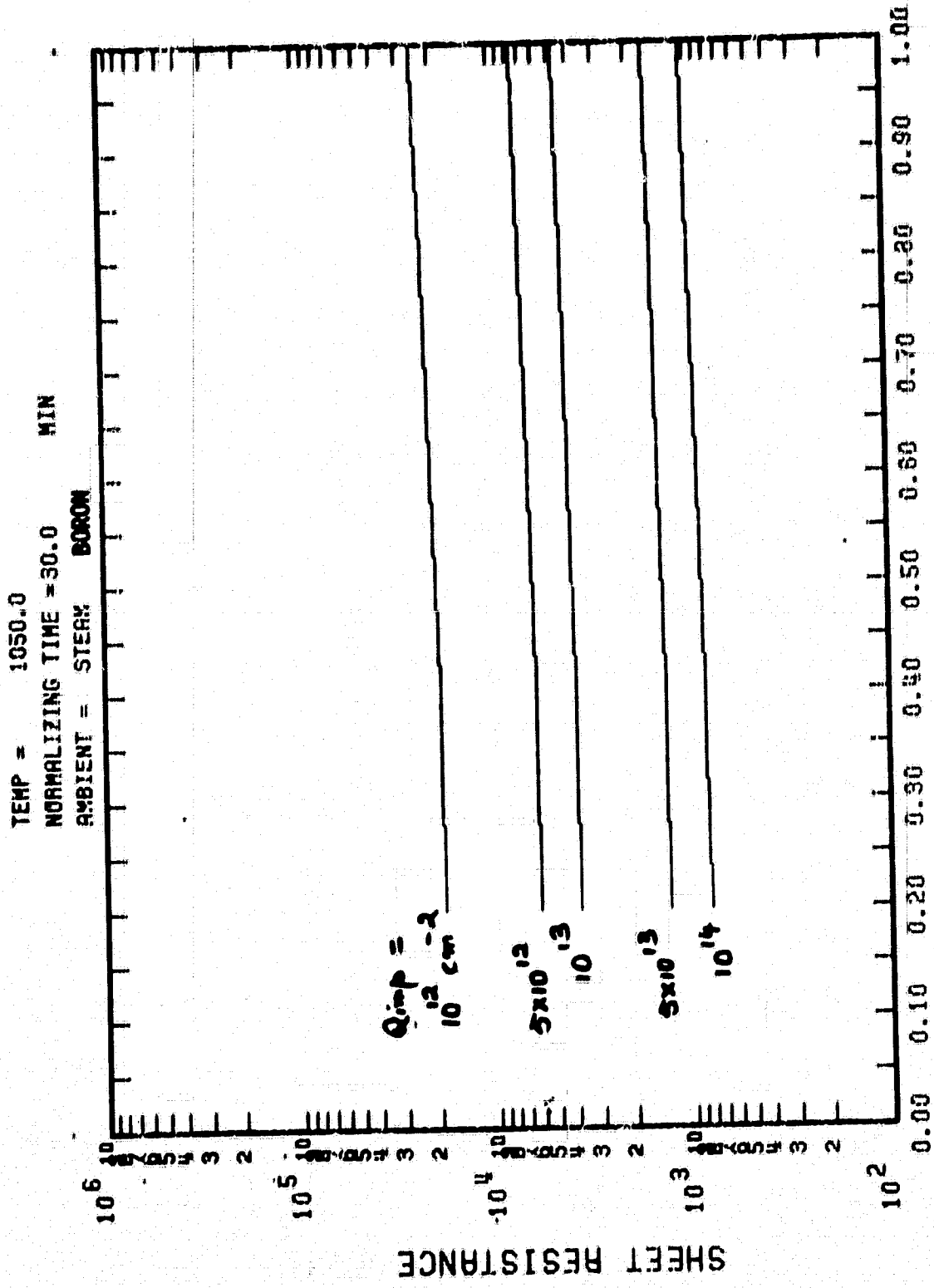
TEMP = 1050.0
NORMALIZING TIME = 30.0 MIN
AMBIENT = STEAM BORON
Qimp = 10^12 cm^-2
5x10^12
10^13
5x10^13
10^14
SHEET RESISTANCE
NORMALIZED TIME
0.00
0.10
0.20
0.30
0.40
0.50
0.60
0.70
0.80
0.90
1.00

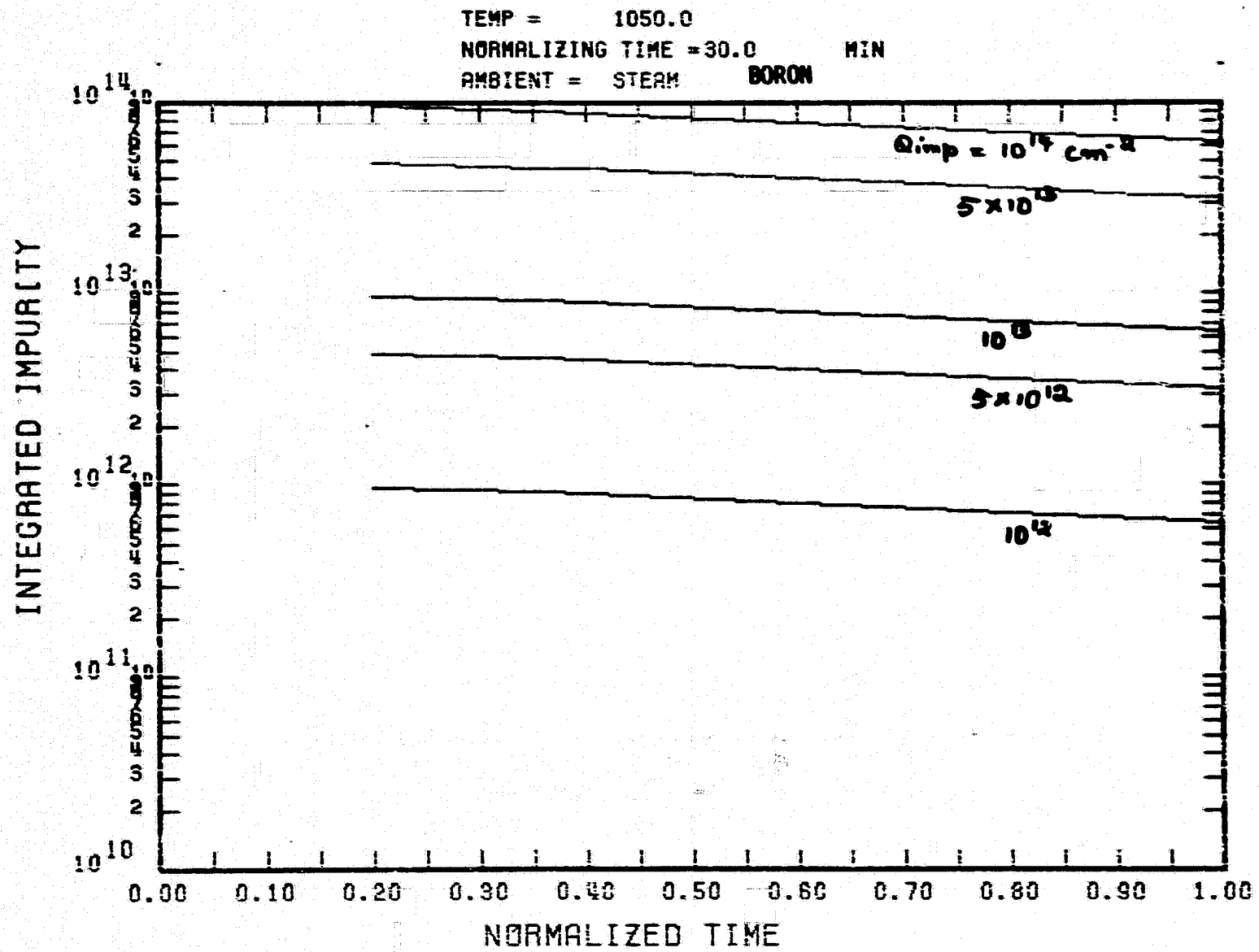
TEMP = 1050.0
NORMALIZING TIME =30.0 MIN
AMBIENT = STEAM BORON
Qimp = 10^14 cm^-2
5x10^13
10^13
3x10^12
10^12
INTEGRATED IMPURITY
NORMALIZED TIME
0.00
0.10
0.20
0.30
0.40
0.50
0.60
0.70
0.80
0.90
1.00

APPENDIX B

PHOSPHORUS DATA

λ^2 =0.0308
TEMPERATURE =1000.
TIME STEP =0
TIME =0.00

- 1.0E20
- 1.0E19
- 1.0E18
- 1.0E17
- 1.0E16
- 1.0E15

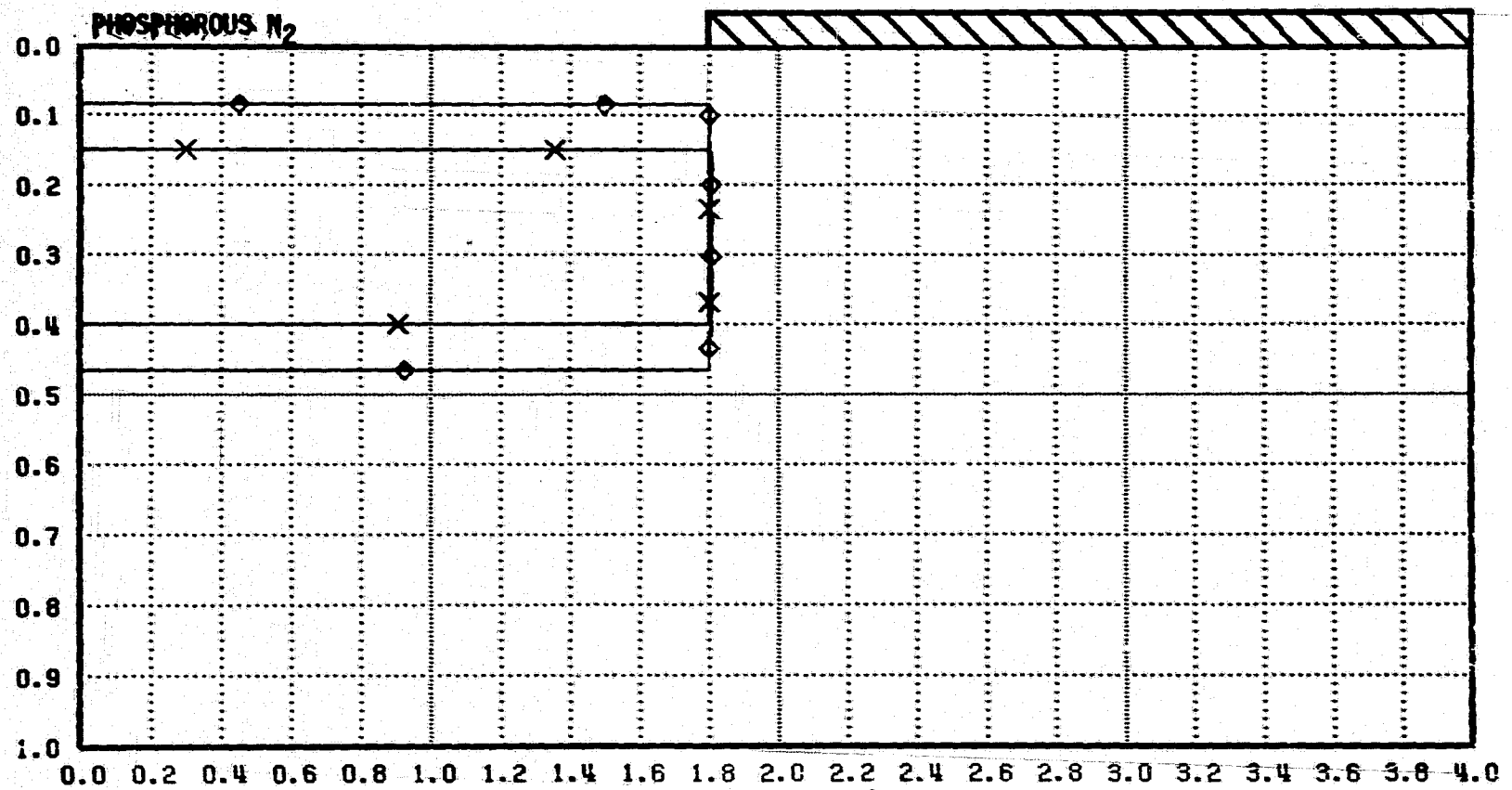

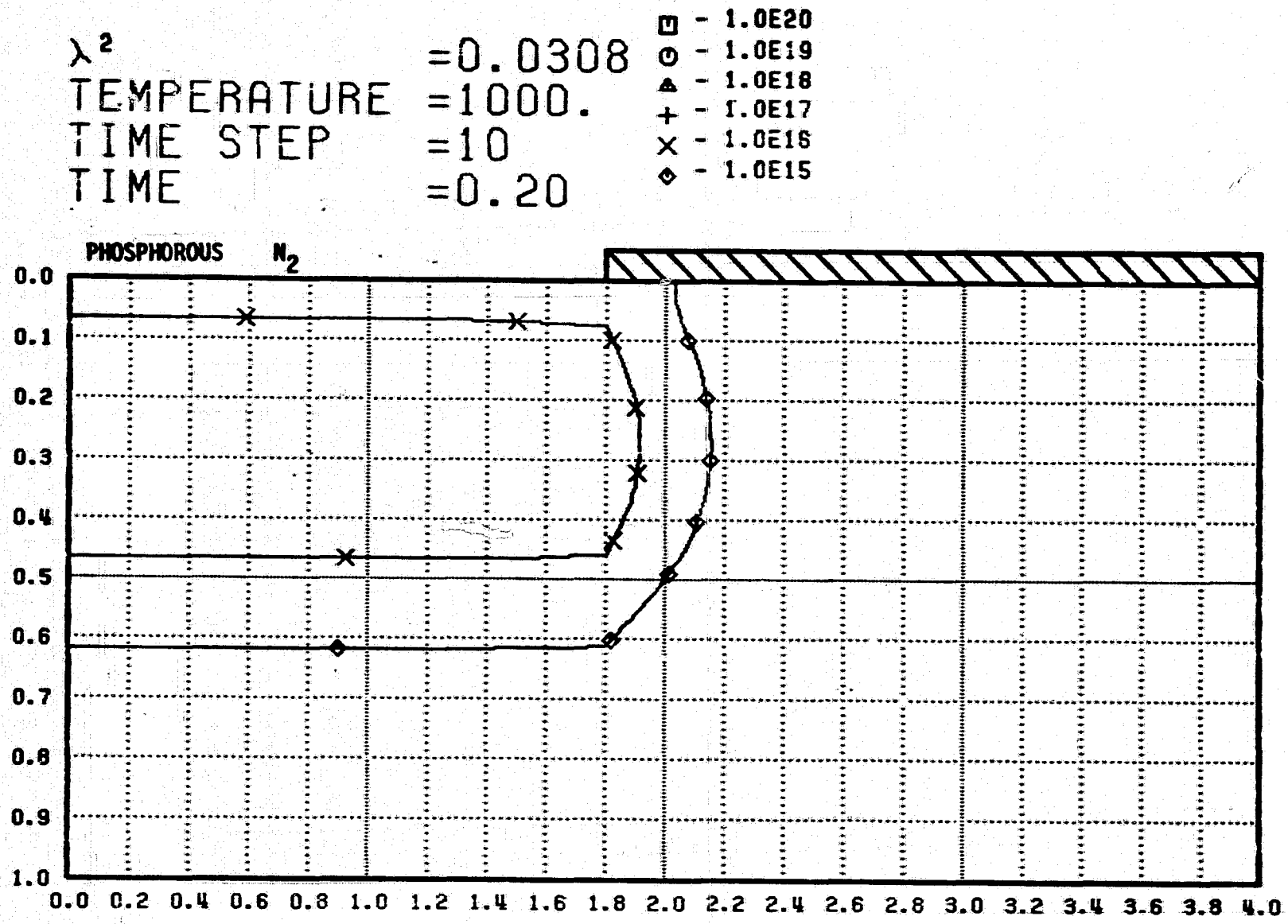
λ² =0.0308
TEMPERATURE =1000.
TIME STEP =10
TIME =0.20
□ - 1.0E20
⊙ - 1.0E19
▲ - 1.0E18
+ - 1.0E17
× - 1.0E16
◇ - 1.0E15
PHOSPHOROUS N2
0.0
0.1
0.2
0.3
0.4
0.5
0.6
0.7
0.8
0.9
1.0
0.0 0.2 0.4 0.6 0.8 1.0 1.2 1.4 1.6 1.8 2.0 2.2 2.4 2.6 2.8 3.0 3.2 3.4 3.6 3.8 4.0

λ^2 =0.0308
TEMPERATURE =1000.
TIME STEP =20
TIME =0.40

- 1.0E20
- 1.0E19
- 1.0E18
- 1.0E17
- 1.0E16
- 1.0E15

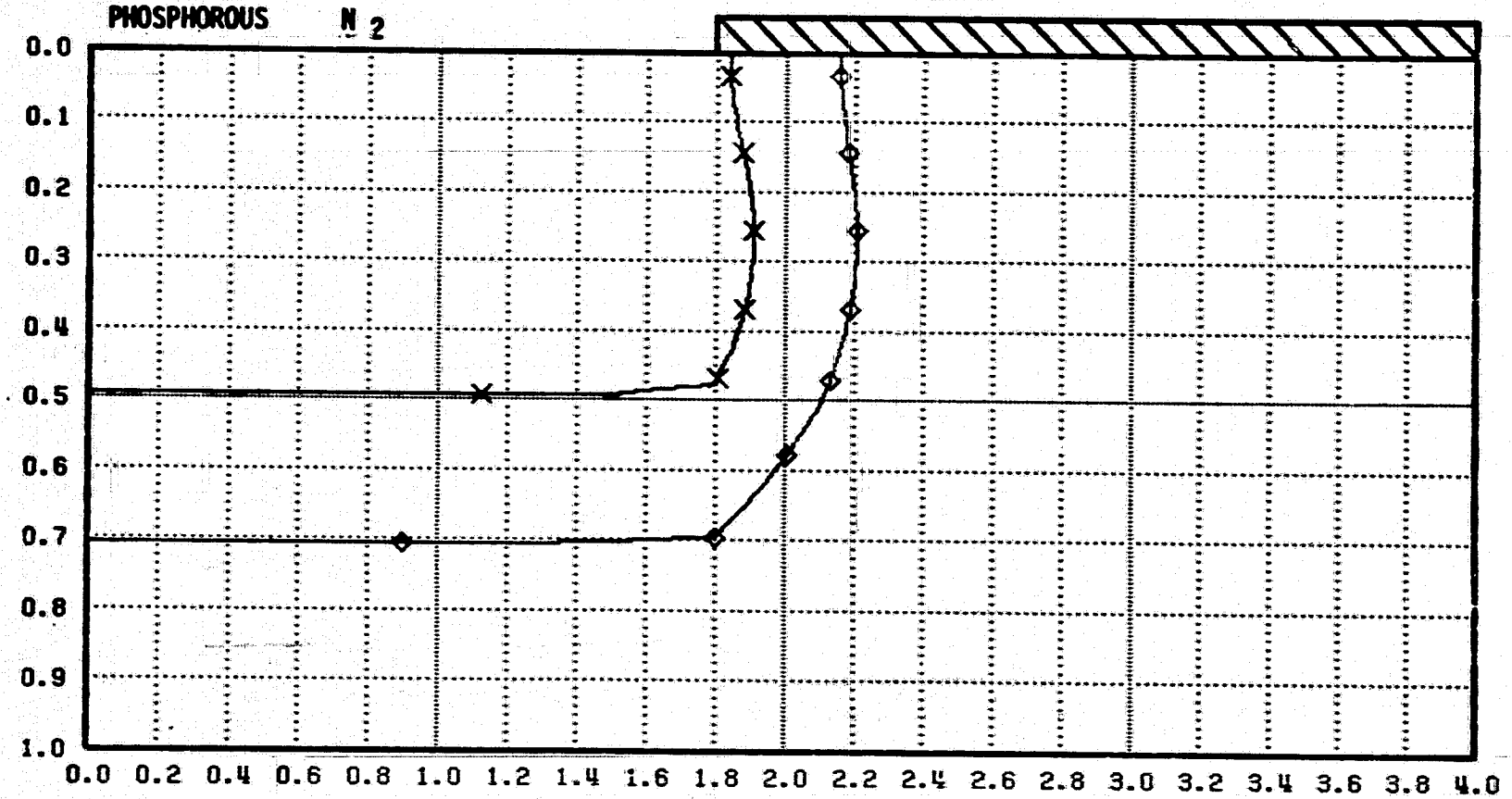

λ^2 =0.0308
TEMPERATURE =1000.
TIME STEP =30
TIME =0.60

□ - 1.0E20
⊙ - 1.0E19
△ - 1.0E18
+ - 1.0E17
× - 1.0E16
◇ - 1.0E15

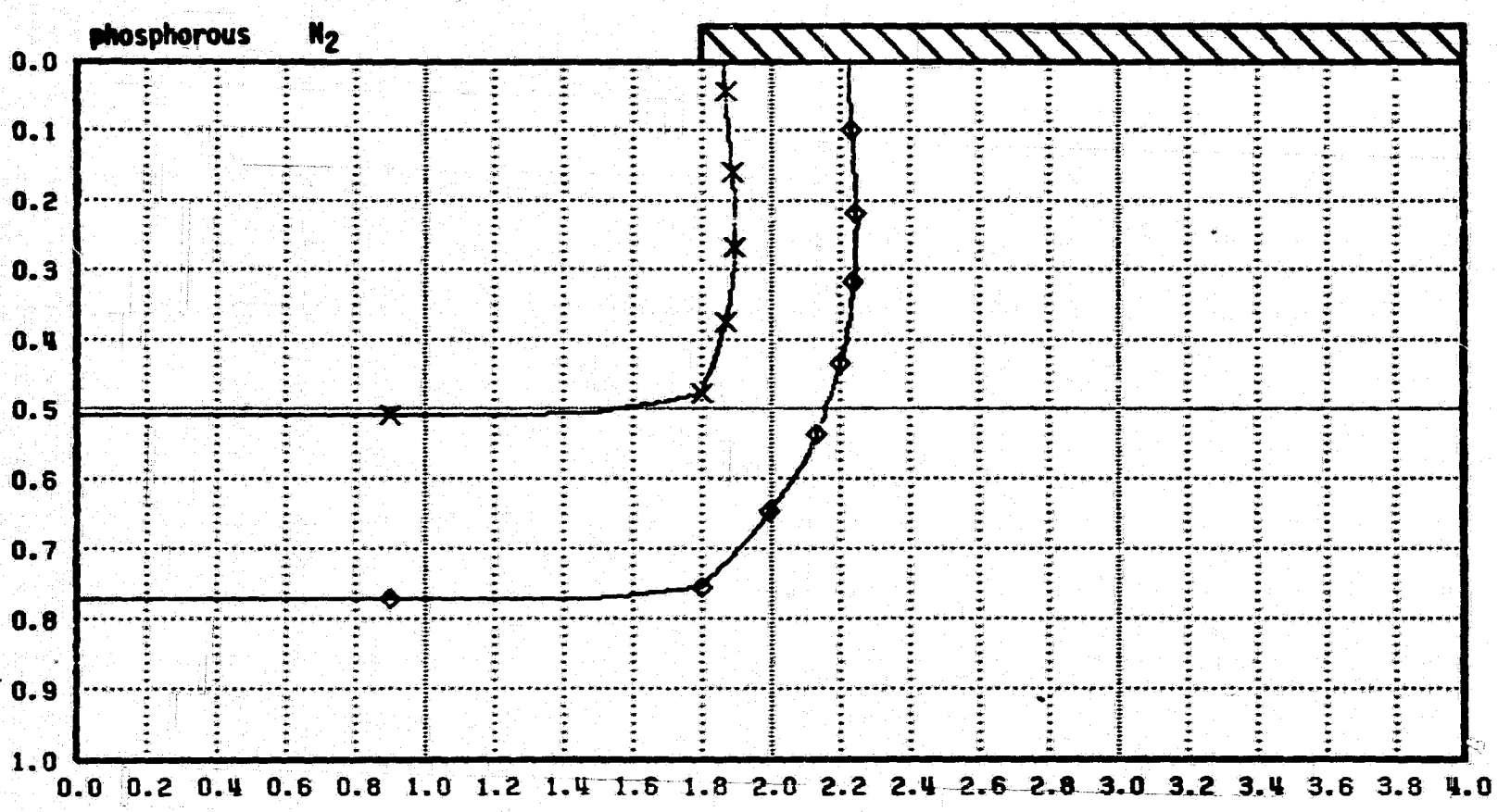

109

λ^2 =0.0308
TEMPERATURE =1000.
TIME STEP =40
TIME =0.80

□ - 1.0E20
⊙ - 1.0E19
△ - 1.0E18
+ - 1.0E17
× - 1.0E16
◇ - 1.0E15

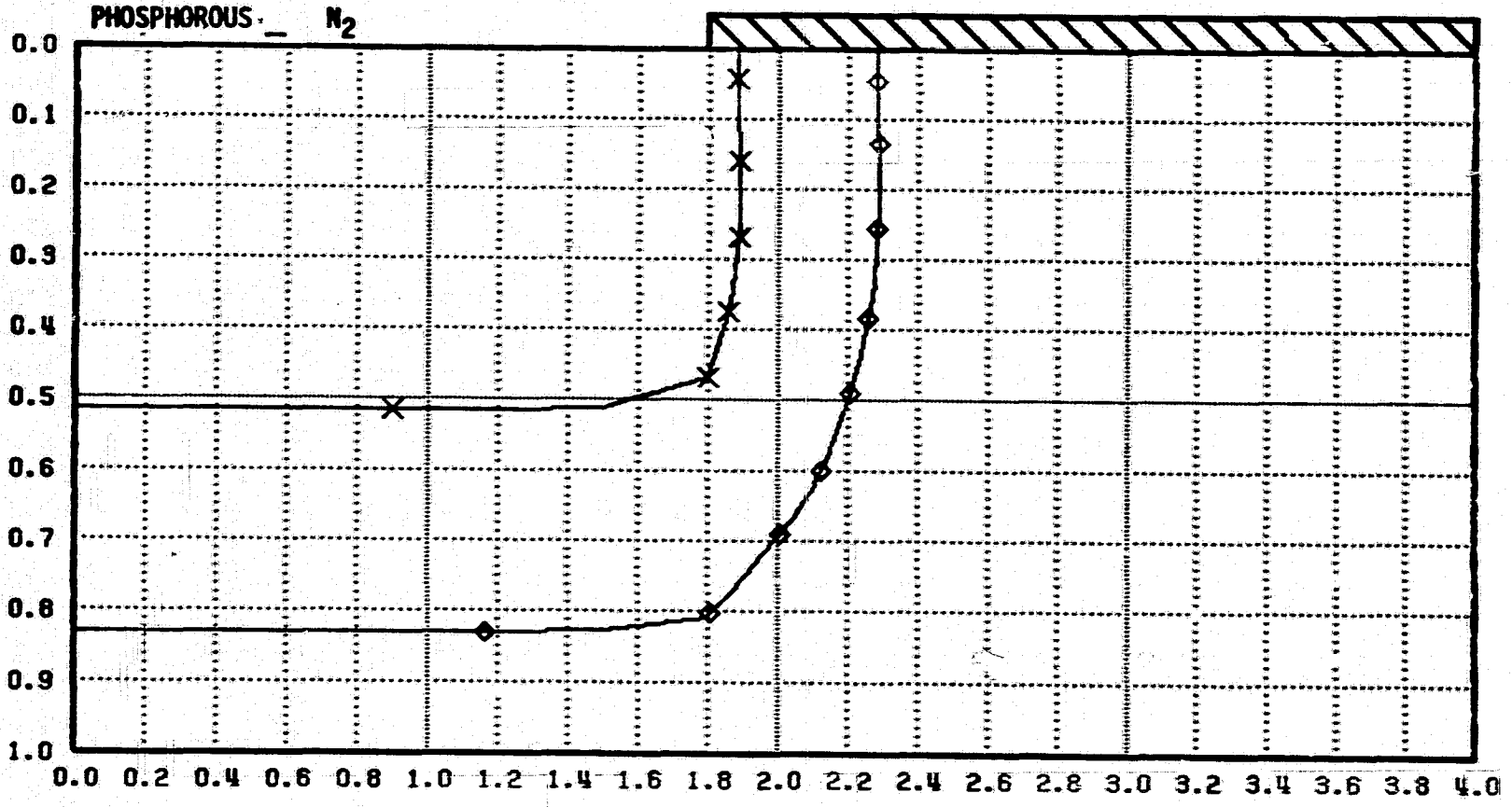

λ^2 =0.0308
TEMPERATURE =1000.
TIME STEP =50
TIME =1.00

□ - 1.0E20
○ - 1.0E19
△ - 1.0E18
+ - 1.0E17
× - 1.0E16
◇ - 1.0E15

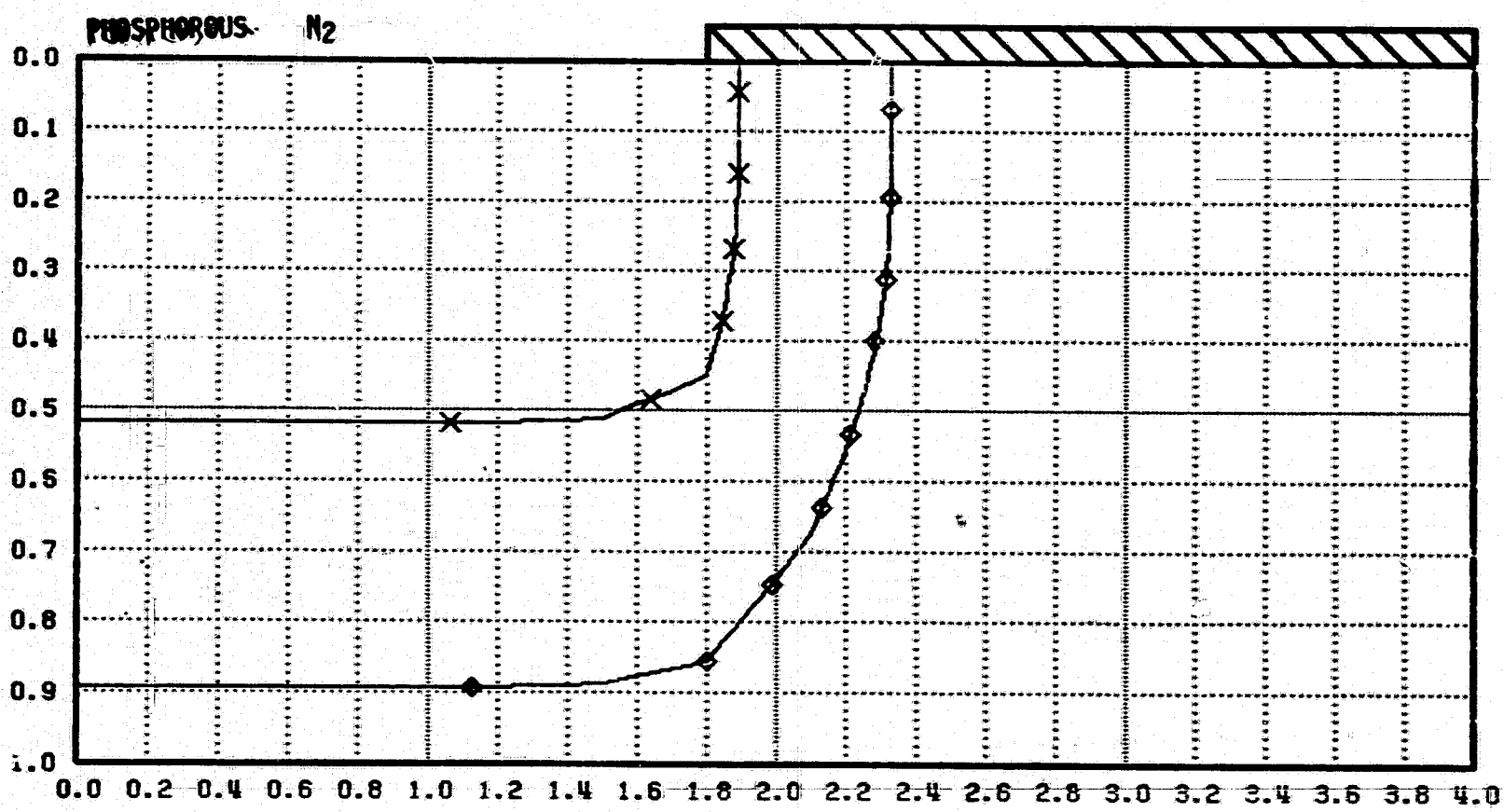

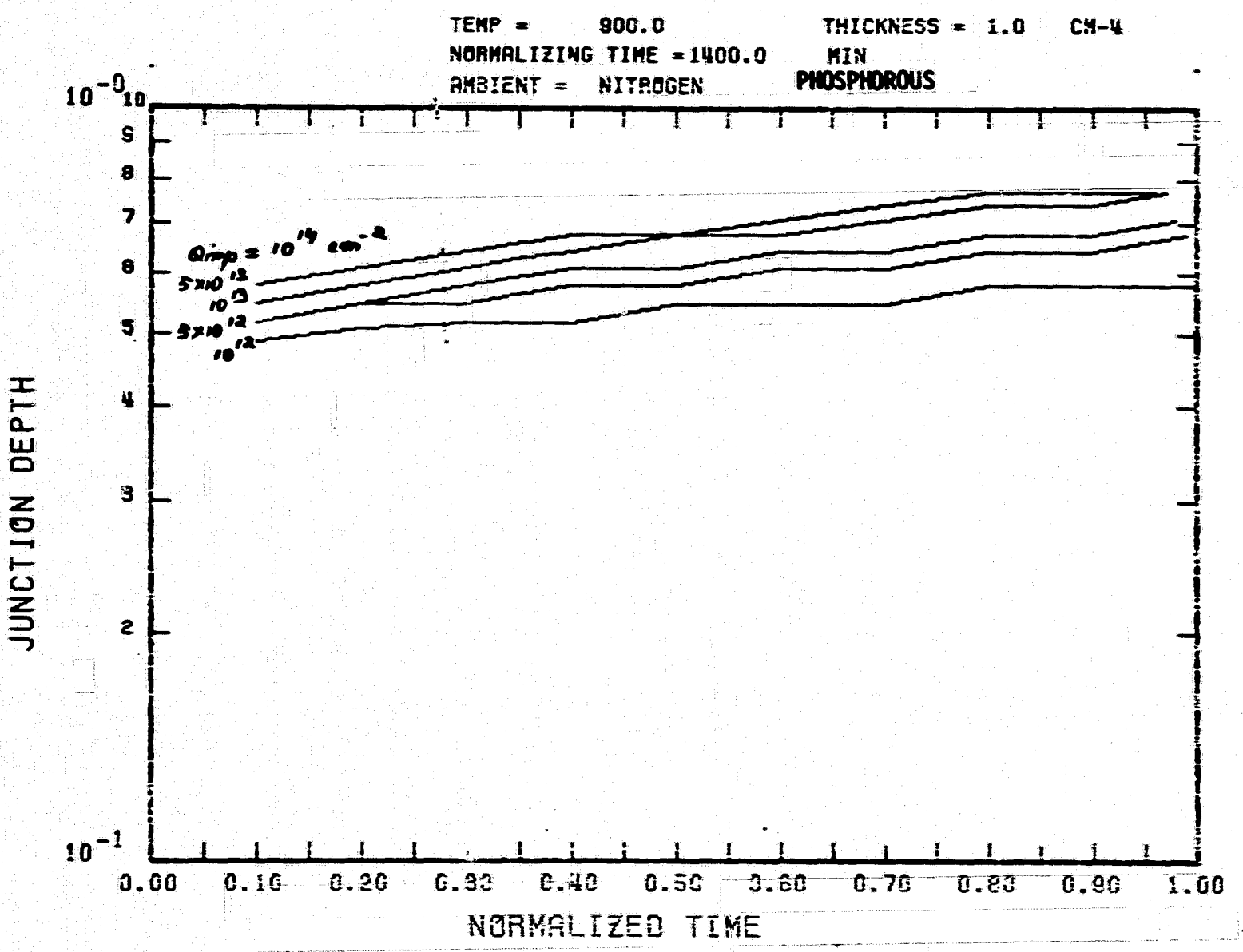
TEMP = 900.0 THICKNESS = 1.0 CM-4
NORMALIZING TIME =1400.0 MIN
AMBIENT = NITROGEN
PHOSPHORUS
10^{-0}
9
8
7
6
5
4
3
2
10^{-1}
$Q_{imp} = 10^{14}$ cm^{-2}
5×10^{13}
10^{13}
5×10^{12}
10^{12}
JUNCTION DEPTH
0.00 0.10 0.20 0.30 0.40 0.50 0.60 0.70 0.80 0.90 1.00
NORMALIZED TIME

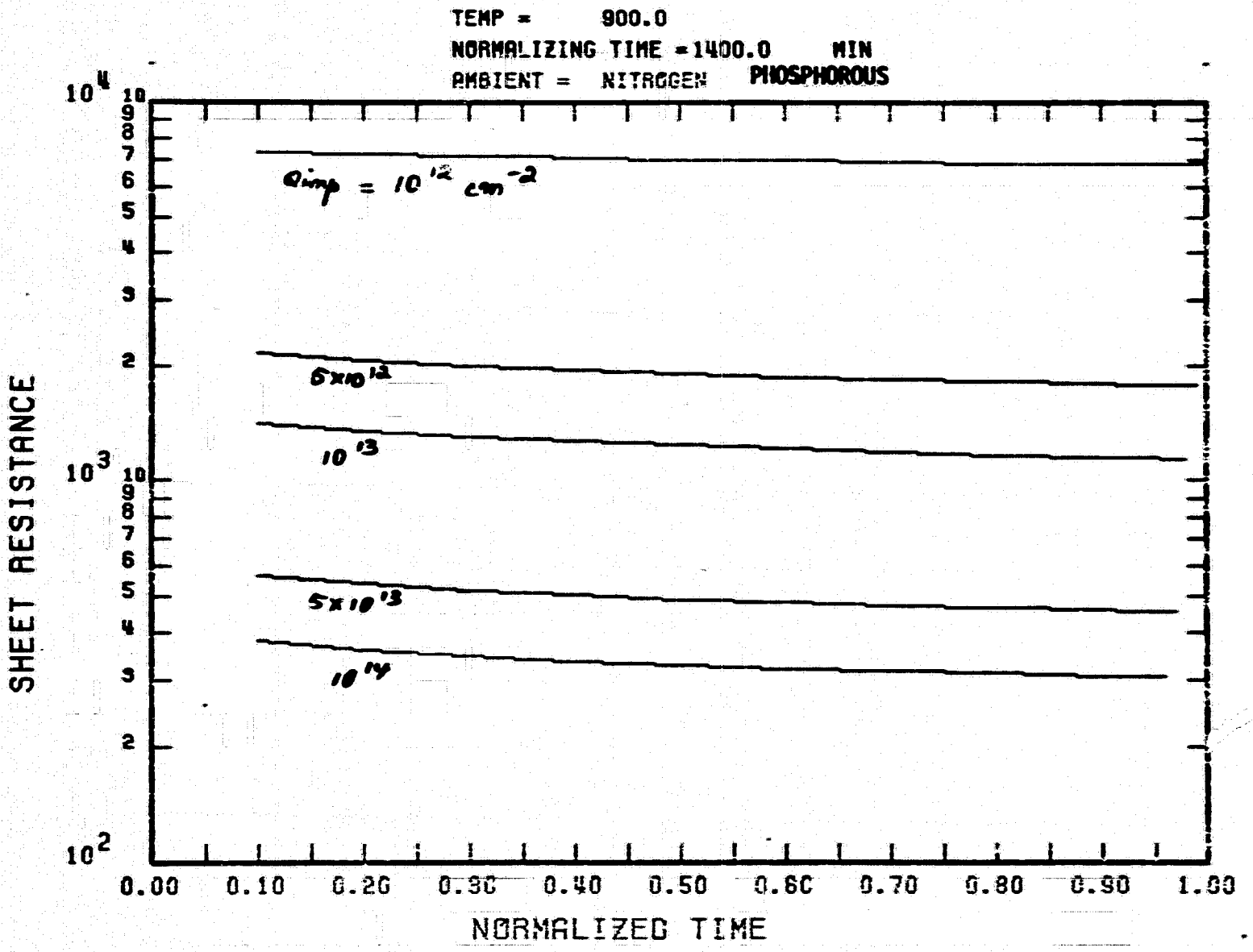
TEMP = 900.0
NORMALIZING TIME = 1400.0 MIN
AMBIENT = NITROGEN PHOSPHOROUS
$Q_{imp} = 10^{12}$ cm^{-2}
6×10^{12}
10^{13}
5×10^{13}
10^{14}
SHEET RESISTANCE
10^4
10^3
10^2
0.00 0.10 0.20 0.30 0.40 0.50 0.60 0.70 0.80 0.90 1.00
NORMALIZED TIME

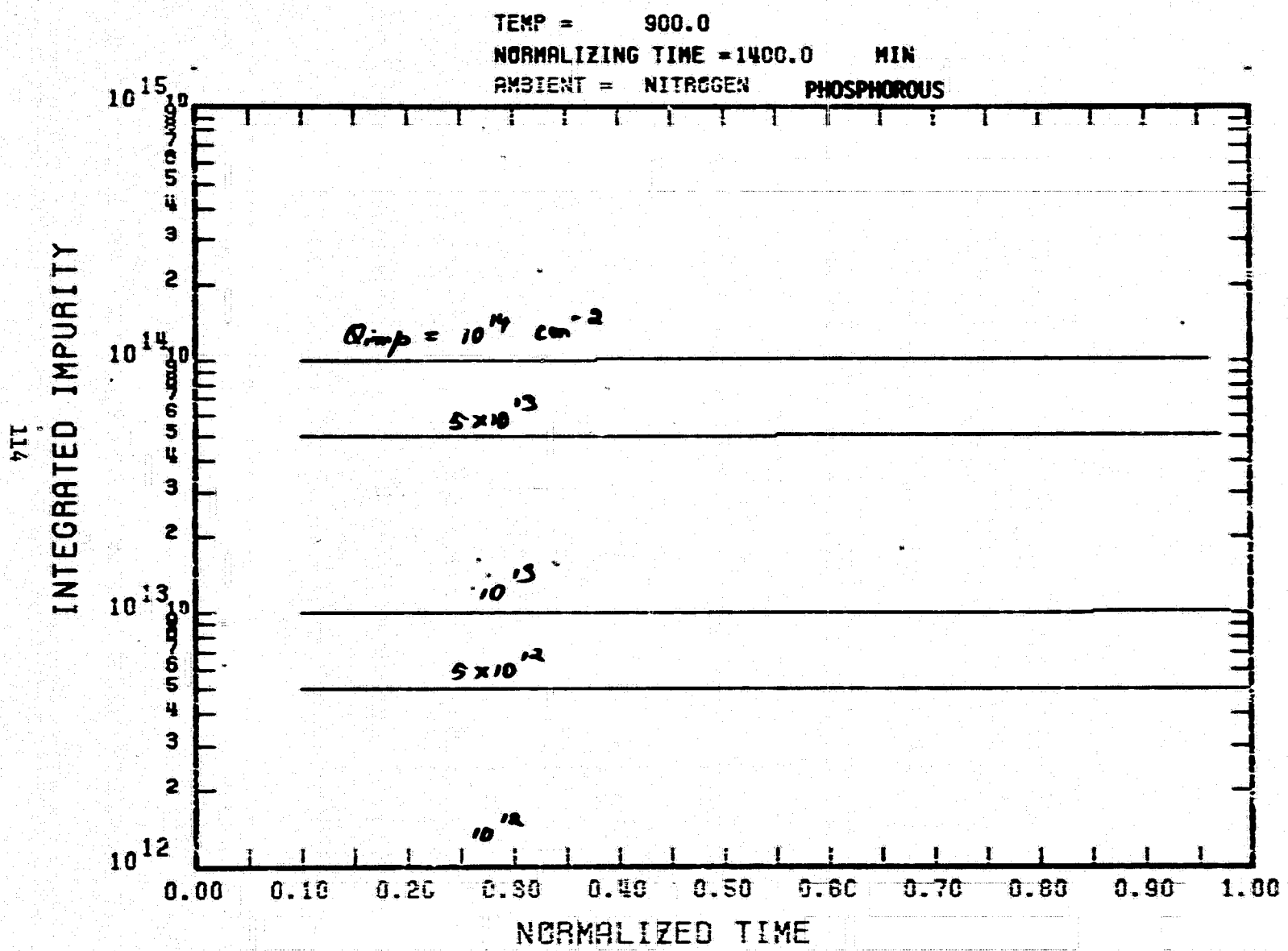
TEMP = 900.0
NORMALIZING TIME = 1400.0 MIN
AMBIENT = NITROGEN
PHOSPHOROUS
INTEGRATED IMPURITY
10^{15}
10^{14}
10^{13}
10^{12}
$Q_{imp} = 10^{14}$ cm^{-2}
5×10^{13}
10^{13}
5×10^{12}
10^{12}
0.00 0.10 0.20 0.30 0.40 0.50 0.60 0.70 0.80 0.90 1.00
NORMALIZED TIME

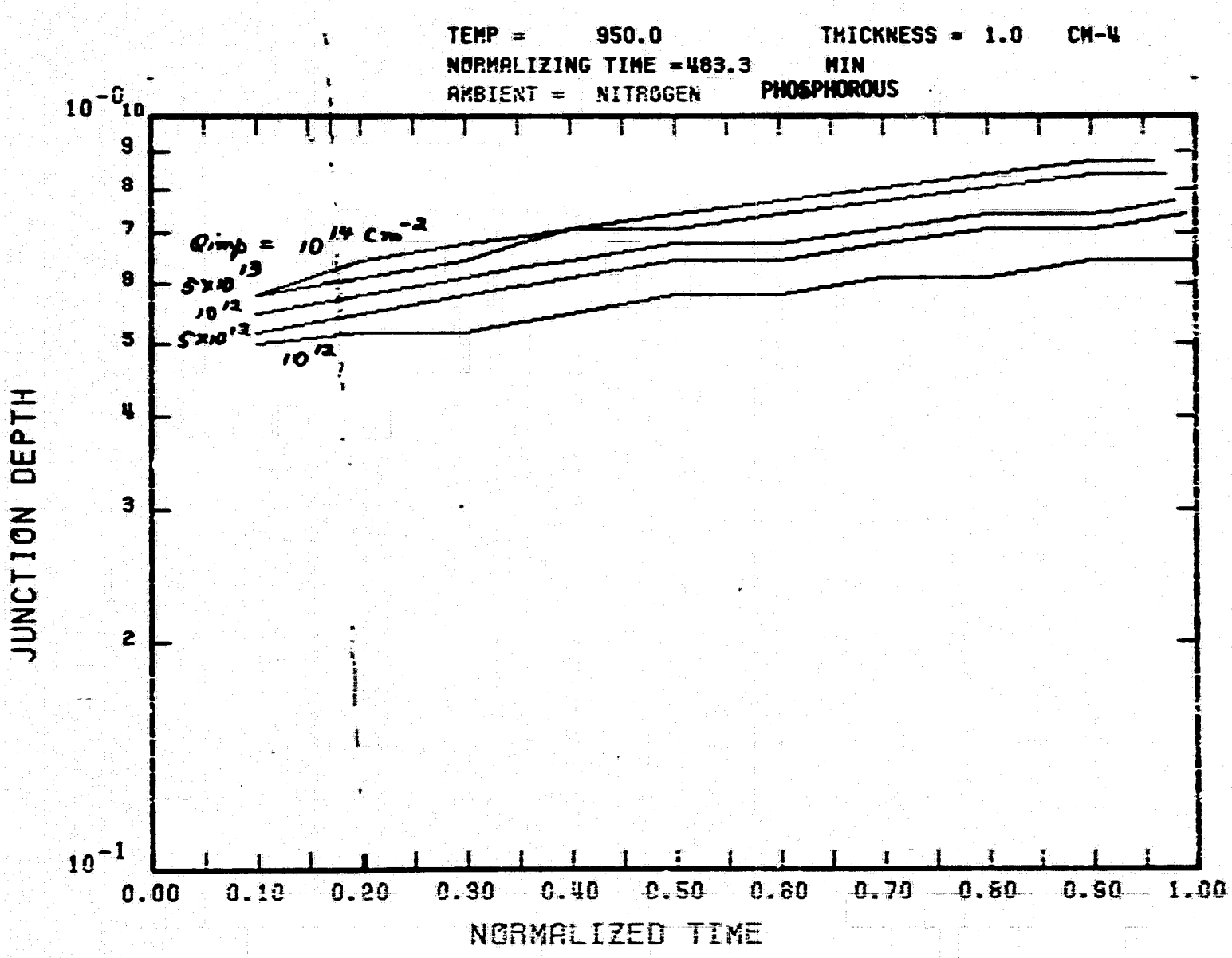
TEMP = 950.0 THICKNESS = 1.0 CM-4
NORMALIZING TIME =483.3 MIN
AMBIENT = NITROGEN PHOSPHOROUS
10^{-0}
10
9
8
7
6
5
4
3
2
10^{-1}
$Q_{imp} = 10^{14}\ cm^{-2}$
5×10^{13}
10^{13}
5×10^{12}
10^{12}
JUNCTION DEPTH
0.00
0.10
0.20
0.30
0.40
0.50
0.60
0.70
0.80
0.90
1.00
NORMALIZED TIME

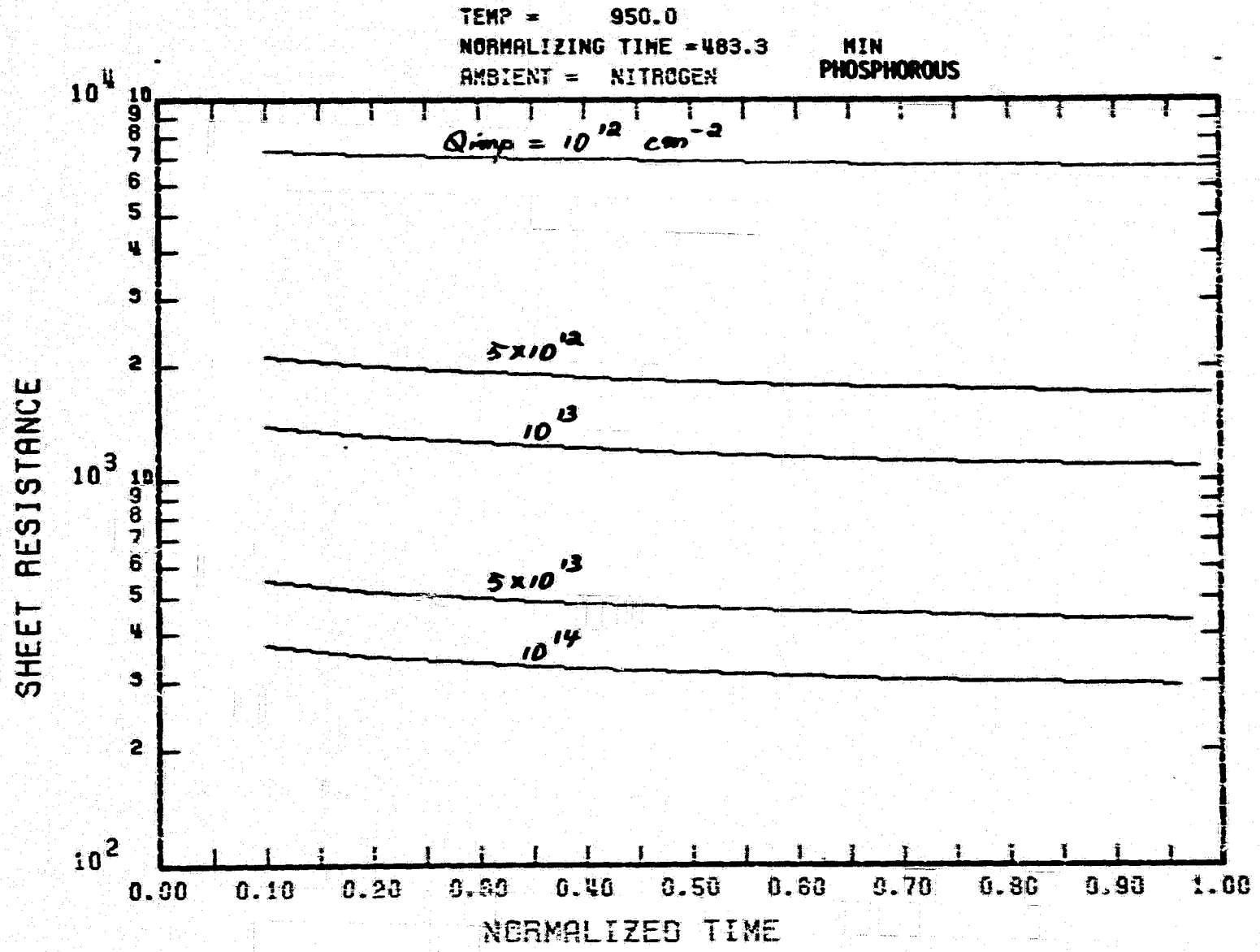
TEMP = 950.0
NORMALIZING TIME =483.3 MIN
AMBIENT = NITROGEN
PHOSPHOROUS
$Q_{imp} = 10^{12}$ cm^{-2}
5×10^{12}
10^{13}
5×10^{13}
10^{14}
SHEET RESISTANCE
10^4
10^3
10^2
0.00 0.10 0.20 0.30 0.40 0.50 0.60 0.70 0.80 0.90 1.00
NORMALIZED TIME

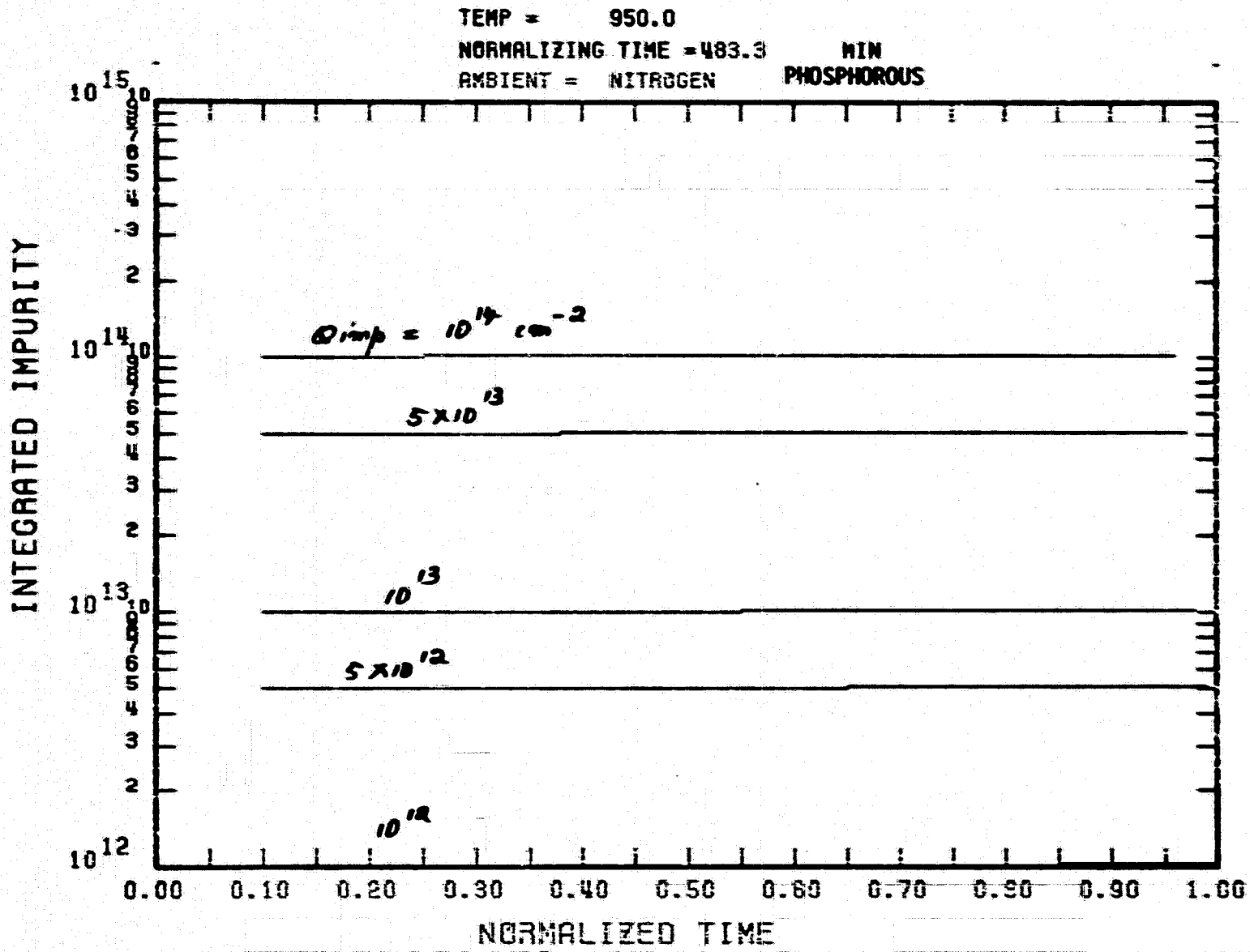
TEMP = 950.0
NORMALIZING TIME =483.3 MIN
AMBIENT = NITROGEN
PHOSPHOROUS
INTEGRATED IMPURITY
NORMALIZED TIME
$Q_{imp} = 10^{14}\ cm^{-2}$
5×10^{13}
10^{13}
5×10^{12}
10^{12}
10^{15}
10^{14}
10^{13}
10^{12}
0.00
0.10
0.20
0.30
0.40
0.50
0.60
0.70
0.80
0.90
1.00

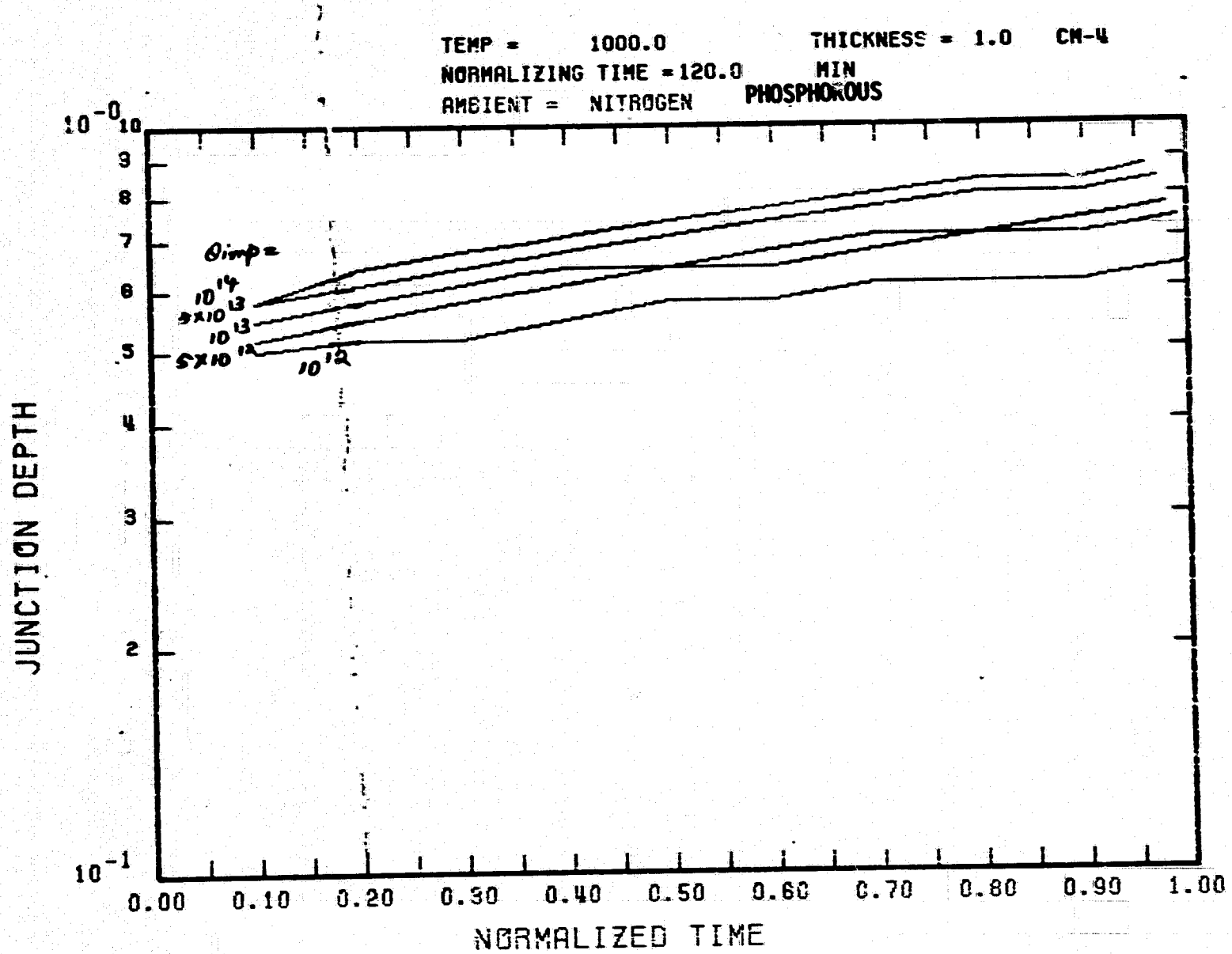
TEMP = 1000.0 THICKNESS = 1.0 CM-4
NORMALIZING TIME = 120.0 MIN
AMBIENT = NITROGEN
PHOSPHOROUS
10^{-0}
10
9
8
7
6
5
4
3
2
10^{-1}
Qimp=
10^{14}
9×10^{13}
10^{13}
5×10^{12}
10^{12}
JUNCTION DEPTH
0.00
0.10
0.20
0.30
0.40
0.50
0.60
0.70
0.80
0.90
1.00
NORMALIZED TIME

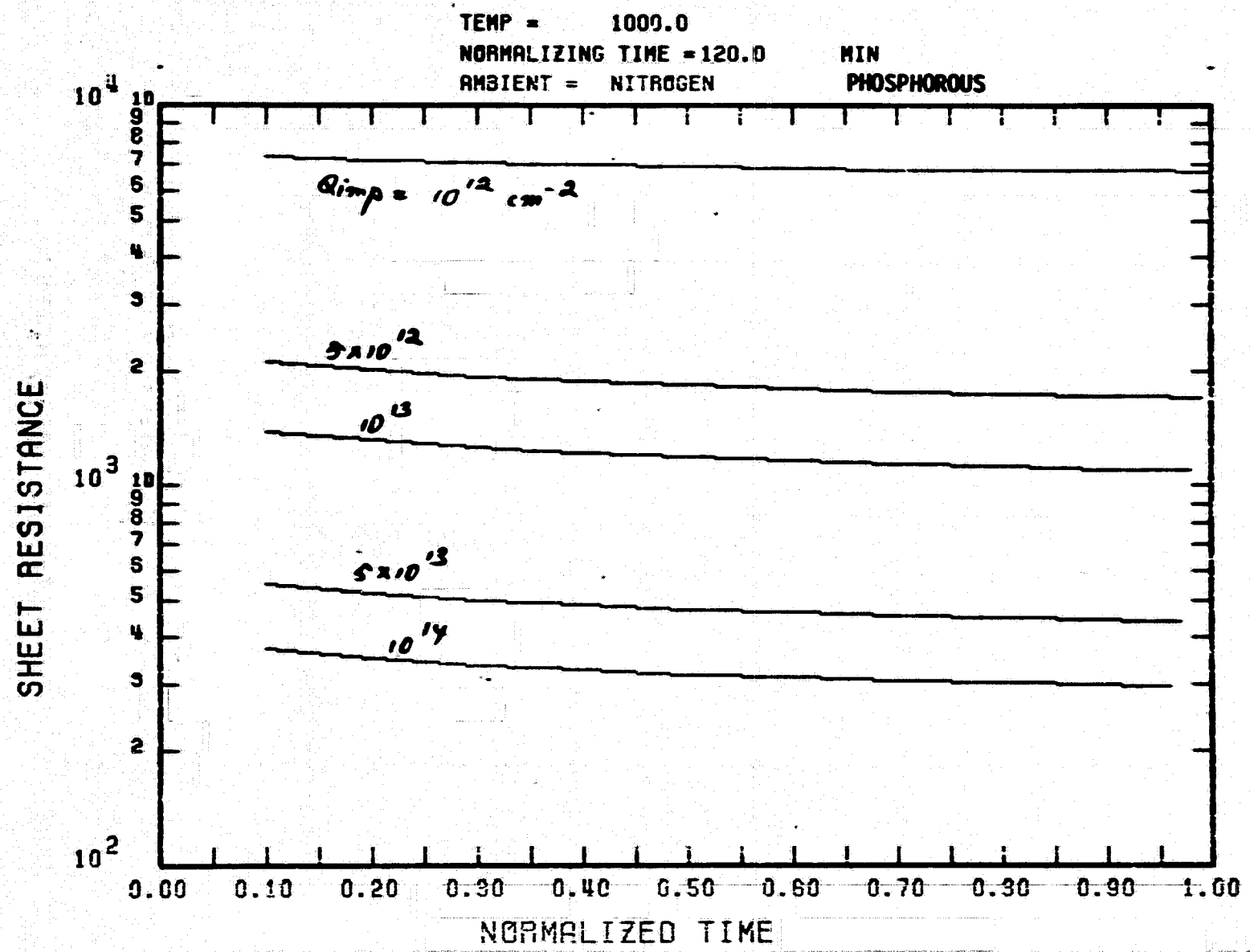
TEMP = 1000.0
NORMALIZING TIME = 120.0 MIN
AMBIENT = NITROGEN PHOSPHOROUS
$Q_{imp} = 10^{12}$ cm^{-2}
5×10^{12}
10^{13}
5×10^{13}
10^{14}
SHEET RESISTANCE
10^4
10^3
10^2
0.00 0.10 0.20 0.30 0.40 0.50 0.60 0.70 0.80 0.90 1.00
NORMALIZED TIME

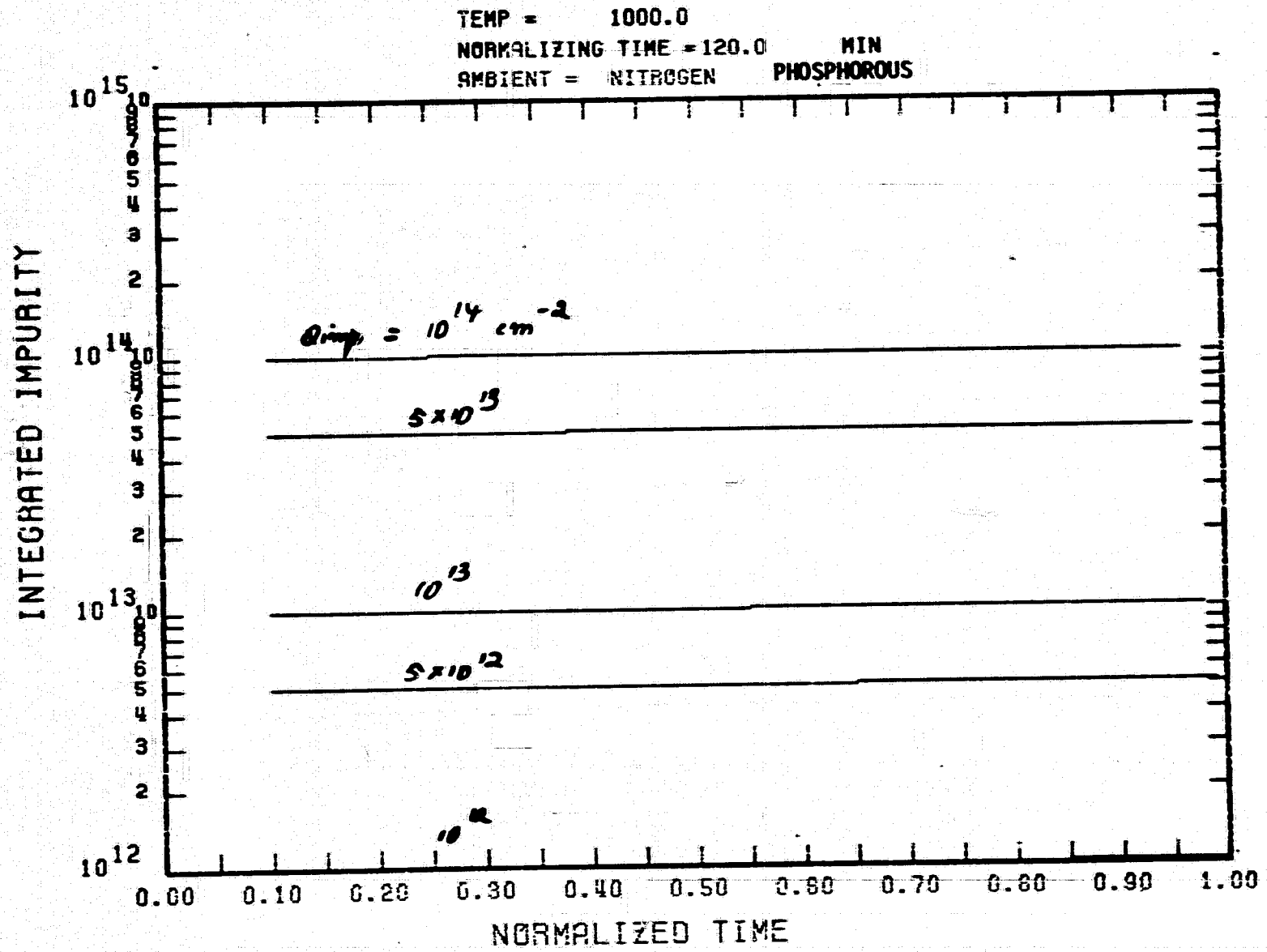
TEMP = 1000.0
NORMALIZING TIME = 120.0 MIN
AMBIENT = NITROGEN
PHOSPHOROUS
INTEGRATED IMPURITY
NORMALIZED TIME
10^{15}
10^{14}
10^{13}
10^{12}
$Q_{imp} = 10^{14}$ cm^{-2}
5×10^{13}
10^{13}
5×10^{12}
10^{12}
0.00
0.10
0.20
0.30
0.40
0.50
0.60
0.70
0.80
0.90
1.00

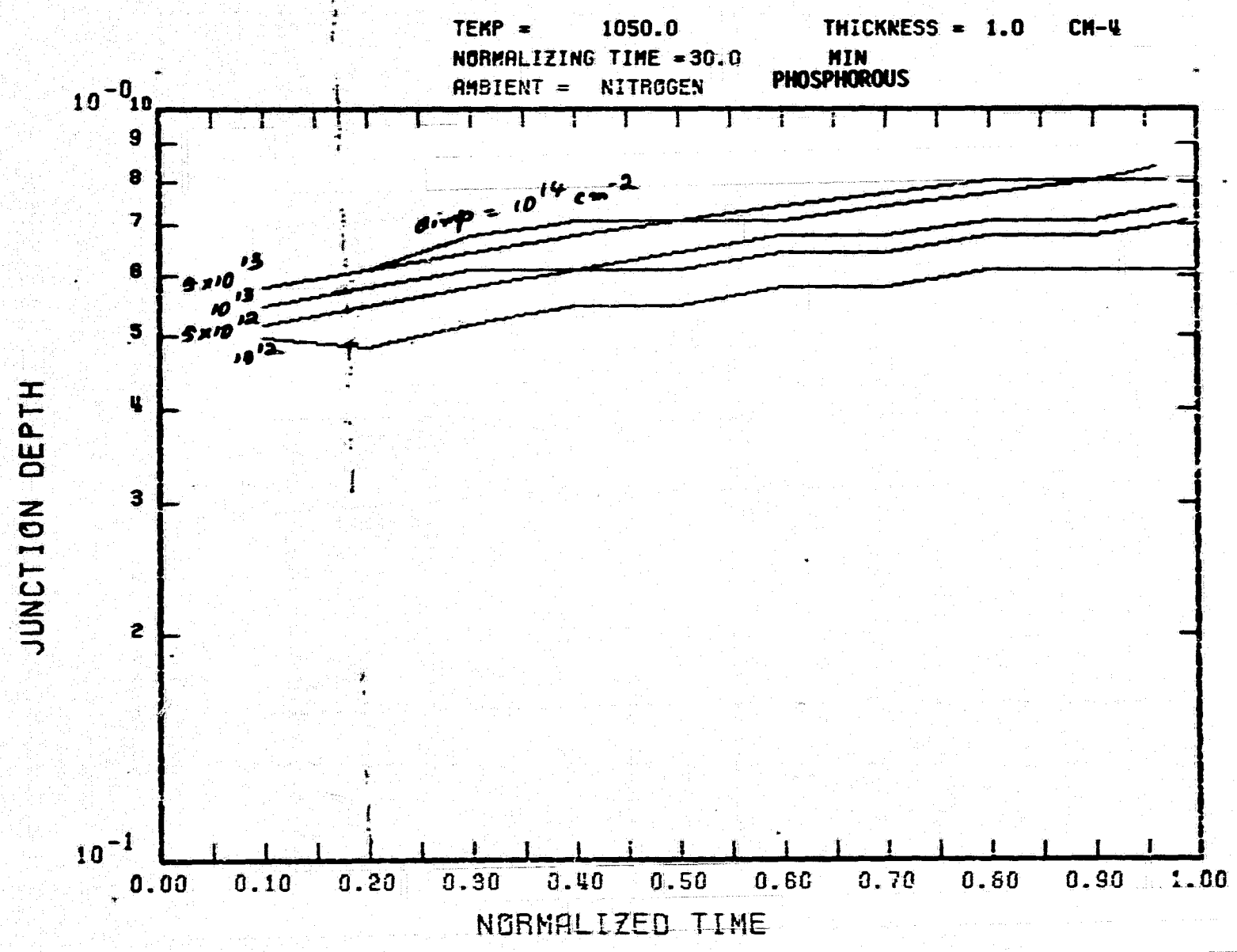
TEMP = 1050.0 THICKNESS = 1.0 CM-4
NORMALIZING TIME =30.0 MIN
AMBIENT = NITROGEN
PHOSPHOROUS
10^{-0}
9
8
7
6
5
4
3
2
10^{-1}
JUNCTION DEPTH
$\phi_{imp} = 10^{14}\ cm^{-2}$
9×10^{13}
10^{13}
5×10^{12}
10^{12}
0.00 0.10 0.20 0.30 0.40 0.50 0.60 0.70 0.80 0.90 1.00
NORMALIZED TIME

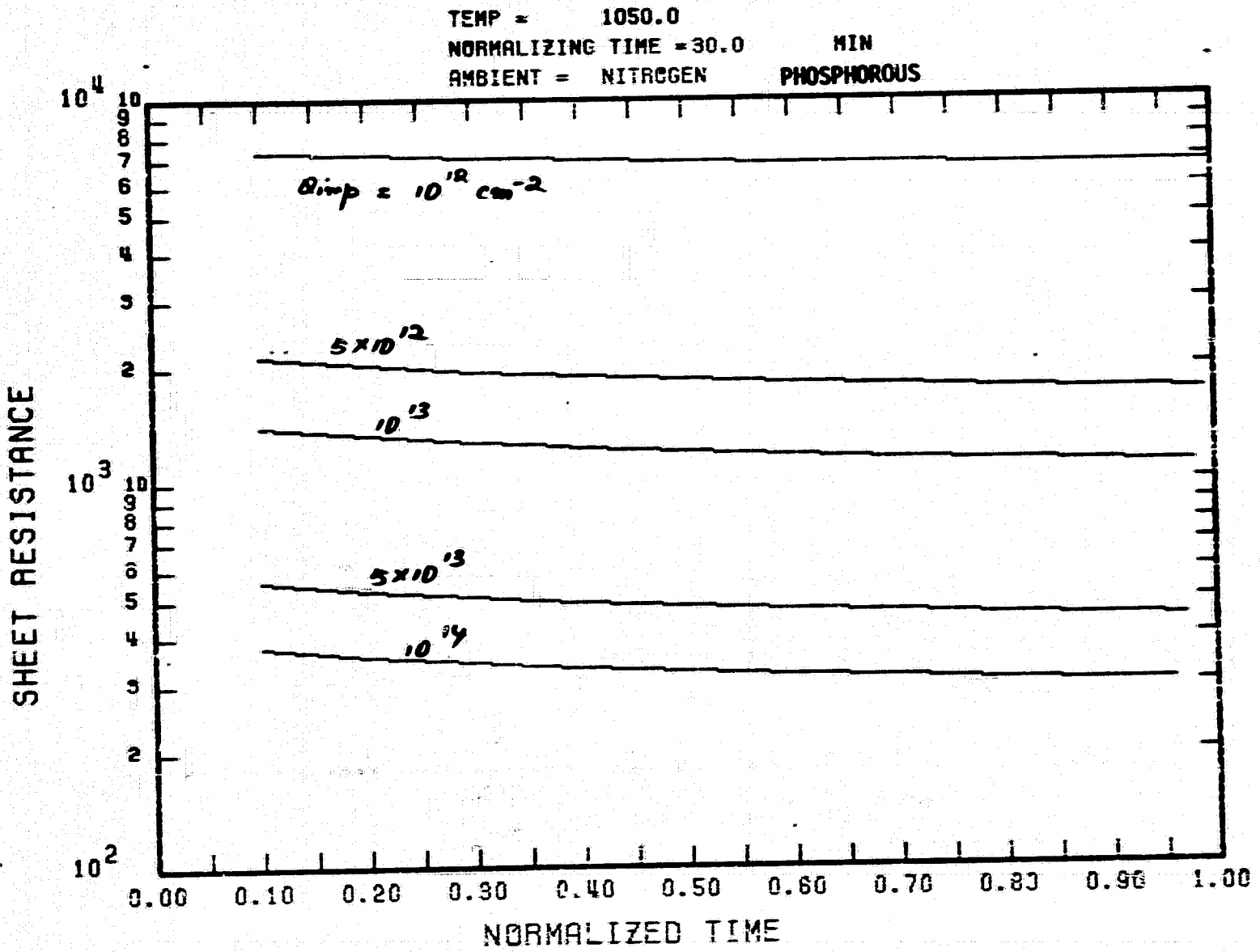
TEMP = 1050.0
NORMALIZING TIME =30.0 MIN
AMBIENT = NITROGEN PHOSPHOROUS
$Q_{imp} = 10^{12}\ cm^{-2}$
5×10^{12}
10^{13}
5×10^{13}
10^{14}
SHEET RESISTANCE
10^4
10^3
10^2
0.00 0.10 0.20 0.30 0.40 0.50 0.60 0.70 0.80 0.90 1.00
NORMALIZED TIME

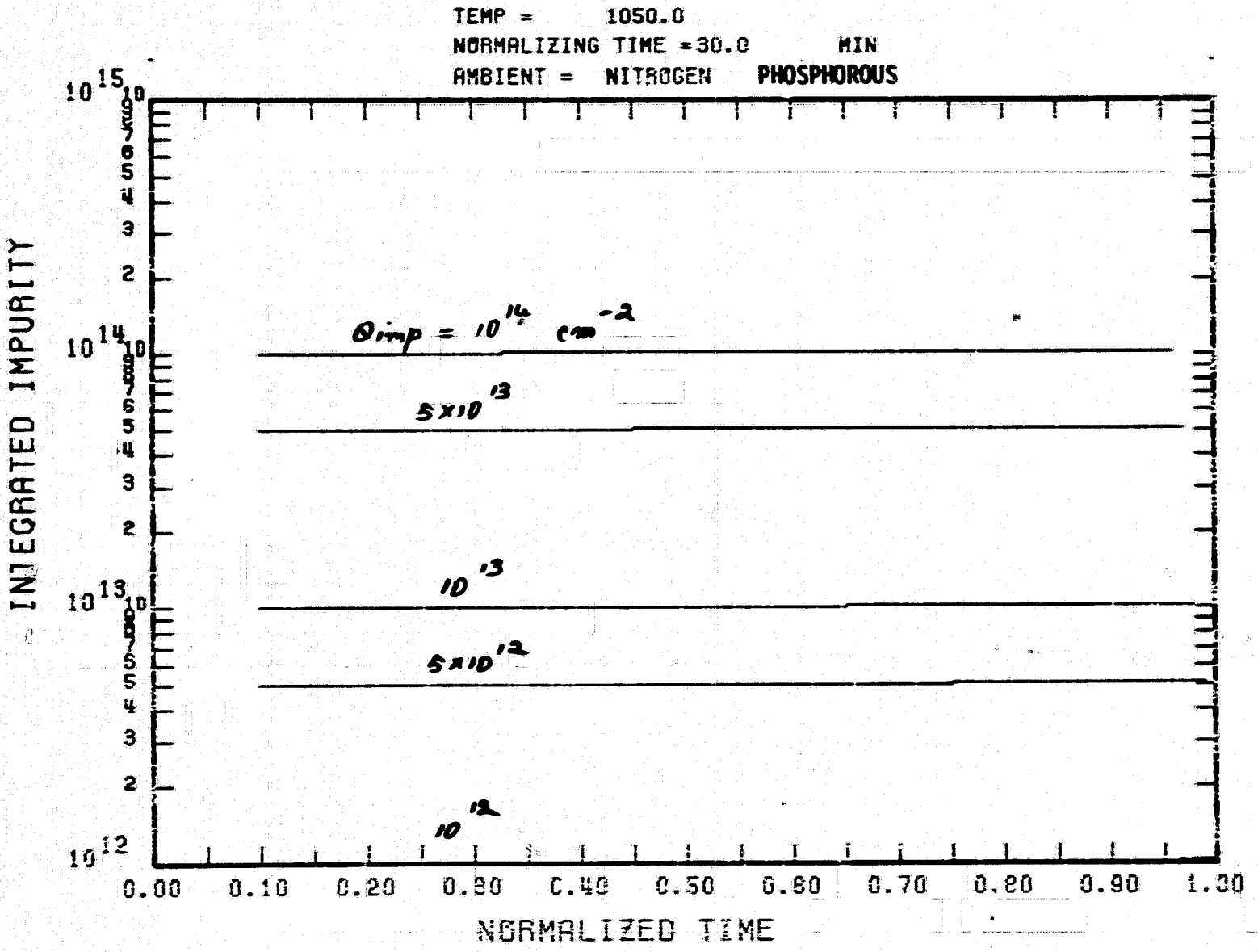
TEMP = 1050.0
NORMALIZING TIME =30.0 MIN
AMBIENT = NITROGEN PHOSPHOROUS
INTEGRATED IMPURITY
NORMALIZED TIME
10^{15}
10^{14}
10^{13}
10^{12}
$Q_{imp} = 10^{14}$ cm^{-2}
5×10^{13}
10^{13}
5×10^{12}
10^{12}
0.00
0.10
0.20
0.30
0.40
0.50
0.60
0.70
0.80
0.90
1.00

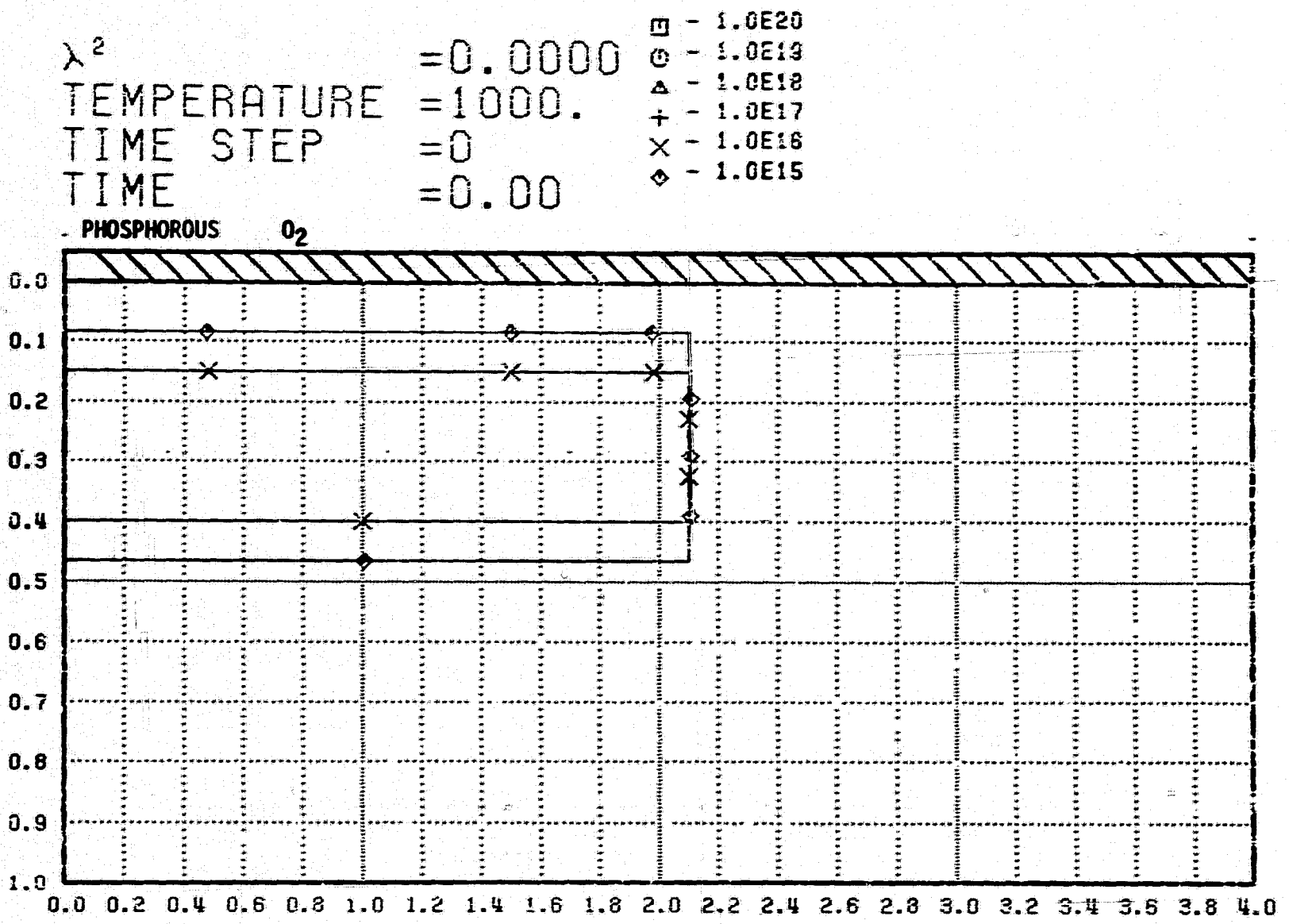
λ² =0.0000
TEMPERATURE =1000.
TIME STEP =0
TIME =0.00
□ - 1.0E20
○ - 1.0E13
△ - 1.0E18
+ - 1.0E17
× - 1.0E16
◇ - 1.0E15
PHOSPHOROUS O2
0.0
0.1
0.2
0.3
0.4
0.5
0.6
0.7
0.8
0.9
1.0
0.0 0.2 0.4 0.6 0.8 1.0 1.2 1.4 1.6 1.8 2.0 2.2 2.4 2.6 2.8 3.0 3.2 3.4 3.6 3.8 4.0

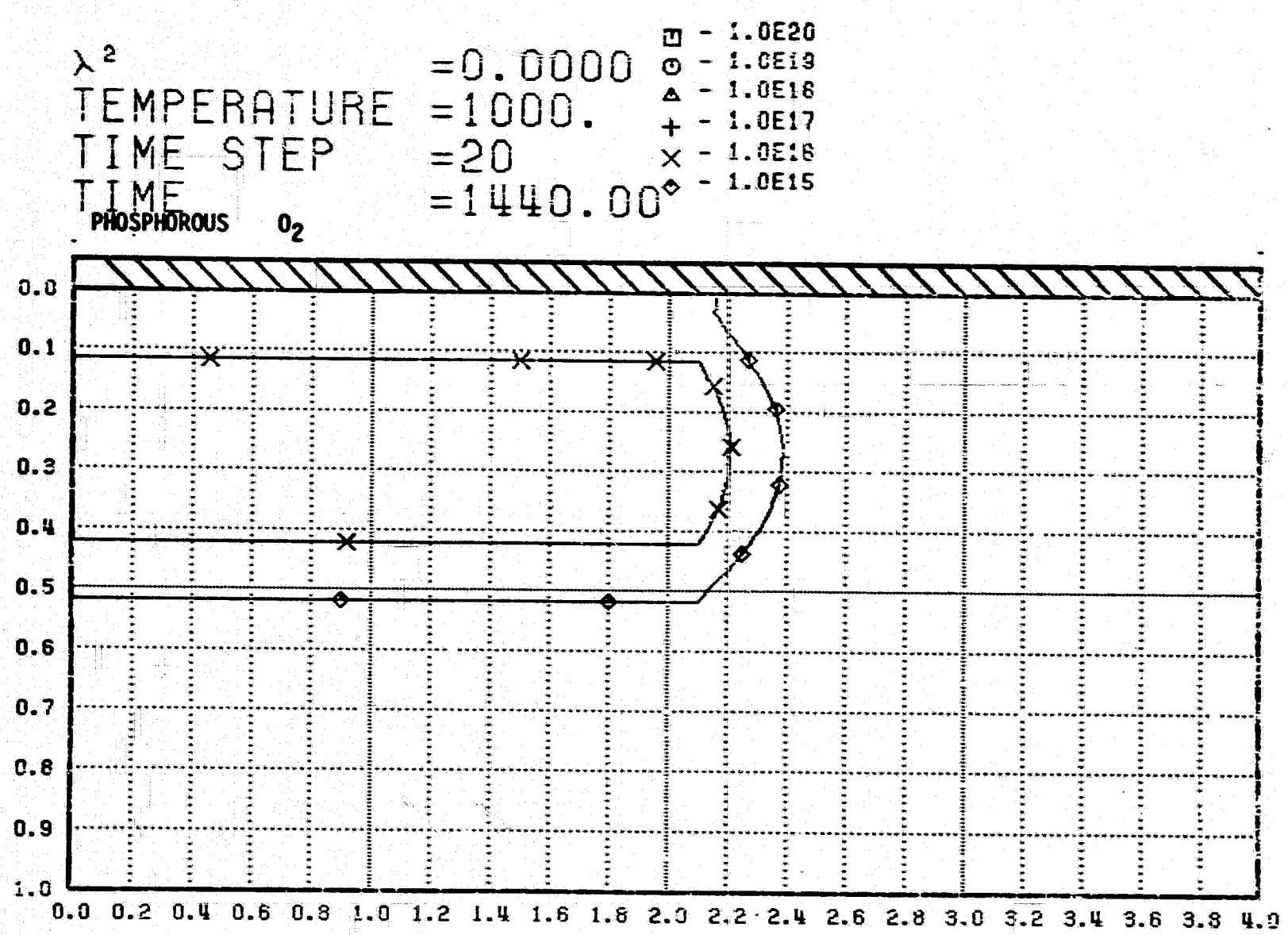
λ² =0.0000
TEMPERATURE =1000.
TIME STEP =20
TIME =1440.00
□ - 1.0E20
⊙ - 1.0E19
△ - 1.0E18
+ - 1.0E17
× - 1.0E16
◇ - 1.0E15
PHOSPHOROUS O2
0.0
0.1
0.2
0.3
0.4
0.5
0.6
0.7
0.8
0.9
1.0
0.0 0.2 0.4 0.6 0.8 1.0 1.2 1.4 1.6 1.8 2.0 2.2 2.4 2.6 2.8 3.0 3.2 3.4 3.6 3.8 4.0

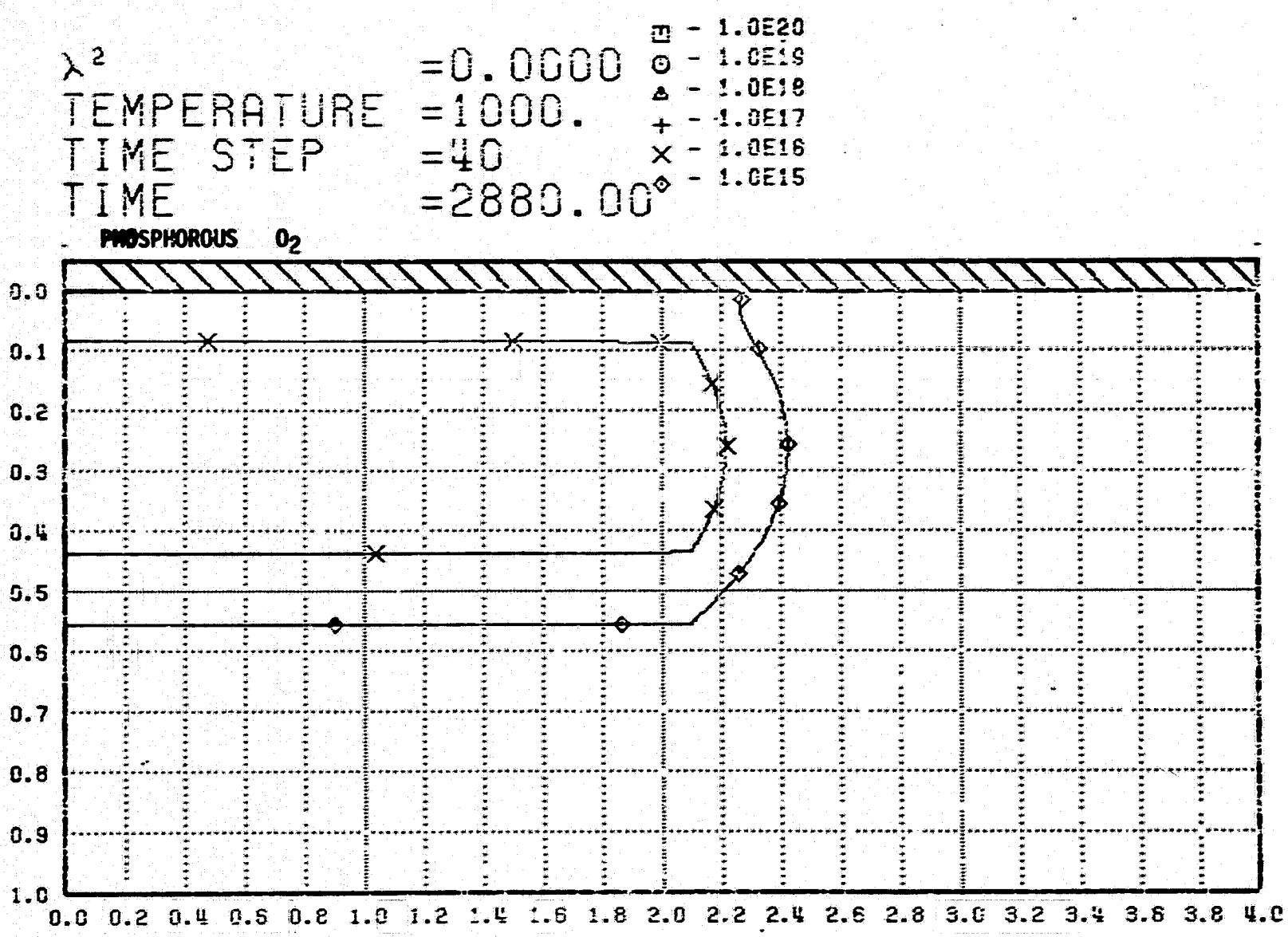
λ² =0.0000
TEMPERATURE =1000.
TIME STEP =40
TIME =2880.00
□ - 1.0E20
⊙ - 1.0E19
△ - 1.0E18
+ - 1.0E17
× - 1.0E16
◇ - 1.0E15
PHOSPHOROUS O2
0.0
0.1
0.2
0.3
0.4
0.5
0.6
0.7
0.8
0.9
1.0
0.0 0.2 0.4 0.6 0.8 1.0 1.2 1.4 1.6 1.8 2.0 2.2 2.4 2.6 2.8 3.0 3.2 3.4 3.6 3.8 4.0

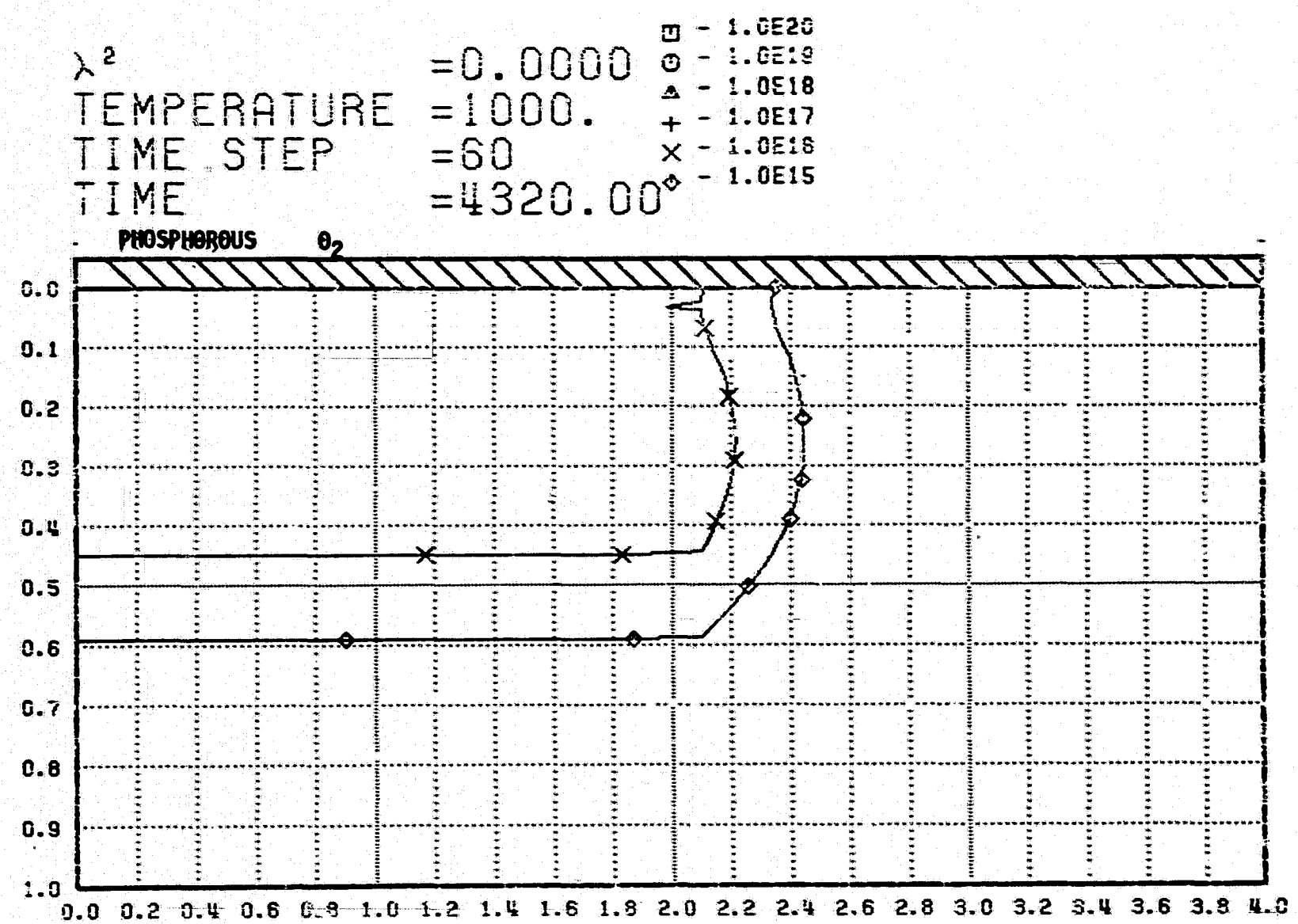
λ² =0.0000
TEMPERATURE =1000.
TIME STEP =60
TIME =4320.00
□ - 1.0E20
⊙ - 1.0E19
△ - 1.0E18
+ - 1.0E17
× - 1.0E16
◇ - 1.0E15
PHOSPHOROUS θ2
0.0
0.1
0.2
0.3
0.4
0.5
0.6
0.7
0.8
0.9
1.0
0.0 0.2 0.4 0.6 0.8 1.0 1.2 1.4 1.6 1.8 2.0 2.2 2.4 2.6 2.8 3.0 3.2 3.4 3.6 3.8 4.0

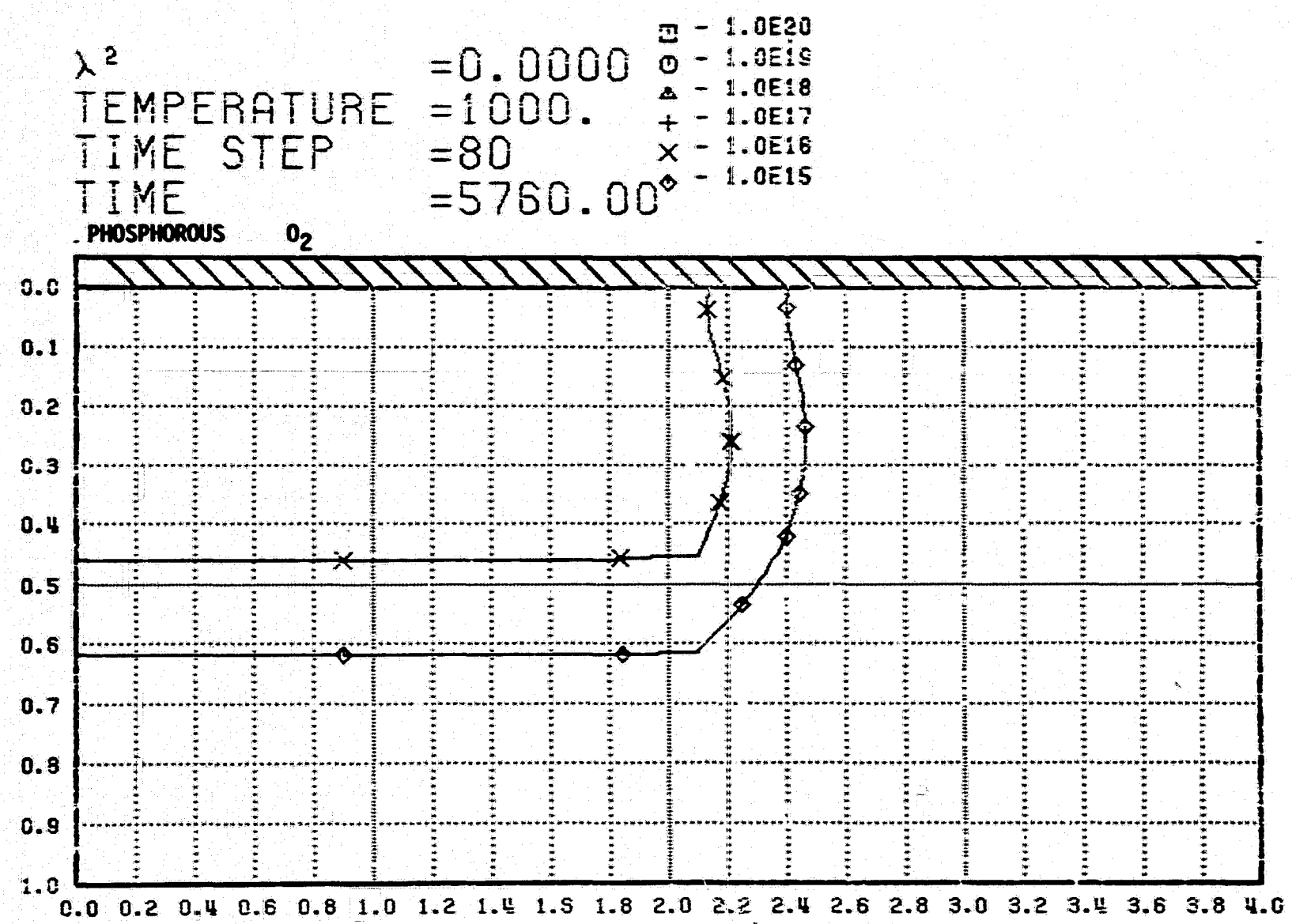
λ² =0.0000
TEMPERATURE =1000.
TIME STEP =80
TIME =5760.00
□ - 1.0E20
○ - 1.0E19
△ - 1.0E18
+ - 1.0E17
× - 1.0E16
◇ - 1.0E15
PHOSPHOROUS O_2
0.0
0.1
0.2
0.3
0.4
0.5
0.6
0.7
0.8
0.9
1.0
0.0 0.2 0.4 0.6 0.8 1.0 1.2 1.4 1.6 1.8 2.0 2.2 2.4 2.6 2.8 3.0 3.2 3.4 3.6 3.8 4.0

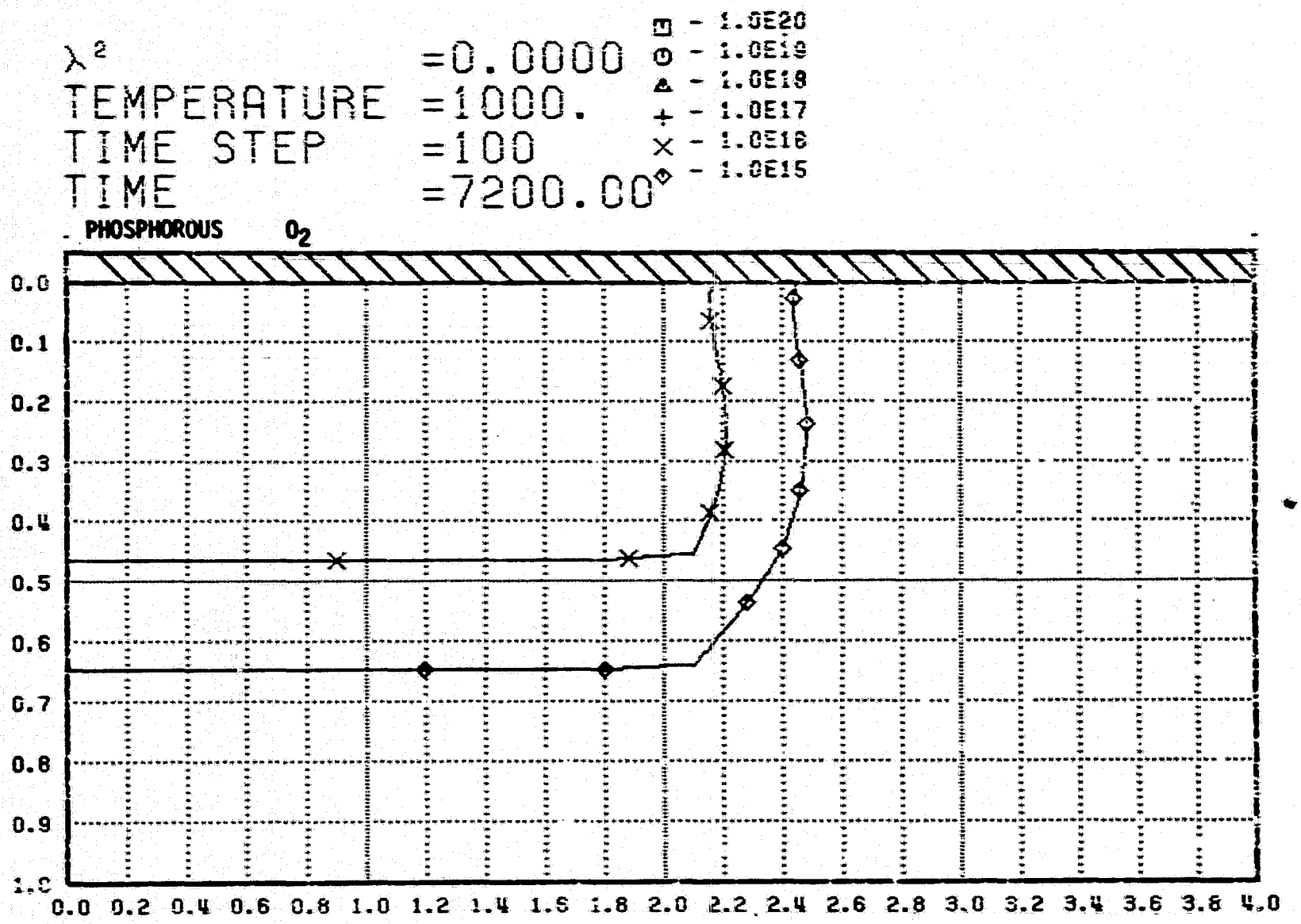
λ² =0.0000
TEMPERATURE =1000.
TIME STEP =100
TIME =7200.00
□ - 1.0E20
○ - 1.0E19
△ - 1.0E18
+ - 1.0E17
× - 1.0E16
◇ - 1.0E15
PHOSPHOROUS O2
0.0
0.1
0.2
0.3
0.4
0.5
0.6
0.7
0.8
0.9
1.0
0.0 0.2 0.4 0.6 0.8 1.0 1.2 1.4 1.6 1.8 2.0 2.2 2.4 2.6 2.8 3.0 3.2 3.4 3.6 3.8 4.0

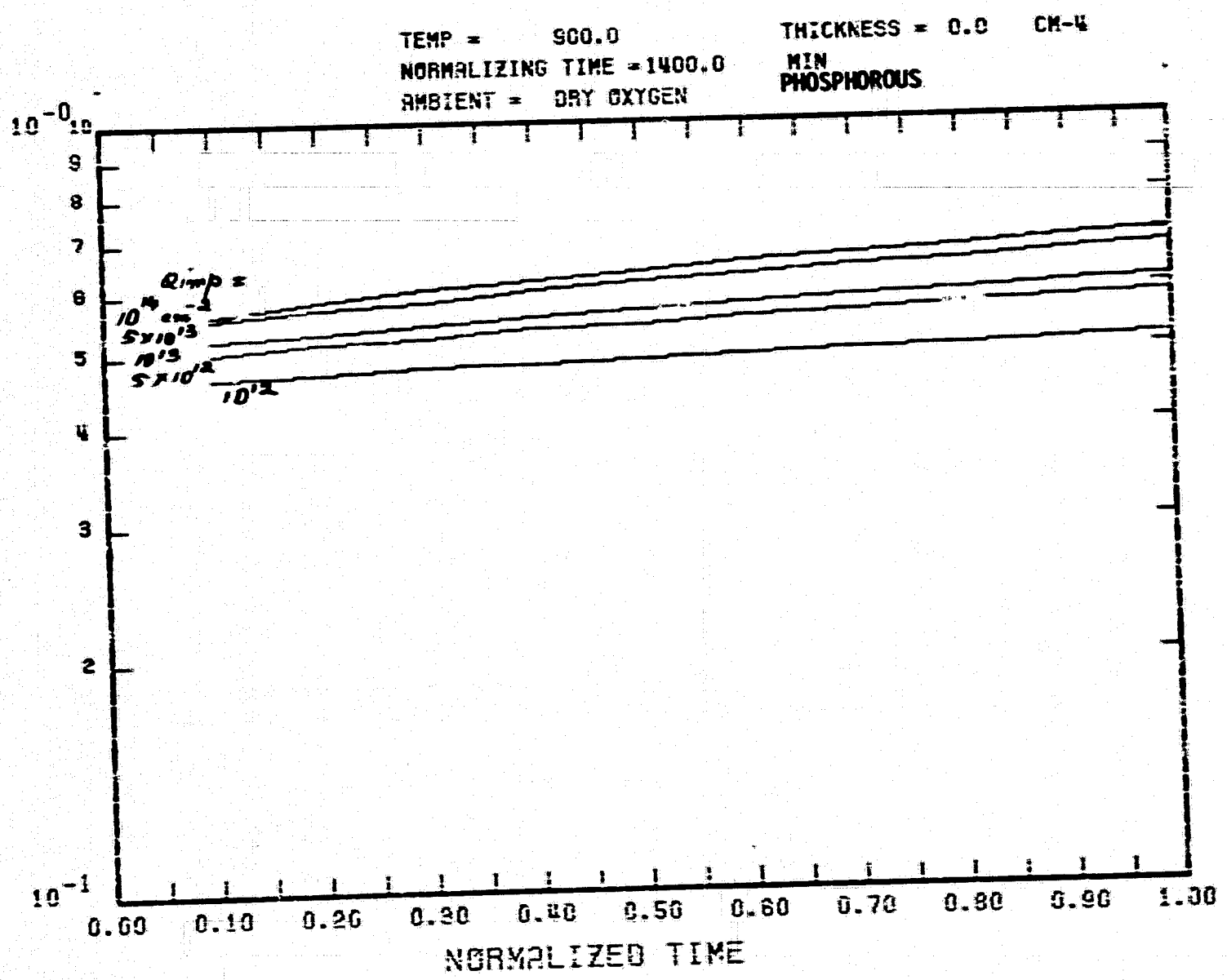
TEMP = 900.0
NORMALIZING TIME = 1400.0
AMBIENT = DRY OXYGEN
THICKNESS = 0.0 CM-4
MIN
PHOSPHOROUS
Qimp =
10^{14} cm^{-2}
5×10^{13}
10^{13}
5×10^{12}
10^{12}
JUNCTION DEPTH
NORMALIZED TIME
10^{-0}
9
8
7
6
5
4
3
2
10^{-1}
0.00
0.10
0.20
0.30
0.40
0.50
0.60
0.70
0.80
0.90
1.00

130

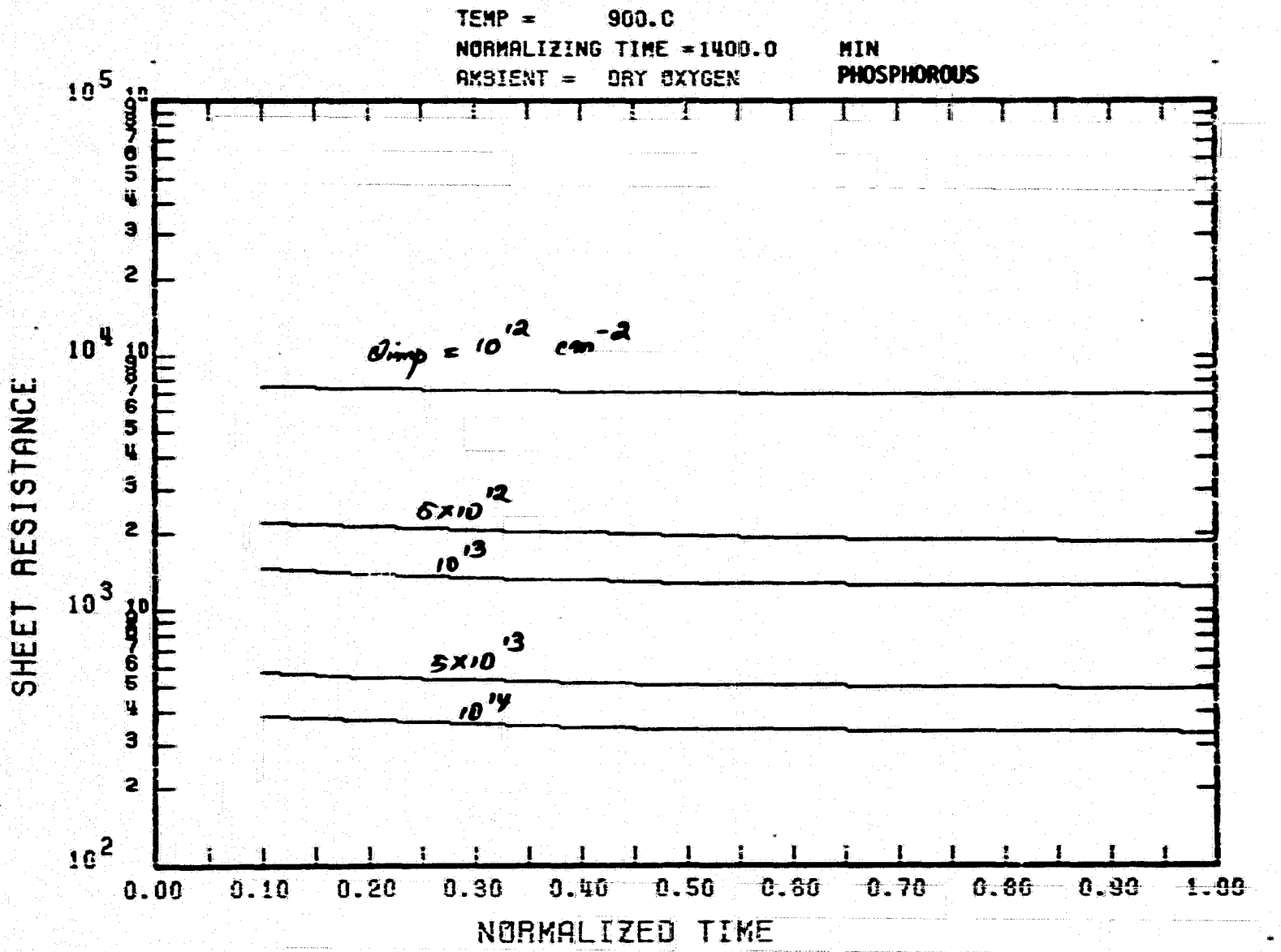
TEMP = 900.C
NORMALIZING TIME =1400.0 MIN
AMBIENT = DRY OXYGEN PHOSPHOROUS
SHEET RESISTANCE
NORMALIZED TIME
10^5
10^4
10^3
10^2
0.00
0.10
0.20
0.30
0.40
0.50
0.60
0.70
0.80
0.90
1.00
$Q_{imp} = 10^{12}$ cm^{-2}
6×10^{12}
10^{13}
5×10^{13}
10^{14}

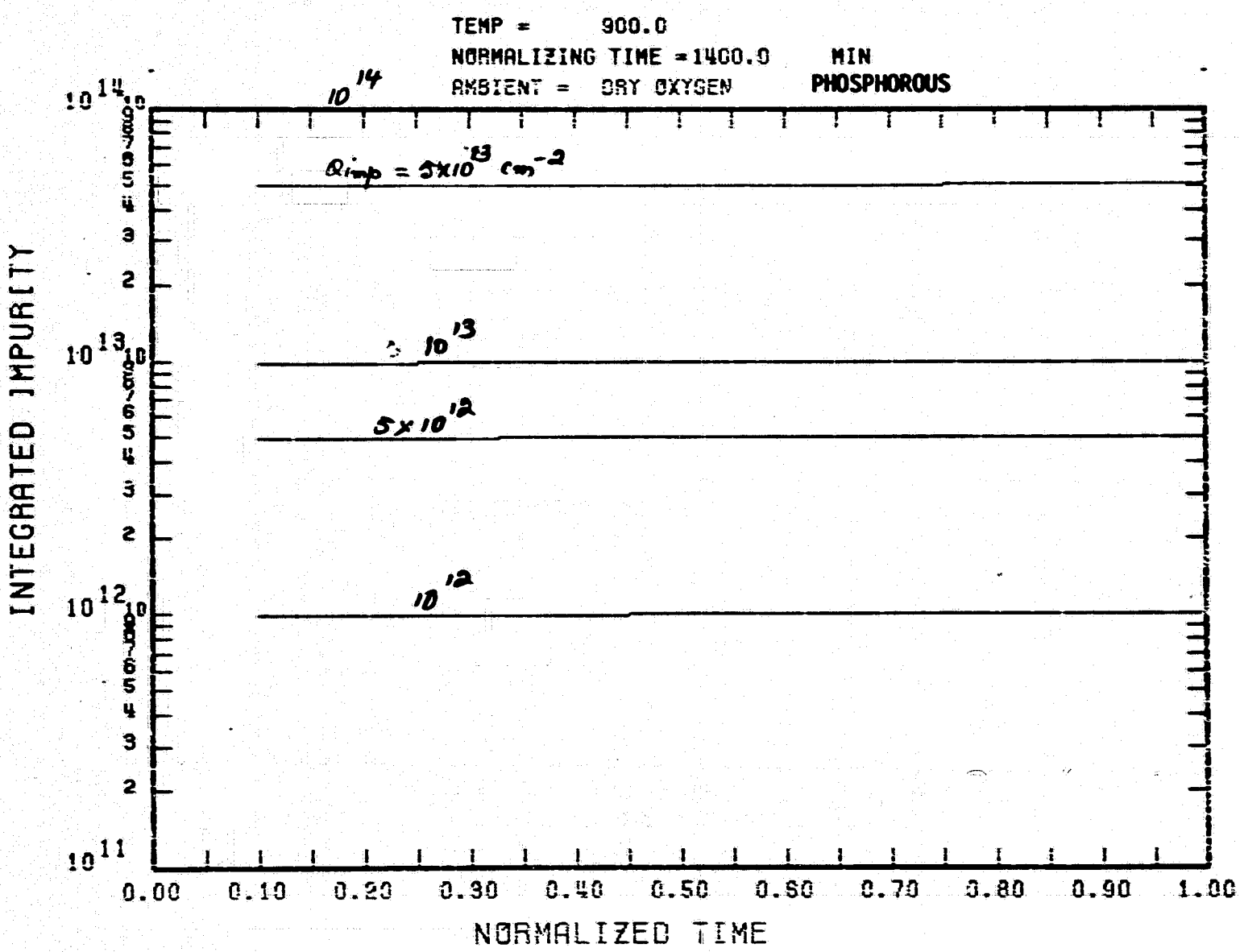
TEMP = 900.0
NORMALIZING TIME = 1400.0 MIN
AMBIENT = DRY OXYGEN
PHOSPHOROUS
10^{14}
$Q_{imp} = 5 \times 10^{13}$ cm^{-2}
10^{13}
5×10^{12}
10^{12}
10^{15}
10^{13}
10^{12}
10^{11}
INTEGRATED IMPURITY
0.00 0.10 0.20 0.30 0.40 0.50 0.60 0.70 0.80 0.90 1.00
NORMALIZED TIME

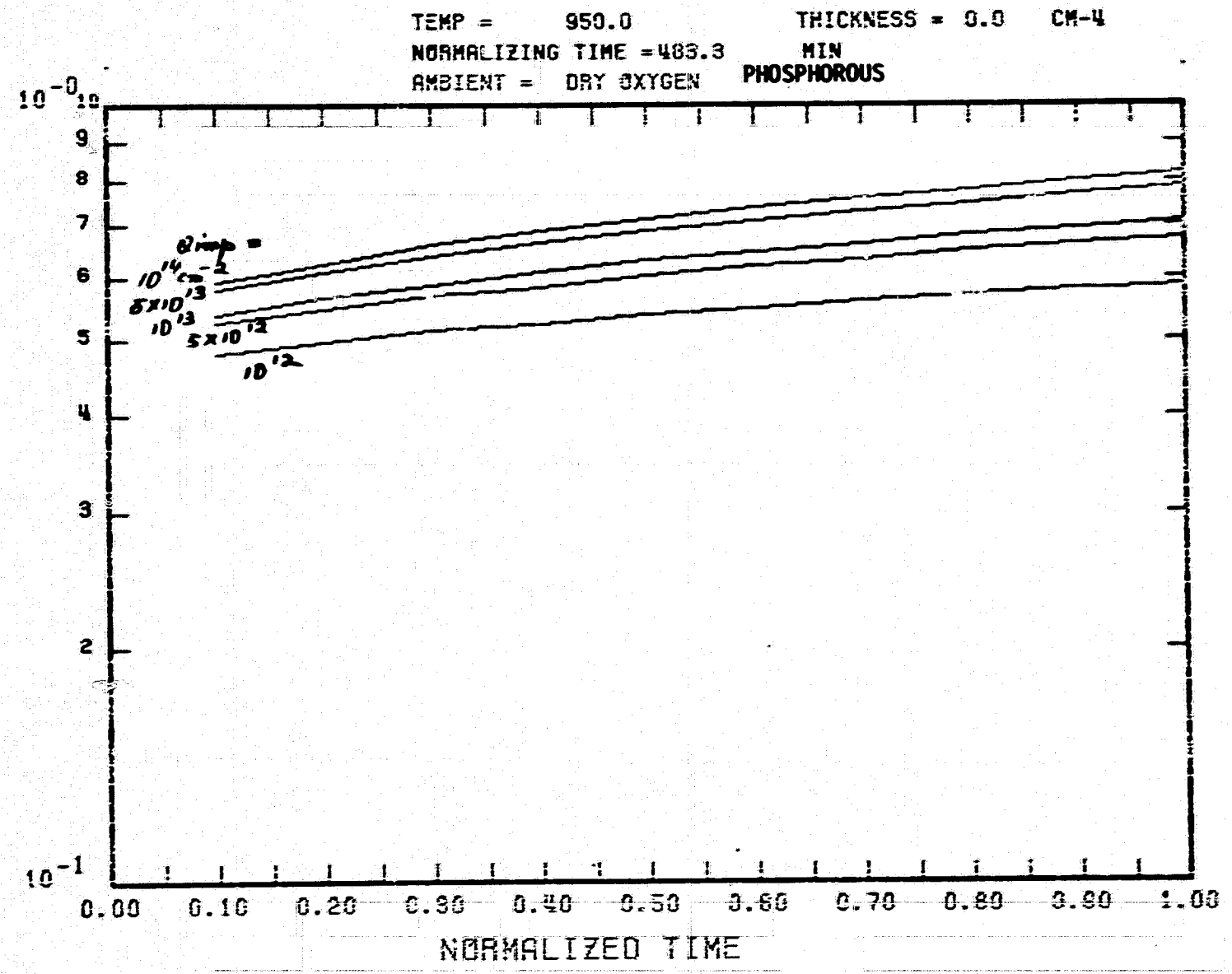
TEMP = 950.0 THICKNESS = 0.0 CM-4
NORMALIZING TIME = 483.3 MIN
AMBIENT = DRY OXYGEN
PHOSPHOROUS
10^{-0}
9
8
7
6
5
4
3
2
10^{-1}
10^{14}
5×10^{13}
10^{13}
5×10^{12}
10^{12}
JUNCTION DEPTH
0.00 0.10 0.20 0.30 0.40 0.50 0.60 0.70 0.80 0.90 1.00
NORMALIZED TIME

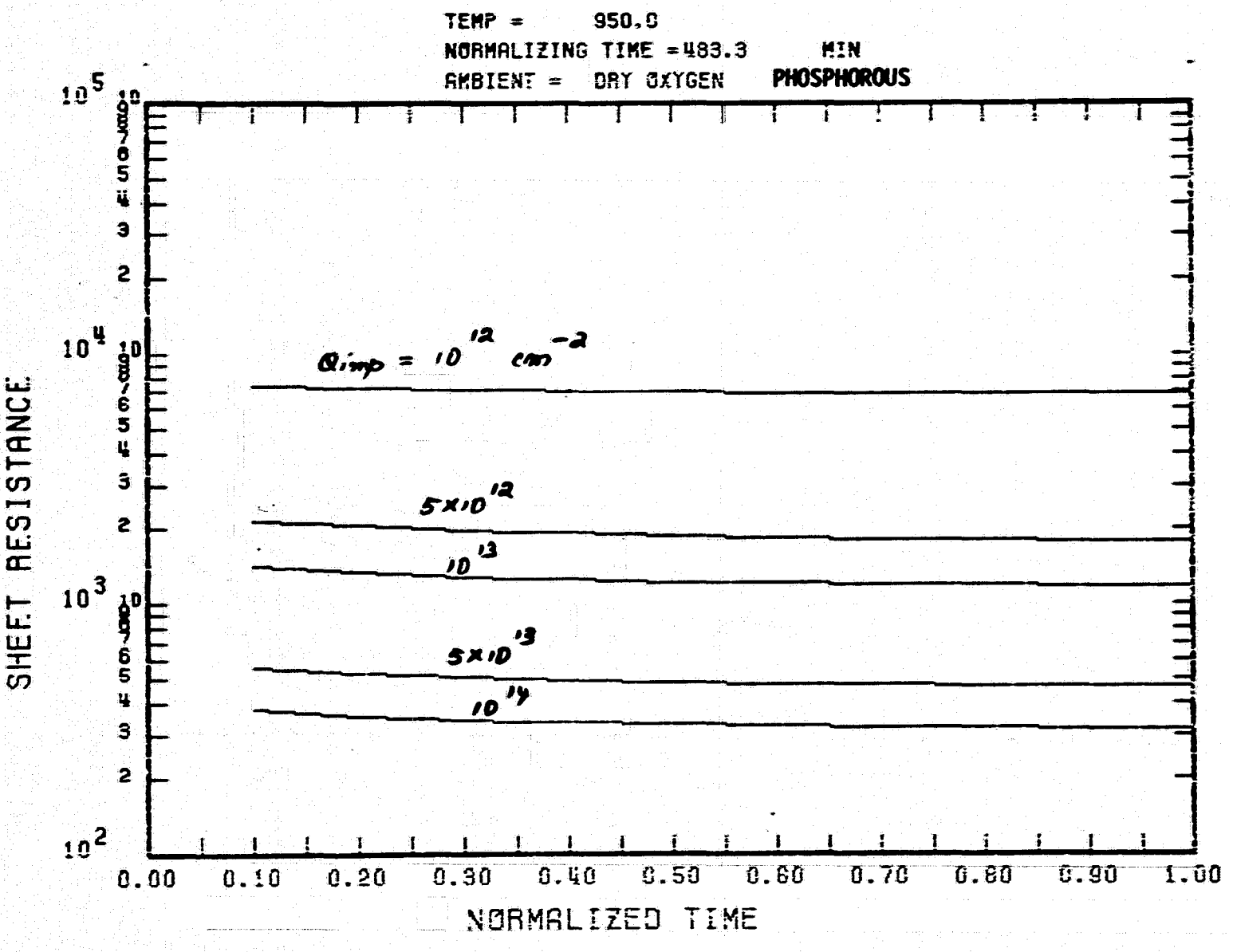
TEMP = 950.0
NORMALIZING TIME =483.3 MIN
AMBIENT = DRY OXYGEN PHOSPHOROUS
SHEET RESISTANCE
NORMALIZED TIME
10^5
10^4
10^3
10^2
0.00
0.10
0.20
0.30
0.40
0.50
0.60
0.70
0.80
0.90
1.00
$Q_{imp} = 10^{12}$ cm^{-2}
5×10^{12}
10^{13}
5×10^{13}
10^{14}

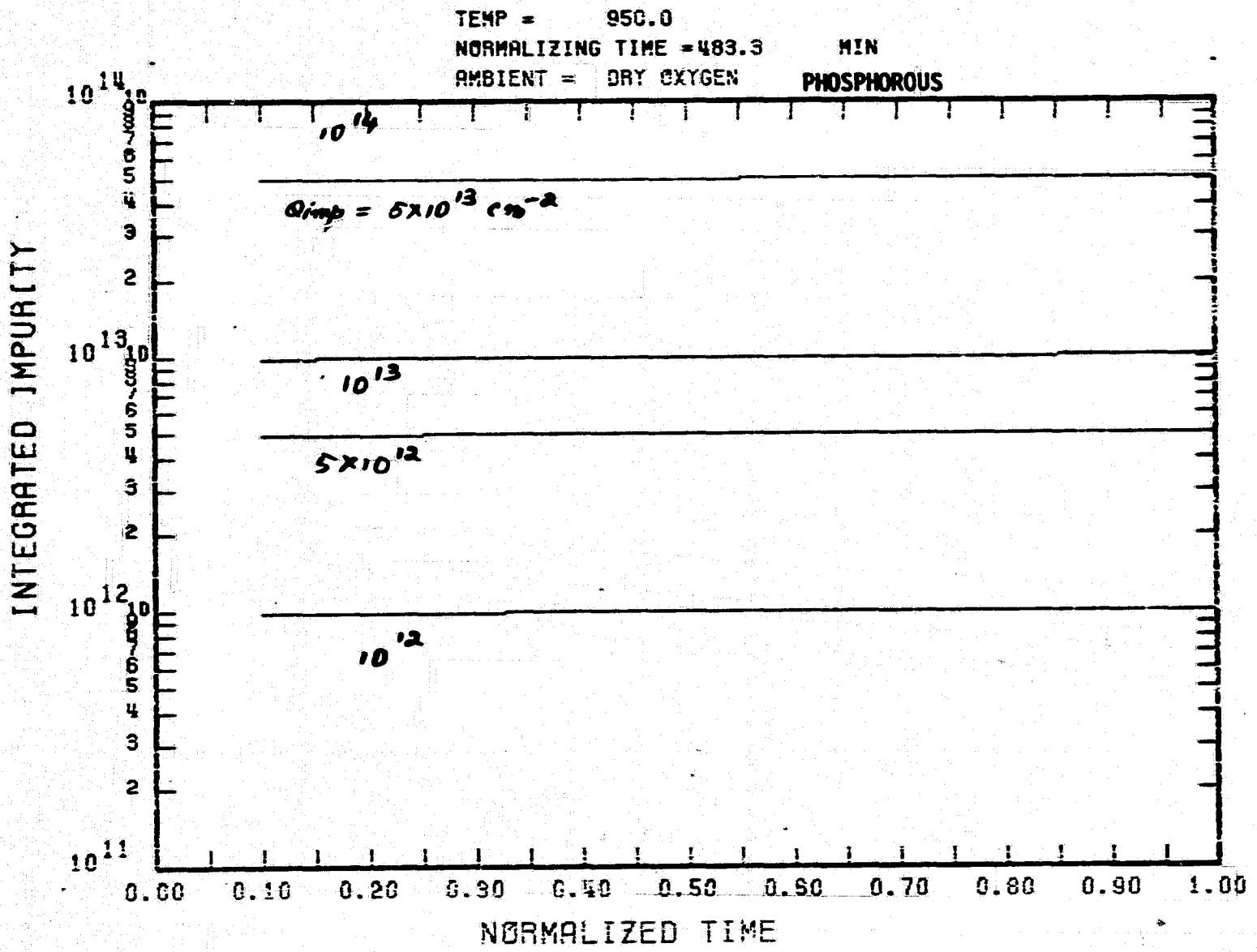
TEMP = 950.0
NORMALIZING TIME =483.3 MIN
AMBIENT = DRY OXYGEN
PHOSPHOROUS
INTEGRATED IMPURITY
NORMALIZED TIME
10^{14}
10^{13}
10^{12}
10^{11}
10^{14}
$Q_{imp} = 5\times10^{13}\ cm^{-2}$
10^{13}
5×10^{12}
10^{12}
0.00
0.10
0.20
0.30
0.40
0.50
0.60
0.70
0.80
0.90
1.00

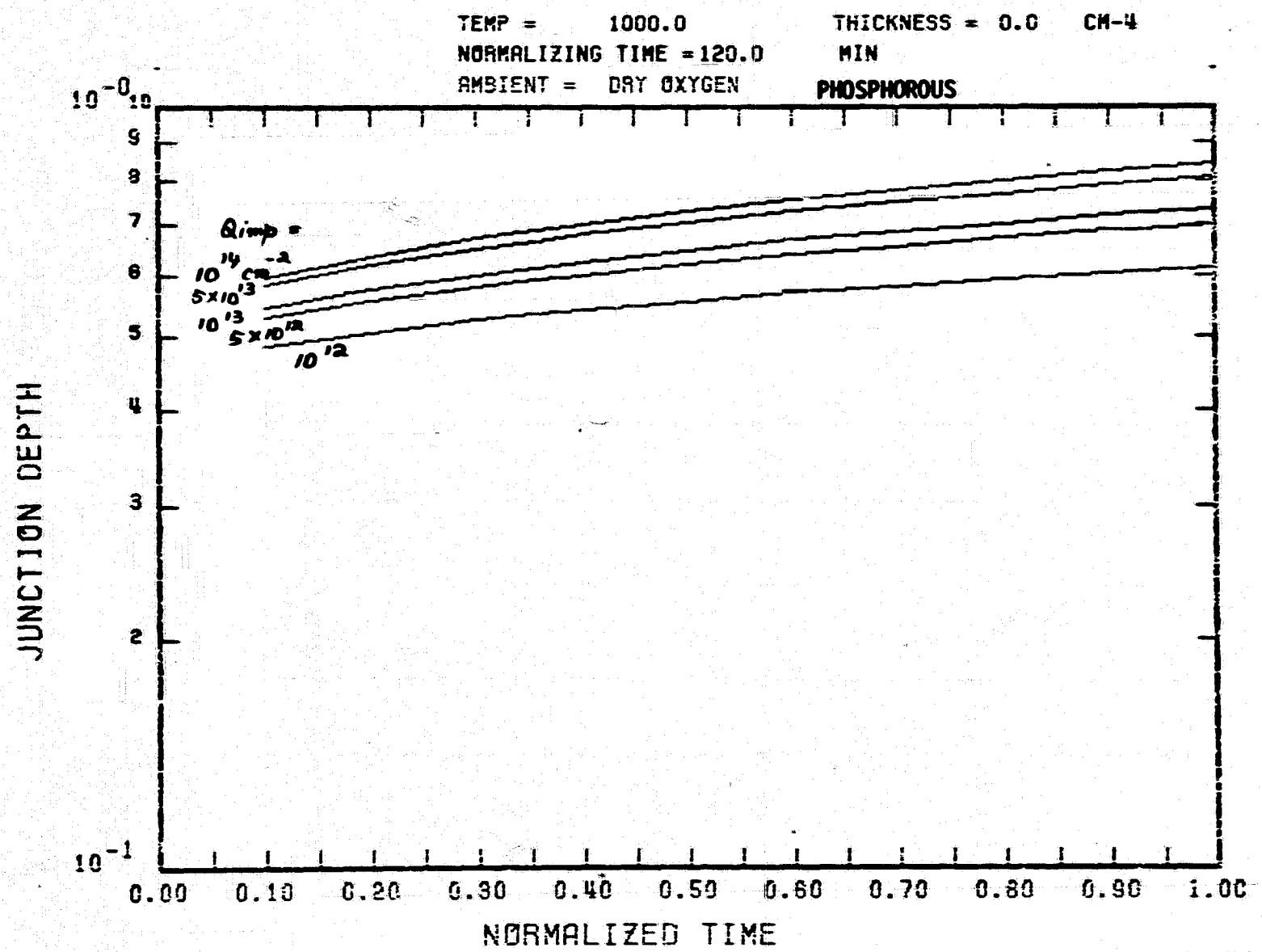
TEMP = 1000.0 THICKNESS = 0.0 CM-4
NORMALIZING TIME = 120.0 MIN
AMBIENT = DRY OXYGEN
PHOSPHOROUS
Qimp =
10^14 cm^-2
5x10^13
10^13
5x10^12
10^12
JUNCTION DEPTH
NORMALIZED TIME
10^-0
9
8
7
6
5
4
3
2
10^-1
0.00
0.10
0.20
0.30
0.40
0.50
0.60
0.70
0.80
0.90
1.00

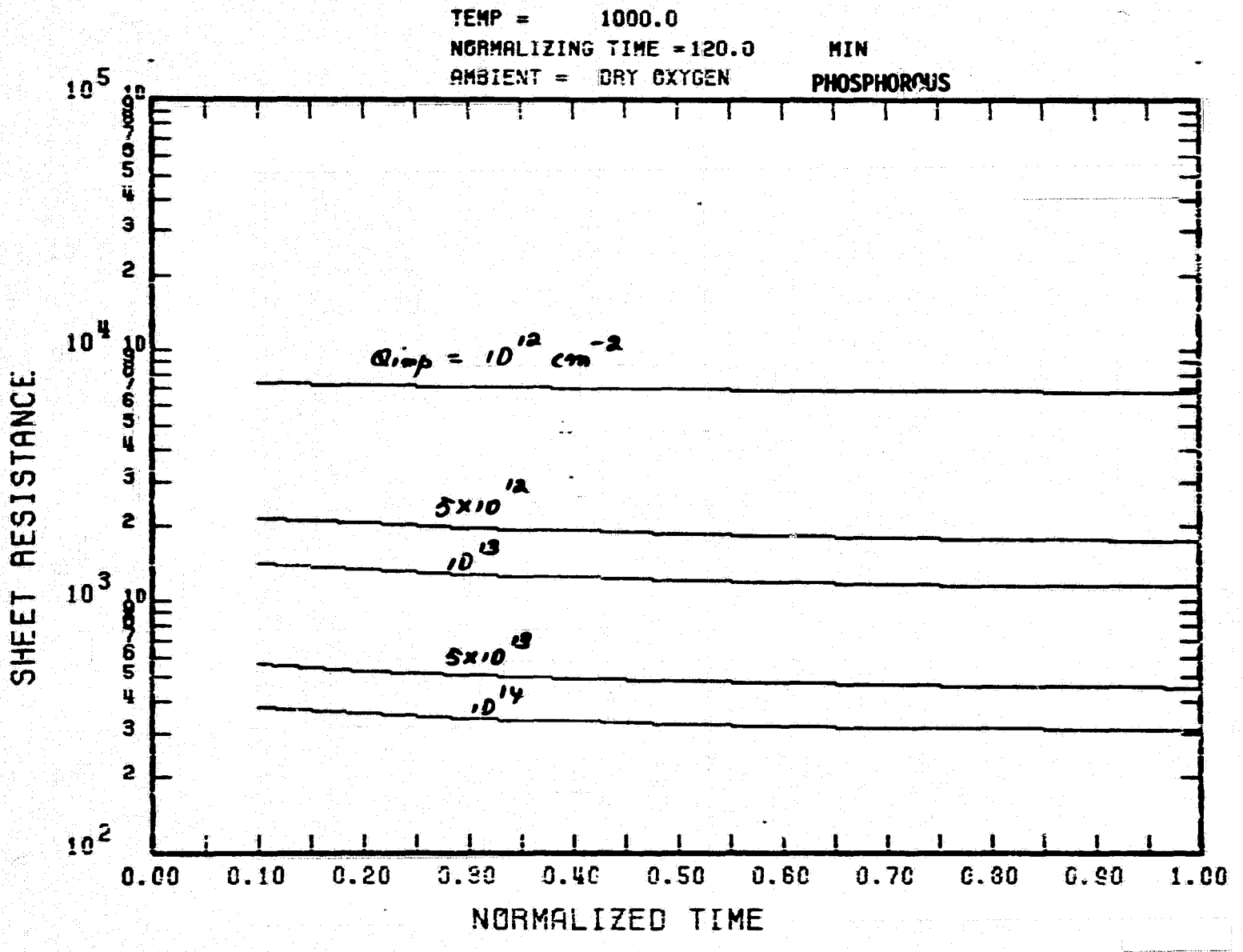
TEMP = 1000.0
NORMALIZING TIME = 120.0 MIN
AMBIENT = DRY OXYGEN
PHOSPHOROUS
$Q_{imp} = 10^{12}\ cm^{-2}$
5×10^{12}
10^{13}
5×10^{13}
10^{14}
SHEET RESISTANCE
NORMALIZED TIME
10^5
10^4
10^3
10^2
0.00
0.10
0.20
0.30
0.40
0.50
0.60
0.70
0.80
0.90
1.00

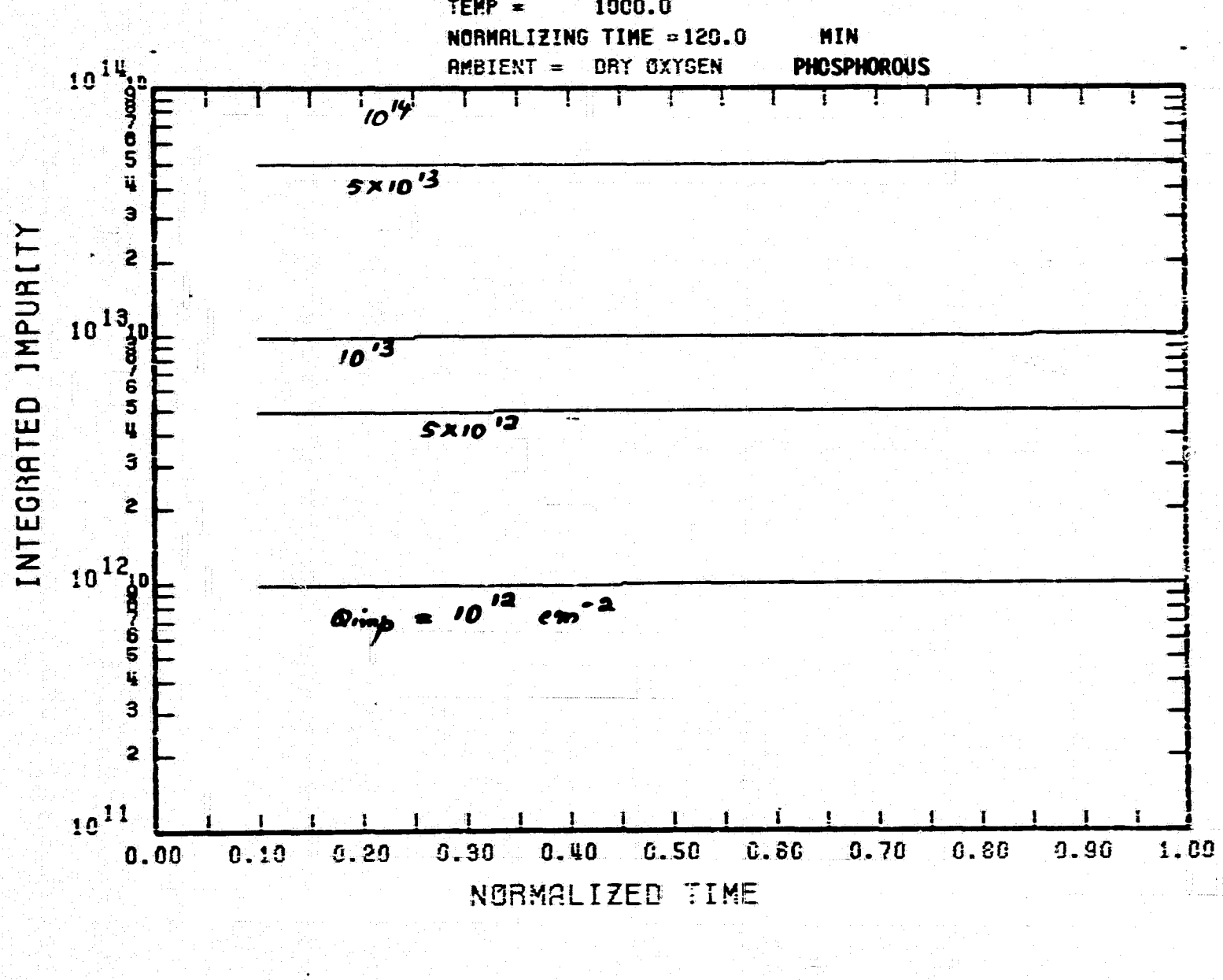
TEMP = 1000.0
NORMALIZING TIME = 120.0 MIN
AMBIENT = DRY OXYGEN PHOSPHOROUS
INTEGRATED IMPURITY
NORMALIZED TIME
10^{14}
5×10^{13}
10^{13}
5×10^{12}
$Q_{imp} = 10^{12}$ cm^{-2}
0.00
0.10
0.20
0.30
0.40
0.50
0.60
0.70
0.80
0.90
1.00

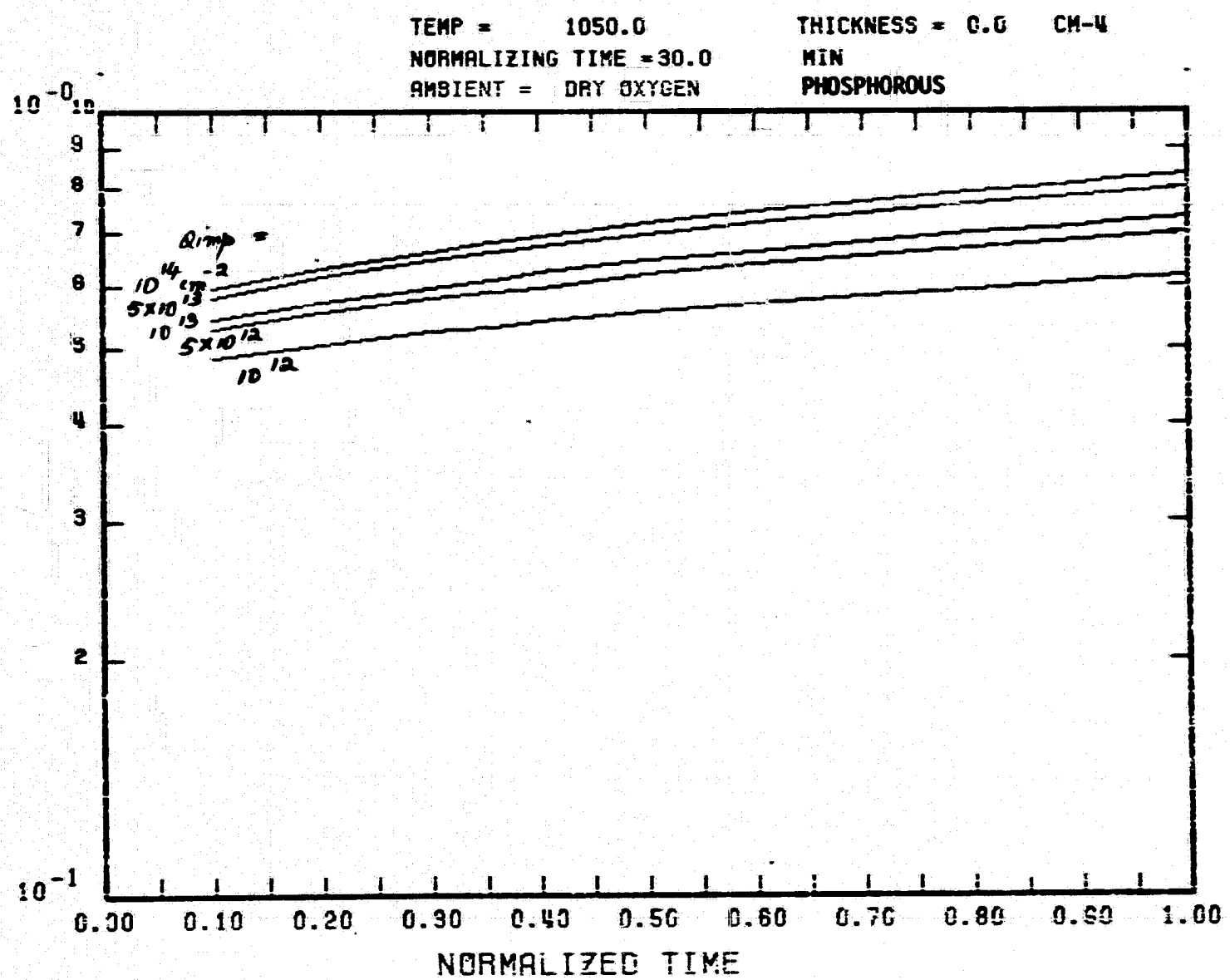
TEMP = 1050.0
NORMALIZING TIME =30.0
AMBIENT = DRY OXYGEN
THICKNESS = 0.0 CM-4
MIN
PHOSPHOROUS
Qimp =
10^14 cm^-2
5x10^13
10^13
5x10^12
10^12
JUNCTION DEPTH
NORMALIZED TIME
10^-0
9
8
7
6
5
4
3
2
10^-1
0.00
0.10
0.20
0.30
0.40
0.50
0.60
0.70
0.80
0.90
1.00

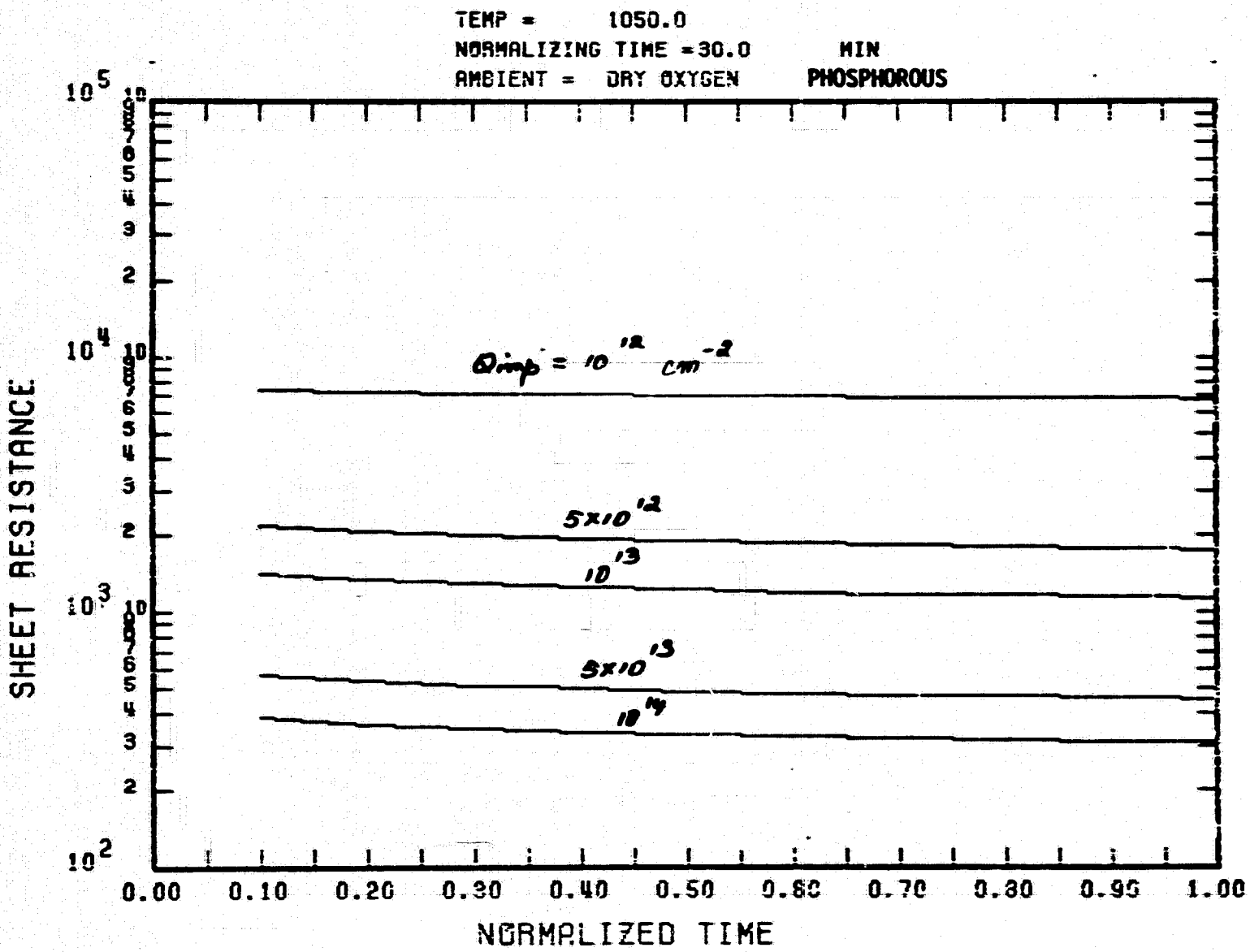
TEMP = 1050.0
NORMALIZING TIME =30.0 MIN
AMBIENT = DRY OXYGEN PHOSPHOROUS
SHEET RESISTANCE
NORMALIZED TIME
10^5
10^4
10^3
10^2
0.00
0.10
0.20
0.30
0.40
0.50
0.60
0.70
0.80
0.90
1.00
$Q_{imp} = 10^{12}\ cm^{-2}$
5×10^{12}
10^{13}
5×10^{13}
10^{14}

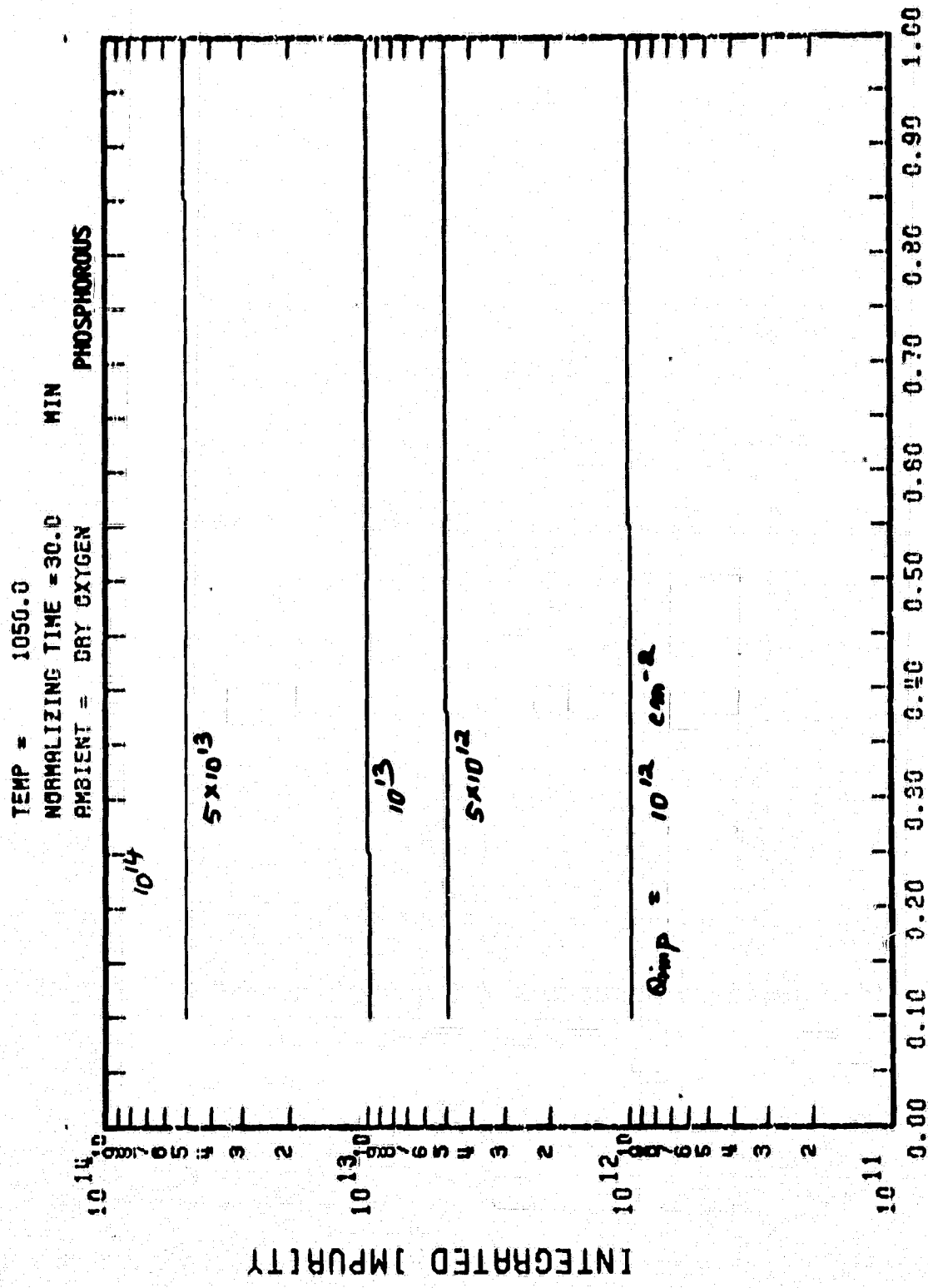
TEMP = 1050.0
NORMALIZING TIME =30.0 MIN
AMBIENT = DRY OXYGEN
PHOSPHOROUS
10^{14}
5×10^{13}
10^{13}
5×10^{12}
$Q_{imp} = 10^{12}$ cm^{-2}
INTEGRATED IMPURITY
NORMALIZED TIME
0.00
0.10
0.20
0.30
0.40
0.50
0.60
0.70
0.80
0.90
1.00

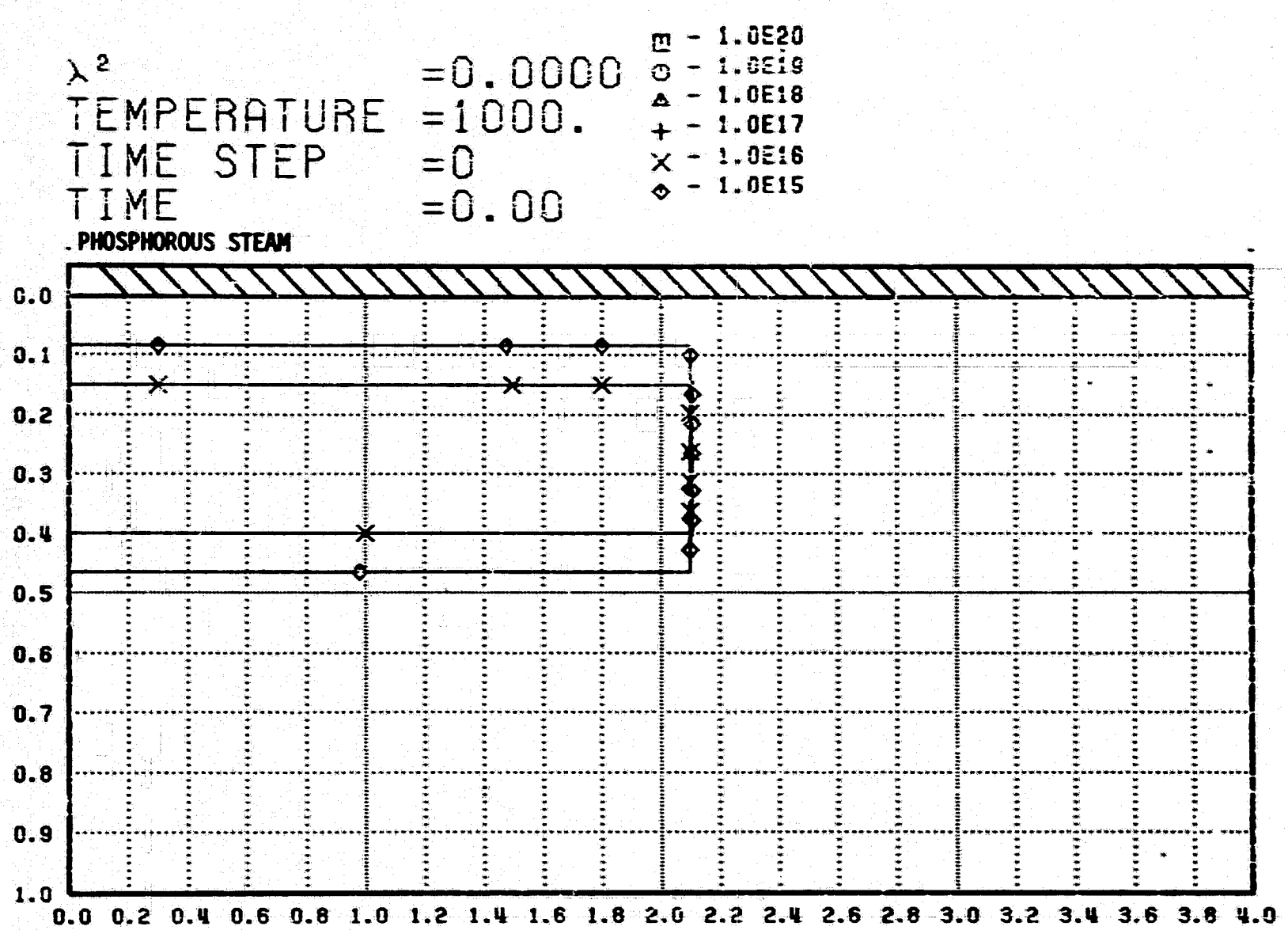
λ²
=0.0000
TEMPERATURE
=1000.
TIME STEP
=0
TIME
=0.00
- 1.0E20
- 1.0E19
- 1.0E18
- 1.0E17
- 1.0E16
- 1.0E15
. PHOSPHOROUS STEAM
0.0
0.1
0.2
0.3
0.4
0.5
0.6
0.7
0.8
0.9
1.0
0.0 0.2 0.4 0.6 0.8 1.0 1.2 1.4 1.6 1.8 2.0 2.2 2.4 2.6 2.8 3.0 3.2 3.4 3.6 3.8 4.0

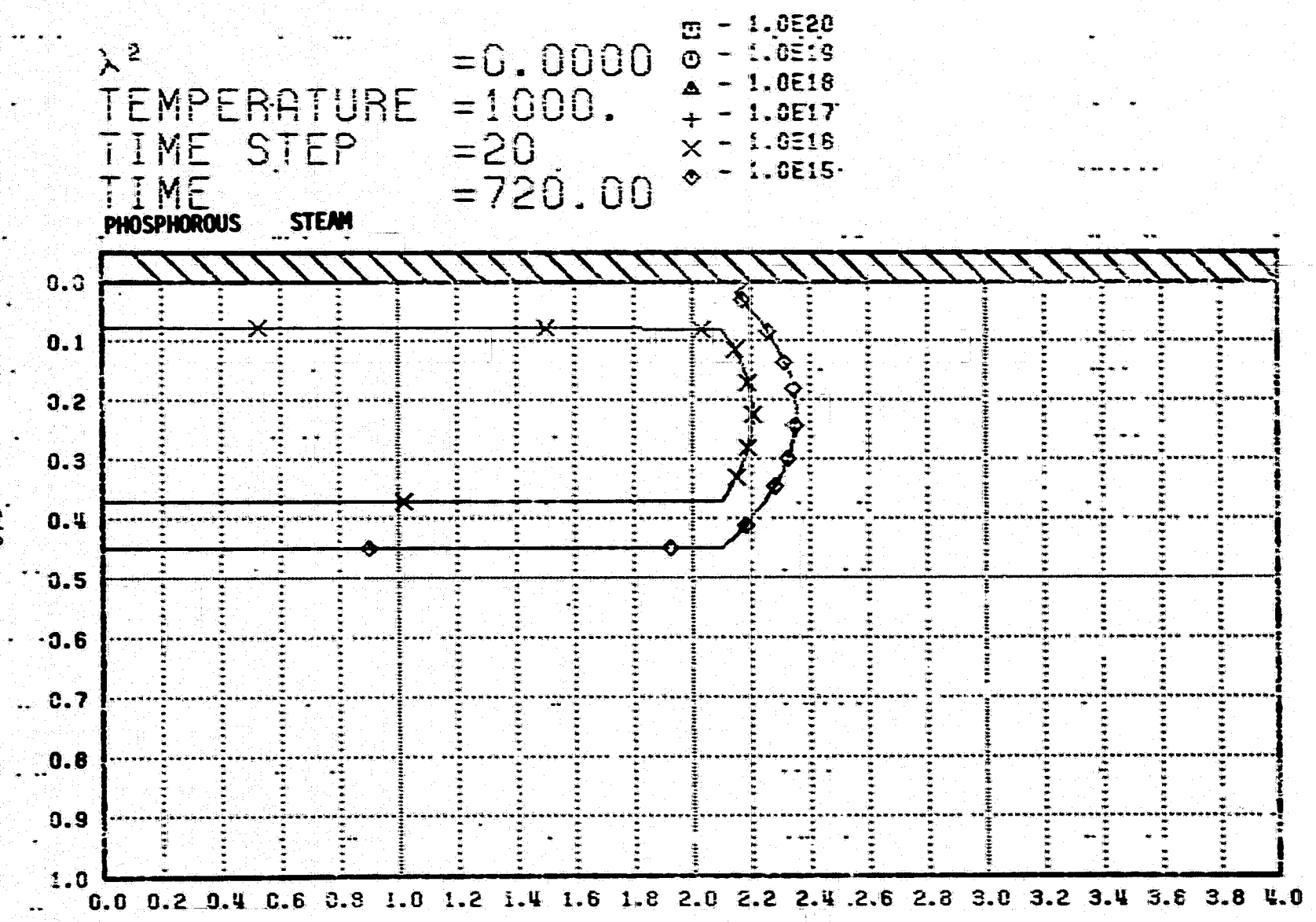
χ^2 =0.0000
TEMPERATURE =1000.
TIME STEP =20
TIME =720.00
□ - 1.0E20
⊙ - 1.0E19
▲ - 1.0E18
+ - 1.0E17
× - 1.0E16
◇ - 1.0E15
PHOSPHOROUS STEAM
0.0
0.1
0.2
0.3
0.4
0.5
0.6
0.7
0.8
0.9
1.0
0.0 0.2 0.4 0.6 0.8 1.0 1.2 1.4 1.6 1.8 2.0 2.2 2.4 2.6 2.8 3.0 3.2 3.4 3.6 3.8 4.0

χ^2 =0.0000

TEMPERATURE =1000.

TIME STEP =60

TIME =2160.00

□ - 1.0E20
○ - 1.0E19
△ - 1.0E18
+ - 1.0E17
× - 1.0E16
◇ - 1.0E15

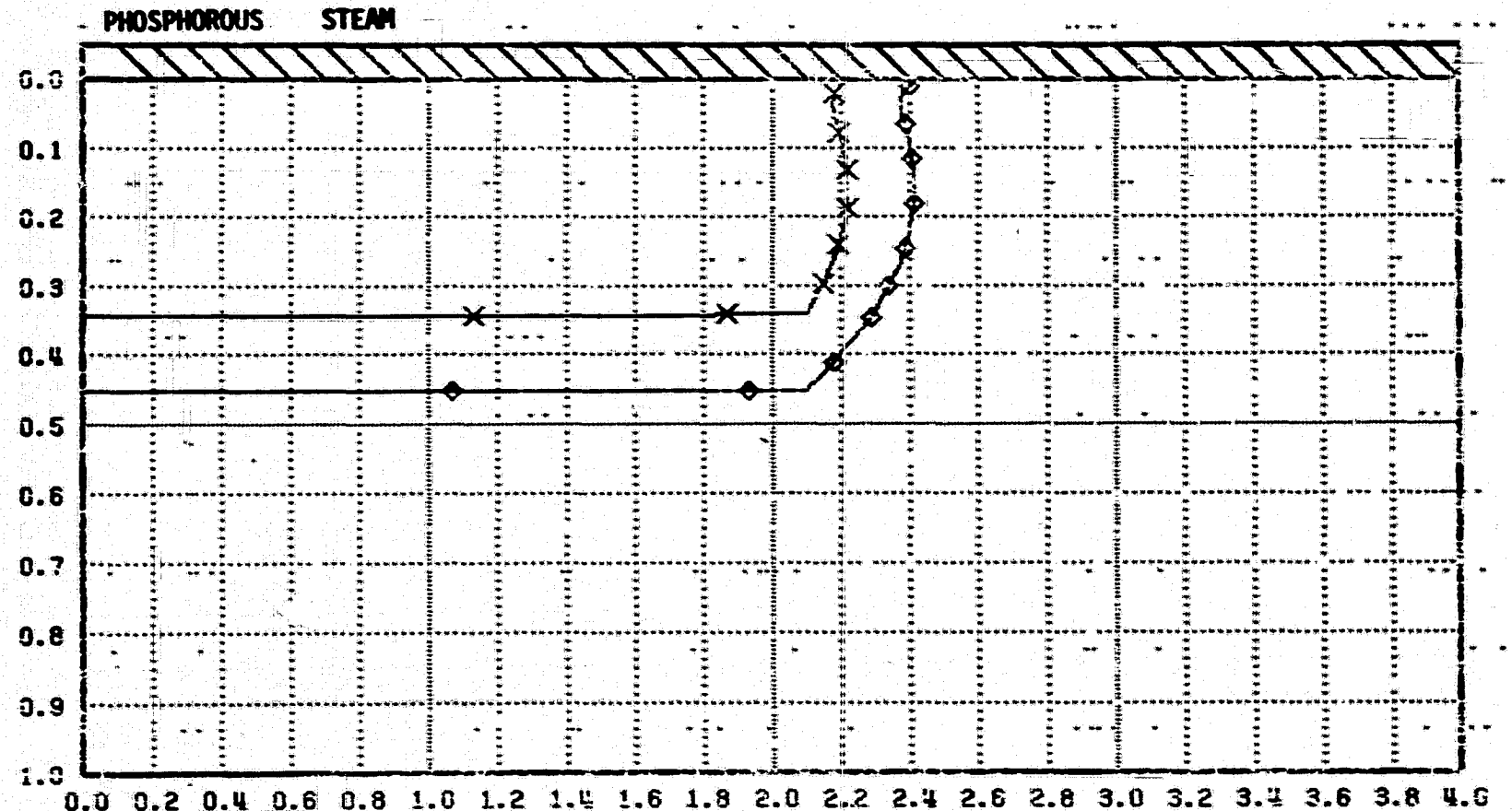

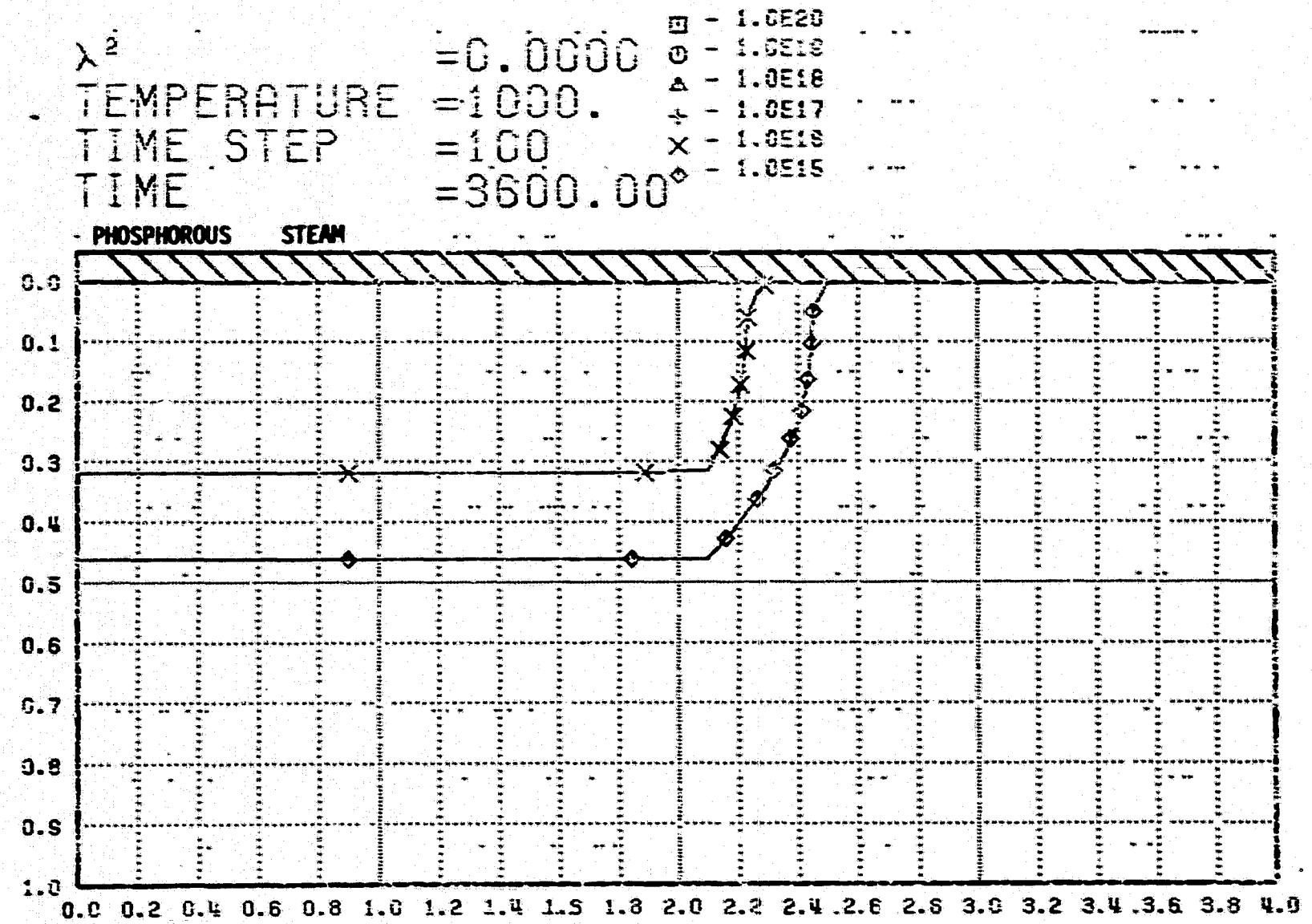
χ^2 =0.0000
TEMPERATURE =1000.
TIME STEP =100
TIME =3600.00
□ - 1.0E20
○ - 1.0E19
△ - 1.0E18
+ - 1.0E17
× - 1.0E16
◇ - 1.0E15
PHOSPHOROUS
STEAM
0.0
0.1
0.2
0.3
0.4
0.5
0.6
0.7
0.8
0.9
1.0
0.0 0.2 0.4 0.6 0.8 1.0 1.2 1.4 1.6 1.8 2.0 2.2 2.4 2.6 2.8 3.0 3.2 3.4 3.6 3.8 4.0

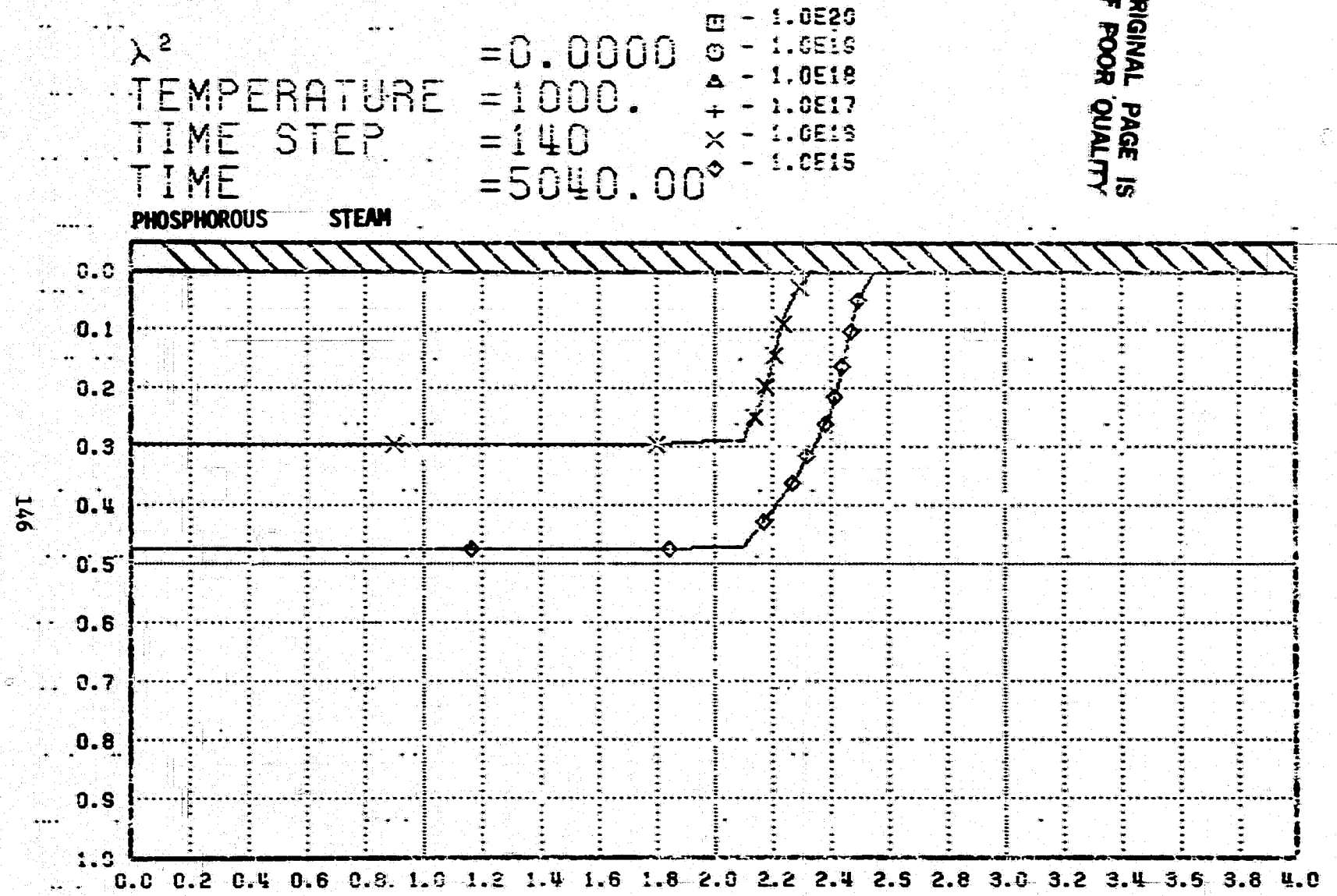

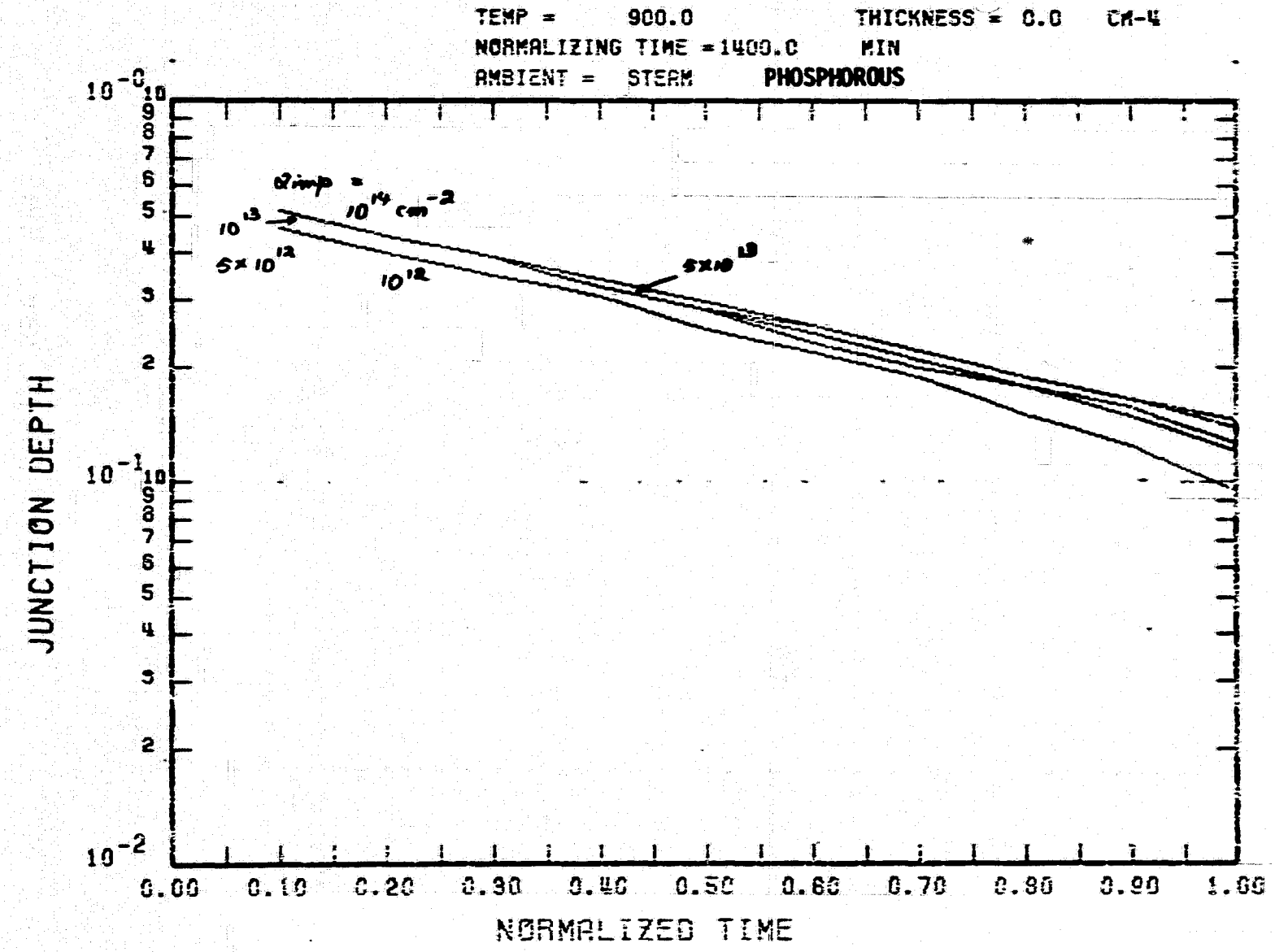
TEMP = 900.0 THICKNESS = 0.0 CM-4
NORMALIZING TIME = 1400.0 MIN
AMBIENT = STEAM PHOSPHOROUS
Qimp = 10^14 cm^-2
10^13
5x10^12
10^12
5x10^13
JUNCTION DEPTH
NORMALIZED TIME
0.00 0.10 0.20 0.30 0.40 0.50 0.60 0.70 0.80 0.90 1.00

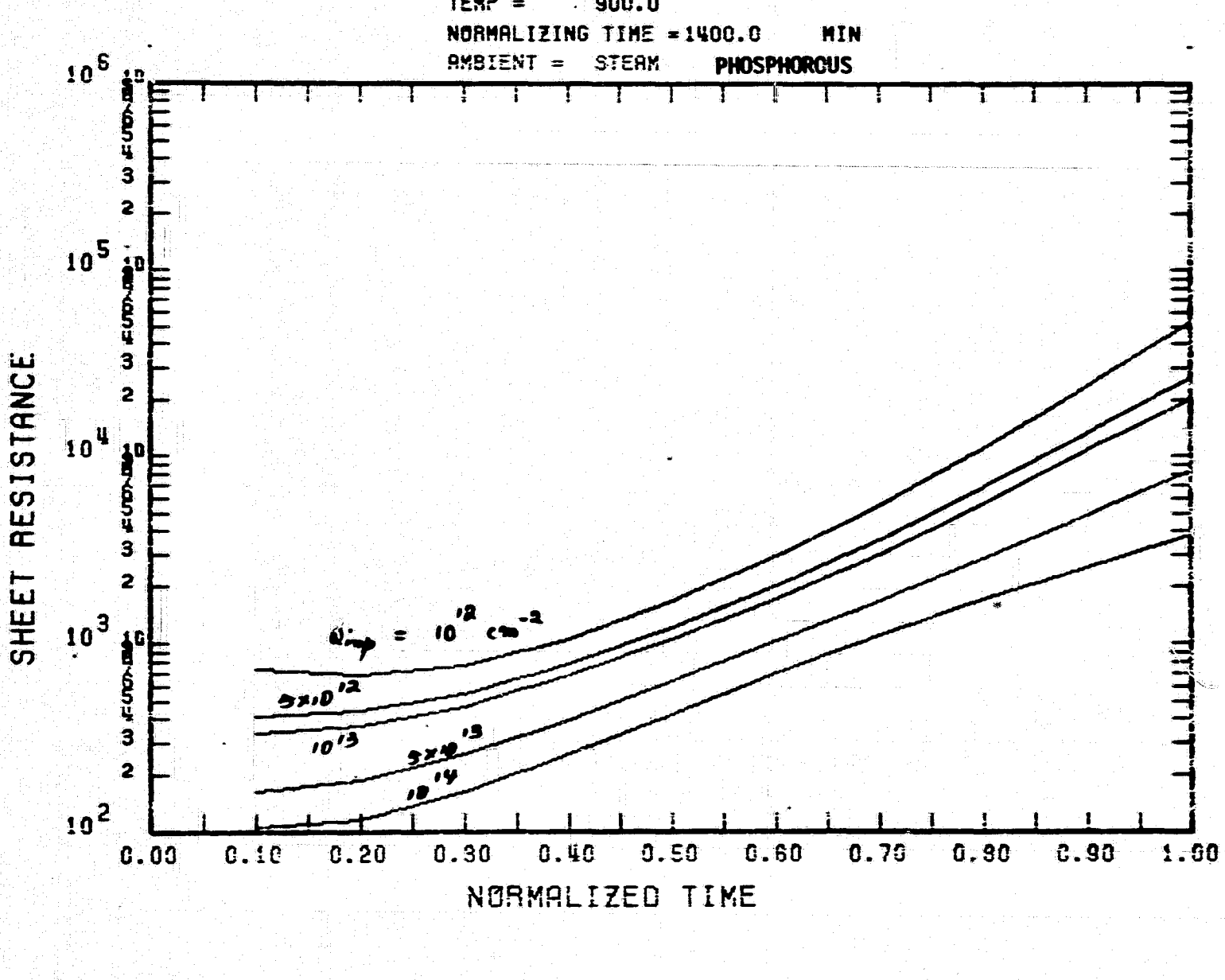
TEMP = 900.0
NORMALIZING TIME = 1400.0 MIN
AMBIENT = STEAM PHOSPHORUS
SHEET RESISTANCE
NORMALIZED TIME
10^6
10^5
10^4
10^3
10^2
0.00
0.10
0.20
0.30
0.40
0.50
0.60
0.70
0.80
0.90
1.00
Q_{inp} = 10^{12} cm^{-2}
5×10^{12}
10^{13}
5×10^{13}
10^{14}

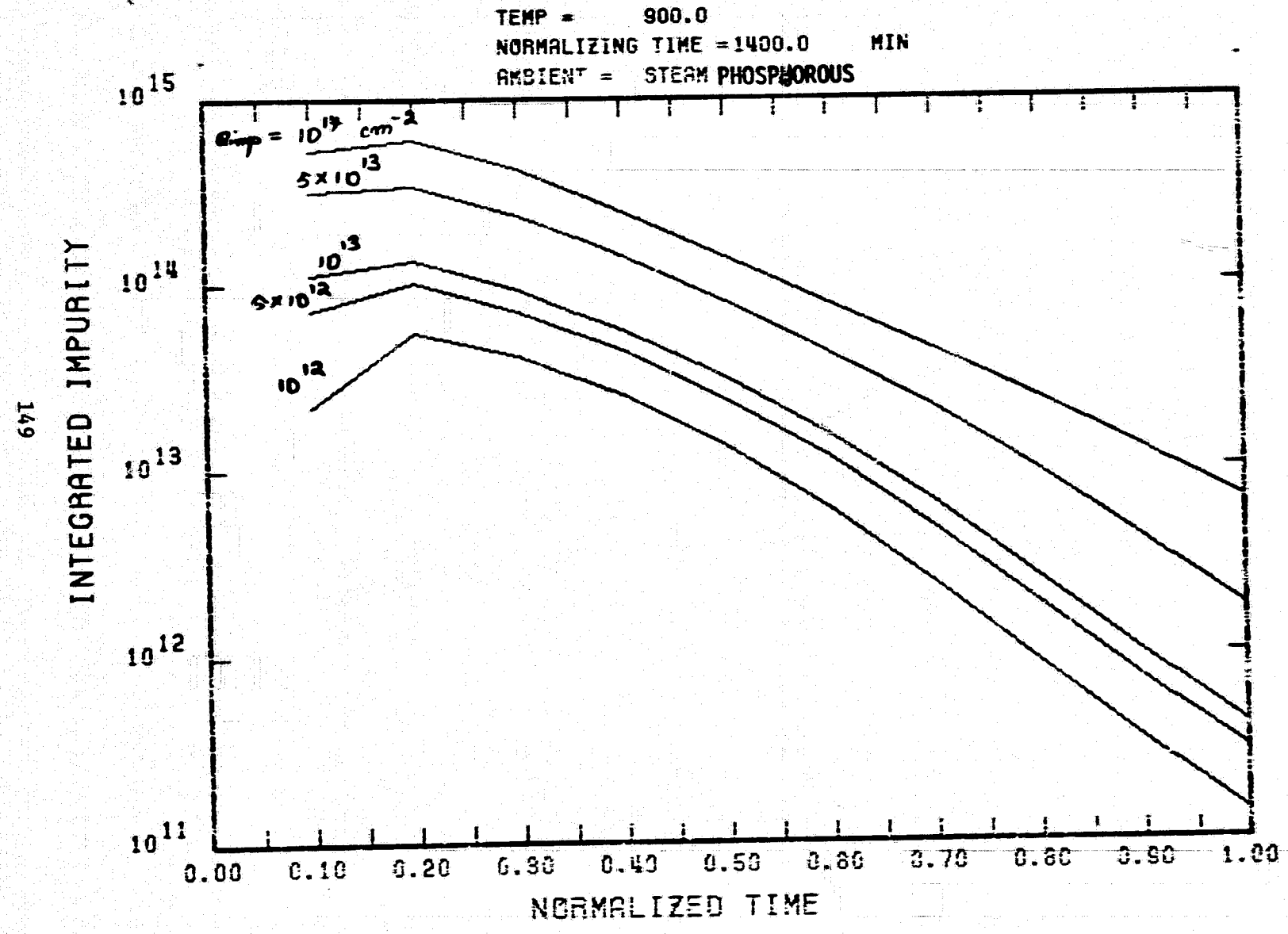
TEMP = 900.0
NORMALIZING TIME = 1400.0 MIN
AMBIENT = STEAM PHOSPHOROUS
Q_{imp} = 10^{13} cm^{-2}
5×10^{13}
10^{13}
5×10^{12}
10^{12}
INTEGRATED IMPURITY
10^{15}
10^{14}
10^{13}
10^{12}
10^{11}
0.00 0.10 0.20 0.30 0.40 0.50 0.60 0.70 0.80 0.90 1.00
NORMALIZED TIME

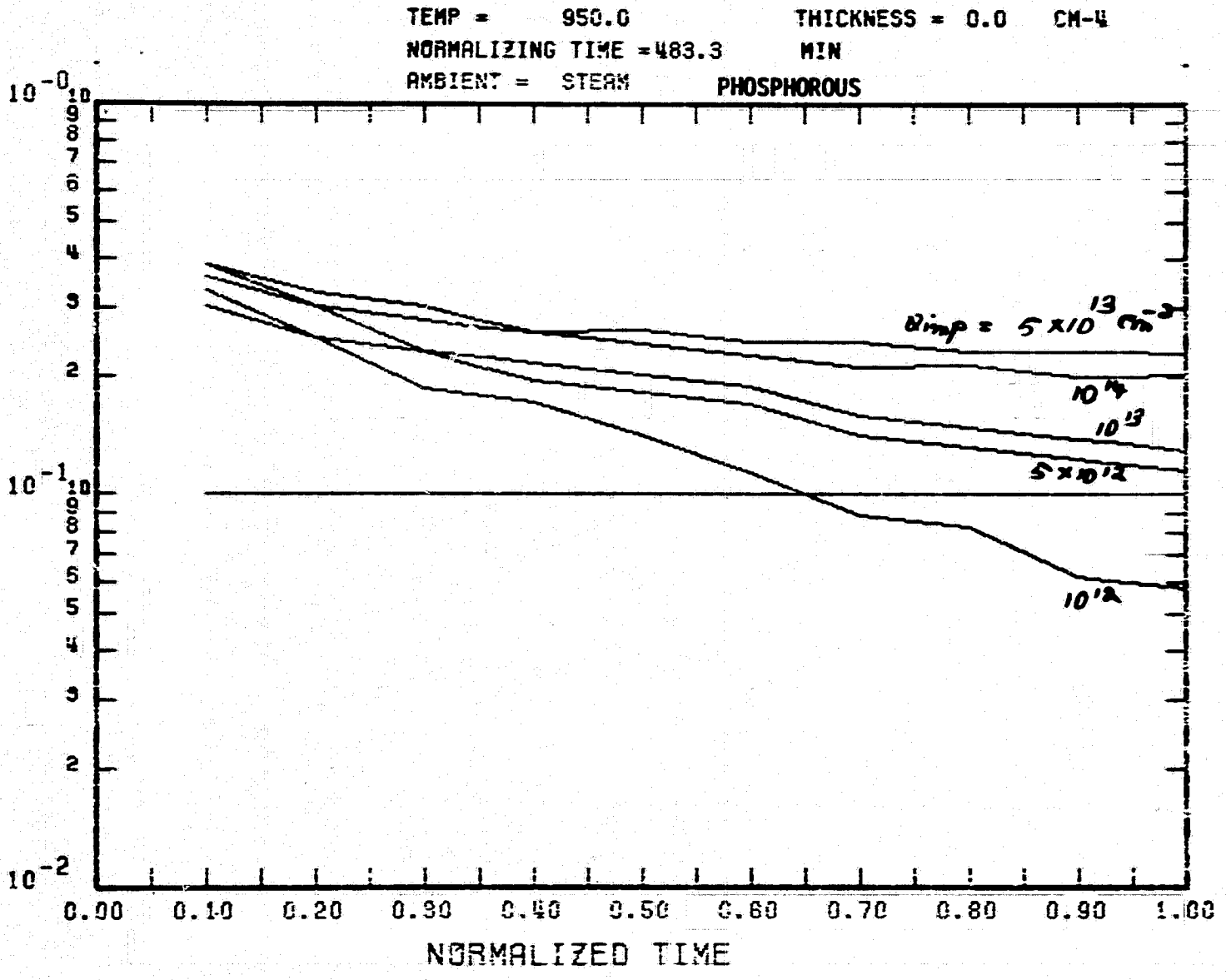
TEMP = 950.0 THICKNESS = 0.0 CM-4
NORMALIZING TIME = 483.3 MIN
AMBIENT = STEAM PHOSPHOROUS
JUNCTION DEPTH
NORMALIZED TIME
10^{-0}
10^{-1}
10^{-2}
0.00
0.10
0.20
0.30
0.40
0.50
0.60
0.70
0.80
0.90
1.00
$Q_{imp} = 5 \times 10^{13}\ cm^{-2}$
10^{14}
10^{13}
5×10^{12}
10^{12}

150

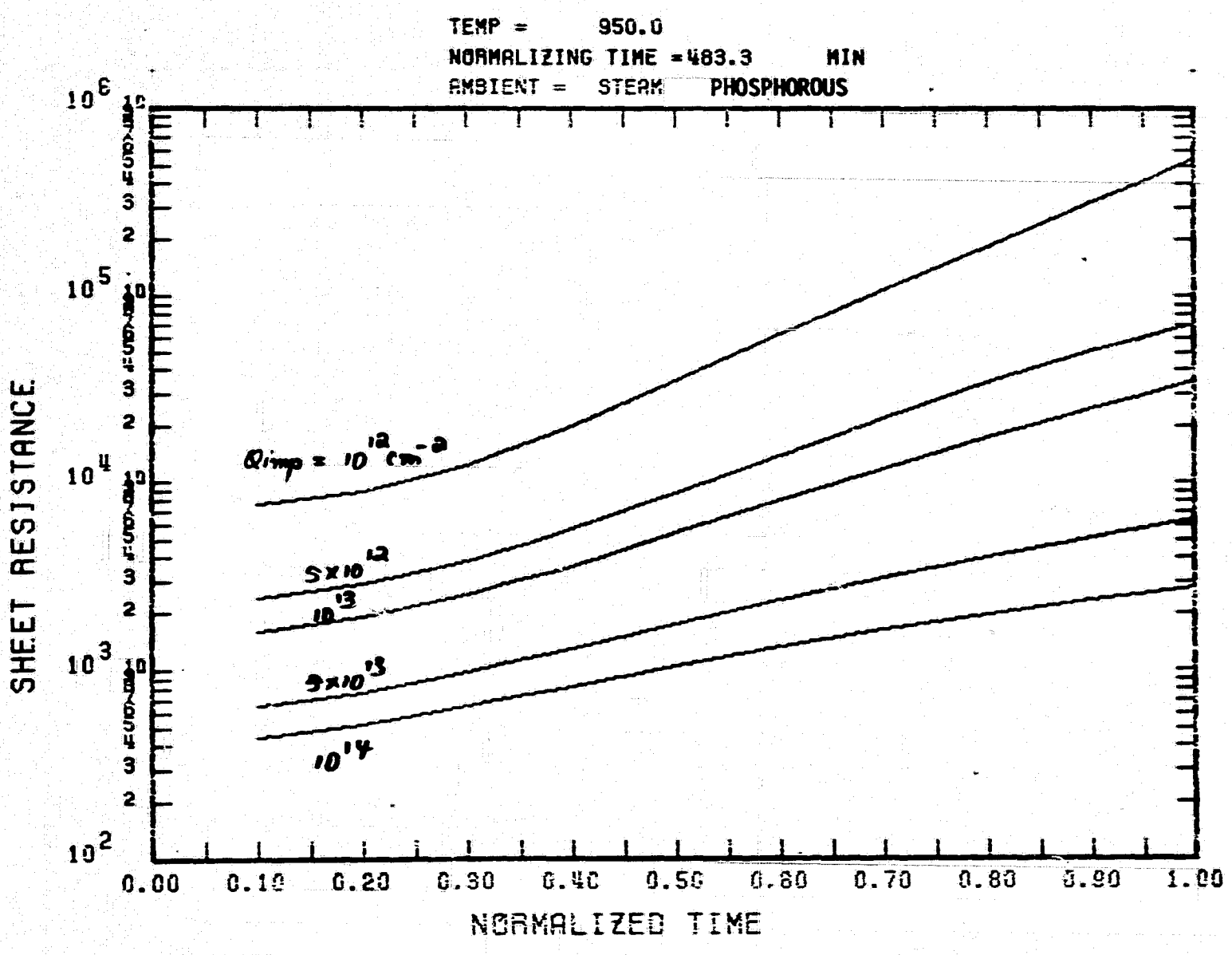
TEMP = 950.0
NORMALIZING TIME =483.3 MIN
AMBIENT = STEAM PHOSPHOROUS
SHEET RESISTANCE
NORMALIZED TIME
10^6
10^5
10^4
10^3
10^2
0.00
0.10
0.20
0.30
0.40
0.50
0.60
0.70
0.80
0.90
1.00
$Q_{imp} = 10^{12}\ cm^{-2}$
5×10^{12}
10^{13}
5×10^{13}
10^{14}

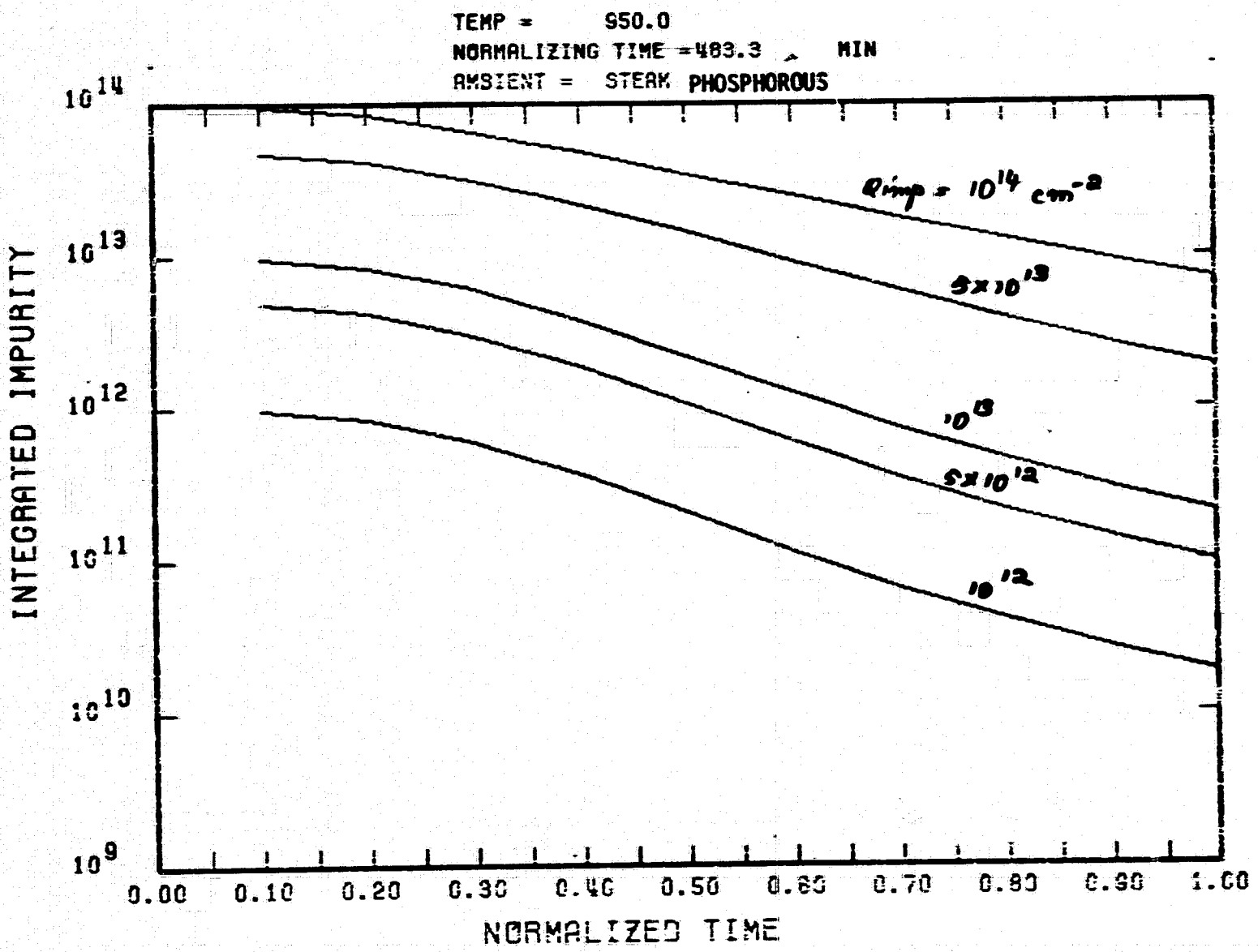
TEMP = 950.0
NORMALIZING TIME =483.3 MIN
AMBIENT = STEAM PHOSPHOROUS
INTEGRATED IMPURITY
NORMALIZED TIME
10^{14}
10^{13}
10^{12}
10^{11}
10^{10}
10^{9}
0.00
0.10
0.20
0.30
0.40
0.50
0.60
0.70
0.80
0.90
1.00
$Q_{imp} = 10^{14}$ cm^{-2}
5×10^{13}
10^{13}
5×10^{12}
10^{12}

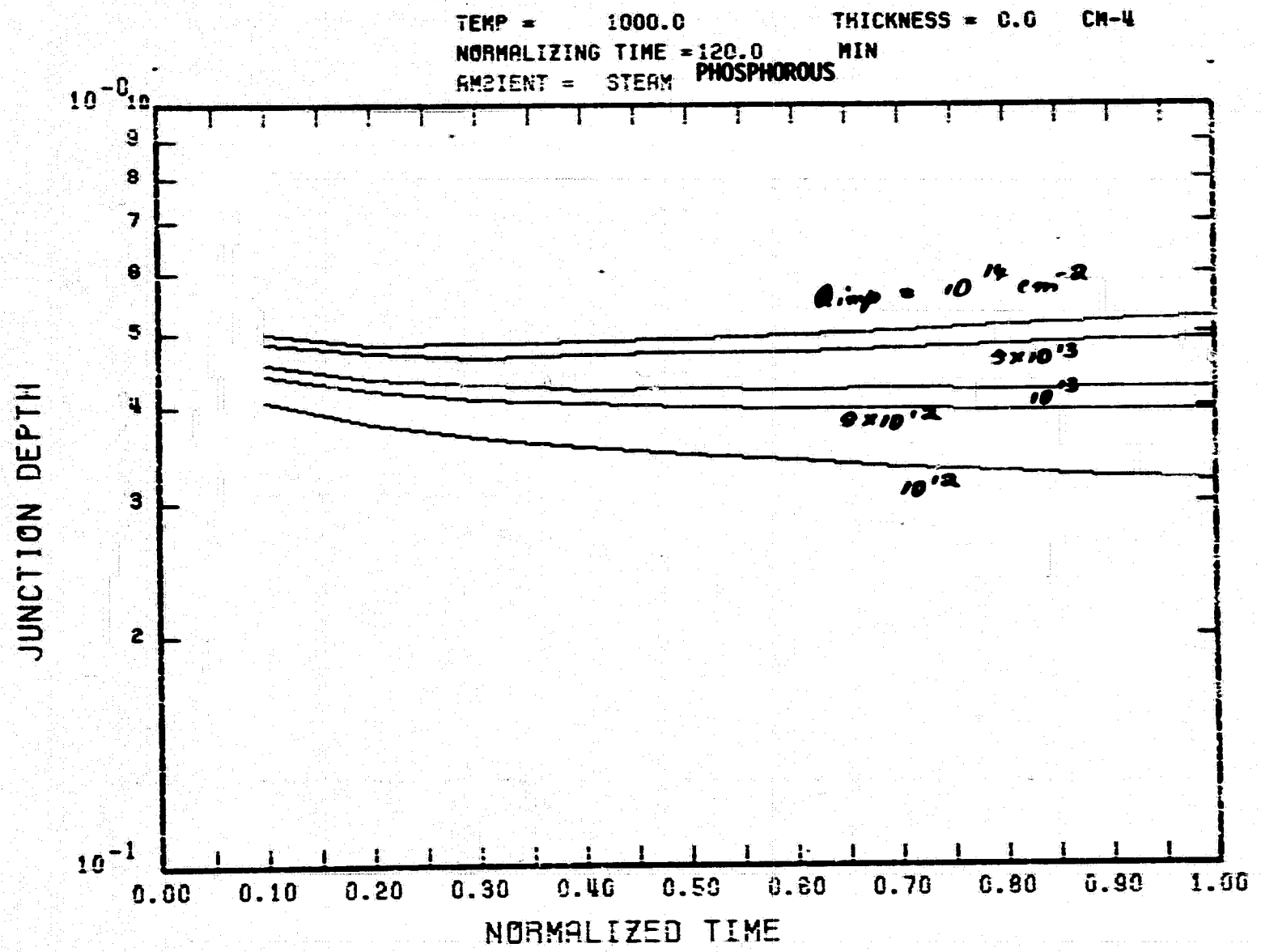
TEMP = 1000.0 THICKNESS = 0.0 CM-4
NORMALIZING TIME = 120.0 MIN
AMBIENT = STEAM PHOSPHOROUS
10^{-0}
9
8
7
6
5
4
3
2
10^{-1}
JUNCTION DEPTH
$Q_{imp} = 10^{14}\ cm^{-2}$
5×10^{13}
10^{13}
8×10^{12}
10^{12}
0.00 0.10 0.20 0.30 0.40 0.50 0.60 0.70 0.80 0.90 1.00
NORMALIZED TIME

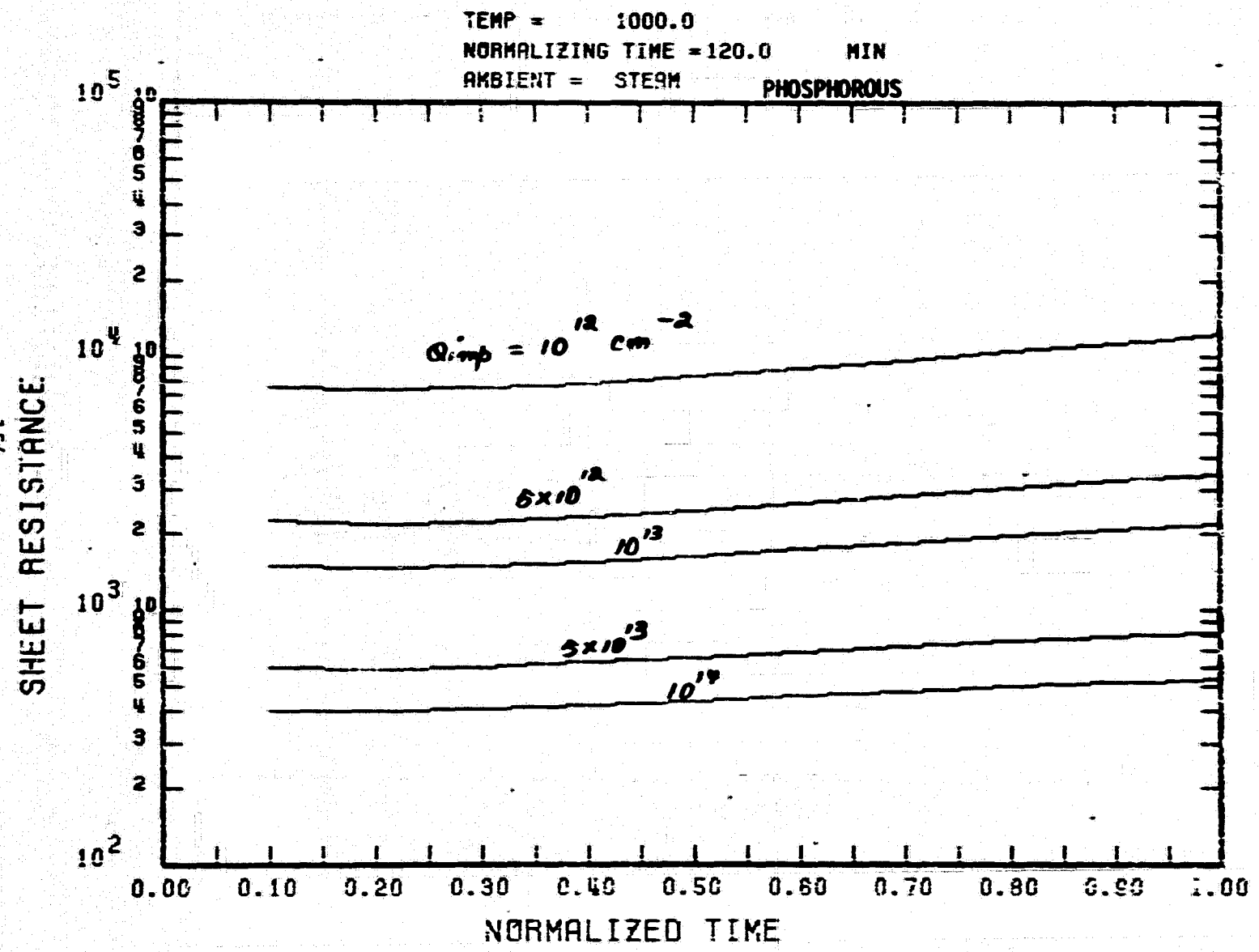
TEMP = 1000.0
NORMALIZING TIME = 120.0 MIN
AMBIENT = STEAM
PHOSPHOROUS
$Q_{imp} = 10^{12}$ cm^{-2}
6×10^{12}
10^{13}
3×10^{13}
10^{14}
SHEET RESISTANCE
154
10^5
10^4
10^3
10^2
0.00
0.10
0.20
0.30
0.40
0.50
0.60
0.70
0.80
0.90
1.00
NORMALIZED TIME

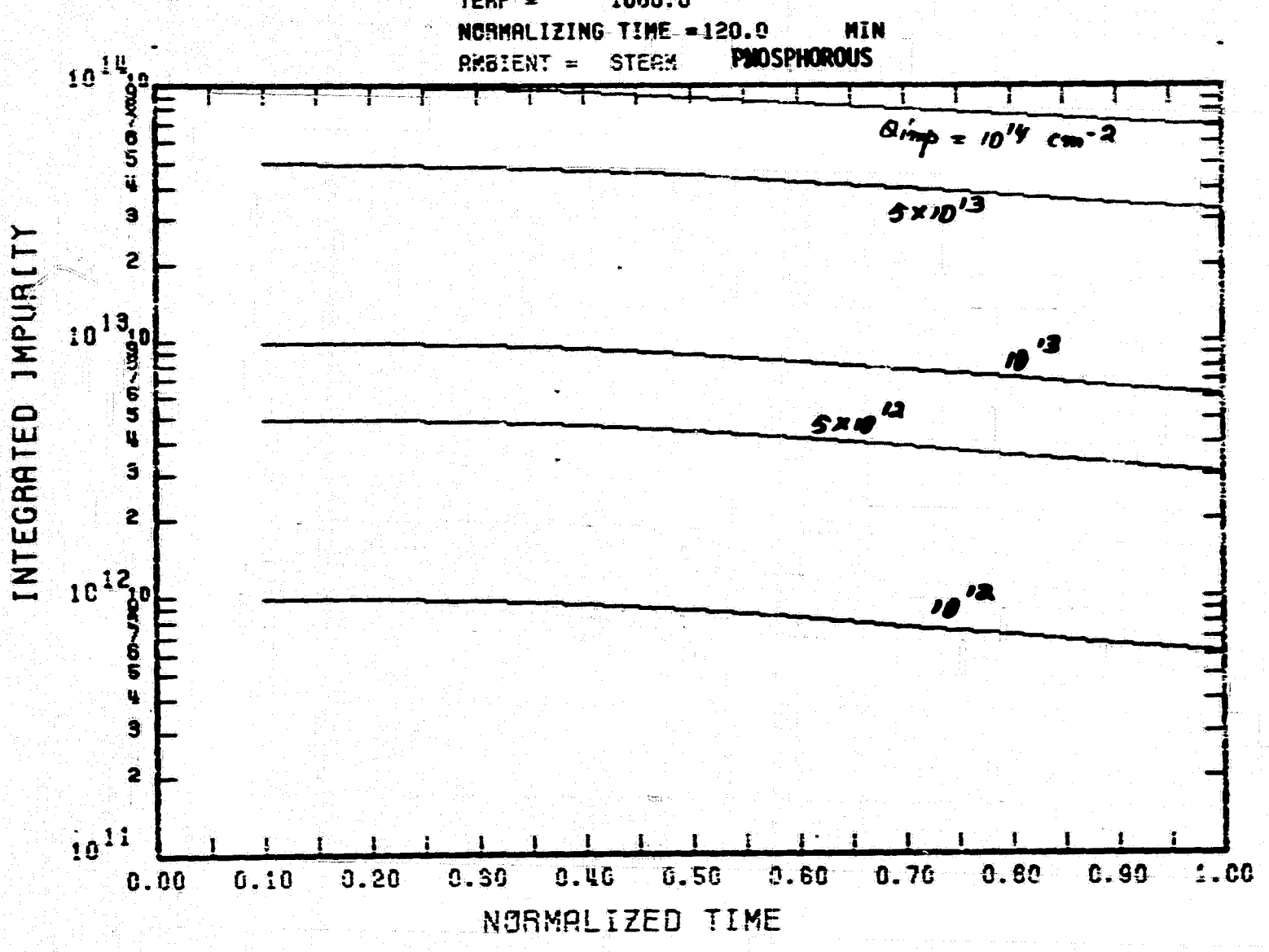
TEMP = 1000.0
NORMALIZING TIME =120.0 MIN
AMBIENT = STEAM PHOSPHOROUS
INTEGRATED IMPURITY
NORMALIZED TIME
0.00
0.10
0.20
0.30
0.40
0.50
0.60
0.70
0.80
0.90
1.00
10^{11}
10^{12}
10^{13}
10^{14}
$Q_{imp} = 10^{14}$ cm^{-2}
5×10^{13}
10^{13}
5×10^{12}
10^{12}

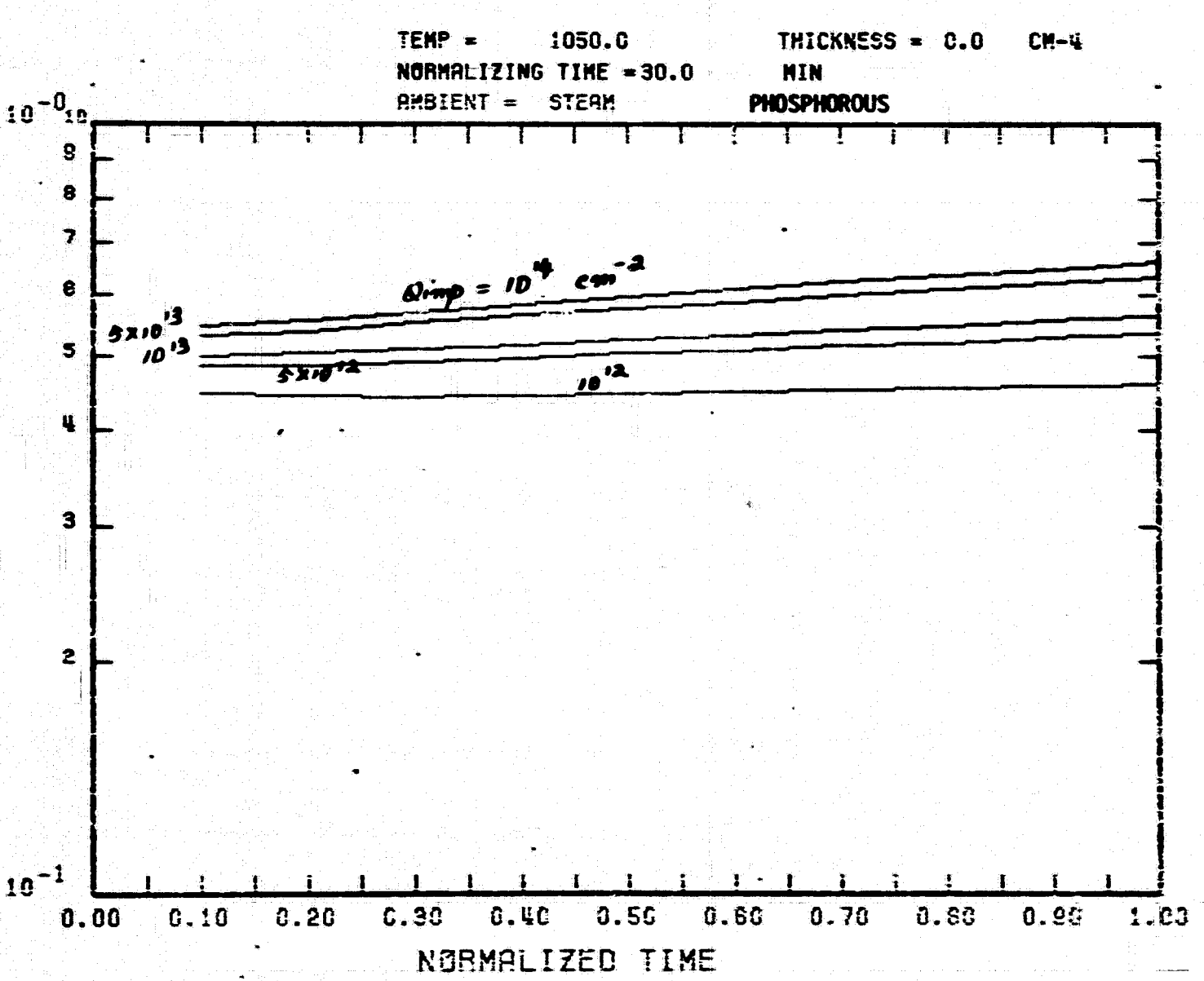
TEMP = 1050.0 THICKNESS = 0.0 CM-4
NORMALIZING TIME =30.0 MIN
AMBIENT = STEAM PHOSPHOROUS
JUNCTION DEPTH
NORMALIZED TIME
10^{-0}
9
8
7
6
5
4
3
2
10^{-1}
0.00
0.10
0.20
0.30
0.40
0.50
0.60
0.70
0.80
0.90
1.00
$Q_{imp} = 10^{14}$ cm^{-2}
5×10^{13}
10^{13}
5×10^{12}
10^{12}

156

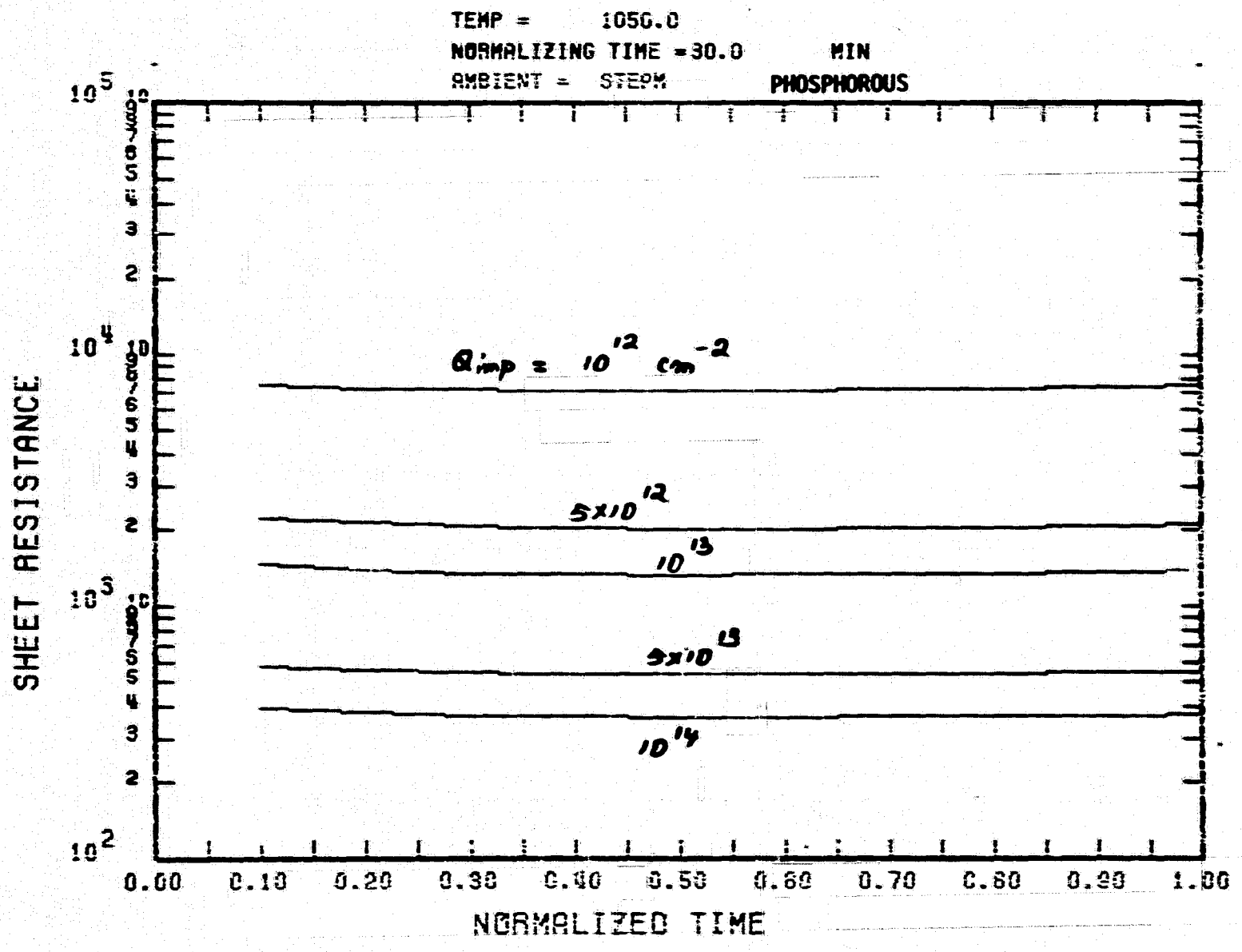
TEMP = 1050.0
NORMALIZING TIME =30.0 MIN
AMBIENT = STEAM
PHOSPHOROUS
SHEET RESISTANCE
$Q_{imp} = 10^{12}$ cm^{-2}
5×10^{12}
10^{13}
5×10^{13}
10^{14}
10^5
10^4
10^3
10^2
0.00
0.10
0.20
0.30
0.40
0.50
0.60
0.70
0.80
0.90
1.00
NORMALIZED TIME

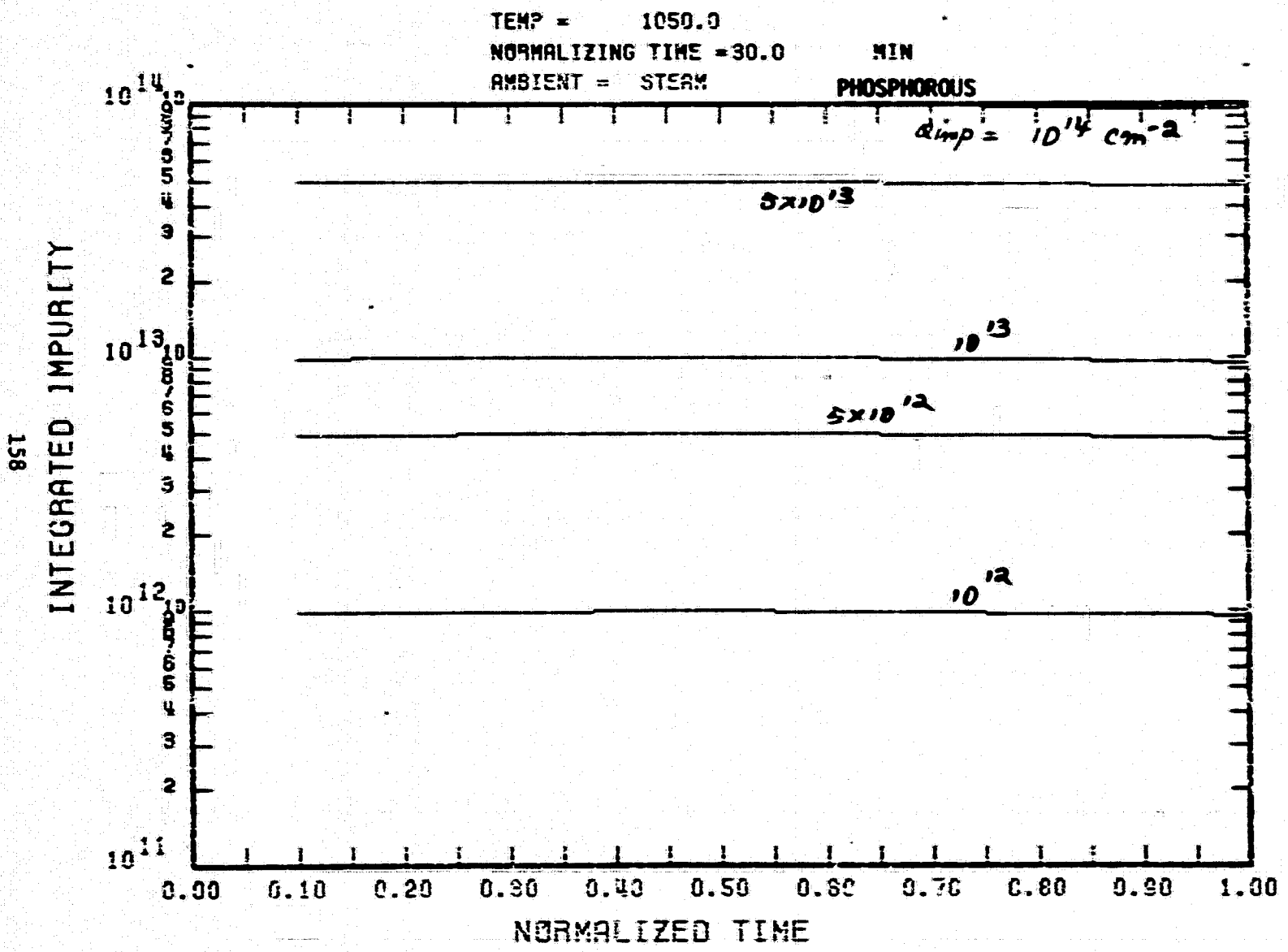
TEMP = 1050.0
NORMALIZING TIME =30.0 MIN
AMBIENT = STEAM
PHOSPHOROUS
$\phi_{imp} = 10^{14}$ cm^{-2}
5×10^{13}
10^{13}
5×10^{12}
10^{12}
INTEGRATED IMPURITY
10^{14}
10^{13}
10^{12}
10^{11}
0.00 0.10 0.20 0.30 0.40 0.50 0.60 0.70 0.80 0.90 1.00
NORMALIZED TIME

APPENDIX C

REVISED PROGRAM LISTING

```
MICRON*SOS2(1).SHPLOT
      C   ***  SHRFJN PLOT PROGRAM  ***
      C
      C        ***  DATA DECK  ***
      C
      C   ***1ST CARD
      C      NPLT - # OF DATA SET(FOR DIFF. VALUES OF IMPLNT. DOSES)
      C      NSTP1 TO NSTP5- # OF TIME STEPS FOR A VALUE OF NPLT(MAX. 5 VALUES)
      C      FIELD 8I10
      C   ***2ND CARD, 4TH AND 6TH CARD
      C      IX,IY - X AND Y AXIS LABELS RESPECTIVELY
      C      1ST, 2ND AND 3RD PLOTS ARE RS, XJ AND Q VS TIME PLOTS RESP.
      C      JCOD - PUT 0 FOR NO GRID
      C      FIELD 2(5A6),2I10
      C   ***3RD CARD
      C      JGRID - # OF DIV. IN Y AXIS
      C      IGRID - # OF DIV. IN X AXIS
      C      NYSTP - SUBGRID DIV. IN Y AXIS
      C              1 GIVES 10 SUBGD.
      C      NXSTP - SUBGRID DIV. IN X AXIS
      C              2 GIVES  1 SUBGD.
      C      YMINV - MIN VAL IN Y AXIS
      C      YMAXV - MAX VAL IN Y AXIS
      C      XMINV - MIN VAL IN X AXIS
      C      XMAXV - MAX VAL IN X AXIS
      C      FIELD 4I10,4E10.5
             DIMENSION RS(10,100),XJ(10,100),Q(10,100),TIME(10,100)
             DIMENSION XI(10,100)
             DIMENSION IX(5),IY(5),IL(2),XO(10,100)
      C   ***  READ IN DATA
             READ 100,NPLT,NSTP1,NSTP2,NSTP3,NSTP4,NSTP5
             DO 10 I=1,NPLT
             IF(I.EQ.1) NSTP=NSTP1
             IF(I.EQ.2) NSTP=NSTP2
             IF(I.EQ.3) NSTP=NSTP3
             IF(I.EQ.4) NSTP=NSTP4
             IF(I.EQ.5) NSTP=NSTP5
             DO 10 J=1,NSTP
             READ(14,104) JMAXI,IAMBNT
             READ(14,101) TEMP,TMAX,DELT,DELY,YDIST
          10 READ(14,101) RS(I,J),XI(I,J),XJ(I,J),Q(I,J),TIME(I,J),XO(I,J)
             IF(IAMBNT.EQ.1) IL(1)='DRY OX'
             IF(IAMBNT.EQ.1) IL(2)='YGEN  '
             IF(IAMBNT.EQ.2) IL(1)='STEAM '
             IF(IAMBNT.EQ.2) IL(2)='      '
             IF(IAMBNT.EQ.3) IL(1)='NITROG'
             IF(IAMBNT.EQ.3) IL(2)='EN    '
      C
         100 FORMAT(8I10)
         101 FORMAT(1H0,6E15.9)
         102 FORMAT(2(5A6),2I10)
         103 FORMAT(4I10,4E10.5)
         104 FORMAT(1H0,8I10)
         105 FORMAT(2A6)
         400 FORMAT(1H0,10X,'XMIN = ',5X,'XMAX = ',5X 'YMIN = ',5X 'YMAX = ',
            *//1H0,3X,4(F10.5,3X))
      C
             DATA HGT,XMAX,YMAX/0.0875,7.,5./
             TMAX=TMAX/60.
             IC=10
      C   ***  INITIATE THE PLOT
             DO 11 N=1,3
             READ 102, (IX(I),I=1,5),(IY(I),I=1,5),JCOD
             READ 103, IGRID,JGRID,NYSTP,NXSTP,YMINV,YMAXV,XMINV,XMAXV
             PRINT 400,XMINV,XMAXV,YMINV,YMAXV
             IF(JCOD.NE.0) ICOD=2
             IF(JCOD.EQ.0) ICOD=3
             CALL PLOTS(10.0,10.0)
             CALL PLOT (1.5,1.5,-3)
      C   ***  DRAW BORDER
             CALL PLOT(0.0,YMAX,2,-1)
             CALL PLOT(XMAX,YMAX,2,-1)
             CALL PLOT(XMAX,0.0,2,-1)
             CALL PLOT(0.0,0.0,2,-1)
      C   ***  DRAW GRID
             YDIV=YMAX/FLOAT(JGRID)
             JK=1
             DO 12 I=1,JGRID
             DO 13 J=1,IC,NYSTP
             YSPC=ALOG10(FLOAT(J*JK))*YDIV
```

ORIGINAL PAGE IS
OF POOR QUALITY

```
      CALL PLOT(0.0,YSPC,3)
      CALL PLOT(0.12,YSPC,2,0)
      CALL PLOT(XMAX-0.12,YSPC,ICOD)
   13 CALL PLOT(XMAX,YSPC,2,0)
   12 JK=JK+10
      IGRID1=IGRID*NXSTP
      IGRID2=IGRID1-1
      XDIV=XMAX/FLOAT(IGRID)
      DO 14 I=1,IGRID2
      XSPC=FLOAT(I)*XDIV
      CALL PLOT(XSPC,0.0,3)
      CALL PLOT(XSPC,0.12,2,0)
      CALL PLOT(XSPC,YMAX-0.12,ICOD)
   14 CALL PLOT(XSPC,YMAX,2,0)
C  ***  AXES NUMBERS
      VAL=YMINV
      JK=1
      JGRID=JGRID+1
      DO 16 I=1,JGRID
      DO 17 J=1,10,NYSTP
      IF(I.EQ.JGRID.AND.J.NE.1) GO TO 17
      YSPC=ALOG10(FLOAT(J+JK))*YDIV
      YSPC1=YSPC
      IF(J.EQ.1) GO TO 200
      VAL=FLOAT(J)
      CALL NUMBER(-0.18,YSPC1,.08,VAL,0.,-1)
      GO TO 17
  200 VAL2=ALOG10(VAL)
      CALL NUMBER(-0.54,YSPC1,0.10,10.,0.,-1)
      CALL NUMBER(-0.35,YSPC1+.09,0.1,VAL2,0.,-1)
   17 CONTINUE
      VAL=VAL*10.
   16 JK=JK+10
      XV=XMAXV/FLOAT(IGRID)
      IGRID3=IGRID+1
      DO 18 I=1,IGRID3
      XSPC=(I-1)*XDIV*NXSTP
      XSPC1=XSPC-0.2
      VAL=XV*(I-1)
   18 CALL NUMBER(XSPC1,-0.20,0.1,VAL,0.0,2)
C  ***  PUT LABELS
      CALL SYMBOL(-0.8,1.0,0.1313,IY,90.,30)
      CALL SYMBOL(2.00,-0.50,0.1313,IX,0.0,30)
      CALL SYMBOL(2.0,5.5,.HGT,'TEMP = ',0.,7)
      CALL NUMBER(3.0,5.5,.HGT,TEMP,0.,1)
      CALL SYMBOL(2.0,5.3,.HGT,'NORMALIZING TIME =            MIN',
     *  0.0,32)
      CALL NUMBER(3.6,5.3,.HGT,TMAX,0.,1)
      CALL SYMBOL(2.0,5.1,.HGT,'AMBIENT = ',0.,10)
      CALL SYMBOL(3.0,5.1,.HGT,IL,0.,12)
      IF(N.EQ.2) CALL SYMBOL(4.5,5.5,.HGT,'THICKNESS =        CM=4',
     *  0.0,23)
      IF(N.EQ.2) CALL NUMBER(5.6,5.5,.HGT,YDIST,0.,1)
C  ***  DRAW CURVES
      YLOG=YMAX/FLOAT(JGRID)
      XVI=XMAX/XMAXV
      YMVR=1./YMINV
      DO 22 I=1,NPLT
      CALL PLOT(0.0,0.0,0,3)
      IF(I.EQ.1) NSTP=NSTP1
      IF(I.EQ.2) NSTP=NSTP2
      IF(I.EQ.3) NSTP=NSTP3
      IF(I.EQ.4) NSTP=NSTP4
      IF(I.EQ.5) NSTP=NSTP5
      DO 21 J=1,NSTP
      IF(J.EQ.1) L=3
      IF(J.NE.1) L=2
      IF(IAMBNT.NE.3) TIME(I,J)=TIME(I,J)/TIME(NPLT,NSTP)
      XMOVE= TIME(I,J)*XVI
      IF(N.EQ.3) GO TO 201
      IF(N.EQ.2) GO TO 202
      YMOVE=YLOG*ALOG10(RS(I,J)*YMVR)
      GO TO 21
  201 YMOVE=YLOG*ALOG10(Q(I,J)*YMVR)
      GO TO 21
  202 YMOVE=YLOG*ALOG10(XJ(I,J)*YMVR)
   21 CALL PLOT(XMOVE,YMOVE,L,0)
      IF(N.NE.2) GO TO 22
      CALL PLOT(0.0,0.0,3)
      DO 23 J=1,NSTP
```

```
160             IF(J.EQ.1) L=3
161             IF(J.NE.1) L=2
162             XMOVE=TIME(I,J)*XV1
163             XI(I,J)=XI(I,J)*(YDIST-0.45*AO(I,J))/1.E-9
164             IF(XI(I,J).LT.1.E-01) XI(I,J)=1.E-01
165             YMOVE=YLOG*ALOG10(XI(I,J)*YMVR)
166          23 CALL PLOT(XMOVE,YMOVE,L,0)
167          22 CONTINUE
168             CALL PLOT(0.,0.,999)
169          11 CONTINUE
170             STOP
171             END
```

```
I(CRON*SnS2(1).PARAM
      SUBROUTINE PARAM(CI,T)
C**************************************************************
C        AFTER THAI AND MORIN AND MAITA.
C**************************************************************
      IMPLICIT DOUBLE PRECISION (A-H,O-Z)
      CI=1.E15
    2 EG=1.21+7.1E-10*SQRT(CI)*(T)**(-.5)
      EG=EG/(8.62E-5*(T))
      CIOLD=CI
      CI=3.87E16*((T)**(1.5))*EXP(-EG/2.)
      R=CIOLD/CI
      IF(R.LT.0.995.AND.R.GT.1.005) GO TO 2
      RETURN
      END
C**************************************************************
```

```
*ICRON.SnS2(1),G
      1            DOUBLE PRECISION FUNCTION G(CN,JJ)
      2            IMPLICIT DOUBLE PRECISION(A-H,O-Z)
      3      C*****************************************************************
      4      C       IRWIN'S CONDUCTIVITY FORMULAS.
      5      C*****************************************************************
      6            IF(JJ.EQ.1) GO TO 3
      7            IF(CN.GT.0.0) A=1.0
      8            IF(CN.GT.0.0) B=7.2D-17
      9            IF(CN.GT.1.6D +14) A=0.65
     10            IF(CN.GT.1.6D +14) B=3.3D-11
     11            IF(CN.GT.2.4D+18) A=0.832
     12            IF(CN.GT.2.4D+18) B=1.47D-14
     13            IF(CN.GT.1.6D+19) A=0.766
     14            IF(CN.GT.1.6D+19) B=4.0-17
     15            GO TO 5
     16        3   IF(CN.GT.0.0) A=1.0
     17            IF(CN.GT.0.0) B=2.0-16
     18            IF(CN.GT.3.5D15) A=0.817
     19            IF(CN.GT.3.5D15) B=6.97D-14
     20            IF(CN.GT.1.0D17) A=0.543
     21            IF(CN.GT.1.0D17) B=6.93D-9
     22            IF(CN.GT.9.6D18) A=0.94
     23            IF(CN.GT.9.6D18) B=2.D-16
     24            IF(CN.GT.6. D19) A=0.744
     25            IF(CN.GT.6. D19) B=1.43D-12
     26            IF(CN.GT.2.35D20) A=0.456
     27            IF(CN.GT.2.35D20) B=1.04D-4
     28        5   G = B*(CN**A)
     29            RETURN
     30            END
```

```
(ICRON*SnS2(1).OXDATA
      SUBROUTINE OXDATA(AMANT,ORINT,T,H,C,M,KB)
C*********************************************************************
C
C        SUBROUTINE FOR OXIDATION PARAMETERS AND SEGREGATION CO-EFFI.
C*********************************************************************
C
      IMPLICIT DOUBLE PRECISION(A-H,O-Z)
      INTEGER AMBNT,ORINT
      DOUBLE PRECISION KB,H,M1,M3
C
      IF(AMANT.EQ.1) GO TO 12
      B=4.40277D-10*DEXP(-7945.74/T)
      IF(ORINT.EQ.1) C=4.74558D-1*DEXP(-22184.07/T)
      IF(ORINT.EQ.2) C=8.13546D-1*DEXP(-21835.313/T)
      IF(ORINT.EQ.3) C=1.400D0*DEXP(-22396.838/T)
      GO TO 14
   12 CONTINUE
      B=1.58507D-9*DEXP(-13016.6449/T)
      IF(ORINT.EQ.1) C=2.0093D-1*DEXP(-24118.98/T)
      IF(ORINT.EQ.2) C=4.33277D-1*DEXP(-24551.98/T)
      IF(ORINT.EQ.3) C=7.07845D-1*DEXP(-24957.028/T)
   14 CONTINUE
      M1=33.3*DEXP(-0.57/(KB*T))
      M3=20.0*DEXP(-0.57/(KB*T))
      IF(ORINT.EQ.1) M=M1
      IF(ORINT.EQ.2) M=(M1+M3)/2.0
      IF(ORINT.EQ.3) M=M3
      RETURN
      END
```

```
MICRON*SAS2(1).FRONT
          SUBROUTINE FRONT(IMAXI,JMAXI,LI,K,TEMP,DFI,DELT,JSTEP,
     *    KTYPE,KOTI,XDIST)
C
C     SUB. FOR CALCULATING CONTOUR FRONT MOVEMENT DATA AND
C     READING AND WRITING THE SAME ON FILE
C
      IMPLICIT DOUBLE PRECISION(A-H,O-Z)
      DIMENSION XFRONT(6), YFRONT(6)
      DATA IDOL,IBLNK,ISTAR/1H$,1H ,1H*/
      IF(KTYPE.NE.1) GO TO 800
C
C     READ FILE
C
      DO 60 KK=1,JSTEP
        READ (9,390) MARK
        IF (MARK.NE.IDOL) GO TO 50
      READ(9,430) TEMP,DFI,DELT
      READ(9,390) MARK
   50   READ (9,430) (DUM,L=1,6)
        READ (9,430) (DUM,L=1,6)
      READ(9,420) IMAXI,JMAXI,K,LM
   60   CONTINUE
      RETURN
  800 CONTINUE
      DO 260 LL=1,6
        CONVAL=10.0**FLOAT(20-LL+1)
        XF=CONDEP(IMAXI,JMAXI,0,-JMAXI,0,0,CONVAL)
      YF=CONDEP(IMAXI,JMAXI,-2,0,0,0,CONVAL)
        IF (XF.EQ.0.0) GO TO 250
        XFRONT(LL)=(XF-FLOAT(K))*(XDIST/FLOAT(IMAXI-1))
  250   CONTINUE
        IF (YF.EQ.0.0) GO TO 260
        YFRONT(LL)=(FLOAT(JMAXI)-YF)/FLOAT(JMAXI-1)
  260   CONTINUE
C
C    STORE CONTOUR FRONT MOVEMENT DATA IF IFILE = 1
C
      MARK=IDOL
      IF (KOTI.GT.1) MARK=IBLNK
      WRITE (9,390) MARK
      IF (KOTI.GT.1) GO TO 270
      WRITE(9,430) TEMP,DFI,DELT
      MARK=IBLNK
      WRITE(9,390) MARK
  270 WRITE (9,430) (XFRONT(LL),LL=1,6)
      WRITE (9,430) (YFRONT(LL),LL=1,6)
      WRITE(9,420) IMAXI,JMAXI,K,LM
  390 FORMAT (1H0,A6)
  400 FORMAT (1H ,3F10.4)
  420 FORMAT (1H ,4I5)
  430 FORMAT (1H ,6(E14.9,2X))
      RETURN
      END
```

```
IICNON*SO52(1).FRPLOT
      C   *** PLOT PROGRAM FOR THE CONTOUR FRONT MOVEMENT ***
      C
      C              READ IN FROM DATA DECK
      C       JSTEP= # OF TIME STEPS TO BE READ IN
      C
      C          'TEMP - SIMULATION TEMPERATURE',
      C                 'DFI - LAMDA**2',
      C                 'DLT - TIME STEP'.
      C
            DOUBLE PRECISION XFRONT(800,6),YFRONT(800,6)
            DOUBLE PRECISION TEMP,DFI,DLT
            DIMENSION TAU(800)
            DIMENSION IX(3),IY(3),IA(6)
            DATA IDOL,IBLNK,ISTAR/1H$,1H ,1H*/
            DATA IA/6HCONCEN,6HTRATIO,6HN FRON,6HT MOVE,6HMENT P,6HLOT    /
            DATA IX/6HIN X D,6HIRECTI,6HON    /
            DATA IY/6HIN Y D,6HIRECTI,6HON    /
        390 FORMAT(1H0,A6)
        420 FORMAT(1H ,4I5)
        430 FORMAT(1H ,6(E14.9,2X))
      C   ***  READ DATA FROM DECK
            READ 200, JSTEP
        200 FORMAT(8I10)
            TIME=0.
            DO 1 KK=1,JSTEP
            READ(8,390) MARK
            IF(MARK.NE.IDOL) GO TO 5
            READ(8,430) TEMP,DFI,DLT
            READ(8,390) MARK
          5 READ(8,430) (XFRONT(KK,LL),LL=1,6)
            READ(8,430) (YFRONT(KK,LL),LL=1,6)
            READ(8,420) IMAX1,JMAX1,LM
            TIME=TIME+DLT
            TAU(KK)=TIME
          1 CONTINUE
            DATA HGT,XMAX,YMAX/0.0875,7.0,5.0/
      C   ***  INITIATE THE PLOT
            DO 80 N=1,2
            CALL PLOTS(10.0,10.0)
            CALL PLOT(1.5,1.5,-3)
      C   ***  DRAW BORDER
            CALL PLOT(0.0,YMAX,2,-1)
            CALL PLOT(XMAX,YMAX,2,-1)
            CALL PLOT(XMAX,0.0,2,-1)
            CALL PLOT(0.0,0.0,2,-1)
      C   ***  SCALE GRID
            TTAU=TAU(JSTEP)*100.
            IDIV=INT(TTAU)
            IS=IDIV/25*25+25
            TAUM=FLOAT(IS)/100.
      C
            YY1=XFRONT(1,6)
            IF(N.EQ.2) YY1=YFRONT(1,6)
            DO 2 I=2,JSTEP
            YY2=XFRONT(I,6)
            IF(N.EQ.2) YY2=YFRONT(I,6)
            YYY=AMAX1(YY1,YY2)
          2 YY1=YYY
            YAP=YYY*100.
            IYD=INT(YAP)
            IT=IYD/25*25+25
            YDMAX=FLOAT(IT)/100.
      C   ***  DRAW GRID
            DX=XMAX/20.
            DO 10 I=1,19
            X=FLOAT(I)*DX
            CALL PLOT(X,0.,3)
            CALL PLOT(X,YMAX,2,1)
         10 CONTINUE
            DY=YMAX/20.
            DO 20 J=1,19
            Y=FLOAT(J)*DY
            CALL PLOT(0.0,Y,3)
            CALL PLOT(XMAX,Y,2,1)
         20 CONTINUE
      C   ***  ERASE LABLE AREA
            DO 30 I=3,14
            XX=(I-1)*DX
            CALL PLOT(XX,17.*DY,3)
```

```
      30 CALL PLOT(XX,19.5*DY,-2)
         DO 40 I=19,20
         YY=(I-1)*DY
         CALL PLOT(DX,YY,3)
      40 CALL PLOT(14.*DX,YY,-2)
C     ***  PUT SYMBOL
         CALL SYMBOL(0.5,4.7,0.1313,1A,0.0,33)
         IF(N.EQ.2) IX=IY
         CALL SYMBOL(1.6,4.45,0.1313,IX,0.0,19)
C     ***  AXES NUMBERS
         Y=-0.2
         DO 50 I=1,11
         X=FLOAT(I-1)*2.*DX-.125
         VAL=FLOAT(I-1)*TAUM/10.
      50 CALL NUMBER(X,Y,HGT,VAL,0.0,2)
         X=-0.5
         DO 60 J=1,2
         Y=FLOAT(J-1)*DY-.063
         VAL=FLOAT(J-1)*YDMAX/2D.
      60 CALL NUMBER(X,Y,HGT,VAL,0.0,2)
         CALL SYMBOL(-.75,5.,.1313,'DISTANCE',90.,8)
         CALL SYMBOL(2.,-.5,.1313,'NORMALIZED TIME = TAU',0.,21)
         DO 70 LL=1,4
         CALL PLOT(0.0,0.0,3)
         XMOVE=0.
         CALL PLOT(TAU,XMOVE,2,0)
         DO 70 ML=1,JSTEP
         TAUP=TAU(ML)*XMAX/TAUM
         XMOVE=XFRONT(ML,LL) *YMAX/YDMAX
         IF(N.EQ.2) YMOVE=YFRONT(ML,LL)*YMAX/YDMAX
         IF(TAU.GT.0.0.AND.YMOVE.EQ.0.0.AND.N.EQ.2) GO TO 70
         IF(N.EQ.2) XMOVE=YMOVE
         IF(XMOVE.LT.0.) XMOVE=0.0
         CALL PLOT(TAUP,XMOVE,2,0)
      70 CONTINUE
         CALL PLOT(0.,0.,999)
      80 CONTINUE
         STOP
         END
```

```
!!CRON.SnS2(1).SHFILE
      1              SUBROUTINE SHFILE(TIME,DELT,DELY,TEMP,THAX,RS,YJI,YJUNC,A
      2             .  ,JMAX1,YDIST,XO,IAMONT)
      3        C
      4        C     SUB WRITES SEET RESISTANCE, JUNCTION DEPTH AND INTIGRATED
      5        C     IMPURITY ON UNIT 13
      6        C
      7              IMPLICIT DOUBLE PRECISION(A-H,O-Z)
      8              WRITE(13,200) JMAX1,IAMONT
      9          200 FORMAT(1HO,8I10)
     10              WRITE(13,100) TEMP,THAX,DELT,DELY,YDIST
     11              WRITE(13,100) RS,YJI,YJUNC,O,TIME,XO
     12          100 FORMAT(1HO,6E15.9)
     13              RETURN
     14              END
```

```
HICHON.SOS2(1).OUTPUT
      1              SUBROUTINE OUTPUT(X,Y,IMAX1,JMAX1,K,LM,JJ,TIME,YDIST,
      2             *ID,ITIME,XO,PTIME,DTIME,IAMBNT)
      3       C
      4       C     TRANSIENT DATA PRINT OUT
      5       C
      6              IMPLICIT DOUBLE PRECISION(A-H,O-Z)
      7              COMMON /CON/CB1(69,64)
      8              DIMENSION X(1),Y(1),ID(15),XO(1)
      9              IMAX=IMAX1-1
     10              IMAX2=IMAX1+1
     11              PRINT 106, ID,ITIME
     12              PRINT 100, LM,TIME,PTIME,DTIME,K,X(K),IMAX1,X(IMAX1)
     13              PRINT 101, (N,N=2,IMAX1,2)
     14              PRINT 102, (X(I),I=2,IMAX1,2)
     15              PRINT 105
     16              W1=YDIST-0.45*XO(2)
     17              DO 2 J=JMAX1,1,-1
     18              Q=YDIST-Y(J)
     19              IF(IAMBNT.NE.3) Q=(JMAX1-J)*(1./FLOAT(JMAX1-1))
     20            2 PRINT 103, Q,(CB1(I,JJ),I=2,IMAX1,2)
     21              PRINT 108, (XO(I),I=2,IMAX1,2)
     22              IF(IAMBNT.NE.3) PRINT 109, W1
     23          109 FORMAT(/1HO,10X,'* SI FILM * = ',F10.5)
     24          108 FORMAT(1HO,10X,'* OXIDE THICKNESS IN CM *'/1HO,13X,11(1PF10.3))
     25              PRINT 104, JJ
     26          100 FORMAT(1HO,10X,12HTIME STEP = ,I4,3X,7HTIME = ,F10.3,
     27             *6X,'ELAPSED TIME ,N SEC.:',2X,'PREDEP = ',F10.3,2X,'DRIVE IN = ',
     28             * F10.3//
     29             *10X,'OXIDE POSITION'//
     30             *10X,'X(',I2,') = ',E6.2,2X,'X(',I2,') = ',E6.2//)
     31          101 FORMAT(//,1HO,  3HI = ,6X,12I10)
     32          102 FORMAT (/,1HO,3X,3HX = ,7X,12(1PF10.3))
     33          103 FORMAT(1H, 2X,'Y=',1PF7.1,2X,11(1PE10.3))
     34          104 FORMAT(//,1HO,'NO. OF ITERATION = ',I5)
     35          105 FORMAT(1HO)
     36          106 FORMAT(1H1,10X,15A4,T98,'TIME',A6)
     37              RETURN
     38              END

PRT SOS2.PLOT-CONTOUR,,SUBION,,TRIANG,,ARC,,XYZ,,PLOT,,CONDEP,,MAIN
```

```
1)CRON*S052(1),PLOT=CONTOUR
      1            SUBROUTINE PLTCON(A,CONVAL,NC,IK,JK)
      2      C
      3      CC    ISOCONCENTRATION PLOT SUBPROGRAM
      4      C
      5            DIMENSION A(64,64),X(1000,3),Y(1000,3),NV(1000)
      6            DIMENSION CS(2,3),CT(2,2,4),OT(2,4),B(4),OS(2,3)
      7            DATA ZERO/1.0E-20/
      8            DATA (((CS(I,J),J=1,3),I=1,2)/0.5,-1.0,0.5,-0.5,0.0,0.5/
      9            DATA (((CT(I,JK),K=1,4),J=1,2),I=1,2)/1.0,0.0,0.0,-1.0,0.0,0.0,0.0,0.0,
     10           *0.0,-1.0,0.0,0.0,-1.0,0.0,0.0,1.0,1.0,0.0,0.0,-1.0,0.0,0.0/
     11            DATA ((OT(I,J),J=1,4),I=1,2)/0.0,0.0,0.0,1.0,1.0,0.0,0.0,1.0,1.0,0.0,0.0/
     12            DATA ((OS(I,J),J=1,3),I=1,2)/0.5,1.0,0.0,0.0,0.5,0.0,0.0,0.0/
     13            DATA XMAX,YMAX/8.0,4.0/
     14            NCM1=NC-1
     15            CONTUR=ALOG10(CONVAL)
     16      C*    * RESET PEN TO ORIGIN
     17            CALL PLOT(0.0,0.0,3)
     18      C*    * COMPUTE SCALING FACTORS
     19            SCALX=XMAX*1.5/(IK-2)
     20            SCALY=YMAX/(JK-1)
     21      C*    * START CONTOUR SEARCH
     22            NT=0
     23            IL=IK-1
     24            JL=JK-1
     25         10 DO 50 I=2,IL
     26            DO 50 J=1,JL
     27      C*    * LOCATE SQUARE CROSSINGS
     28            II=I-2
     29            JJ=J-1
     30            B(1)=0.25*(ALOG10(A(I,J))+ALOG10(A(I+1,J))+ALOG10(A(I,J+1))+
     31           *ALOG10(A(I+1,J+1)))
     32            B(1)=10.0**B(1)
     33            B(4)=B(1)
     34      C*    * LOCATE TRIANGLES
     35         20 DO 40 K=1,4
     36            NP=0
     37            GO TO (21,22,23,24),K
     38         21 B(2)=A(I+1,J)
     39            B(3)=A(I,J)
     40            GO TO 30
     41         22 B(2)=A(I,J)
     42            B(3)=A(I,J+1)
     43            GO TO 30
     44         23 B(2)=A(I,J+1)
     45            B(3)=A(I+1,J+1)
     46            GO TO 30
     47         24 B(2)=A(I+1,J+1)
     48            B(3)=A(I+1,J)
     49            GO TO 30
     50      C*    * LOCATE INTERSECTIONS
     51         30 DO 35 M=1,3
     52            IF (CONVAL.LT.AMIN1(B(M),B(M+1)).OR.CONVAL.GT.AMAX1(B(M),B(M+1)))
     53           * GO TO 35
     54            NP=NP+1
     55            BB=ALOG10(B(M+1))-ALOG10(B(M))
     56            IF (ABS(BB).GT.ZERO) GO TO 33
     57            D=0.5
     58            GO TO 34
     59         33 D=(CONTUR-ALOG10(B(M)))/BB
     60         34 CONTINUE
     61            TX=OS(1,M)+CS(1,M)*D
     62            TY=OS(2,M)+CS(2,M)*D
     63            X(NT+1,NP)=OT(1,K)+CT(1,1,K)*TX+CT(1,2,K)*TY+II
     64            Y(NT+1,NP)=OT(2,K)+CT(2,1,K)*TX+CT(2,2,K)*TY+JJ
     65         35 CONTINUE
     66            IF (NP.LE.1) GO TO 40
     67            NT=NT+1
     68            NV(NT)=NP
     69         40 CONTINUE
     70         50 CONTINUE
     71      C*    * SCALE POINTS
     72            IF (NT.EQ.0) GO TO 80
     73         60 DO 65 K=1,NT
     74            NM=NV(K)
     75            DO 65 L=1,NM
     76            X(K,L)=X(K,L)*SCALX
     77            Y(K,L)=Y(K,L)*SCALY
     78         65 CONTINUE
     79      C*    * PLOT CONTOUR
```

```
      DO 71 K=1,NT
      NH=NV(K)
      CALL PLOT(X(K,1),Y(K,1),3)
      IF (MOD(K,10).EQ.0) CALL SYMBOL(X(K,1),Y(K,1),0.10,NCH(1),0.0,-1)
      DO 71 L=2,NH
      CALL PLOT(X(K,L),Y(K,L),2)
      IF (NH.EQ.3) CALL PLOT(X(K,1),Y(K,1),2)
   71 CONTINUE
C     MOVE PEN TO ORIGIN
   80 CALL PLOT(0.0,0.0,3)
      RETURN
      END
```

```
MICRON.SnS2(1).TRIDAG
      1             SUBROUTINE TRIDAG(JF,L)
      2       C*****************************************************************
      3             IMPLICIT DOUBLE PRECISION (A-H,O-Z)
      4             COMMON /TRI/ A(64),B(64),C(64),D(64),V(64)
      5       C
      6             DIMENSION GAMMA(64),BETA(64)
      7             BETA(JF)=B(JF)
      8             GAMMA(JF)=D(JF)/BETA(JF)
      9             JFP1=JF+1
     10             DO 100 I=JFP1,L
     11             BETA(I)=B(I)-A(I)*C(I-1)/BETA(I-1)
     12       100   GAMMA(I)=(D(I)-A(I)*GAMMA(I-1))/BETA(I)
     13             LAST=L-JF
     14             V(L)=GAMMA(L)
     15             DO 200 K=1,LAST
     16             I=L-K
     17       200   V(I)=GAMMA(I)-C(I)*V(I+1)/BETA(I)
     18             RETURN
     19             END
```

MICRON*SnS2(1).SUBION

```
      1            SUBROUTINE SUBION(IMAXI,JMAXI,K,,YDIST,CSTOP)
      2      C*****************************************************************
      3      C     SUBROUTINE FOR GENERATING ION IMPLANT DATA
      4      C*****************************************************************
      5            IMPLICIT DOUBLE PRECISION(A-H,O-Z)
      6            COMMON /CON/CBI(64,64)
      7            DIMENSION Y(1)
      8            ISS=0
      9            JM=JMAXI/2
     10            IF(Y(JM).LT.1.D-3) ISS=1
     11            READ 100, CMAX,RP,DRP,VOLT
     12        100 FORMAT(3E15.6,F10.5)
     13            PRINT 200, CMAX,RP,DRP,VOLT,CSTOP
     14        200 FORMAT(//1HO,'CMAX = ',E10.5,' CM-3',3X,'RP = ',E10.5,' MICRON'/
     15           *  1H ,'DRP = ',E10.5,' MICRON',/1H ,'ION IMPLANTATION WITH
     16           *  BORON IMPLANT AT ',F10.5,' KEV',5X,'CSTOP = ',E15.6)
     17            IF(ISS.EQ.1) RP=RP+1.D-4
     18            IF(ISS.EQ.1) DRP=DRP+1.D-4
     19            DO 1 J=1,JMAXI
     20          1 CBI(1,J)=CMAX*DEXP(-0.5*((YDIST-Y(J)-RP)/DRP)**2)
     21            DO 2 J=1,JMAXI
     22            DO 3 I=2,K
     23          3 CBI(I,J)=CBI(1,J)
     24          2 CONTINUE
     25            RETURN
     26            END
```

MICRON*SnS2(1).ABC

```
      1            SUBROUTINE ABC(IMAXI,,JMAXI,X,Y,LM,TIME,K,DFI,TEMP,TMAX,KOTI,XO,
     *  YDIST,IAMBNT)
      2      C*****************************************************************
      3      C**                                                             **
      4      C**  SUBROUTINE WRITES TRANSIENT DATA ON DATA FILE ON UNIT 11   **
      5      C**                                                             **
      6      C*****************************************************************
      7            DOUBLE PRECISION CBI,X,Y,TIME,TEMP,TMAX,DFI,XO,YDIST
      8            COMMON /CON/CBI(64,64)
      9            DIMENSION XO(1)
     10            DIMENSION X(1),Y(1)
     11            DATA IDOL,IBLNK/1H$,1H /
     12            KOTI=KOTI+1
     13            MARK=IDOL
     14            IF(KOTI.GT.1) MARK=IBLNK
     15            WRITE(11,400) MARK
     16        400 FORMAT(1HO,A6)
     17            IF(KOTI.GT.1) GO TO 2
     18            WRITE(11,100) DFI,TMAX,TEMP,YDIST
     19            WRITE(11,200)K,IMAXI,,JMAXI,IAMBNT
     20        200 FORMAT(1H ,8I10)
     21            WRITE(11,100) (X(I),I=2,IMAXI)
     22            WRITE(11,100) (Y(I),I=1,JMAXI)
     23            MARK=IBLNK
     24            WRITE(11,400) MARK
     25          2 CONTINUE
     26            WRITE(11,200) LM
     27            WRITE(11,100) TIME
     28            DO 1 J=JMAXI,1,-1
     29          1 WRITE(11,100) (CBI(I,J),I=2,IMAXI)
     30            WRITE(11,100) (XO(I),I=2,IMAXI)
     31        100 FORMAT(1H ,5E15.9)
     32            PRINT 300, KOTI
     33        300 FORMAT(1HO,10X,'KOTI = ',I10/)
     34            RETURN
     35            END
```

```
MICRON.SnS2(1),XYZ
      1            SUBROUTINE XYZ(IMAX1,JMAX1,X,Y,LM,TIME,K,DFI,TEMP,TMAX,KOTI,XO,
      2           *  YDIST,IAMBNT)
      3      C.....................................................................
      4      C
      5      C     SUBROUTINE READS THE TRANSIENT DATA FILE ON UNIT 11
      6      C
      7            DOUBLE PRECISION CBI,X,Y,TIME,TEMP,TMAX,DFI,XO,YDIST
      8            COMMON /CON/CBI(64,64)
      9            DIMENSION XO(1)
     10            DIMENSION X(1),Y(1)
     11            DATA IDOL,IBLNK/1H$,1H /
     12            DO 3 KLM=1,KOTI
     13            READ (11,400) MARK
     14            IF(MARK.NE.IDOL) GO TO 5
     15            READ(11,100) DFI,TMAX,TEMP,YDIST
     16            READ(11,200) K,IMAX1,JMAX1,IAMBNT
     17        100 FORMAT(1H ,5E15.9)
     18        200 FORMAT(1H ,8I10)
     19            READ(11,100) (X(I),I=2,IMAX1)
     20            READ(11,100) (Y(I),I=1,JMAX1)
     21            READ(11,100) MARK
     22          5 CONTINUE
     23            READ(11,200) LM
     24            READ(11,100) TIME
     25            DO 1 J=JMAX1,1,-1
     26          1 READ(11,100) (CBI(I,J),I=2,IMAX1)
     27            READ(11,100) (XO(I),I=2,IMAX1)
     28          3 CONTINUE
     29        400 FORMAT(1HO,A6)
     30      C     APPLY PERIODIX B.C.
     31            IMAX2=IMAX1+1
     32            IMAX =IMAX1-1
     33            DO 7 J=1,JMAX1
     34            CBI(1,J)=CBI(3,J)
     35          7 CBI(IMAX2,J)=CBI(IMAX,J)
     36            RETURN
     37            END
```

```
MICRON•SnS2(1).PLOT
      1            SUBROUTINE PLOT(CS,IMAX1,JMAX1,U)
      2      C*****************************************************************
      3      C
      4      C     SUBROUTINE PLOTS THE TWO DIMENSIONAL PROFILE
      5      C     IN THE OUTTPUT PRINTOUT IF IPLOT = 1
      6      C
      7      C*****************************************************************
      8            DOUBLE PRECISION CBI,CS
      9            COMMON /CON/CBI(44,44)
     10            DIMENSION SYMBL(21),ULINE(43)
     11            DIMENSION IX(32)
     12            DATA SYMBL/1HA,1H ,1HB,1H ,1HC,1H ,1HD,1H ,1HE,1H ,1HF,1H ,
     13           •1HG,1H ,1HH,1H ,1HI,1H ,1HJ,1H ,1HK/
     14            DATA DOT,STAR/1H.,1H•/,KP/21/
     15            DATA IX/6•1H ,  1HY,1H ,1HA,1HX,1HI,1HS,90•1H /
     16            IMAX=IMAX1-1
     17            PRINT 11
     18            AT=ALOG10(2.2D11)
     19            FACT=(ALOG10(CS)-AT)/(FLOAT(KP-1))
     20            K=0
     21            DO 2 J=JMAX1,1,-1
     22            DO 1 I=2,IMAX1
     23            IF(CBI(I,J).LE.0.0) GO TO 3
     24            K=((ALOG10(CBI(I,J))-AT)/FACT)+1.0
     25         3  CONTINUE
     26            IF(K.LT.1) ULINE(I)=DOT
     27            IF(K.GE.1.AND.K.LE.KP) ULINE(I)=SYMBL(K)
     28         1  IF(K.GT.KP) ULINE(I)=STAR
     29            L=JMAX1+1-J
     30         2  PRINT 10,IX(L), (ULINE(I),I=2,IMAX1),(ULINE(I),I=IMAX,2,-1)
     31            PRINT 12
     32            PRINT 13
     33            PRINT 14,SYMBL(KP),CS
     34            KD=KP-1
     35            DO 4 I=KD,1,-1
     36            CBL=10.••((I-1)•FACT+AT)
     37            CBH=10.••(I•FACT+AT)
     38         4  PRINT 15, SYMBL(I),CBH,CBL
     39            PRINT 16
     40        10  FORMAT(1H ,A1,1X,1H),70A1)
     41        11  FORMAT(1H1,'IMPURITY CONCENTRATION PROFILE'//
     42           •1HO,41(1HW),///)
     43        12  FORMAT(1H ,1X,50(1H-)//1H ,15X,'X AXIS')
     44        13  FORMAT(  /,1HO,'SYMBOLIC REPRESENTATION OF CONCENTRATION RANGES'
     45           •//1HO,T10,'SYMBOL',T30,'CONCENTRATION RANGE'/1H ,T10,6(1H-),T30,
     46           •19(1H-)/ 1HO,T13,1H•,T29,'ABOVE SURFACE CONC.')
     47        14  FORMAT(1H ,T13,A1,T29,'AT CS = ',E10.3)
     48        15  FORMAT(1H ,T13,A1,3X,'LESS THAN',E10.3,3X,'GREATER THAN OR EQUAL T
     49           •O',E10.3)
     50        16  FORMAT(1H ,T13,1H•,T29,'BELOW 1.0D0E11')
     51            RETURN
     52            END
```

```
MICRON•SnS2(1).CONDEP
      1              FUNCTION CONDEP(M,N,I,J,MIN,MAX,CONVAL)
      2         C•   • LOCATES CONCENTRATION CONTOURS ALONG EITHER          •
      3         C•   • A VERTICAL OR HORIZONTAL GRID LINE. EITHER           •
      4         C•   • LINEAR OR LOGRITHIMIC INVERSE INTERPOLATION          •
      5         C•   • CAN BE USED.                                         •
      6         C•   •                                                      •
      7         C•   • A      -  ARRAY BEING CONTOURED (DIMENSIONED         •
      8         C•   •           (M,N) IN CALLING PROGRAM                   •
      9         C•   •                                                      •
     10         C•   • I,J    -  NON-ZERO VALUE SPECIFIES GRID LINE         •
     11         C•   •           TO BE CONTOURED. POSITIVE VALUE FOR         •
     12         C•   •           LINEAR INTERPOLATION. NEGATIVE FOR          •
     13         C•   •           LOGRITHIOMIC INTERPOLATION. EITHER          •
     14         C•   •           I OR J MUST BE ZERO.                        •
     15         C•   • CONVAL-  CONOUR VALUE                                •
     16         C•   •                                                      •
     17         C•   • MIN,   -  MINIMUM AND MAXIMUM SUBSCRIPTS OF          •
     18         C•   • MAX       GRID LINE TO BE CONTOURED. (MAY BE         •
     19         C•   •           ZERO IF ENTIRE GRID LINE IS TO BE          •
     20         C•   •           CONTOURED.)                                •
     21         C•   • CONDEP-  POSITION OF CONVAL ON GRID LINE. IF         •
     22         C•   •           CONVAL IS OUT OF RANGE OF GRID LINE        •
     23         C•   •           VALUES CONDEP RETURNS A VALUE OF           •
     24         C•   •           ZERO.                                      •
     25         C•   •                                                      •
     26              IMPLICIT DOUBLE PRECISION(A-H,O-Z)
     27              COMMON /CON/A(64,64)
     28              DO 100 I=1,M
     29              DO 100 J=1,N
     30          100 IF(A(I,J).LT.1.D-100) A(I,J)=1.D-100
     31              ILOG=1
     32              IF (I.NE.0) GO TO 10
     33              IINC=1
     34              IMIN=MIN
     35              IMAX=MAX-1
     36              IF ( MIN.EQ.0) IMIN=1
     37              IF ( MAX.EQ.0) IMAX=M-1
     38              IF (J.LT.0) ILOG=-1
     39              JINC =0
     40              JMIN=IABS(J)
     41              JMAX=JMIN
     42              GO TO 20
     43           10 CONTINUE
     44              JINC=1
     45              JMIN=MIN
     46              JMAX=MAX-1
     47              IF ( MIN.EQ.0) JMIN=1
     48              IF ( MAX.EQ.0) JMAX=N-1
     49              IF (I.LT.0) ILOG=-1
     50              IINC=0
     51              IMIN=IABS(I)
     52              IMAX=IMIN
     53           20 CONTINUE
     54              CONDEP=0.0
     55              DO 45 II=IMIN,IMAX
     56              DO 40 JJ=JMIN,JMAX
     57              IF(CONVAL.LT.AMIN1(A(II,JJ),A(II+IINC,JJ+JINC))
     58             1.OR.CONVAL.GT.AMAX1(A(II,JJ),A(II+IINC,JJ+JINC)))
     59             2GO TO 40
     60              IF (ILOG.LT.0) GO TO 30
     61              CONDEP=((CONVAL-A(II,JJ))/(A(II+IINC,JJ+JINC)-A(II,JJ)))
     62             1+FLOAT(II+IINC+JJ+JINC)
     63              RETURN
     64           30 CONTINUE
     65              CONLOG=ALOG10(CONVAL)
     66              CONDEP=((CONLOG-DLOG10(A(II,JJ)))/(DLOG10(A(II+IINC,JJ+JINC))-
     67             1DLOG10(A(II,JJ))))+FLOAT(II+IINC+JJ+JINC)
     68              RETURN
     69           40 CONTINUE
     70           45 CONTINUE
     71              RETURN
     72              END
```

```
MICRON.SnS2(1).MAIN
      1       C***********************************************************
      2       C***********************************************************
      3       C**                                                       **
      4       C**                      PROCSIM  II                      **
      5       C**                                                       **
      6       C**   SOLUTION OF DIFFUSION PROBLEM FOR SILICON ON SAPPHIRE**
      7       C**            *** NORMALIZED SOLUTION ***                **
      8       C**                                                       **
      9       C***********************************************************
     10       C***********************************************************
     11       C**                                                       **
     12       C**          DATA IS READ FROM DECK IN FOLLOWING SEQUENCE: **
     13       C**                                                       **
     14       C**   FIRST CARD:                                         **
     15       C**   LIST - # OF TIME STEPS TO BE SKIPPED WHILE PRINTING **
     16       C**   IFILE - PUT 1 TO WRITE ON FILE AND ALSO TO LOCATE   **
     17       C**           CONTOUR POSITION,CONTOUR FRONT MOVEMENT DATA IS**
     18       C**           WRITTEN ON UNIT 9 AND CONCENTRATION PROFILE IS**
     19       C**           WRITTEN ON UNIT 11.                         **
     20       C**   LFILE - # OF TIME STEPS TO BE SKIPPED WHILE WRITING ON FILE**
     21       C**   IPLOT - PUT 1 TO PLOT PROFILE    PRINT OUT          **
     22       C**   IREAD - PUT 1 TO READ DATA FROM FILE                **
     23       C**         - PUT 2 TO READ ION IMPLANT DATA AND TO       **
     24       C**           DO REDISTRIBUTION.                          **
     25       C**   JSTEP - # OF DATA STEPS TO BE READ FROM FILE IF IREAD = 1**
     26       C**   IMAX1,JMAX1 - # OF GRID POINTS IN X AND Y DIRECTIONS**
     27       C**                 RESPECTIVELY.CHECK DIMENSION BEFORE CHANGING**
     28       C**           FORMAT FIELD - 8I10                         **
     29       C**                                                       **
     30       C**   SECOND CARD:                                        **
     31       C**   JSTP - PUT 0 IF CONST. SOURCE DIFF. IS DESIRED.     **
     32       C**        - PUT 1 IF REDISTRIBUTION IS DESIRED.          **
     33       C**        - PUT> 1 IF TWO-STEP DIFF. IS DESIRED          **
     34       C**   ORINT - PUT 1 FOR 100 CRYSTAL ORIENTATION           **
     35       C**         - PUT 2 FOR 110 CRYSTAL ORIENTATION           **
     36       C**         - PUT 3 FOR 111 CRYSTAL ORIENTATION           **
     37       C**   AMBNT - PUT 1 FOR DRY OXYGEN                        **
     38       C**         - PUT 2 FOR STEAM                             **
     39       C**         - PUT 3 FOR NITROGEN                          **
     40       C**           FIELD 3I10                                  **
     41       C**                                                       **
     42       C**   THIRD CARD:                                         **
     43       C**   CSUB - SUBSTRATE DOPING/1.E15                       **
     44       C**   CS - SURFACE CONCENTRATION/1.E18                    **
     45       C**   TEMP - TEMPERATURE IN DEG. CENT.                    **
     46       C**   TMAX - NORMALIZATION TIME IN SECOND                 **
     47       C**          THIS HAS NO EFFECT IF LAMDA IS SPECIFIED AS DATA**
     48       C**   XDIST, YDIST - WIDTH AND THICKNESS(IN MICRON) OF THE TWO**
     49       C**                  DIMENSIONAL REGION IN QUESTION       **
     50       C**   OXTHIC - WIDTH(IN MICRON) OF THE OXIDE IN THE REGION**
     51       C**   DELT - NORMALIZED TIME STEP                         **
     52       C**           FORMAT FIELD - 8F10.3                       **
     53       C**                                                       **
     54       C**   FORTH CARD:                                         **
     55       C**   IMTYPE - SPECIFY TYPE OF IMPURITY BY PUTTING N OR P **
     56       C**            NO SPEC. IS NECESSARY IF IT IS BORON       **
     57       C**   IMPUTY - PUT BORON,ARSENIC, PHOSPHOROUS OR ANY      **
     58       C**            OTHER NAME.                                **
     59       C**   EA - ACTIVATION ENERGY OF THE DIFFUSION             **
     60       C**        IF BLANK AND BORON DIFF., DATA IS SUPPLIED INTERNALLY**
     61       C**   DI - DIFFUSIVITY CONST. OF THE IMPURITY .           **
     62       C**        IF BLANK AND BORON DIFF., DATA IS SUPPLIED INTERNALLY**
     63       C**           FIELD A4,4A4,2F10.3                         **
     64       C**                                                       **
     65       C**   FIFTH CARD:                                         **
     66       C**   ID - IDENTIFICATION COMMENT TO BE PRINTED ON TOP OF **
     67       C**        PROFILE PRINT OUT                              **
     68       C**   ITEST - PUT 0 TO READ LAMDA FROM DATA DECK          **
     69       C**   CSTOP - CONCENTRATION/1.E15 AT WHICH SIMULATION STOPS**
     70       C**           WHEN THE LEFT END CORNER OF SILICON AND SAPPHIRE**
     71       C**           INTERFACE REACHES THIS VALUE(DURING PREDEP)  **
     72       C**           FORMAT FIELD - 15A4,I5,F15.9                **
     73       C**                                                       **
     74       C**   SIXTH CARD(USE IF JSTP>0):                          **
     75       C**   RDTEMP - REDISTRIBUTION TEMPERATURE                 **
     76       C**   RDTMAX - REDISTRIBUTION NORM. TIME                  **
     77       C**            REDISTRIBUTION FINAL TIME IS 1.            **
     78       C**   RDDLT - REDISTRIBUTION NORM. TIME STEP.             **
     79       C**   XOA - REDISTRIBUTION INITIAL OXIDE THICKNESS IN CM  **
```

```
C**              WHERE SURF. CONC. WAS CS                              **
C**   XOR ,- REDISTRIBUTION INITIAL OXIDE THICKNESS IN CM              **
C**              WHERE SURF. HAS THE THICK OXIDE                       **
C**   CM -    SEGREGATION COEFFICINT, GENERATED INTERNALLY IF          **
C**         IMPURITY IS BORON AND NO VALUE IS GIVEN                    **
C**   FIELD 6F10.3                                                     **
C**                                                                    **
C**   SEVENTH  CARD(USE WHEN ITEST=0)!                                 **
C**   LAMDA - LAMDA**2/1.E-3                                           **
C**           FORMAT FIELD - F10.3                                     **
C**                                                                    **
C**   EIGHTH CARD(USE IF IREAD=2)!                                     **
C**   ION IMPLANTATION DATA                                            **
C**   CMAX - MAX. CONCENTRATION                                        **
C**   RP - RANGE OF DISTRIBUTION. MEAN VALUE (IN MICRON )              **
C**   DRP - STRAGGLE. STANDARD DEVIATION. (IN MICRON )                 **
C**   VOLT - IMPLANTATION ENERGY LEVEL IN KEV                          **
C**           FIELD 3E15.6,F10.5                                       **
C**                                                                    **
C************************************************************************
C
      IMPLICIT DOUBLE PRECISION (A-H,O-Z)
      INTEGER ORINT,AMBNT
      DOUBLE PRECISION KB,NI,LAMDA
      COMMON /TRI/ A(64),B(64),D(64),E(64),V(64)
      COMMON /CON/ CB(64,64)
      DIMENSION X(64), Y(64), CB(64,64), CB2(64,64), G(64,64), ID(16)
      DIMENSION IMTYPE(1), IMPUTY(4), IBRON(4),
      DIMENSION XOLAST(64), XO(64), DRMXO(64),YP(64)
      DIMENSION  IMAT(2),IORNT(1),IDOX(2),INIT(2),ISTM(1)
C
C     DEFINE COMPUTING FUNCTIONS
C
      RHS(Q,G1,G3,C10,C00,C20)=C00+Q*(G1*C20+G3*C10)
      RATIO(C,CSUB,NI)=(C-CSUB)/(2.*NI)
      ROOT(RATIO)=DSQRT((RATIO**2)+1.0)
      FU(RATIO,ROOT)=((RATIO+ROOT)**2)/ROOT
      CALL ERTRAN (9,IDATE,ITIME)
C
C     READ SIMULATION INITIAL DATA
C
      READ 360, LIST,IFILE,LFILE,IPLOT,IREAD,JSTEP,IMAXI,JMAXI
      READ 360, JSTP,ORINT,AMBNT
      IF(IREAD.EQ.2) JSTP=1
      READ 370, CSUB,CS,TEMP,TMAX,XDIST,YDIST,OXTHIC,DELT
      READ 320, IMTYPE,IMPUTY,EA,DI
      READ 380, ID,ITEST,CSTOP
      IF (JSTP.GT.0) READ (5,370,ERR=310) RDTEMP,RDTMAX,RDDLT,XOA,XOR,CM
      IF (ITEST.EQ.0) READ (5,370,ERR=310) LAMDA
C
C     DEFINE DATA!
C
C     KB - BOLTZMANN'S CONSTANT
C     JLIM - # OF ALLOWABLE ITERATIONS
C     DVLIM - ALLOWABLE ERROR IN CONVERGENCE
C     TIMAX - NORMALIZED TIME AT WHICH SIMULATION STOPS
C     EAB AND DIB - BORON DIFFUSIVITY DATA
C
      DATA EAB,DIB /3.59D0,3.17D0/
      DATA IBRON /4HBORO,4HN   ,4H    ,4H    /
      DATA NYP,IPT /1HN,1HP/
      DATA KB /8.616D-5/
      DATA JLIM,DVLIM /60,1.D-6/ ,TIMAX /1.D0/
      DATA IDOX/6HDRY O2,6HHYGEN  /
      DATA INIT/4HNITROG,6HEN    /
      DATA ISTM/6HSTEAM /
C
      IF (IMPUTY.EQ.IBRON) IMTYPE=IPT
      IER=0
      IF (JSTP.EQ.1.AND.IREAD.EQ.0) IER=1
      IF (IMPUTY.NE.IBRON.AND.EA.EQ.0.D0) IER=1
      IF (IMPUTY.NE.IBRON.AND.DI.EQ.0.D0) IER=1
      IF (IER.EQ.1) PRINT 450
      IF (IER.EQ.1) GO TO 310
      IF (IMTYPE.EQ.IPT) ITYPE=0
      IF (IMTYPE.EQ.NYP) ITYPE=1
      IF (IMPUTY.EQ.IBRON.AND.EA.EQ.0.D0) EA=EAB
      IF (IMPUTY.EQ.IBRON.AND.DI.EQ.0.D0) DI=DIB
      PRINT 410, ID
      PRINT 330, IMPUTY,IMTYPE
```

```
      NAMELIST /PUT/ LIST,IFILE,LFILE,IPLOT,IREAD,JSTEP,IMAX1,JMAX1,JSTP
     1,ORINT,AMBNT,CSUB,CS,TEMP,TMAX,XDIST,YDIST,OXTHIC,DELT,EA,DI,ITEST
     2,CSTOP,LAMDA,ROTEMP,ROTMAX,RODLT,XOA,XOB,CM,JLIM,DVLIM,TIMAX
      WRITE (6,PUT)
C
CC    REFORMATION OF COMPUTING, GEOMETRIC AND PHYSICAL PARAMETERS
C
      IF(JSTP.EQ.0.OR.JSTP.GT.1) ICOND=1
      IF(ICOND.EQ.1) AMBNT=3
      IF(AMBNT.NE.3) XDIST=XDIST*1.D-4
      IF(AMBNT.NE.3) YDIST=YDIST*1.D-4
      IF(AMBNT.NE.3) OXTHIC=OXTHIC*1.D-4
      JMAX=JMAX1-2
      KOTI=0
      IMAX=IMAX1-1
      IMAX2=IMAX1+1
      IF(IMAX1.GT.3) GO TO 5
      DELX=6.D0
      IF(AMBNT.NE.3) DELX=6.D-4
      GO TO 6
    5 DELX=XDIST/FLOAT(IMAX2-3)
    6 DELY=YDIST/FLOAT(JMAX)
      CSUB=CSUB*1.D15
      CSTOP=CSTOP*1.D15
      LAMDA=LAMDA*1.D-3
      CS=CS*1.D18
      T=TEMP+273.
      WINDO=(XDIST-OXTHIC)+1.D-5
      CM=CM
      CM=1.0
      TMX=TMAX
      IF(AMBNT.EQ.1) IMAT(1)=IDOX(1)
      IF(AMBNT.EQ.1) IMAT(2)=IDOX(2)
      IF(AMBNT.EQ.2) IMAT=ISTM
      IF(AMBNT.EQ.3) IMAT(1)=INIT(1)
      IF(AMBNT.EQ.3) IMAT(2)=INIT(2)
      IF(ORINT.EQ.1) IORNT='100'
      IF(ORINT.EQ.2) IORNT='110'
      IF(ORINT.EQ.3) IORNT='111'
C
CC    CALCULATE DISTANCE X AND Y
C
      DO 10 I=2,IMAX1
        X(I)=(I-2)*DELX
   10   IF (X(I).LE.WINDO) K=I
      DO 20 J=1,JMAX1
   20   Y(J)=(J-1)*DELY
      DO 30 I=2,IMAX1
   30   XOLAST(I)=XOA
      DO 31 J=JMAX1,1,-1
   31 YP(J)=(JMAX1-J)*(1./FLOAT(JMAX))
C
CC    SPECIFY PREDEP CONDITIONS
C
      DO 40 I=1,IMAX2
        DO 40 J=1,JMAX1
          CA(I,J)=0.0
          CB1(I,J)=0.0
   40     CB2(I,J)=0.0
      DO 50 I=2,K
        CA(I,JMAX1)=CS
        CB1(I,JMAX1)=CS
   50   CB2(I,JMAX1)=CS
      TIME=0.0
      LM=0
C
CC    SPECIFY INITIAL PROFILE
C
      IF(IREAD.EQ.2) CALL SUBION(IMAX1,JMAX1,K,Y,YDIST,CSTOP)
      IF (IREAD.EQ.1) CALL XYZ (IMF1,JMF1,X,Y,LM,TIME,KA,DFA,TMP,TIMX,JS
     1TEP,XOLAST,YDIST,AMBNT)
      IF(IREAD.EQ.1) TIMAX=TIME+1.0
      STIME=TIME
      IF (JSTP.EQ.1) ICOND=2
C
CC    READ CONTOUR FRONT MOVEMENT FROM DATA FILE IF IREAD = 1
C
      IF (IREAD.EQ.1) CALL FRONT (IM1,JM1,LA,KC,TMPR,DFB,DLT,LM,1,KOTI,X
     1DIST)
      IF (IREAD.EQ.1) PRINT 430, LM,TIME,TMP,DFA,TIMX,IMF1,JMF1,KA
```

```
      IF (IREAD.EQ.1) PRINT 440, TMFR,DFB,LA,IMI,JMI
      IF (IREAD.NE.1) GO TO 60
      IF (IMFI.NE.IMAXI.OR.JMFI.NE.JMAXI.OR.KA.NE.K) IER=1
      IF (IMI.NE.IMAXI.OR.JMI.NE.JMAXI.OR.KC.NE.K.OR.LA.NE.LM) IER=1
      IF (IER.EQ.1) PRINT 450
      IF (IER.EQ.1) GO TO 310
C
CC    START SIMULATION STEP
C
   60 IF (ICOND.EQ.1) GO TO 70
      KOTI=0
      TEMP=RDTEMP
      T=TEMP+273.
      DELT=RDDLT
      TMAX=RDTMAX
      IF(AMBNT.NE.3) DELT=DELT*TMAX
      IF(AMBNT.NE.3) TMAX=TMAX
      TIME=0.
   70 CONTINUE
C
CC    CALCULATE NI
C
      TMAX=TMAX-DELT
      CALL PARAM (NI,T)
      DF=DI*DEXP(-EA/(KB*T))
      IF (ITEST.NE.0) DFI=DF*TMAX/((YDIST*1.D-4)**2)
      IF(AMBNT.NE.3) DFL=DF
      IF (ITEST.EQ.0) DFI=LAMDA
      IF (ICOND.EQ.1) PRINT 340
      IF (ICOND.EQ.2) PRINT 350
      PRINT 390, NI,DF
      PRINT 420, IMPUTY,TEMP,DFI,TMAX
C
      P=(DFI*DELT)/(DELY**2)
      Q=(DFI*DELT)/(DELX**2)
C
CC    PRINT INITIAL PROFILE
C
      CALL OUTPUT (X,Y,IMAXI,JMAXI,K,LM,JJ,TIMF,YDIST,ID,ITIME,XOLAST,
     * PTIMF,DTIME,AMBNT)
      IF (IREAD.EQ.2.AND.IFILE.EQ.1) CALL ABC (IMAXI,JMAXI,X,Y,LM,TIMF,K
     1,DFI,TEMP,TMAX,KOTI,XOLAST,YDIST,AMBNT)
      AM=1.0
      CC=1.0
      BB=1.0
      IF (ICOND.NE.1) CALL OXDATA (AMBNT,ORINT,T,BB,
     1CC,AM,KB)
      IF(ICOND.EQ.2.AND.GM.EQ.0.) CM =AM
      IF(ICOND.EQ.2.AND.GM.NE.0.) CM =GM
      IF(ICOND.EQ.2)   PRINT 421, IMBT,IORNT,BB,CC,CM
C
CC    START TIME STEP LOOP
C
   80 LM=LM+1
C
CC    STORE N TH. RESULT FOR R.H.S.,WILL NOT BE CHANGED DURING ITER.
C
      TIME=TIME+DELT
      IF(ICOND.EQ.1) STIME=TIME
      PTIME=TMX*STIME
      IF(ICOND.EQ.2) PTIME=TMX
      DTIME=RDTMAX*(TIME-STIME)
      IF(AMBNT.NE.3) DTIME=TIME
      DO 90 I=1,IMAX2
        DO 90 J=1,JMAXI
   90     CR2(I,J)=CB1(I,J)
      IF (ICOND.EQ.1) GO TO 110
C
CC    CALCULATE OXIDE THICKNESS
C
      IF(AMBNT.NE.3) GO TO 95
      DO 94 I=2,IMAXI
   94   XO(I)=XOLAST(I)
      GO TO 110
   95 PS=BB*DELT
      QS=BB/CC
      DO 100 I=2,IMAXI
        XO(I)=XOLAST(I)+PS/(2.*XOLAST(I)+QS)
  100   DRRXO(I)=(XO(I)-XOLAST(I))/DELT
      XO(1)=XO(2)
```

```
      IF((YDIST-0.45*XO(I)).LT.0.1D 4) GO TO 310
  110 CONTINUE
      DELY=(1./FLOAT(JMAX))*(YDIST-0.45*XOLAST(2))
      IF(AMBNT.NE.3) P=(DFI*DELT)/(DELY**2)
      JJ=0
      JM=0
C
CCC   START ITERATION LOOP
C
  120 JJ=JJ+1
      IF (JJ.GT.JLIM) PRINT 400, CTER
      IF (JJ.GT.JLIM) GO TO 290
C
CCC   TRANSFER SOLN. VECTOR FROM LAST ITERA. FOR CAL. OF G
C
      DO 130 I=1,IMAX2
        DO 130 J=1,JMAX1
  130     CR1(I,J)=CR(I,J)
C
CCC   CAL.G
C
      DO 140 I=1,IMAX2
        DO 140 J=1,JMAX1
          RA=RATIO(CR(I,J),CSUB,NI)
          RO=ROOT(RA)
  140     G(I,J)=FU(RA,RO)
C
CCC   SOLVE SYSTEM IN Y DIRECTION
C
      DO 220 I=2,IMAX1
C
CCC   CALCULATE THE COEFF. IN Y DIRECTION
C
      SR=0.
        DO 150 J=2,JMAX
          G1=(G(I,J)+G(I+1,J))/2.0
          G2=(G(I,J)+G(I,J+1))/2.0
          G3=(G(I,J)+G(I-1,J))/2.0
          G4=(G(I,J)+G(I,J-1))/2.0
      IF(AMBNT.EQ.3) GO TO 151
      SR=0.45*DRRXO(I)*(YP(J)-1.0)*DELT/DELY
  151 CONTINUE
          A(J)=-P*G4
          B(J)=1.+Q*(G1+G3)+P*(G2+G4)+SR
          D(J)=-P*G2-SR
  150     E(J)=RHS(Q,G1,G3,CB(I-1,J),CR2(I,J),CB(I+1,J))
C
CCC   PUT BOUNDARY CONDITION ON Y AXIS
C
        B(2)=A(2)+B(2)
        A(2)=0.0
        IF (ICOND.NE.1) GO TO 170
        IF (I.GT.K) GO TO 160
        E(JMAX)=E(JMAX)-D(JMAX)*CS
        D(JMAX)=0.0
        GO TO 180
  160   CONTINUE
        B(JMAX)=B(JMAX)+D(JMAX)
        D(JMAX)=0.0
        GO TO 180
  170   IF (AMBNT.EQ.3) DRRXO(I)=0.
        HA=-DELY*(1./CM-0.45)*DRRXO(I)
      HB=2.*DFI
        HK1=HA/(HB*G(I,JMAX1))
        HK2=HA/(HB*G(I,JMAX))
        B(JMAX)=B(JMAX)+((1.+HK2)/(1.-HK1))*D(JMAX)
        D(JMAX)=0.
  180   CONTINUE
C
        CALL TRIDAG (2,JMAX)
C
CCC   CONVERT MATRIX SOLUTION
C
        DO 190 J=2,JMAX
          CR1(I,J)=V(J)
  190 CONTINUE
C
CCC   PUT BOUNDARY VALUES IN Y
C
        CR1(I,1)=CR1(I,2)
```

```
      IF (ICOND.NE.1) GO TO 210
      IF (I.GT.K) GO TO 200
      CBI(I,JMAX1)=CS
      GO TO 220
  200 CBI(I,JMAX1)=CBI(I,JMAX)
      GO TO 220
  210 CONTINUE
      CBI(I,JMAX1)=((Y+HK2)/(1.-HK1))*CBI(I,JMAX)
      IF(CBI(I,JMAX1).LT.1.D-300) CBI(I,JMAX1)=1.D-300
  220 CONTINUE
C
CCC   PUT BOUNDARY VALUES IN AXIS X(PERIODIC BOUNDARY)
C
      DO 230 J=1,JMAX1
      CBI(1,J)=CBI(3,J)
  230 CBI(IMAX2,J)=CBI(IMAX,J)
C
CCC   CHECK FOR CONVERGENCE
CC
      IF (JJ.EQ.1) GO TO 120
      ICK=0
      DO 240 I=1,IMAX1
        DO 240 J=1,JMAX
          IF (CBI(I,J).LE.0.0) GO TO 240
          CTEST=DABS((CBI(I,J)-CB(I,J))/CBI(I,J))
          IF (CTEST.LE.CVLIM) GO TO 240
          CTER=DMAX1(CTEST,CTER)
          ICK=1
  240     CONTINUE
      IF (ICK.NE.0) GO TO 120
      JM=JM+1
      DO 241 I=1,IMAX1
      DO 241 J=1,JMAX1
  241 IF(CBI(I,J).LT.0.0D0)    CBI(I,J)=CBI(I,J)
      IF(JM.EQ.1) GO TO 120
C
CCC   PRINT RESULTS
CC
      IS=LM/LIST*LIST-LM
      IF (IS.EQ.0) GO TO 250
      IF (TIME.GE.TIMAX.AND.CS.NE.0.0) GO TO 260
      IF(CBI(2,1).GE.CSTOP.AND.ICOND.EQ.1) GO TO 250
      IF(CBI(2,1).GE.CSTOP.AND.CS.EQ.0.0.AND.JSTP.EQ.1) GO TO 250
      GO TO 260
  250 CALL OUTPUT (X,Y,IMAX1,JMAX1,K,LM,JJ,TIME,YDIST,ID,ITIME,XO,
     * PTIME,DTIME,AMBNT)
      CALL SHREJN (CSUR,YDIST,JMAX1,Y,TIME,DELT,DELY,TEMP,TMAX,IFILE,ITY
     IPE,AMANT,XO(2))
      IF (IPLOT.NE.1) GO TO 260
      CALL PLOT (CS,IMAX1,JMAX1,K)
C
CCC   STORE TRANSIENT DATA
CC
  260 IF (IFILE.EQ.0) GO TO 270
      IT=LM/LFILE*LFILE-LM
      IF(IT.EQ.0) GO TO 265
      IF(TIME.GE.TIMAX) GO TO 265
      IF(CBI(2,1).GE.CSTOP.AND.ICOND.EQ.1) GO TO 265
      GO TO 266
  265 CALL ABC(IMAX1,JMAX1,X,Y,LM,TIME,
     1K,DFI,TEMP,TMAX,KOTI,XO,YDIST,AMANT)
C
CCC   LOCATE CONTOUR POSITION AND STORE DATA
C
  266 CONTINUE
      CALL FRONT (IMAX1,JMAX1,LM,K,TEMP,DFI,DELT,JSTEP,0,KOTI,XDIST)
  270 CONTINUE
C
CC    GO TO NEXT TIME STEP
C
      IF (CBI(2,1).GE.CSTOP.AND.ICOND.EQ.1) GO TO 290
      IF (TIME.GE.TIMAX) GO TO 290
      XO(1)=XO(2)
      DO 280 I=2,IMAX1
  280   XOLAST(I)=XO(I)
      GO TO 80
  290 IF (JSTP.GT.1.AND.ICOND.EQ.1) GO TO 300
      GO TO 310
  300 TIMAX=TIME+1.
```

```
400               IF(AMBNT.NE.3) TIMAX=TIME*RDTMAX
401               ICOND=2
402               GO TO 60
403           310 IF(LM.EQ.0) PRINT 450
404               STOP
405           C
406           320 FORMAT (A4,4A4,2F10.3)
407           330 FORMAT (1H0,20X,'IMPURITY = ',4A4,2X,'IMPURITY TYPE = ',A4)
408           340 FORMAT (1H0,20X,'*** PREDEPOSITION CYCLE ***')
409           350 FORMAT (1H1,20X,'*** REDISTRIBUTION CYCLE ***')
410           360 FORMAT (8I10)
411           370 FORMAT (8E10.5)
412           380 FORMAT (15A4,I5,F5.9)
413           390 FORMAT (///,1H0,10X,'NI = ',D10.3,5X,'DFI = ',D10.3//)
414           400 FORMAT (///,1H0,10X,'ITERATION DID NOT CONVERGE, ERROR = ',D10.3)
415           410 FORMAT (1H1,10X,'*** SOLUTION OF DIFFUSION PROBLEM FOR SILICON
416              1 ON SAPPHIRE ***'//1H0,31X,'NORMALIZED SOLUTION'//1H ,10X,15A4//1
417              2H0,10X,'FOLLOWINGS ARE THE DATA VALUE')
418           420 FORMAT (//,1H0,10X,'NI - INTRINSIC CARRIER CONC.'//1H ,10X,'DFI -
419              1 ,INTRINSIC DIFFUSIVITY OF',1X,4A4,2X,'AT',2X,F10.3,2X,'DEG. CENT.
420              2'//1H ,10X,'LAMDA = LAMDA**2 = DFI*TMAX/(YMAX*1.E-4**2)'//1H ,10X,
421              3'LAMDA = ',D10.3,6X,'FOR NORMALIZATION TIME = ',E12.4,2X,'SEC.')
422           421 FORMAT(//,1H0,10X,'AMBIENT = ',2A4/1H0,5X,'CRYSTAL ORIENTATION = '
423              *A4//1H0,5X,'OXIDATION PARAMETERS',6X,2X,'B = '
424              *E10.3,2X,'C = ',E10.3,/
425              *1H0,6X,'SEGREGATION COEFF. = ',E10.3)
426           430 FORMAT (1H0,10X,'*** INITIAL PROFILE AT TIME STEP = ',I5,2X,'TIME
427              1= ',D10.3,2X,'HAS BEEN READ IN FROM DATA FILE 11 ***'//1H0,15X,'FO
428              2LOWING DATA ARE PROVIDED'//1H ,15X,'TEMP = ',D10.3,2X,'LAMDA**2 =
429              3 ',D10.3,2X/1H ,15X,'NORM. TIME = ',D10.3,2X,'IMAXI = ',I10,2X,'JM
430              4AXI = ',I10,2X,'OXIDE GRID = ',I6)
431           440 FORMAT (1H0,10X,'*** FOLLOWING DATA ARE OBTAINED FROM THE DATA
432              1 FILE 9 ***'//1H ,10X,'TEMP = ',F10.3/1H ,10X,'LAMDA**2 = ',D10.
433              23/1H ,10X,'TIME STEP = ',I10/1H ,10X,'IMAXI = ',I5/1H ,10X,'JMAXI
434              3 = ',I5)
435           450 FORMAT (1H0,10X,'***DATA INPUT ERROR ***'/1H0,8X,'RUNSTREAM TERMIN
436              1ATED')
437           C
438               END
```

@PRT 5059.SWREJN:.MAIN-PLOT

```
MICRON*SnS2(1).SHREJN
      SUBROUTINE SHREJN(CSUB,YDIST,JMAX1,X,TIME,DELT,DELY,
     *  TEMP,TMAX,IFILE,ITYPE,IAMBNT,XO)
C*****************************************************************
C        SUBROUTINE FOR CALCULATING SHEET RESISTANCE AND JUNCTION
C*****************************************************************
      IMPLICIT DOUBLE PRECISION(A-H,O-Z)
      COMMON /CON/C(64,49)
      DIMENSION CNET(64),CBI(64),X(1),Y(64)
      DEL=YDIST/FLOAT(JMAX1-1)
      IF(IAMBNT.NE.3) DEL=DEL/YDIST
      YWJ=0.0
      YWJI=0.0
      DO 6 I=1,JMAX1
      IJ=JMAX1-I+1
      Y(I)=YDIST-X(IJ)
    6 IF(IAMBNT.NE.3) Y(I)=(I-1)*(1./FLOAT(JMAX1-1))
      JNI=1
      ICK=0
      DO 5 J=JMAX1,1,-1
      I=JMAX1+1-J
      CBI(I)=C(2,J)
      IF(CBI(I).LT.CSUB.AND.ICK.EQ.0) JNI=I
      IF(CBI(I).GT.CSUB) ICK=1
      IF(CBI(I).GT.CSUB) JN=I
    5 CNET(I)=CBI(I)-CSUB
      IF(JNI.EQ.1.OR.JN.EQ.(JMAX1-1).OR.JN.EQ.JMAX1) GO TO 7
      YWJ=(YDIST/(JMAX1-1))*(CBI(JN)-CSUB)/(CBI(JN)-CBI(JN+1))
      IF(IAMBNT.NE.3) YWJ=YWJ/YDIST
      YWJI=DEL*(CSUB-CBI(JNI))/(CBI(JNI+1)-CBI(JNI))
    7 K=0
      SIGMA=0.0D0
      Q=0.D0
C
C        START INTEGRATION
C
    1 K=K+1
      IF(K.GE.JMAX1) GO TO 2
      Q=Q+(CBI(K+1)+CBI(K))*DEL/2.D0
      IF(K.LE.JNI.OR.K.GE.JN) GO TO 1
      SIG1=G(DABS(CNET(K)),ITYPE)
      SIG2=G(DABS(CNET(K+1)),ITYPE)
      SIGMA=SIGMA+(Y(K+1)-Y(K))*((SIG2+SIG1)/2.0D0)
      GO TO 1
    2 CONTINUE
      IF(JN.EQ.JMAX1) YWJ=0.0
      IF(JNI.EQ.1.AND.CBI(JNI).GT.CSUB) YWJI=0.0
      SIGA=G(DABS(CNET(JN+1)),ITYPE)
      SIGB=G(DABS(CNET(JNI)),ITYPE)
      SIGC=G(DABS(CNET(JNI+1)),ITYPE)
      YJUNC=Y(JN)+YWJ
      SIGIN=G(DABS(CNET(JN)),ITYPE)
      SIGWJ=0.5*(YWJ*(SIGIN+SIGA)+(DEL-YWJI)*(SIGB+SIGC))
      YWJI=Y(JNI)+YWJI
      SIGMA=SIGMA+SIGWJ
      RS=1.0D0/SIGMA
      WRITE(6,203)  YWJI,YJUNC,RS,Q
  203 FORMAT(/,5X,'JUNCTION IS AT ',2D15.9,' CM',5X,/,
     *5X,'SHEET RESISTANCE = ',D15.9,3X,
     * /3X,'INTEGRATED IMPURITY=',D15.9)
      WRITE(6,201) JNI,JN
  201 FORMAT('0',5X,'JN=',2I5/)
      AFAC=1.0
      IF(IAMBNT.NE.3) AFAC=(YDIST-0.45*XO)/1.D-4
      YJUNC=YJUNC*AFAC
      RS=RS/(AFAC*1.D-4)
      Q=Q*AFAC*1.D-4
      IF(IFILE.EQ.1) CALL SHFILE(TIME,DELT,DELY,TEMP,
     *  TMAX,RS,YWJI,YJUNC,Q,JMAX1,YDIST,XO,IAMBNT)
      RETURN
      END
```

```
MICRON*SnS2(1).MAIN-PLOT
      1         C     ** ISOCONCENTRATION PLOT PROGRAM **
      2         C
      3         C           READ IN FROM DATA DECK
      4         C       FIRST CARD: LL - # OF TIME STEPS TO BE
      5         C                   READ IN FROM DATA FILE, FIELD 13.
      6         C       SECOND CARD: IIT - TIME STEPS TO BYE SKIPPED WHILE
      7         C                          PLOTTING PROFILE. DEFAULT PLOT AT
      8         C                          TIME STEPS 1 AND AT LL. FIELD 13.
      9         C
     10               DIMENSION CB(64,64),XC(64),YC(64),XO(64)
     11               DATA XMAX,YMAX/8.0,4.0/OX/3.6/
     12               DATA IDOL,IRLNK/1H$,1H /
     13               DATA HGT/0.0875/
     14               READ (5,3) LL
     15               READ(5,3) IIT
     16          3    FORMAT (I3)
     17          C*   * READ DATA FILE 11
     18               DO 100 L=1,LL
     19               READ(7,4) MARK
     20          4    FORMAT(1HO,A6)
     21               IF(MARK.NE.IDOL) GO TO 5
     22               READ(7,1) DFI,TMAX,TEMP,YDIST
     23               READ(7,2) K,IMAX1,JMAX1,IAMBNT
     24               IK=IMAX1
     25               JK=JMAX1
     26          1    FORMAT(1H ,5E15.9)
     27          2    FORMAT(1H ,8I10)
     28               READ(7,1) (XC(I),I=2,IK)
     29               READ(7,1) (YC(I),I=1,JK)
     30               READ(7,4) MARK
     31          5    CONTINUE
     32               READ(7,2) LM
     33               READ(7,1) TIME
     34               DO 99 J=JK,1,-1
     35               READ(7,1) (CB(I,J),I=2,IK)
     36               DO 60 I=2,IK
     37          60   IF(CB(I,J).LE.1.E-30) CB(I,J)=1.E-30
     38          99   CONTINUE
     39               READ(7,1) (XO(I),I=2,IK)
     40               IS=L/IIT*IIT-L
     41               IF(IS.EQ.0) GO TO 11
     42               IF(L.EQ.1.OR.L.EQ.LL) GO TO 11
     43               GO TO 100
     44          11   CONTINUE
     45          C*   * INITIALIZE PLOT.
     46               CALL PLOTS(10.0,10.0)
     47          C*   * RESET PEN TO ORIGIN
     48               CALL PLOT(1.0,2.0,-3)
     49          C*   * DRAW BORDER
     50               CALL PLOT(0.0,YMAX,2,-1)
     51               CALL PLOT(XMAX,YMAX,2,-1)
     52               CALL PLOT(XMAX,0.0,2,-1)
     53               CALL PLOT(0.0,0.0,2,-1)
     54          C*   * DRAW OXIDE MASK
     55               XP=(XC(IK)-2.)
     56               IF(IAMBNT.NE.3) XP=(XC(IK)-2.E-4)/1.E-4
     57               OX=(8./XP)*XC(K)
     58               CALL PLOT(OX,YMAX,3)
     59               CALL PLOT(OX,YMAX+0.2,2,-1)
     60               CALL PLOT(XMAX,YMAX+0.2,2,-1)
     61               CALL PLOT(XMAX,YMAX,2,-1)
     62               X=XMAX
     63               PAT=8.-OX
     64               INC=INT(PAT/0.2)
     65               DO 10 I=1,INC
     66               X=X-0.2
     67               CALL PLOT(X,YMAX+0.2,2,-1)
     68               CALL PLOT(X,YMAX,3)
     69          10   CONTINUE
     70               CALL PLOT(0.0,0.0,3)
     71          C*   * HORIZONTAL GRID LINES
     72               DO 20 I=1,9
     73               Y=0.4*FLOAT(I)
     74               LNWT=+3
     75               IF (I.EQ.5) LNWT=.1
     76               CALL PLOT(0.0,Y,3)
     77               CALL PLOT(XMAX,Y,2,LNWT)
     78          20   CONTINUE
     79          C*   * VERTICAL GRID LINES
```

```
      DO 30 I=1,19
      X=0.4*FLOAT(I)
      LNWT=+3
      IF (MOD(I,5).EQ.0) LNWT=+1
      CALL PLOT(X,0.0,3)
      CALL PLOT(X,YMAX,2,LNWT)
   30 CONTINUE
C*    * HORIZONTAL AXIS NUMBERS
      DEX=XP/20.
      IE=21
      IS=1
      IF(DEX.LT.0.1) IE=11
      IF(DEX.LT.0.0) IE=2
      IF(DEX.LT.0.01) DEX=XP/10.
      IF(IAMBNT.EQ.3) GO TO 31
      IS=1
      DEX=XP/20.
      IE=21
   31 CONTINUE
      DO 40 I=1,IE
      VAL=DEX*FLOAT(I-1)
      X=0.4*FLOAT(I-1)-0.5*HGT+0.04
      Y=-0.2
      CALL NUMBER(X,Y,HGT,VAL,0.0,16)
   40 CONTINUE
C*    * VERTICAL AXIS NUMBERS
      IF(IAMBNT.NE.3) YAK=YC(JK)/1.E-4
      DEY=YAK/10.
      DO 50 I=1,11
      VAL=DEY*FLOAT(I-1)
      X=-3.0*HGT-0.1
      Y=YMAX-0.4*FLOAT(I-1)-0.5*HGT
      CALL NUMBER(X,Y,HGT,VAL,0.0,1)
   50 CONTINUE
      CALL SYMBOL(4.2,5.7,0.1,'= 1.0E20',0.0,8)
      CALL SYMBOL(4.2,5.5,0.1,'= 1.0E19',0.0,8)
      CALL SYMBOL(4.2,5.3,0.1,'= 1.0E18',0.0,8)
      CALL SYMBOL(4.2,5.1,0.1,'= 1.0E17',0.0,8)
      CALL SYMBOL(4.2,4.9,0.1,'= 1.0E16',0.0,8)
      CALL SYMBOL(4.2,4.7,0.1,'= 1.0E15',0.0,8)
      CALL SYMBOL(4.0,5.7,0.1,0.0,0.0,-1)
      CALL SYMBOL(4.0,5.5,0.1,1.0,0.0,-1)
      CALL SYMBOL(4.0,5.3,0.1,2.0,0.0,-1)
      CALL SYMBOL(4.0,5.1,0.1,3.0,0.0,-1)
      CALL SYMBOL(4.0,4.9,0.1,4.0,0.0,-1)
      CALL SYMBOL(4.0,4.7,0.1,5.0,0.0,-1)
      CALL SYMBOL(0.0,5.4,0.2,'                    = ',0.0,14)
      CALL SYMBOL(0.,5.4,2.41,0.,-1)
      CALL SYMBOL(999.,5.5,.1,2,0.,1)
      CALL NUMBER(2.6,5.4,0.2,DF1,0.,4)
      CALL SYMBOL(0.0,5.1,0.2,'TEMPERATURE = ',0.0,14)
      CALL NUMBER(2.6,5.1,0.2,TEMP,0.0,n)
      CALL SYMBOL(0.0,4.8,0.2,'TIME STEP   = ',0.0,14)
      TLH=LH
      CALL NUMBER(2.6,4.8,0.2,TLH,0.0,-1)
      CALL SYMBOL(0.0,4.5,0.2,'TIME        = ',0.0,14)
      CALL NUMBER(2.6,4.5,0.2,TIME,0.0,2)
      DO 200 II=1,6
      CONVAL=10.0**FLOAT(20-II+1)
      CALL PLTCON(CB,CONVAL,II,IK,JK)
  200 CONTINUE
      CALL PLOT(0.0,0.0,999)
  100 CONTINUE
      STOP
      END
```

BEGIN

APPENDIX D.

FINITE-ELEMENT EVALUATION

In order to better understand the applicability of the finite element method, it was applied to a one-dimensional linear diffusion problem. This simple problem is one for which familiar results are available for comparison and at the same time taxes the finite-element method. In its most valid form, the finite element method is applicable to variational problems in which a true minimum of an energy-related function exists. Such a minimum does not apply for the semiconductor problem in which current flow occurs by diffusive and conductive mechanisms. It has been proposed that a "weak form", the so-called Galerkin method, be applied to such problems. The typical semiconductor problem is a non-linear boundary value and initial condiction problem of which the linear diffusion problem is a very special case. In the example chosen, the diffusion variable u, obeys:

$$u(x,t)\big|_{x=0} = u_s = 1 \qquad \text{(a)} \qquad \text{(D.1)}$$

$$u_x(x,t)\big|_{x=a} = 0 \qquad \text{(b)}$$

$$u(x,t)\big|_{t=0} = \begin{matrix} 1 \text{ , } x=0 \\ 0 \text{ , } x>0 \end{matrix} \qquad \text{(c)}$$

$$u_t - u_{xx} = f(x,t) = 0 \qquad \text{(D.2)}$$

The Galerkin formulation of this problem is:

$$\int_0^a (u_t v - u_x v_x - fv)\, dx = 0 \qquad \text{(D.3)}$$

C-3

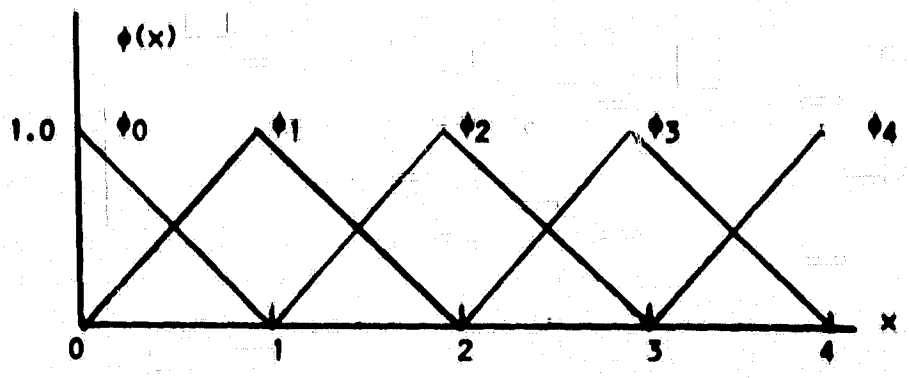

(a) Bilinear hill functions

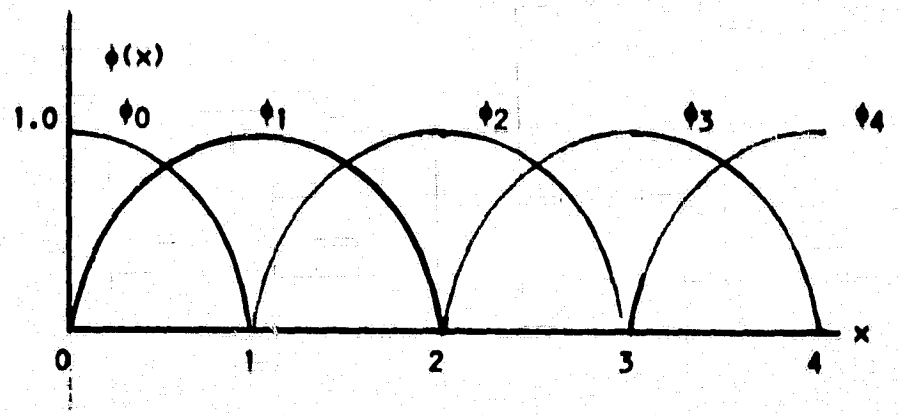

(b) Bicubic (Hermite) hill functions

Figure D-1. Illustration of hill functions used in finite element method.

where $v(x,t)$ represents a "trial function" which is used to approximate $u(x,t)$. The finite element methods uses a set of "hill functions" as illustrated in Figure D.1 to construct the $v(x,t)$ approximation. Two of the popular hill functions are the Hermite bicubic and the bilinear functions which are illustrated in the figure and were used in the example. The final form of the approximate solution is;

$$v(x,t) = \sum_{i=1}^{N} q_i(t)\ \phi_i(x) \quad . \tag{D.4}$$

On the node points the solution is approximated by the set $\{q_i(t)\}$ for the type of hill functions which overlap as illustrated in Figure D-1. Solution for the set $\{q_i(t)\}$ is then analogous to solving for the set $\{u_i(t)\}$ on the node points using the finite difference technique. The quations for the set $\{q_i(t)\}$ are obtained by substituting (D-4) into (D-3).

$$\sum_{i=1}^{N} \int_0^a \left(\frac{\partial q_i}{\partial t}\ \phi_i\phi_j + q_i\ \frac{\partial\phi_i\partial\phi_j}{\partial x\partial x} + f\phi_j\right) dx = 0$$

$$j = 1,2,3,.....N \tag{D.5}$$

From (D-5) a set of time differential equations is obtained which is solved using an implicit numerical method.

The solution of the problem posed by the example is closely approximated by the erfc function in the range $0 \leq x \leq 3$ if $a=6$, and this solution was used to compare the accuracy of the finite element and finite differnece methods. Figures D-2, D-4 show the

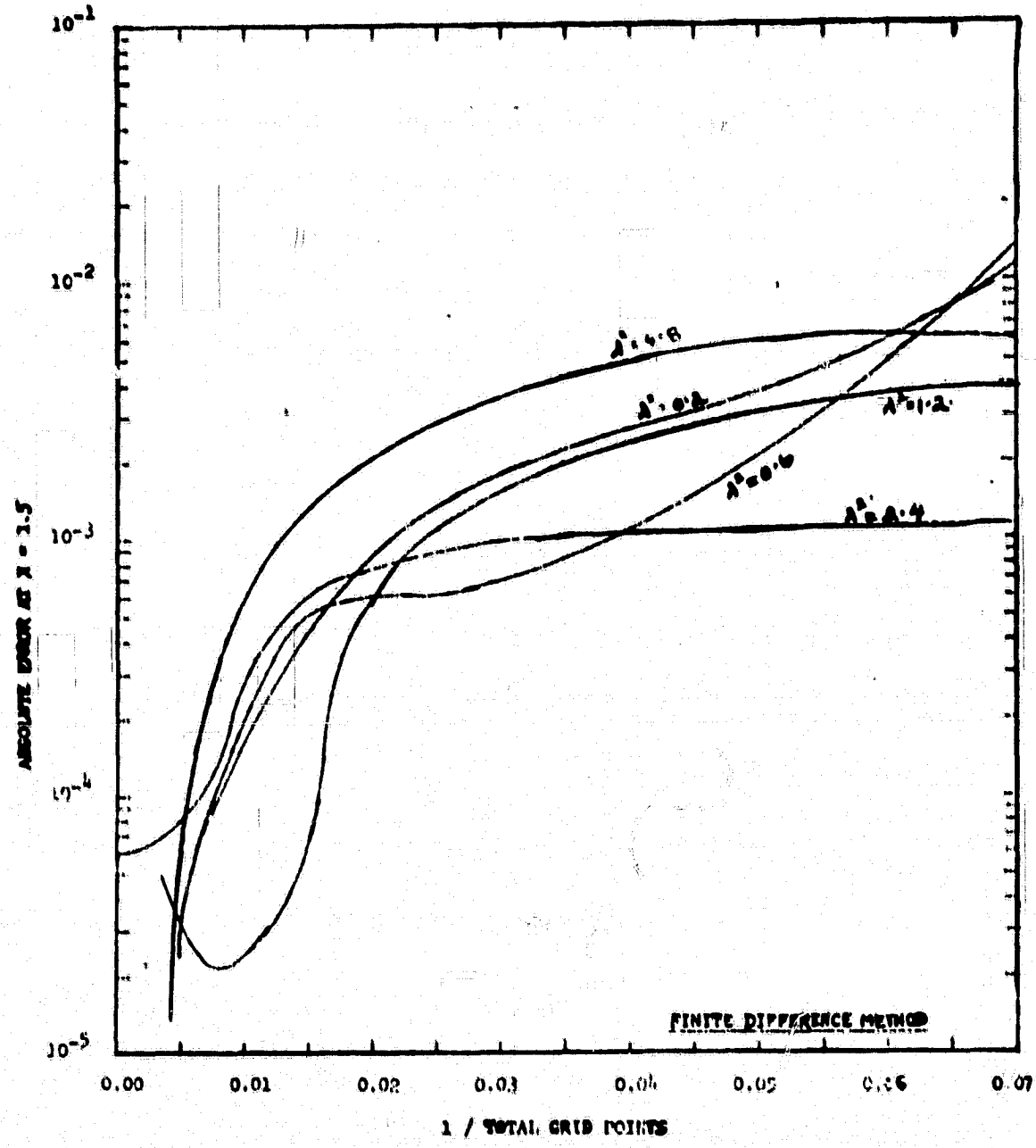

Figure D-2. Error for finite-difference vs. reciprocal of total number of grid points.

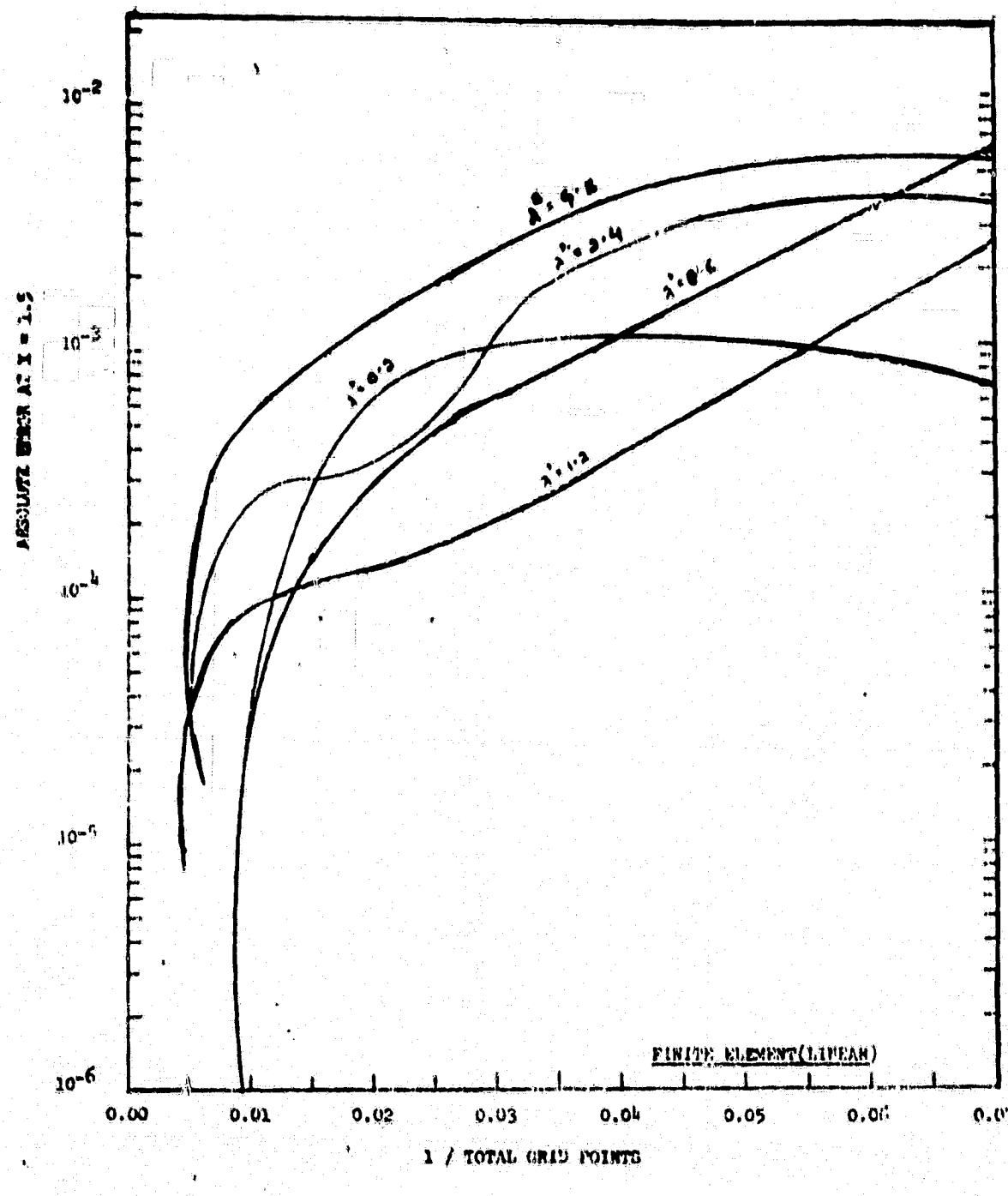

Figure D-3. **Error for finite-bilinear element vs. reciprocal of total number of grid points.**

Figure D-4. Error for finite-bicubic-element vs. reciprocal of total number of grid points.

maximum error as a function of the reciprocal of the number of grid points and the size of the time step, i.e. $\lambda^2 = \Delta t/\Delta x^2$.

The error obtained in the solution by the bilinear finite element method is very nearly the same as that obtained with the finite difference method. This was not surprising because the system of equations for $\{q_i(t)\}$ and $\{u_i(t)\}$ were quite similar. What was surprising was that the Hermite bicubic finite element produced such poor results, although this surprize was based upon the intuition that since this element was more difficult to use it should provide some reward for the difficulty.

APPENDIX E

MICROELECTRONICS AT MISSISSIPPI STATE UNIVERSITY

A. Introduction

The new microelectronics facility at Mississippi State consists of approximately 6600 square feet of space located in the newly constructed (1977) Harry Charles Fleming Simrall Electrical Engineering Building. The space and equipment represent a million dollars investment. Approximately 3000 square feet consists of class 10,000 clean rooms. Within this space, facilities exist for mask-making and photolithography, for chemical preparation, oxidation, etching, diffusion of impurities, for metallization, die-bonding and lead attachment, and for the evaluation of device and integrated circuit parameters. In addition, the hybrid facilities allows fabrication of thick and thin film circuits and encapsulation. Close research ties with NASA Marshall Space Flight Center makes available to EE students and faculty additional research tools, including scanning electron microscope, Auger analysis, electron microprobe, etc.

The vast field of solid state electronics has experienced radical changes since the invention of the transistor in 1949, and the invention of the integrated circuit in 1959. Today's hand held calculator, for instance, contains more than 50,000 active solid

state devices on a single substrate (called a "chip"); electronic watches and appliances touch every aspect of our daily lives.

The rapidly changing technology which has made such electronic marvels possible poses a continuing challenge to an electrical engineering faculty not only to keep abreast, but to devise a curriculum which passes such knowledge on to students, both graduate and undergraduate, and to motivate them in a manner adequate to enable them to join that technology as actively contributing graduate engineers. To this end, the Electrical Engineering Department at Mississippi State University has recently established an extensive laboratory facility and revised curriculum aimed at meeting the threefold purpose of transmitting knowledge through teaching, at the undergraduate and graduate levels; opening new frontiers through research; and extending these efforts and findings to others through service.

Success in these endeavors depends on several important ingredients:

1) A dedicated faculty possessing interest and expertise in the various areas of physical electronics.

2) An undergraduate curriculum devised to teach students not only fundamental principles of physical electronics and of solid state electron devices, but also of the technology which is used in their realization. Students should be provided the opportunity to achieve "hands-on" experience in device fabrication.

3) A graduate teaching program offering education which enables students to do practical design and creative research contributing to the state-of-the-art.

4) A comprehensive research program which simultaneously provides for the education of advanced students while contributing knowledge, basic and applied, to the advancement of the field.

5) The availability of adequate laboratory facilities to support both teaching and research activities.

B. New Electrical Engineering Facilities

The Harry Charles F. Simrall Electrical Engineering building was completed in January, 1977, consisting of 95,000 square feet of floor space at a construction cost of 4.25 million dollars. This building was built under the direction of the State of Mississippi Building Commission with funds appropriated by the State Legislature.

The general theme of the building is classrooms, computer terminal and other heavily populated areas on the first floor, department offices and student activity areas on the second floor with teaching and research laboratories on the third and fourth floors. The features of the Harry Charles F. Simrall Electrical Engineering building include:

1) 10 classrooms with 382 seats total.

2) Computer terminal operated by computing center housing 1004 terminal and other special purpose equipment.

3) 254 seat Auditorium.

4) Microelectronics laboratory complex for instruction and research.

5) High voltage laboratory complex for instruction and research and testing.

6) Computer design and application laboratory complex for instruction and research.

7) Dedicated laboratories for instruction and research in control systems, microwave systems, communication systems, and electronic systems.

8) Dedicated instructional laboratories for study of digital devices, networks and electronics.

9) Student activities and organization area.

10) Faculty and Departmental office complex.

The building now houses all programs and activities of the Electrical Engineering Department which have previously been housed in parts of five buildings.

The Electrical Engineering Department includes 26 faculty members, some with duties outside the department, 410 undergraduate electrical engineering students, 42 undergraduate electronic engineering technology students and some 45 electrical engineering graduate students for a total enrollment of some 500 students.

C. Microelectronics

The objectives of the microelectronics program at Mississippi State are consistent with the University charge to provide education, research and service. These objectives are:

1) To provide an outstanding facility for research dealing with the electronic properties of materials, electron device research, circuit fabrication technology, and computer aided design of electronic circuits.

2) To provide circuit technology accessible at several levels of sophistication which will support research and teaching activities within the department, college and University.

3) To provide a facility available for prototype development of electronic apparatus by industrial concerns and to provide an expertise in electronic fabrication technology to assist industrial start-up operations.

4) To provide operational strategies to allow utilization of the facilities on an economically feasible basis consistent with the commitment to supporting agencies.

The SCOPE of the developing facility is detailed below:

I. Fabrication and processing capability

A. Silicon Integrated Circuit

1. Thermal oxidation and impurity diffusion
2. Photolithography
3. Chemical vapor deposition
   a. Polysilicon
   b. silicon dioxide
   c. other (phosphosilicate glass, silicon nitride, etc.)
4. Aluminum film deposition
   a. sputtering
   b. E-beam evaporation
5. Expitaxial silicon
6. Ion-implantation

B. Hybrid Integrated Circuits

1. Thick film screen printing and firing

2. Chip and wire bonding

3. Component trimming

4. Substrate scribing

5. Packaging and encapsulation

C. Printed Circuits

1. Board sensitization, exposure, and development

2. Baord etching and drilling

3. Board plating

4. Board lamination

II. Computer Aided Design

A. Art work generation by computer

1. Printed circuit layout from line drawing

2. Custom art work for hybrid and monolithic IC's

3. Art work from cell librairies and layout programs

B. Art work processing

1. Reduction

2. Step and repeat reduction of IC master masks (presently thru NASA)

3. Development of working masks

C. Circuit Analysis

1. PCAP

2. Nonlinear circuit analysis program

3. Digital logic and timing analysis

III. Experimental Evaluation

A. Electrical: C-V, sheet resistance, curve tracing, probe testing, circuit testing.

B. Electrochemical: lap and stain, anodization

C. Optical: Microscopic, interferometric, ellipsometric

D. Surface analysis: SEM with SIMS or Auger attachment (presently thru NASA)

D. Description of Facilities

As indicated earlier, the new $4.25 million Harry F. C. Simrall Electrical Engineering Building became occupied in January of 1977. In the electronics area, the department owned or had custody of approximately $250,000 worth of equipment related to microelectronics prior to moving into the new facilities. Primarily the existing equipment consisted of that furnished by the state (mostly in the in the past 3 to 5 years), surplus equipment from NASA, much built in-house, and GFE items.

The microelectronics facilities are located on the fourth floor of the building and consume in excess of 6,600 square feet. Approximately 3,000 square feet of this consist of class 10,000 clean rooms. At a conservative building cost of $45 per square foot, this represents approximately a $300,000 investment in floor space alone. In addition, the department either has purchased or is in the process of purchasing some $175,000 worth of new equipment to furnish the microelectronics laboratory and associated supporting labs. Thus, a total commitment by the University of well over a half million dollars is being invested in this area for purposes of fundamental research and teaching. In addition, equipment obtained through industrial donations represents well over $350,000 to date.

Through University acquisition and industrial donations, the department will be equipped to do significant research in silicon integrated circuits, thick film and chip hybrid circuits.

The following describes the fourth floor microelectronics laboratories and related support facilities. All rooms have compressed air, vacuum, chemical drains, and extensive venting for safe and convenient operation.

A. Silicon Fabrication

This activity is to be carried out in three different rooms, all class 10,000. The water supply consists of an evaporation still, a storage tank with ultraviolet light source, a deionizer, and submicron filters for delivering a minimum of two gallon/minute of 15-18 megohm/cm. water.

A1. Process Room

This large 30 x 40 foot room has one fume hood with etching sink and D. I. water. Benches and cabinets and a quartz/mullite tube closet are also included. There exist five vented gas bottle closets capable of storing ten large cylinders. Water, drains and 3-phase power are available for furnaces and reactor equipment. The basic equipment includes:

. Thermco Spartan 6-tube furnace with class-100 load station and source cabinets.

. Three single tube furnaces (Lindberg, Marshall and BTU), all with electronic controls.

. One class 100 clean bench

. Vaponics deionized water system with additional reservoir for continuous cycle filtering

. Wafer dicer

. Unicorp. Inc. Unipole VIII Epitaxial reactor with dual 8" susceptors driven by a LEPEL solid state power supply (143KVA)

. Four point probe

. Lap and stain facilities

. Ellipsometer/Laser source

. Microscopes

. Multiple probe station

. Capacitance-Voltage test station

. Anodization equipment

. Large dewars for liquid nitrogen and liquid oxygen

For the furnaces, two tubes will be equipped to operate as hot-walled low pressure CVD reactors. The remaining tubes will be used for diffusion and oxidation. One or more tubes will be available for non-silicon work.

A2. Photolithographic Room

This room is 10 x 24 feet and is equipped with three in-line class 100 clean benches and two pass-through ovens with nitrogen ambients. All photo resist and developing operations are done in class 100 environment. Photo-resist spinning is done under temperature and humidity control. Oxide etching and wafer washing is done in end stations with high quality water. Other equipment includes:

. Two-head spinner, plus a single-head spinner

. Electroglass mask aligner for 1 1/2" wafers, plus two Casper aligners for 1 1/2" to 3" wafers

. Balance table's

. Interference microscope

. Hot plate/stirrers, etc.

A3. Metallization and Bonding Room

This large 30 x 20 foot class 10,000 clean room if for the deposition of metal films and thermal-compression bonding. It is equipped with compressed air, vacuum, D. I. water and chemical drains. Pertinent equipment includes:

. NRC-Varian 6" diffusion pump vacuum station equipped with a Sloan sputtering system and a thickness monitor

. Hughes pulse tip thermal compression bonder

. Class 100 clean station for bonder

. Varion Vacion vacuum station equipped for thermal evaporation of aluminum including film thickness monitor and class 100 clean station

. Class 100 clean benches for multiple probe station and vacuum system work areas

. Work benches and cabinets

. Large dewars for liquid nitrogen

. A 200 KeV ion implanter is to be added to this room in early 1979.

. Perkin-Elmer Vacion vacuum station equipped with dual E-beam guns for depositing alloys.

B. Hybrid Fabrication

This activity will be carried out in one large 48 x 42 foot room equipped with fume heads, sinks compressed air, vacuum and three-phase power. Ample bench tops and storage cabinet space is also available. Equipment includes:

- Thick film screen printer
- Class 100 clean bench for printer
- Drying oven
- Thermco belt furnace
- Thick film trimmer
- Thick film trimmer
- Multiple probe station
- Electronic instrumentation for circuit evaluation
- Packaging and sealing station

C. Artwork and Mask Making

This work will be carried out in four different rooms.

C1. Computer Aided Plotting Room

This 30 x 50 foot room was initially scheduled for all artwork but a more comprehensive computer aided graphics facility is being developed. Equipment includes:

- Gerber Scientific 1200 plotter with HP minicomputer tape drive (36 x 36 inch plotting surface with ink or photo exposure heads)
- Tektronix graphics terminal with hard copy capability
- Uniscope CRT terminal to the central campus UNIVAC 1108 computer

. Data General Eclipse S/130 minicomputer with video monitors and Varian Statos 42 high density electrostatic printer/ plotter

. Lexidata color graphics terminal

. Digitizing table for generating check plots on Gerber plotter

C2. Manual Graphics

This will be done in the reduction room. Equipment includes drafting tables and a Unitech coordinatograph with digital read-out. Rubylith masks are produced with this system.

C3. Dark Room

This is a small dark room with modern developing sink temperature controlled water source, and ample storage cabinets and bench top space.

C4. Reduction Room

This room is part of the printed circuits lab and is equipped with a precision Dekacon reduction camera (36 x 36 inch mask mounting capabilities).

C5. Step and Repeat Room

This is an 8 x 24 foot class 10,000 clean room and is part of the silicon IC complex. It is equipped with two class 100 clean benches. One bench has a sink and hood for development and one bench is for a step and repeat camera. The first bench is equipped with compressed air, nitrogen blow gun, and a DI submicron filtered water.

It is hoped that a step and repeat camera will be added soon.

D. Printed Circuit Lab

This laboratory is equipped with benches, a fume hood and sink, and two spray etchers, water dryer, KPR developer unit, IR oven, dip coater, rinse unit, shear, pilot hole punch, drill press, light table, etc. Almost all of this equipment is new.

E. Other Equipment

The microelectronics laboratory has a wide assortment of electronic equipment for evaluation of semiconductor devices and circuits, including signal sources, meters, counters, curve tracers, scopes, etc. A partial listing of new equipment just purchased includes:

- 100 meg Hz Oscilloscope (Tektronics Mod 465);
- Sampling Oscilloscope (HP Mod 182C main frame with HP 1810A sampler);
- Digital to Analog Converter, HP 49303A;
- X-Y recorder, HP Mod. 7015;
- LRC meter, HP Mod 4332A;
- Precision multimeters, HP 3490A;
- Interface bus, HP 59310A;
- etc.

F. Supporting Laboratories

F1. Electro-optic Laboratory

This lab is equipped with a vibration free table, optical benches, detectors, lens, filter, optical radiation detector, two lasers (5 watt argon and 100 milliwatt Helium-Neon), and several items of standard electronic instrumentation.

F2. Communications Laboratory

This facility includes extensive electronic instrumentation for microwave measurements and for signal analysis. Equipment includes wave guides, slotted lines, microwave sources, UHF sources, wave analyzers, antennas, etc. New equipment will include a spectrum analyzer (up to 1.8 G Hz) and a vector voltmeter for s-parameter measurements. Also included are maximal length pseudo-random noise generators and bit pattern generators. The laboratory is located in two rooms on the fourth floor and has two antenna locations on the roof of the building.

F3. Instruction Laboratory

Two large rooms and several smaller rooms are dedicated to teaching and project laboratories. A wide variety of instrumentation, breadboarding equipment, logic trainers, power supplies, etc. are available for instruction, training and project work.

APPENDIX F

POST-HEAT TREATMENT EFFECTS ON DOUBLE LAYER METAL STRUCTURES FOR VLSI APPLICATIONS

A. Introduction

The increasing demands toward greater packing densities in LSI and VLSI make it imperative that multilevel metallization systems be developed. Although several reviews have been written [F1-7], the realization of reproducible and reliable results have yet to be forthcoming. The most common problem associated with double layer metal has been the inability to make electrical contacts between metal layers through via holes etched in the dielectric to provide electrical communication between metals. The problem is more acute when the number of vias is large (>500) and are relatively small in size ($\leq$0.2 mil square). Another, less important problem is associated with shorts between metal layers due to pinholes in the dielectric film, thin spots, or poor coverage of hillocks in the first level metal. An example of the use of double layer metal for circuit application [F-8] is given in Figure F-1.

In order to study the effects associated with double layer metal structures having a large number of small vias, a test pattern was generated consisting of a string of 560 vias. The via size was varied from 0.5 mil square to 0.2 mil square per string. Electrical measurements were made on the test pattern after initial sintering and subsequent heat treatments in order to monitor

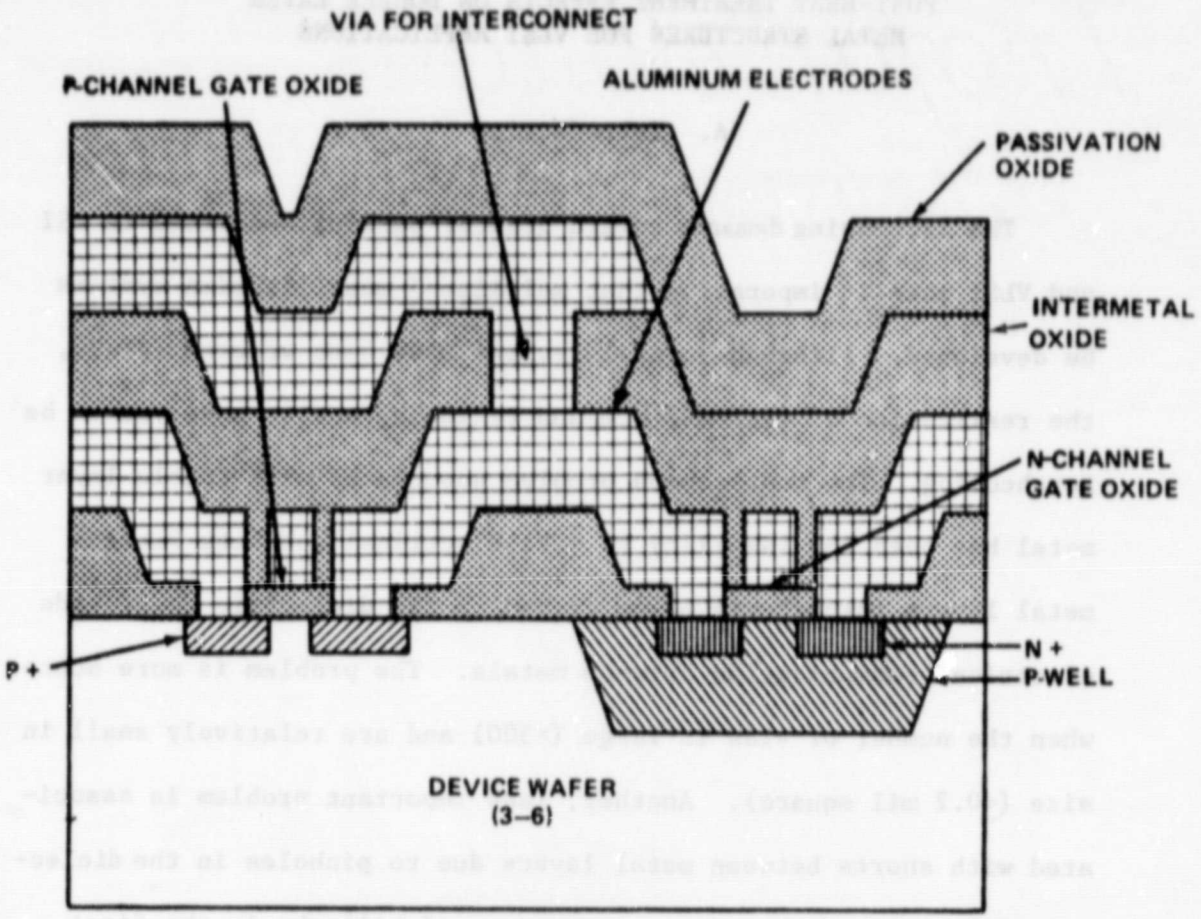

COMPLETED
AL GATE C-MOSFET
DOUBLE LEVEL METALLIZATION

Figure F-1. An example of the use of double layer metal in the realization of an aluminum gate C-MOSFET structure.

contact resistance behavior and variations in yield. Metal interconnects between vias were typically 0.7 mils wide although samples were also prepared and tested having interconnects of 0.4, 0.5, and 0.6 mil wide Al, with little or no variation in results.

B. Preparation of Test Vehicle

The steps involved in preparing the test vehicle consist of the following. The starting material was 3-8 ohm-cm, (100) oriented, n-type phosphorous doped silicon wafers. A field oxide was thermally grown in dry O_2 for 5 minutes, boiling H_2O for 60 minutes and then dry O_2 for an additional 15 minutes at 900°C resulting in an oxide thickness of $14^{K\text{Å}}$. Prior to depositing the first layer metal, a cleaning step was performed, this consisted of a one-minute rinse in deionized water. The wafer was then dehydrated at 900°C in an N_2 ambient for 10 minutes. The first metal layer was d.c. sputtered structural grade Al alloy 6061 of 0.5μm thickness. The metal was patterned using conventional photolithographic techniques with Waycoat-31 negative photoresist.

Prior to depositing the dielectric, scribe lines (0.7 mils wide) were etched around the test patterns through the thermally grown field oxide down to the silicon substrate. These lines were used as an etch end-point monitor in etching vias in the intermetal dielectric.

The intermetal oxide was next deposited at 400°C using CVD of SiH_4 (4% in Ar) and O_2 (and later P_2O_5 of approximately 3 mole

percent) to a thickness of $8^{K}\mathring{A}$. Dielectric thickness was measured with an (laser) ellipsometer. Vias were etched in this dielectric film with buffered HF using standard photolithographic masking. This etching was done first by dipping the wafers in a stirred solution of etchant, using the scribe lines as reference to determine when etching was completely through the dielectric film. In later processes, this etching was done ultrasonically in a totally enclosed container.

The second layer metal was also deposited using dc sputtering of the same target used in the first layer metal and patterned. Typically a 15 minute aluminum sintering process at 470°C preceded the first testing of the completed test vehicle.

C. Experimental Results

Approximately 50 wafers were processed. Each wafer had 200-220 test patterns with via sizes ranging from 0.2 mils square to 0.5 mils square. Table I represents a summary of results in terms of percent yield obtained for each via size as a function of fabrication process. Process A through L are explained below. Among other variables it will be noted that each process is characterized by an etch time associated with etching the vias in the intermetal dielectric film. The scribe lines were used as reference. When all dielectric was etched from these scribe lines, this was defined as the 'break' time. Any additional etching beyond this break time is measured in seconds.

	Percentage Yield Via Resistance for 560 Vias < 20 Meg Ohm Process Identification											
Via Size	A	B	C	D	E	F	G	H	I	J	K	L
0.5 mils	81	76	95	98	99	98	94	84	94	98	98	98
0.4 mils	70	56	88	94	97	98	92	82	89	90	97	97
0.3 mils	61	53	64	85	93	94	92	83	87	80	100	100
0.2 mils	40	18	64	82	91	94	93	89	72	67	98	98

Table I-A

	Percentage Yield Via Resistance for 560 Vias < 10 Kil Ohms Process Identification											
Via Size	A	B	C	D	E	F	G	H	I	J	K	L
0.5 mils	17	59	86	97	97	94	84	61	92	93	98	98
0.4 mils	8	48	73	89	94	96	88	64	82	90	97	97
0.3 mils	0	30	45	64	89	92	88	74	85	80	100	100
0.2 mils	0	14	13	26	44	59	64	52	38	67	98	98

Table I-B

	Percentage Yield Via Resistance for 560 Vias < 1 Kil Ohm Process Identification											
Via Size	A	B	C	D	E	F	G	H	I	J	K	L
0.5 mils	0	59	78	85	86	82	74	56	92	92	98	98
0.4 mils	0	46	47	66	72	72	68	54	82	90	97	97
0.3 mils	0	28	85	36	47	55	58	56	85	80	100	100
0.2 mils	0	8	10	15	22	27	30	30	32	67	75	98

Table I-C

Table I Percentage yield as a function of processing with via size as a parameter for contact resistance of 560 vias less than 20 Megohm, 10 Kilohm, and 1 Kilohm for tables I-A, I-B, and I-C, respectively.

Process Definitions:

1) Wafers were processed as described in section B. The width of the first level metal interconnect of 0.4, 0.5, 0.6 and 0.7 mils corresponded to test patterns having square vias of 0.2, 0.3, 0.4, and 0.5 mils, respectively. The width of the second metal was 0.7 mils. Via etch time was break plus 10 seconds.

2) Wafers were processed as described in section B. The metal interconnects on both levels were 0.7 mils wide. (This is true for all processes 2 through 7). Via etch time was break plus 10 seconds.

3) Wafers processed as described in section B with via etch time in stirred dielectric etchant extended 20 seconds beyond break time.

4 thru 7) correspond to wafers processed as described in section B but with via etch time in stirred dielectric etchant extended 40, 60, 80, 100 and 120 seconds beyond break, respectively. (Note that the values given for processes 1) through 7) represent an average of five different process runs of eight wafers for each run.)

8) Wafers processed as described in section B but having a phosphorous doped intermetal dielectric of 3.1 mole percent (as determined by Auger spectroscopy) and with vias etched in stirred dielectric etchant for 20 seconds beyond break.

9) Wafers processed as described in 8 above except via etching was done ultrasonically in a closed container for 20 seconds beyond break.

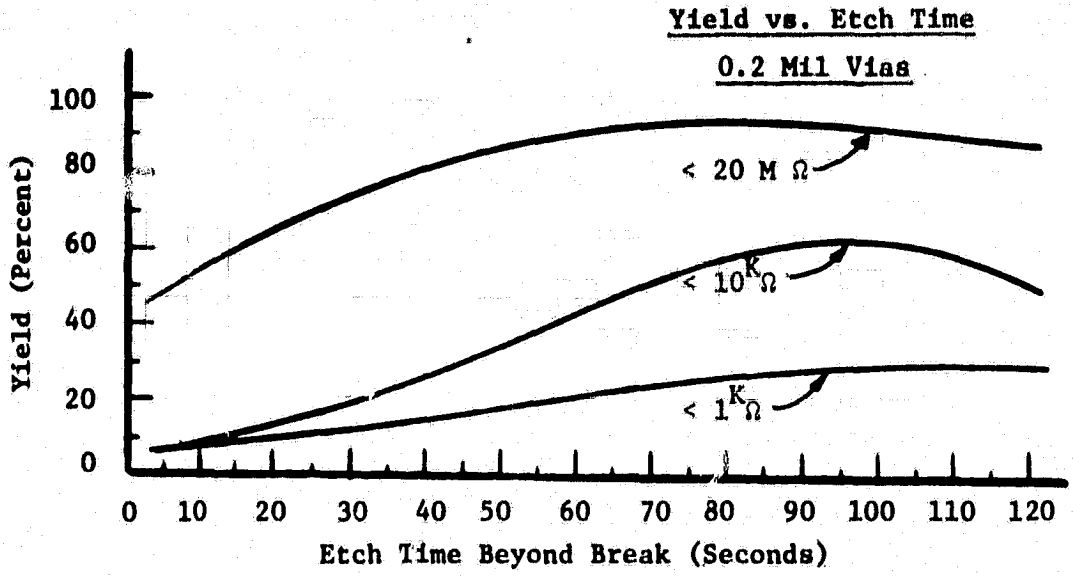

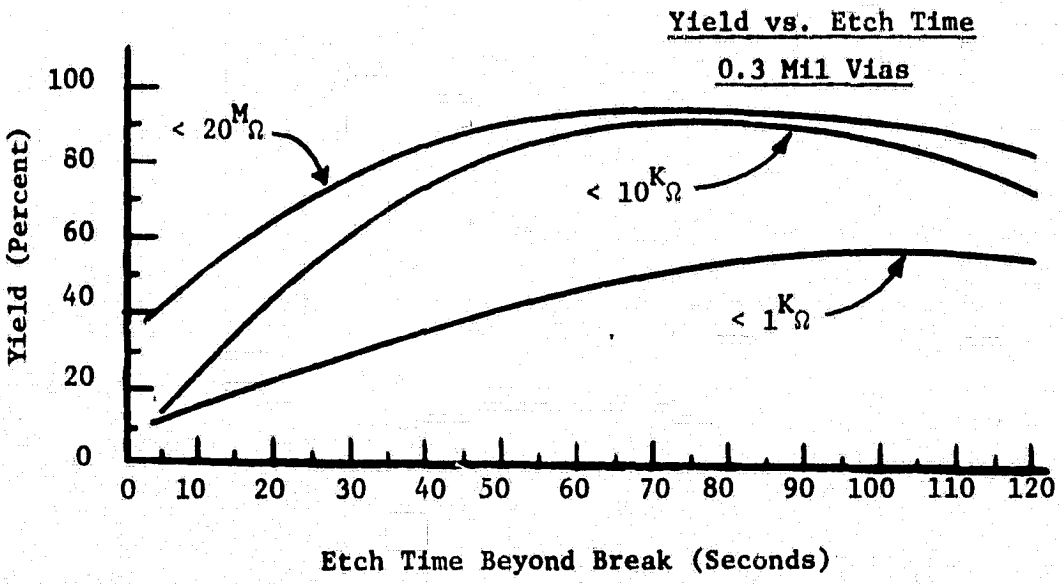

Figure F-2. Percent yield as a function of etch time beyond break with via size as a parameter. Intermetal dielectric etch accomplished with stirred B.O.E.

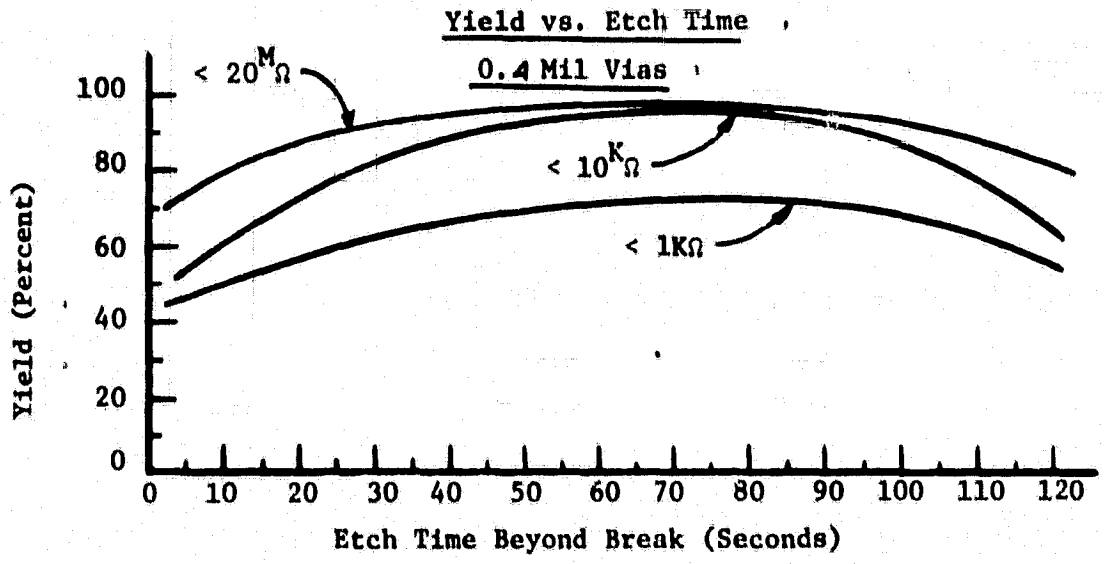

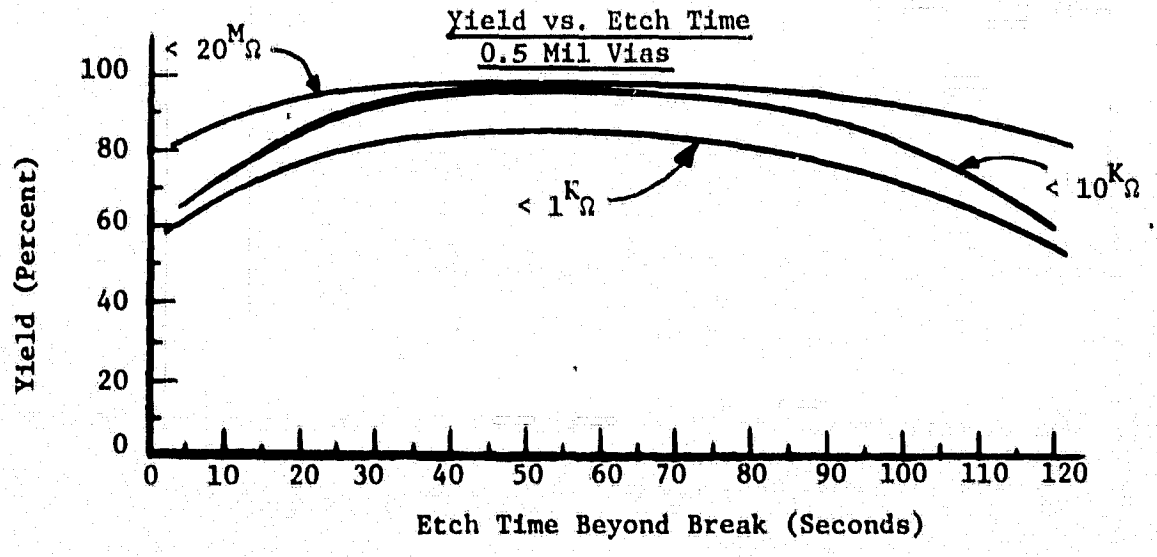

Figure F-2. (continued). Percent yield as a function of etch time beyond break with via size as a parameter. Intermetal dielectric etch accomplished with stirred B. O. E.

10) Wafers processed as described in 9 above with the addition of a first level metal cleaning step through the vias prior to depositing the second level metal. The metal cleaning solution consisted of an ethylene glycol-buffered HF-H_2O solution for the removal of Al_2O_3 from the first level metal prior to deposition of second level metal [F-10].

11) Wafers processed as described in 10 above but having undergone a one-half hour post heat (sintering) treatment at 490°C.

The results of processes 3 through 8 are displayed graphically in Figure F-2. The data are shown in Tables F1-A, B, and C which give the percent yield for via contact resistances less than 20 meg-ohms, 10 kil-ohms and 1 kil-ohm. It is desirable to have minimum contact resistance (i.e. less than 250 ohms) since as the number of vias increase from 600 to approximately 3000 for a VLSI circuit, the resistance will increase proportionately. Any pattern having a contact resistance greater than 20 meg-ohm is assumed to be an open-circuit in Table F1.

Wafers processed as described in D in Table F1 were used for an Auger surface analysis of the first level metal through a 0.5 mil via just prior to depositing the second level metal. The purpose of the Auger analysis was to determine what insulating mateials reside on the surface of the first level metal which prevented good low resistance ohmic contact between metal levels. The results of this analysis indicated the following materials were present with an accuracy of ± 5%:

Al_2O_3		64%
C		31%
N		1.8%
Mg		1.3%
Si		0.6%
F		0.6%
S		0.7%
O	(other than Al_2O_3)	<0.1%

For this contact, the amounts of Mg and Si were about the same as the bulk Al alloy so there did not seem to be any surface enrichment of Mg_2Si which was suspected as a source of the high resistance. When about 100Å of this surface was removed by ion etching, the N,S,F, and C were greatly reduced, which suggested that they may be a source of interfacial contamination.

The large percentage of carbon measured (31%) is believed to be a result of the photoresist leaving a carbon residue on the wafer. The composition of this photoresist could not be obtained from the manufacturer.

It should be noted that the composition of the structural grade Al 6061 consist of the following impurities:

Si	0.4 - 0.8%
Cu	0.15 - 0.4%
Fe	0.7%
Mg	0.8 - 1.2%
Mn	0.15%
Cr	0.15 - 0.35%
Zn	0.25%
Ti	0.15%

The primary reason for using this Al alloy was for the prevention of hillock formation.

Post heat treatment or sintering of a wafer exhibiting an initial poor yield (i.e. less than one kil-ohm for a chain of 560 vias in series) can increase the effective yield by 500 to 700% as

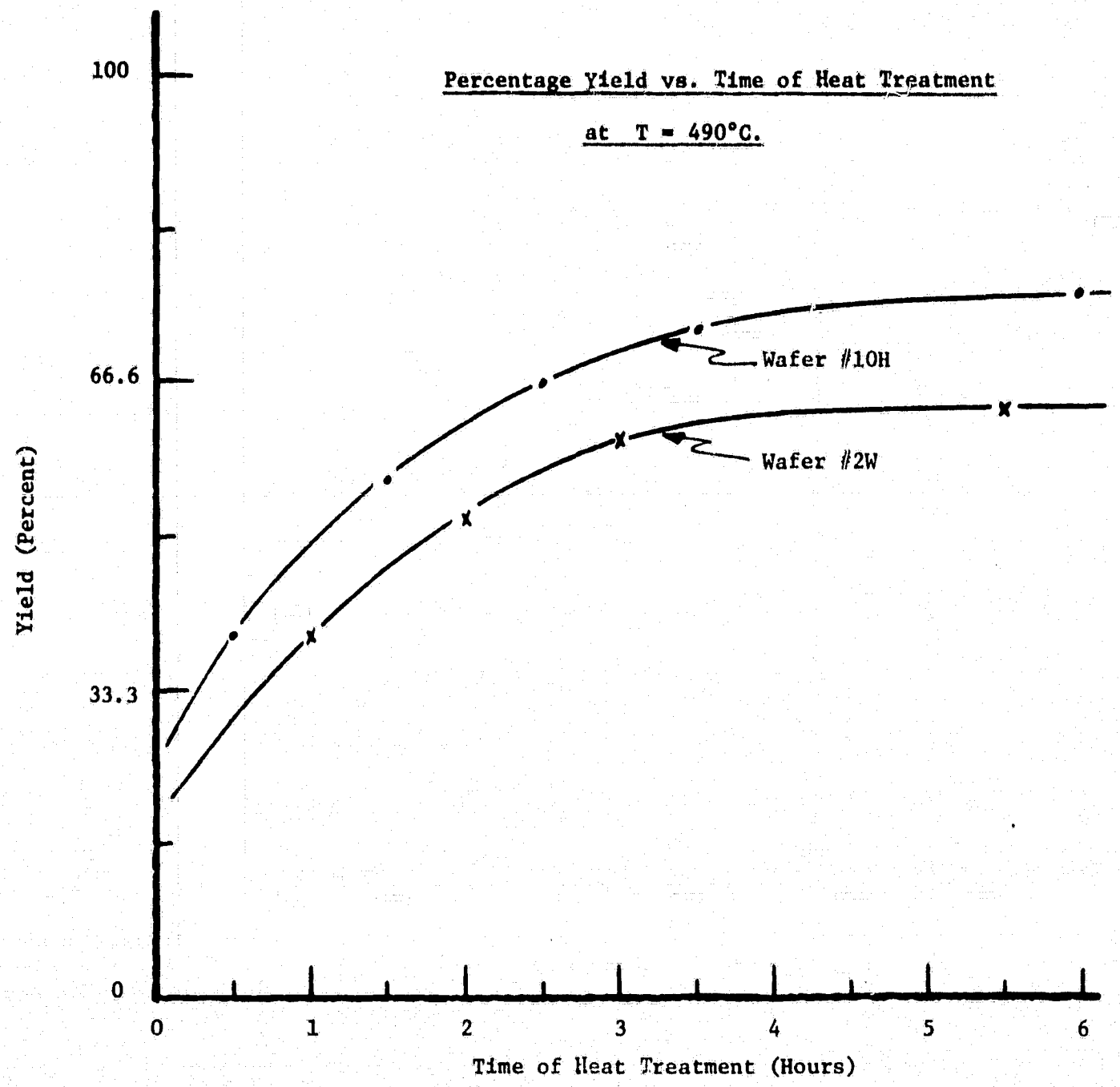

Figure F-3. Percentage yield of number of chips less than 1 kil ohm as a function time of heat treatment at 490°C for wafers with undoped intermetal dielectric.

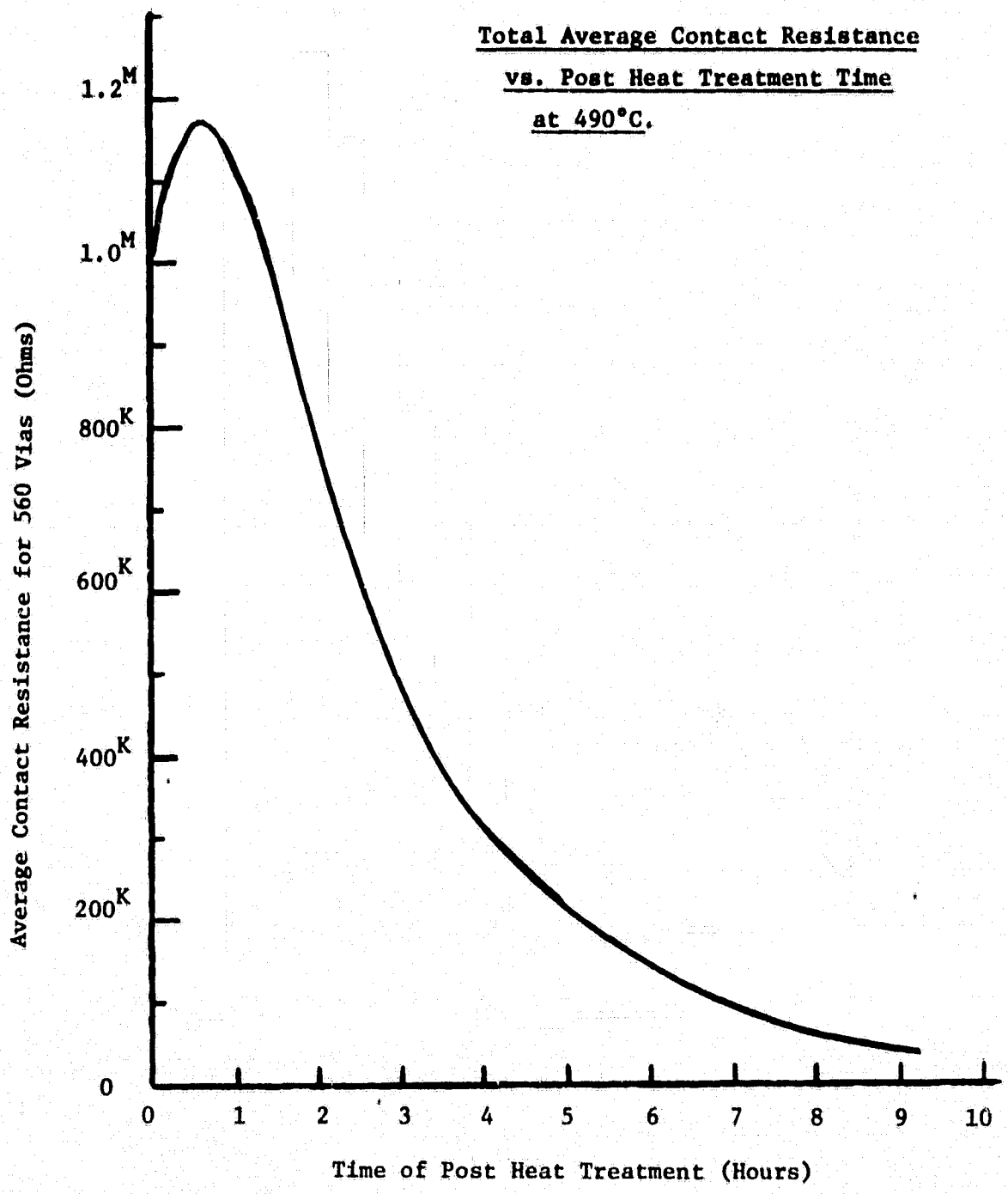

Figure F-4. Average contact resistance for 560 vias of all 0.5 mil square chips as a function of post heat treatment time for wafer #2W. (Total number of chips = 55)

illustrated in Figure 3 for wafers 10H and 2W. These wafers were processed as in 'C' above, having only a 15 minute 470°C sintering before initial testing. All addition sintering was done at 490°C in a nitrogen ambient.

The primary reason for this increase in yield with post heat treatment is due to the fact that the Al-to-Al contact resistance decreases with sintering, as demonstrated in Figure 4. Here, the average resistance for all test patterns having 0.5 mil square vias (approximately 55 of the total 212 chips) is plotted as a function of sintering time. As the time of sintering increases, the number of test patterns having a contact resistance < 1 kil-ohm increases, hence the yield increases.

On an individual chip basis, the contact resistance for 560 vias per chip behaved as shown in Figure F-5. For a given wafer which initially exhibits a relatively poor yield, the number of chips behaving in the manner shown for chips #10C and 10W was approximately 51%, those behaving like chip #10R was 27% and those like chip #10T was 10%. The remaining chips either exhibited low initial contact resistance (<300 ohms) or were open-circuited (>20 meg-ohms). Those chips initially exhibiting a low contact resistance generally had their resistance lowered with increasing heat treatment, how4ver a few chips showed a gradual increase in resistance with increased heat treatment time as shown in Figure F-6. It is believed that this increase in resistance is due primarily to the consumption of Al by SiO_2 to lessen the Al thickness. Since at 490°C Al reacts chemically with SiO_2 to lessen the Al thickness.

Since at 490°C Al reacts chemically with SiO_2 to form Al_2O_3 and free Si,Al is consumed at a rate of 210Å/hr. [F-15]

The most predominant trend found in sintering of double level metal test patterns is demonstrated in Figure F-7. As inferred from this plot of contact resistance as a function of post-heat treatment for these two wafers, the average contact resistance decreases drastically for the first few hours of sintering. Because of this feature, the realization of multiple level metal LSI having a large number of vias (>2000) is a distinct possibility.

One major problem involved in post heat treatment of double layer metal structures is that the dielectric (C.V.D. - SiO_2) has a tendence to crack or "craze" at elevated temperatures (>500°C). This cracking, as illustrated in Figure F-8, is due to excess stress on the insulating layer [F.9]. One method to lessen, if not-alleviate this problem, is to use a phosphorous doped dielectric of 3 to 5 mole percent. This increases the effective temperature for which sintering can be done before cracking is observed [F.9].

Using this phosphorous doped dielectric (also called phosphosilicate glass or PSG) resulted in a much higher yield as shown in Table 1 and also a considerable less contact resistance as shown in Figure F-9. Here the average contact resistance as a function of via size is plotted for a test pattern with a doped dielectric layer for no heat treatment (curve B0 and with 30 minutes post heat treatment at 490°C (curve A). These results are compared to the best results obtained for the undoped case (curve C),

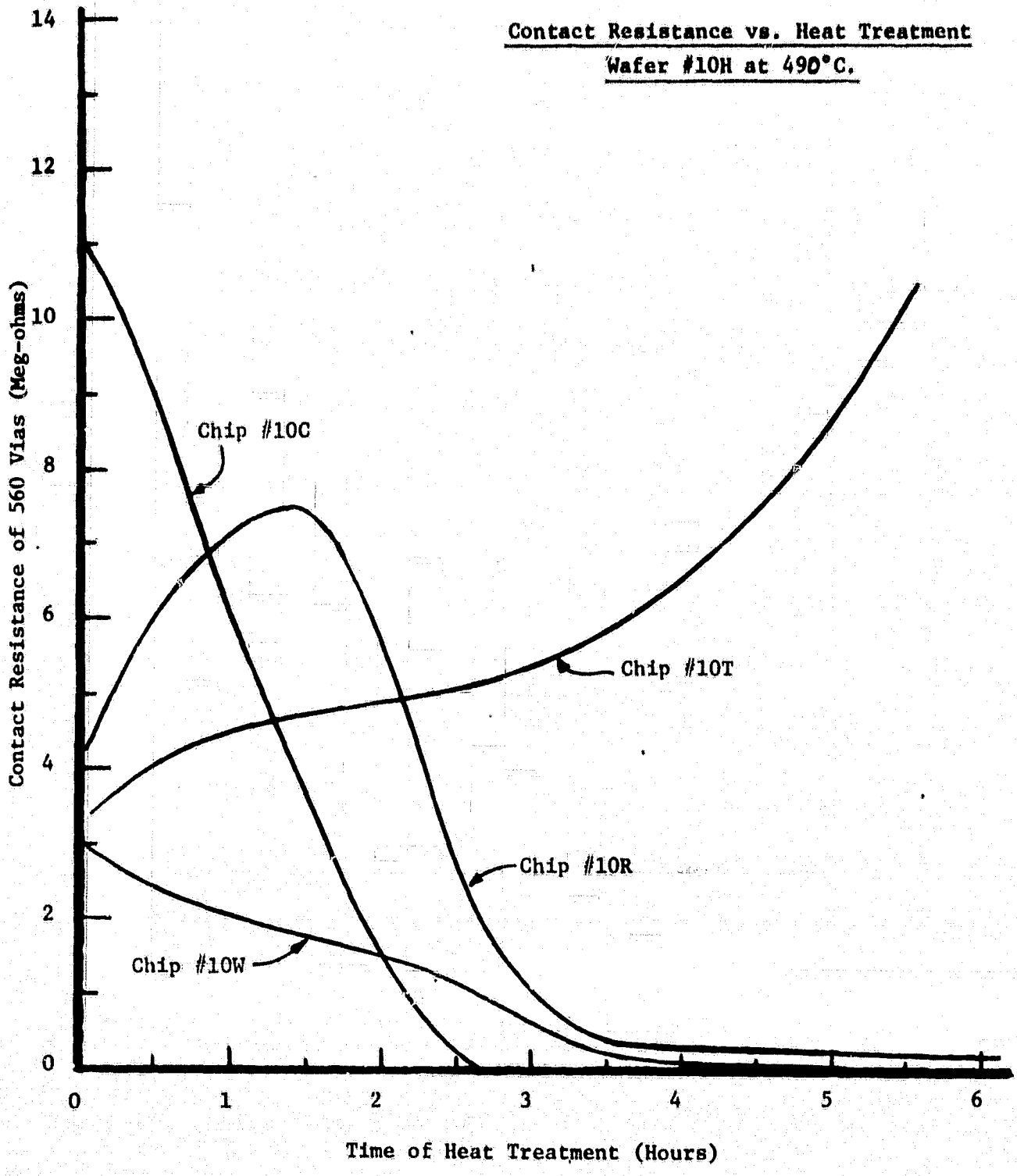

Figure F-5. Contact resistance of 560 vias as a function of heat treatment time for several different chips of wafer #10H at a temperature of 490°C.

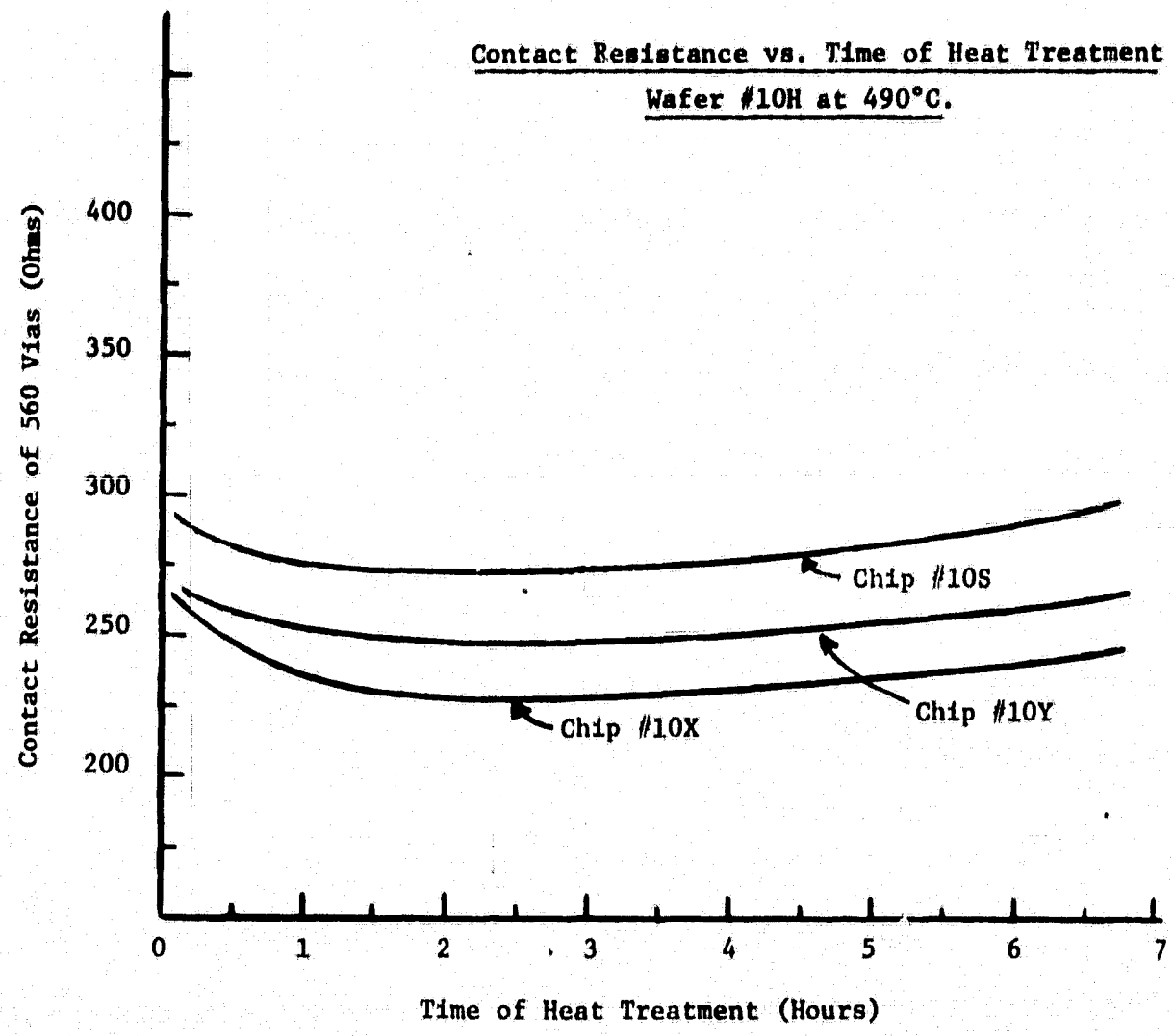

Figure F-6. Contact resistance of 560 vias as a function of heat treatment time for wafer #10H showing slight increase in resistance with time of heat treatment for ~6% of the chips on the wafer.

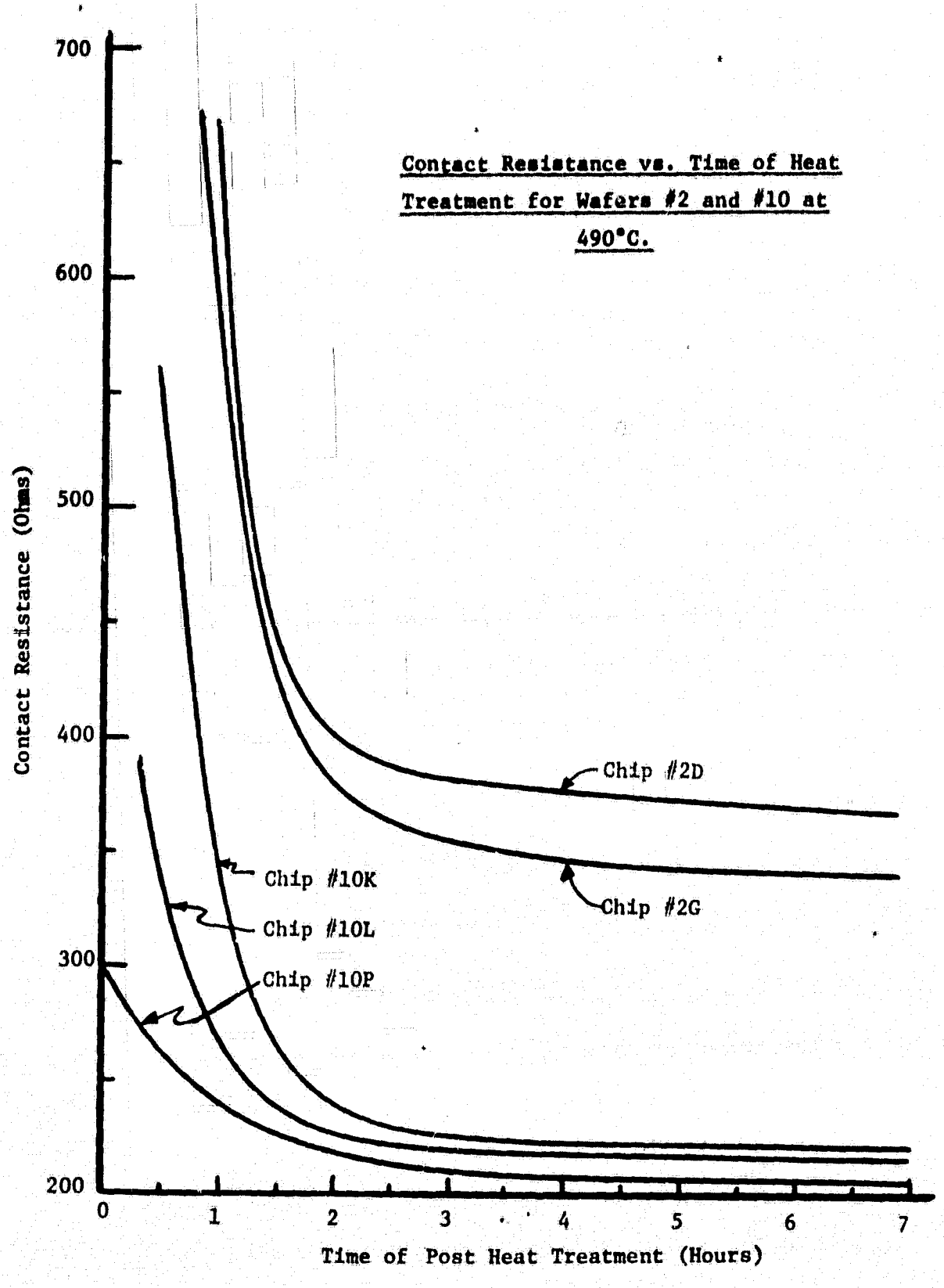

Figure F-7. Contact resistance trends as a function of heat treatment time for wafers #2 and #10.

even after many hours of heat treatment. The table in the figure indicates resistance and percent yield for each case presented.

A resistance map of the wafer shown in curve B is given below:

			173	159	154	217	161	143	158	196	176					
		170	171	∞	157	231	158	161	159	183	171	158				
	166	163	168	158	166	226	162	162	162	171	167	161	164			
	164	164	167	161	158	208	164	159	161	172	170	163	165	173		
	168	170	170	160	159	212	163	161	163	228	169	164	∞	172	164	
157	168	169	170	165	158	219	162	161	160	234	168	163	163	170	160	
164	170	170	171	164	156	213	161	163	159	221	173	159	163	170	165	
112	173	201	176	164	151	143	173	∞	163	192	174	162	162	170	171	
164	175	375	181	167	159	405	172	162	158	181	167	161	164	167	165	
	177	202	182	169	159	211	164	161	154	176	164	160	156	166		
	176	216	184	171	161	228	169	158	154	∞	162	156	154	165		
	44	198	179	171	162	228	164	158	153	173	160	157	151			
		260	181	171	163	231	166	159	154	172	160	153				
				177	166	200	167	159	151	167	157					

Via size	.4	.5	.2	.3	.4	.5	.2	.3	.4	.5	.2	.3	.4	.5	.2	.3	.4

D. Analysis and Conclusions

The following comments and conclusions may be derived from this investigation.

1) The variation in width of the metal interconnects between vias had little influence on yield, as expected. It may have had a slight effect on total resistance, expecially for the 0.4 mil compared to 0.7 mil wide interconnect, but this was not detectable. The major difficulty came in mask alignment of the smaller interconnects.

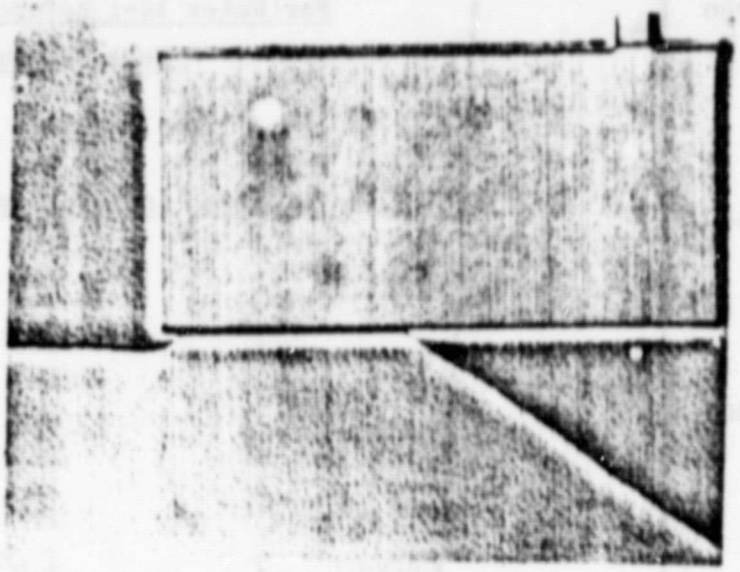

Photomicrograph (A)

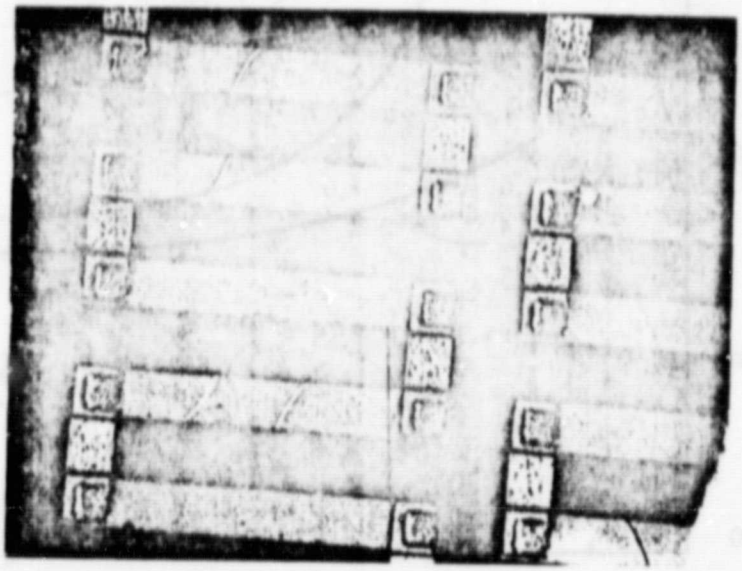

Photomicrograph (B)

Figure F-8. Photomicrograph of test pattern at 300X magnification illustrating crazing tendency at temperatures >500°C and for fast pull from the furnace. Photomicrograph (A) shows crazing around a test pad whereas (B) shows crazing in the test pattern itself.

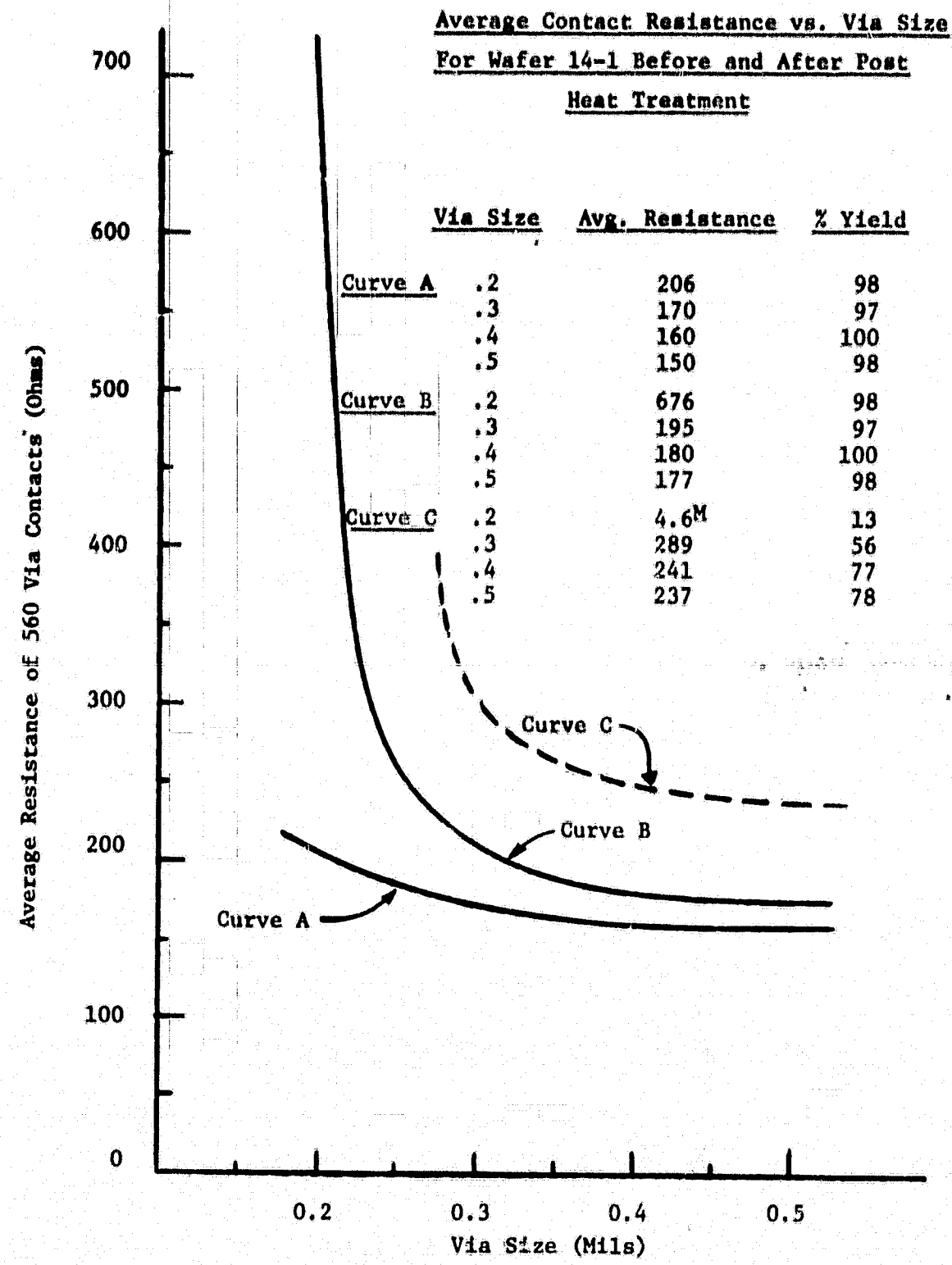

Figure F-9. Average contact resistance vs. via size for wafer #14-1 having phosphorous doped intermetal dielectric before post heat treatment (curve B) and after 30 minutes at 490°C (curve A). For comparison with a wafer having an undoped dielectric, curve C represents such a wafer after undergone 8 hours of post heat treatment at 490°C. (Note contact resistance for 0.5 mil via of wafer in curve C prior to post heat treatment was 90 kilohms.)

2) The extension of the via etch time of the dielectric film for both the dipped (stirred) etching and the ultrasonic etching indicated a substantial improvement in yield with only a slight undercutting for extended times below 90 seconds. (As expected, the doped dielectric etched faster than the undoped.) For etch times beyond break in excess of 110 seconds; the yield decreased. This is believed to be attributed to an increase in contact resistance- and thus a decrease in yield - due to a chemical reaction between the dielectric etchant and the alloys of the sputtered aluminum to form an insulating layer at the surface of the first level metal prior to depositing the second layer.

As indicated in Figure F-2, the optimum etch time is dependent on the size via being etched.

3) The addition of phosphorous doping to the oxide eliminated the possiblity of intermetal dielectric cracking for post heat treatment temperatures below 500°C. A considerable increase in yield was also realized, having total average contact resistances slightly over 200 ohms for 0.5 mil vias and 250 ohms for 0.2 mil as per Figure F-9. (A slow pull of the wafer from the furnace was also practiced to eliminate cracking.)

4) The use of an ultrasonic etching bath for etching vias gives a much better probability of etching small vias (<0.2 mils). This etching was accomplished in a completely enclosed container.

5) The chemical cleaning of the first level metal through the vias prior to depositing the second level metal also increased yield. The first layer Al develops a thin oxide coating as soon as

it is exposed to the atmosphere and this oxide skin creates a high resistance upon depositing the second layer. This coupled with the difficulty of removing all of the dielectric film from the via and the formation of oxides of the alloys contained within the Al all tend toward low yield, high resistance contacts. There are actually two approaches for solving this problem, back sputtering and chemical etching. Back sputtering has the advantage that the oxide thickness can in principle be reduced to zero if the subsequent metallization is applied without exposure to air. The disadvantages include: possibility of radiation induced MOS damage; potential for contamination of the sputtering system; redeposition of previously sputtered materials especially from the substrate table; etc. The chemical etch procedure does not have these disadvantages, but the oxide thickness can never be reduced to zero. [F.14]

The use of a 1:1:1 ethylene glycol: buffered -HF : H_2O etch removes all but 30-50 Å of oxide [F.10] without attacking the Al. (The second layer sputtered Al can easily penetrate this oxide thickness to form good ohmic contacts.) This etch was done just prior to second level metallization.

6) The application of post heat treatments can drastically increase yield by lowering total via contact resistance. There are several possible reactions which could occur to cause this temperature effect. [F.11] Aluminum could react with aluminum suboxides and thus break up the continuous layer of dielectric. Alternately, the recrystallization of aluminum in both of the

level could mechanically disrupt the thin native oxide layer, therefore forming aluminum-to-aluminum contact. As yet, there is no evidence for this speculation.

Figures F-4 and F-5 indicate that in some cases the contact resistance increases with post heat treatment time prior to the "diffusion" through this 'interfacial contamination' by the two layers of aluminum. If this contamination were SiO_2, then it could be said that there exists excess ionic silicon in the oxide which becomes tied-up upon the application of post heat treatments [F-1]]. Since the contamination is probably Al_2O_3, one might say there exist excess ionized Al in the oxide which reacts with the oxidizing species during the sintering process, thus decreasing the total ionic charge in the oxide layer causing the net resistance to increase.

7) Testing the via test pattern can be tedious. For high resistance vias the measured resistance was seen to be both light sensitive and current sensitive. As a result, all testing was accomplished in the dark. Ideally, very low testing potentials are applied in order not to break down a barrier layer thus turning a defective via into a good one. Also, theoretically, vias should not be tested in series, since the entire applied voltage will be dropped across a defective via, probably causing it to break down and appear good. However, in our testing, all vias were measured at once in series using a digital voltmeter.

8) Recently, a new planar multilevel interconnection technology was introduced [F.13] using polyimide films. Although

this procedure appears to be very promising for future applications if taken at face value, it is felt there is still many facets of "magic" associated with it.

REFERENCES

1.1 Woo, D., Private communication provided the range-straggle data.

1.2 Deal, B. E. and A. S. Grove, "General Relationship for the Thermal Oxidation of Silicon," J. Appl. Physics, Vol. 35, No. 12, December 1965, p. 3770, Deal, Sklar, Grove and Snow, "Characteristics of the Surface-State Charge of Thermally Oxidized Silicon," J. Electrochem. Soc., Vol. 114, No. 3, March 1967, p. 266.

1.3 Gassaway, J. D. and Q. Mahmood, Computer Simulation of Two Dimensional Impurity Diffusion in Silicon-on-Sapphire Films, Interim report, NASA Contract NAS8-36749, March 1978.

1.4 Barry, M. L., "Doped Oxides as Diffusion Sources," J. Electrochem. Soc., Vol. 117, No. 11, November 1970, p. 1405.

1.5 Fair, R. B. and J. C. C. Tsai, "A Quantitative Model for the Diffusion of Phosphorus in Silicon and the Emitter Dip Effect," J. Of Electrochem. Soc., Vol. 124, No. 7, July 1977, p. 1107.

1.6 Fair, R. B., "Boron Diffusion in Silicon-Concentration and Orientation Dependence, Background Effects, and Profile Estimation," J. Electrochem. Soc., Vol. 122, No. 6, June 1975, p. 800.

3.1 Kennedy, D. P. and R. R. O'Brien, "Computer Aided Two-Dimensional Analysis of the Junction Field-effect Transistor," IBM J. Research/Development, Vol. 14, pp. 95-116, March 1970.

3.2 Reiser, Martin, "A Two-Dimensional Numerical FET Model for DC, AC, and Large-Signal Analysis," IEEE Trans. Electron Devices, Vol. ED-20, pp. 35-45, January 1973.

3.3 Barnes, J. T., "A Two-Dimensional Simulation of MESFETs," Ph.D. dissertation, Univ. of Mich., Ann Arbor, 1976.

3.4 Schroeder, J. E. and R. S. Muller, "IGFET Analysis Through Numerical Solutions of Poisson's Equation," IEEE Trans. on Electron Devices, Vol. ED-15, No. 12, pp. 954-961, December 1968.

3.5 Barron, M. B., "Low Level Currents in Insulated-Gate Field Effect Transistors," Solid State Electronics, Vol. 15, pp. 293-302, 1972.

3.6 Armstrong, G. A. and J. A. Magowan, "The Distribution of Mobile Carriers in the Pinch-Off Region of An Insulated Gate Field-Effect Transistor and Its Influence on Device Breakdown," Solid-State Electronics, Vol. 14, pp. 723-733, 1971.

3.7 Kennedy, D. P., "Mathematical Simulation of the Effects of Ionizing Radiation on Semiconductors," Contract No. F19628-70-C-0098, Final Report No. AF CRL-72-0257 (1972).

3.8 Kennedy, D. P. and P. C. Marley, "Steady State Mathematical Theory for the Insulated Gate Field Effect Transistor," IBM J. Res. Develop., Vol. 17, pp. 2-12, January 1973.

3.9 Mock, M. S., "A Two-Dimensional Mathematical Model of the Insulated-Gate Field-Effect Transistor," Solid-State Electronics, Vol. 16, pp. 601-609, 1973.

3.10 Motta, R. F., "Steady-State Theory for the Metal-Oxide-Semiconductor Field Effect Transistor," Ph.D. Dissertation, Univ. of Florida, 1976.

3.11 El-Mansyet, Y. A. and A. R. Boothroyd, "A Simple Two-Dimensional Model for IGFET Operation in the Saturation Region," IEEE Trans. on Electron Devices, Vol. ED-24, No. 3, pp. 254-262, March 1977.

3.12 Strang, G. and F. J. Fix, An Analysis of the Finite Element Method, Prentice-Hall, 1973.

3.13 Hohl, J. H., "Variational Principles for Semiconductor Divice Modeling with Finite Elements," IBM J. Res. Develop., Vol. 22, No. 2, March 1978, p. 159.

3.14 Sutherland, A. D., "A Two-Dimensional Computer Model for the Steady-State Operation of MOSFETs," ARPA Report ECOM-75-1344-F Supplement, September 1977.

APPENDIX F (References)

F-1. Schnable, G. L. and R. S. Keen, Jr., IEEE Trans. on Electron Devices, ED-16, 322, No. 4, (1969)

F-2 Bleck, I., H. Sello and L. V. Gnegor, in Handbook of Thin Film Technology, edited by L. I. Maissel and G. Glang (McGraw-Hill, N. Y. 1970), Chapter 23.

F-3 Santoro, C. J. and D. L. Talliver, Proc. IEEE, 59, 1403 (1971)

F-4 Schlacter, M. M., R. S. Keen and G. L. Schnable, IEEE J. Solid-State Circuits, SC-6, 327 (1971)

F-5 Cox, R. H. and H. Hentzschel, J. Electrochem. Soc., 118, 2006 (1971).

F-6 Schnable, G. L. and R. S. Keen, Adv. Electron. Electron Phys., 30, 79 (1971).

F-7 Vossen, J. L., G. L. Schnable and W. Kern, J. Vac. Sci. Tech. 11, 59 (1974)

F-8 Bouldin, D. L., R. W. Eastes, W. R. Feltner, B. R. Hollis, D. E. Routh, NASA Technical Memorandum 78188, September 1978.

F-9 Sunami, H., Y. Itoh, and K. Sato, Jap. J. Appl. Phys., 40, 67 (1971).

F-10 Chang, C. C., et. al., J. Electrochem Soc., Solid-State Science and Technology 125, No. 5, 787 (1978)

F-11 Schnable, G. L., R. S. Keen, Proc. of IEEE 57, #9, 1570 (1969)

F-12 Grove, A. S., Physics and Technology of Semiconductor Devices, Wiley, (1967) p. 343.

F-13 Mukai, K., S. Saiki, K. Yamanaka, S. Harada and S. Sheji, IEEE J. of Solid State Ckts, SC-13, p. 462, 1978.

F-14 Shankoff, T. A., C. C. Chang, S. E. Haszko, J. Electrochem. Soc., Solid State Science and Technology, 125 No. 3, 467 (1978).

F-15 Black, T., "The Reaction of Al With Vitreous Silica", 15th Annual Proceedings Reliability Physics, April 1977.